THE MINOR PLANET BULLETIN

BULLETIN OF THE MINOR PLANETS SECTION OF THE ASSOCIATION OF LUNAR AND PLANETARY OBSERVERS

VOLUME 46, NUMBER 1, A.D. 2019 JANUARY-MARCH 1.

ROTATIONAL PERIODS AND LIGHTCURVES OF FOUR ASTEROIDS

Klay Fuller, Cristo Sanchez, Kent Montgomery
Texas A&M University–Commerce
P.O. Box 3011
Commerce, TX 75429-3011
kent.montgomery@tamuc.edu

(Received: 2018 Aug 2)

Lightcurves were observed for 1603 Neva, 2304 Slavia, 3230 Vampilov, and 3744 Horn-d'Arturo. From the lightcurves, the rotational periods were determined to be 6.426 ± 0.001 hr, 2.914 ± 0.002 hr, 6.149 ± 0.005 hr, and 6.118 ± 0.008 hr, respectively.

The purpose of this research was to find the rotational periods of four asteroids: 1603 Neva, 2304 Slavia, 3230 Vampilov, and 3744 Horn-d'Arturo. These asteroids were chosen based on opposition date, apparent magnitude, and declination. The asteroids were all within two weeks of their opposition date to ensure maximum observing time.

Three different telescopes were used for this research. All three are part of the Southeastern Association for Research in Astronomy (SARA). The SARA-South telescope is 0.6-m and equipped with an FLI CCD camera. SARA-South is located at the Cerro Tololo Inter-American Observatory (CTIO) in La Serena, Chile. The SARA-North telescope is 0.9-m and equipped with an Alta-E6-1105 CCD camera. SARA-North is located at the Kitt Peak National Observatory (KPNO) in Arizona. The SARA-ORM telescope is 1.0-m and equipped with an Andor Ikon-L 2048 CCD camera. SARA-ORM is located at Observatorio del Roque de los Muchachos (ORM) on the island of La Palma in the Canary Isles.

In order to calibrate the images, a set of dark, bias, and flat calibration images were taken each night. The dark images were exposed for the same period of time as their respective light images: 150-sec for 2017 September 24, 120-sec for 2017 September 17, and 2017 September 18 for 1603 Neva, and 180-sec for the other three asteroids. Flat images were taken against the twilight sky each night. For SARA-North, an IR-blocking filter was used; for SARA-ORM, a UV-blocking filter was used; for SARA-South, a luminance 5 filter was used.

The image processing program *Maxim DL* was used to both reduce and align the light images. The program *MPO Canopus* v10.8.1.0 (Warner, 2011) was used to perform time-series photometry on the reduced images. For each observing session, five comparison stars were selected and their brightness compared to the asteroid. The average magnitude difference between the comparison stars and the asteroid was plotted versus the Julian Date. This resulted in a lightcurve that was used to determine the rotational period of the asteroid by applying a Fourier transform to the lightcurve data.

<u>1603 Neva.</u> The asteroid 1603 Neva was imaged 190 times on 2017 September 17, 175 times on September 18 both with SARA-South, and 129 times on September 24 with SARA-ORM. Analysis of the lightcurve found a rotation period of 6.426 ± 0.001 hours with an amplitude of 0.24 magnitudes. A previous study of this asteroid found a similar rotation period of 6.430 ± 0.015 hr with an amplitude of 0.28 mag (Macías, 2016).

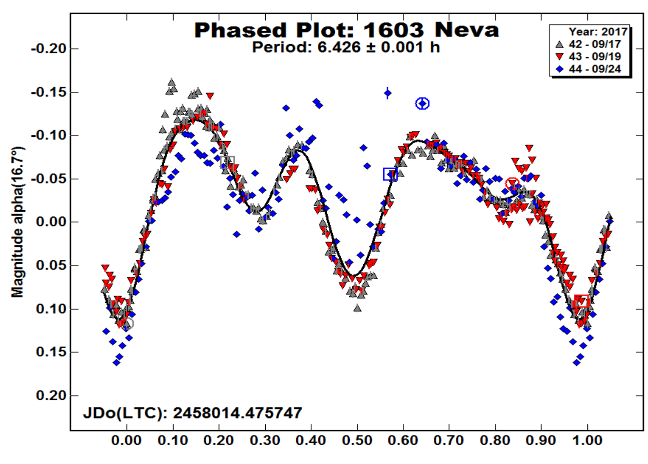

Number	Name	2017 mm/dd	Pts	Phase	L_{PAB}	B_{PAB}	Period(h)	P.E.	Amp	A.E.	Grp
1603	Neva	09/17-09/24	494	7.7,10.5	339	-6	6.426	0.001	0.24	0.02	MB-O
2304	Slavia	06/12-06/13	304	10.0,10.2	254	+16	2.914	0.002	0.20	0.02	EUN
3230	Vampilov	08/30-08/31	271	14.5,14.7	324	-21	6.149	0.005	0.27	0.02	MB-O
3744	Horn-d'Arturo	10/24-10/25	268	8.3,8.8	18	+2	6.118	0.008	0.11	0.01	MB-M

Table I. Observing circumstances and results. Pts is the number of data points. The phase angle is given for the first and last date. L_{PAB} and B_{PAB} are the approximate phase angle bisector longitude and latitude at mid-date range (see Harris *et al.*, 1984). Grp is the asteroid family/group (Warner *et al.*, 2009). Some data are from the JPL SBN website (JPL, 2017).

2304 Slavia. The asteroid 2304 Slavia was imaged 155 times on 2017 June 12, and 149 times on June 13. Both sets of images were obtained with SARA-South. Analysis of the lightcurve found a rotation period of 2.914 ± 0.002 hr with an amplitude of 0.20 mag. A previous study of this asteroid found a similar rotation period of 2.916 hr with an amplitude of 0.28 mag (Behrend et al., 2009).

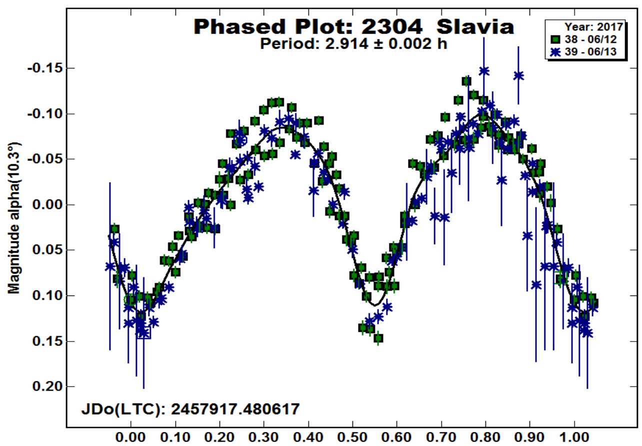

230 Vampilov. The asteroid 3230 Vampilov was imaged 132 times on 2017 August 30, and 139 times on August 31. All observations of this asteroid were done with SARA-South. Analysis of the lightcurve found a rotation period of 6.149 ± 0.005 hr and amplitude of 0.27 mag. A previous study of this asteroid found a similar period of 6.141 ± 0.001 hr and amplitude of 0.24 mag (Waszczak et al., 2016).

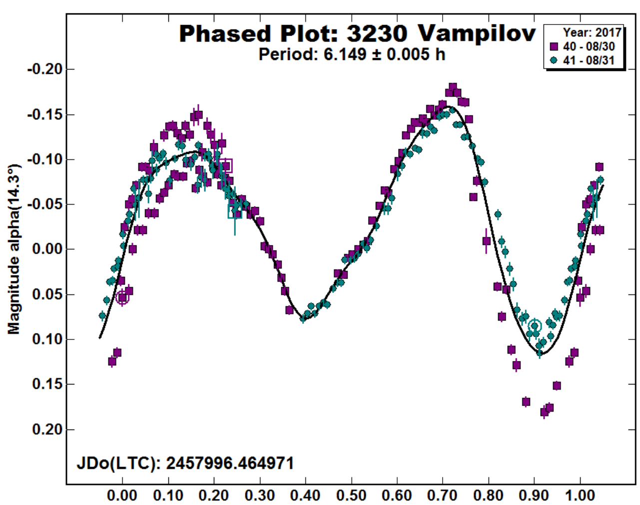

3744 Horn-d'Arturo. The asteroid 3744 Horn-d'Arturo was imaged 141 times on 2017 October 24 with SARA-North, and 127 times on October 25 with SARA-ORM. Analysis of the lightcurve found a rotation period of 6.118 ± 0.008 hr and amplitude of 0.11 mag. A previous study found this asteroid to have a rotation period of 7.18 ± 0.01 hr and amplitude of 0.45 mag (Carbognani, 2014). It is unknown what caused this large discrepancy in rotational period. In this study, both sets of data covered more than one rotational period, and distinctly show a 6.118 ± 0.008 hr period. The higher 7.18 ± 0.01 hr period of the previous study does not fit our data. In addition, their observations did not cover a complete rotation period.

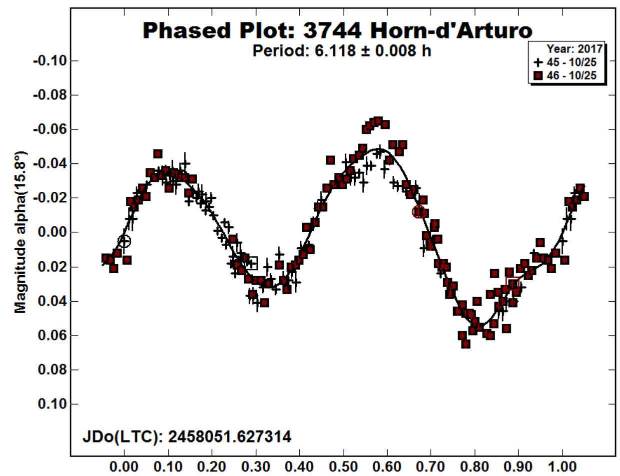

References

Behrend, R. (2009). Observatoire de Geneve web site. *http://obswww.unige.ch/~behrend/page_cou.html*

Carbognani, A. (2014). "Asteroids Lightcurves at OAVdA: 2013 December-2014 June." *Minor Planet Bull.* **41**, 265-270.

Harris, A.W., Young, J.W., Scaltriti, F., Zappala, V. (1984). "Lightcurves and phase relations of the asteroids 82 Alkmene and 444 Gyptis." *Icarus* **57**, 251-258.

JPL (2017). Small-Body Database Browser. *https://ssd.jpl.nasa.gov/sbdb.cgi*

Macías, A. (2016). "Parameters of Rotation and Shapes of Main-Belt Asteroids from APT Observatory Group: Second Quarter 2016." *Minor Planet Bull*. **43**, 350-353.

Warner, B.D., Harris, A.W., Pravec, P. (2009). "The Asteroid Lightcurve Database." *Icarus* **202**, 134-146. Updated 2017 Sep. *http://www.minorplanet.info/lightcurvedatabase.html*

Warner, B.D. (2011). *MPO Canopus* software v10.8.1.0 Bdw Publishing. *http://www.minorplanetobserver.com/*

Waszczak, A., Chang, C.-K., Ofek, E.O., Laher, R., Masci, F., Levitan, D., Surace, J., Cheng, Y.-C., Ip, W.-H., Kinoshita, D., Helou, G., Prince, T.A., Kulkarni, S. (2015). "Asteroid Light Curves from the Palomar Transient Factory Survey: Rotation Periods and Phase Functions from Sparse Photometry." *Astron. J.* **150**, A75.

PHOTOMETRIC OBSERVATIONS OF ASTEROIDS 570 KYTHERA, 1334 LUNDMARKA, 2699 KALININ, AND 5182 BRAY

Michael Fauerbach
Francisco Zabala
Florida Gulf Coast University
10501 FGCU Blvd.
Ft. Myers, FL33965-6565
mfauerba@fgcu.edu

(Received: 2018 July 20)

Photometric observations of 4 main-belt asteroids were obtained during three nights from 2018 June 18 to 2018 June 21, using the SARA-South telescope located at Cerro Tololo Inter-American Observatory in Chile.

We report on the results of photometric observations obtained with the Southeastern Association for Research in Astronomy (SARA) consortium 0.6m (f/13.5) telescope coupled with an Andor iKon-L series CCD. The telescope is located at Cerro Tololo Inter-American Observatory in Chile. The data was calibrated using MaximDL and photometric analysis was performed using MPO Canopus (Warner, 2017). The targets were selected to take advantage of the long winter nights and their accessibility from the southern hemisphere. Utilizing the asteroid lightcurve database (LCDB; Warner et al., 2009a) we searched for asteroids that fulfilled these criteria and had a high uncertainty in their rotational periods associated with previous observations. Unfortunately, the weather was not favorable and high cirrus clouds and an almost full Moon made for less than ideal observing conditions. A fourth night scheduled for 2018 June 22 was completed clouded out.

570 Kythera. There are six previously published rotational periods for 570 Kythera ranging from 5.682 h to 10.2 h, with an adopted value of 8.120 ± 0.002 h (Behrend (2004)). All previous measurements reported amplitudes ranging from 0.12 to 0.20 mag. We observed the asteroid on two nights but were unfortunately not able to determine a rotational period. Due to the non-ideal observing conditions our data is rather noisy and unlike in previous years our measured lightcurve amplitude was only 0.05 mag, significantly smaller than in previous years. We display our data with the adopted rotational period of 8.120 h only to highlight the small amplitude -and unfortunately high noise- of our data. We will restrict ourselves to only reporting the amplitude for our measurement.

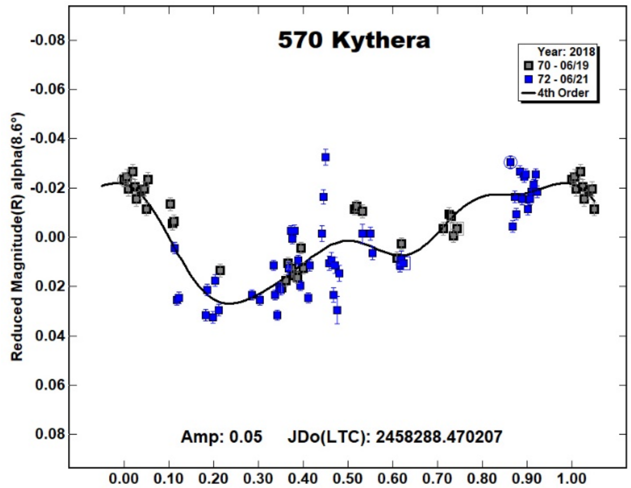

1334 Lundmarka. We observed 1334 Lundmarka over a period of three nights. We derived a rotational period of 6.250 ± 0.002 h with an amplitude of 0.88 mag. This agrees with the measurement by Bohn et al. (2015) and Ďurech at al. (2016). It would be interesting to combine the data presented here and the data by Bohn et al. with the sparse data used by Ďurech at al. to derive a shape model. This could be another test case for the accuracy of shape models from sparse data.

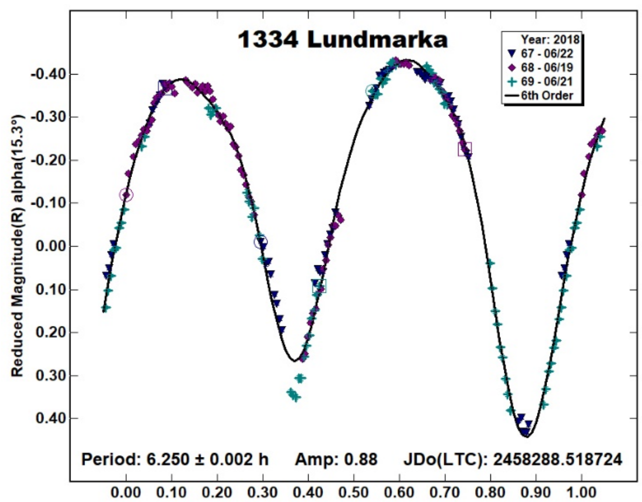

2699 Kalinin. We observed 2699 Kalinin on two nights for approximately 2.5 h and 4 h respectively. Only one prior measurement of the rotational period exists. Ambrosioni (2011) measured a period of 2.9279 h. We obtained a rotational period of 2.928 ± 0.001 h with an amplitude of 0.28 mag in excellent agreement with the previous measurement.

Number	Name	2018 mm/dd	Pts	Phase	L_{PAB}	B_{PAB}	Period(h)	P.E.	Amp	A.E.	Grp
570	Kythera	06/19,06/21	84	8.7,9.2	237.8	0.6			0.05	0.02	MB-O
1334	Lundmarka	06/19-06/21	214	14.6,15.1	236.0	13.3	6.250	0.001	0.88	0.02	MB-M
2699	Kalinin	06/19,06/21	136	13.3,12.7	290.8	-14.1	2.928	0.001	0.28	0.02	MB-I
5182	Bray	06/18	38	10.8	276.4	16.3	2.86	0.04	0.28	0.02	EUN

Table I. Observing circumstances and results. Pts is the number of data points. The phase angle is given for the first and last date. L_{PAB} and B_{PAB} are the approximate phase angle bisector longitude and latitude at mid-date range (see Harris *et al.*, 1984). Grp is the asteroid family/group (Warner *et al.*, 2009).

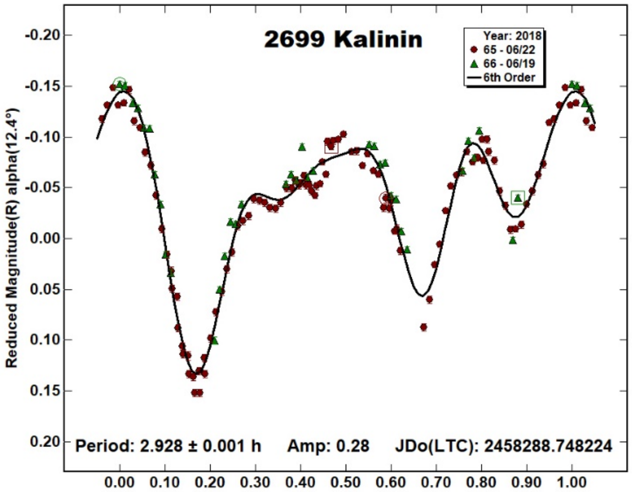

5182 Bray. This is a member of the Eunomia family. We observed 5182 Bray on a single night and measured a rotational period of 2.86 ± 0.04 h with an amplitude of 0.28 mag. The only previously reported rotational period is by Klinglesmith (2014). The data was reported to the CALL website but does not seem to be published elsewhere. Klinglesmith reported a period of 2.883 ± 0.001 h in good agreement with our result.

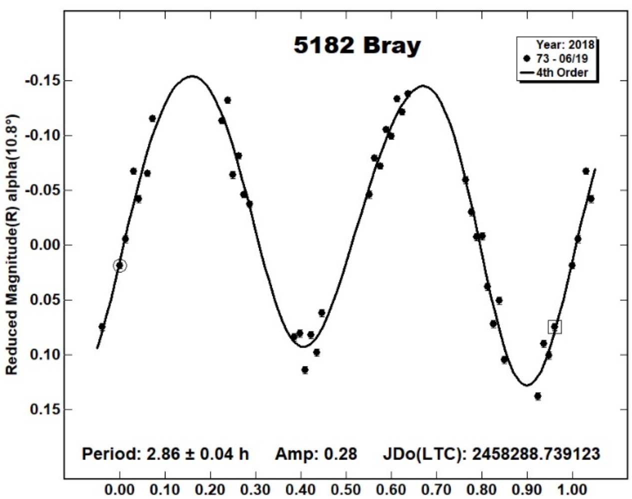

Acknowledgements

One of the authors (F.Z.) would like to acknowledge support from the NASA/Florida Space Grant Consortium Summer Research Scholarship program.

References

Ambrosioni, C., Colazo, C., Mazzone, F. (2011). "Period Determination for 1996 Adams and 2699 Kalinn by AOACM." Minor Planet Bulletin 38, 102.

Behrend, R. (2004). Observatoire de Geneve web site. *http://obswww.unige.ch/~behrend/page_cou.html*

Bohn, L., Hibbler, B., Stein, G., Ditteon, R. (2015). "Asteroid Lightcurve Analysis at the Oakley Southern Sky Observatory: 2014 September." *Minor Planet Bulletin* **42**, 89-90.

Ďurech, J., Hanuš, J., Oszkiewicz, D., Vančo, R. (2016). "Asteroid models from the Lowell photometric database." Astronomy & Astrophysics, Volume 587, id.A48, 6 pp.

Harris, A.W., Young, J.W., Scaltriti, F., Zappala, V. (1984). "Lightcurves and phase relations of the asteroids 82 Alkmene and 444 Gyptis." *Icarus* **57**, 251-258.

Klinglesmith III, D.A. (2014). Posting on CALL web site. *http://www.MinorPlanet.info/call.html*

Warner, B.D., Harris, A.W., Pravec, P. (2009). "The Asteroid Lightcurve Database." *Icarus* **202**, 134-146. Updated 2017 Nov. *http://www.minorplanet.info/lightcurvedatabase.html*

Warner, B.D. (2017). MPO Canopus software version 10.7.10.0. *http://www.bdwpublishing.com*

CORRIGENDUM: WARNER (2018), *MPB* 45, PAGE 380

For the published article:
Warner, B.D. (2018). "Asteroid Lightcurve Analysis at CS3-Palmer Divide Station: 2018 April-June." *Minor Planet Bulletin* **45**, 380-386.

Incorrect references were given for previous works on 132 Aethra. Instead of those for Galad (2010) and Pilcher (2017), two of the many relevant references would be Behrend (2010; 5.16792 h) and McDonald (2012; 5.168 h). Accordingly, the full references for the References section would read:

Behrend, R. (2010). Observatoire de Geneve web site. September results. *http://obswww.unige.ch/~behrend/page_cou.html*

McDonald, D. (2012). "Lightcurve Photometry of 132 Aethra." *Minor Planet Bull.* **39**, 105.

VISUAL OBSERVATION OF MINOR PLANETS

Andrew Salthouse
560 Heritage Road, Millington NJ 07946 USA
asalthouse@hotmail.com

(Received: 2018 Aug 5)

The author describes the processes for identifying minor planet targets, observational planning, identification criteria, and record keeping. He presents his lifetime observational totals from 50+ years of observing.

A worthwhile challenge for amateur astronomers is hunting asteroids. Since they are constantly on the move, they can be more difficult to locate than most other celestial objects. To be successful, the amateur needs to identify targets, prepare charts, observe, and keep good records.

Identifying Potential Targets

There are several sources a minor planet observer can use to identify potential targets. One such resource is maintained by Brian Warner (*http://www.MinorPlanet.info*). By clicking "Observation Planning" on the main menu, one can access the "Ephemeris Generator" page, which allows the user to select parameters such as month and year, magnitude limit, declination limits, etc. Once these parameters are entered, the site produces a list of minor planets ordered by date of brightest appearance. The output includes the dates of closest approach and opposition, minimum distance, brightness, declination, etc.

This list is a starting point; the user will need to cull objects from this list based on personal criteria. A useful second step is to access the Minor Planet and Comet Ephemeris Service web site of the IAU Minor Planet Center

http://minorplanetcenter.net/iau/MPEph/MPEph.html

Entering the minor planet numbers from the list, and the desired date range, the IAU website will then provide an ephemeris for each selected minor planet for the desired range of dates. This information can be used to further cull the list of potential targets.

Observational Preparation

Next, the observer must prepare a chart for each target. The author has used two different methods for producing charts.

The first is the *Minor Planet Observer Asteroid Viewing Guide* (Warner, 2018). This software package will produce a sky chart showing the path of the minor planet on selected dates. The user can select the minor planet, chart scale, magnitude limit of the background stars, and dates. Another useful source is the AAVSO site (*http://aavso.org/apps/vsp*). Like the *MPOAVG*, users can select the scale and magnitude limits, but this software does not produce a path track.

Finally, the user needs to select the targets for observation on a given night. In the author's youth he would select up to 30 targets for a single night, but as his stamina declined with age he limited it to just 10 or so. Observing minor planets visually can be hard work, and an observer needs to understand his limitations.

Observing

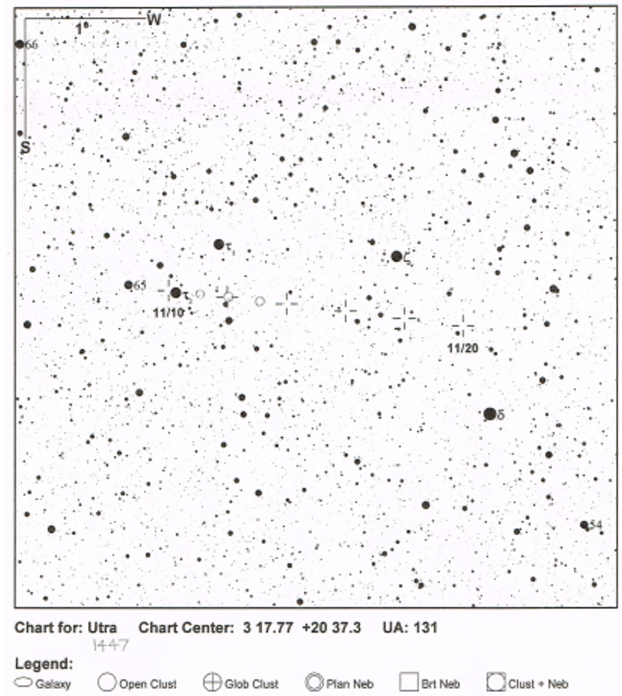

Figure 1. Chart of the path of 1447 Utra, produced from the *Asteroid Viewing Guide* on 2001 Nov 10. The hand-drawn circles along the path show the positions during times of observation. North is up.

Figure 2. Motion of 1447 Utra recorded by the author at the telescope on 2001 Nov 10. Positions "A" and "B" correspond to local times 22:20 and 23:25 EST respectively (03:20 and 04:25 UT on 2001 Nov 11). North is to the lower right. [The image was digitally enhanced during production to increase contrast – Editor].

Once the observer has selected a list of targets and produced star charts (with tracks plotted on them) for each one, he is ready to observe. If the observer has a "go-to" telescope with RA and Dec inputs, then he can locate the star field quickly. Otherwise, he must identify the bright stars on the chart and locate them in the sky with a good quality atlas. The author uses the *Atlas of the Heavens* (Becvar, 1962), *Sky Atlas 2000* (Tirion and Sinnott, 1998), or the *Sky & Telescope Pocket Atlas* (Sinnott, 2006), depending on the brightness of the targets. Standard star-hopping techniques can be used to find the target.

When observing, one should record the telescope aperture, magnifications used, date and time, transparency, seeing, and other relevant factors such as moonlight. Once a target is located in the telescope, the observer draws the relevant field of view, and identifies suspected targets. This drawing must be sufficiently accurate that a motion of 0.5 arc minutes would be noticeable. The less accurate the drawing, the greater the motion must be to be noticed and, therefore, the longer the wait until that motion becomes clear. The author has found that eyepieces producing a field of view of 10 to 20 arc minutes are most helpful. Figure 1 shows a target path created from the *Asteroid Viewing Guide*, and Figure 2 shows the drawing of the visual field made by the author at the eyepiece.

After sufficient time has passed for the motion of the suspect to be identified, the observer must re-observe the field of view and note the second position of the target, if it has moved. If no motion is detected, then either the target was not seen at all, or the time interval to detect its motion was insufficient. Most minor planets move at least 0.5 arc minutes per hour, although some may be slower, particularly near stationary points. Like the outer planets, nearly all minor planets will retrograde at opposition, but they can be near a stationary point several weeks before or after opposition. Thus, the middle of the opposition is the best time to observe any given minor planet because the motion will be most obvious and the target will be at or near its brightest.

Once the observer has confirmed the observation of the minor planet by showing it at two different locations at two different times on the same night, the observation needs to be logged and recorded. The author recommends making a visual estimate of the object's magnitude.

In the early years, the author came to realize that drawings can be imperfect and errors of identification can be made. For example, multiple faint stars very near the target can cause the observer to misidentify the target, especially if the transparency changes between the first and second observations. For this reason, the author does not consider the observation of the minor planet to be fully confirmed until additional observations can be made on subsequent nights. This is the "three observations" rule: the object should be seen on two different nights and at least twice on one of those nights. This rule was always followed when observing a minor planet for the first time, but eventually it was relaxed when observing brighter asteroids ($V < \sim 13$) at second and subsequent oppositions.

Record Keeping

It is critical that clear records be maintained. Besides the actual drawings and notes made at the eyepiece, there is a need for a summary record, generally digital. The author has kept all of his notes and drawings since 1965, and also maintains several digital records covering the last 50+ years. Microsoft Excel® is useful for this purpose since pivot tables can be constructed that allow slicing the data by minor planet number (or groups of numbers), month or year, and other parameters. Of course, Microsoft Excel® did not exist when the author started observing, but he began converting paper records to digital form in the 1990s.

Successful minor planet observing requires all the aforementioned processes, and some skill at the eyepiece, but also the discipline to keep observing night after night. One will not find any minor planets by staying indoors on cold winter nights or on sweltering hot summer evenings. The author has endured hundreds of bitterly cold nights in an effort to identify as many asteroids as possible. Largely because of this persistence, he has accumulated over 28,000 visual observations of nearly 2,900 distinct objects.

Seasonality

The orbits of the main-belt asteroids lie between the orbits of Mars and Jupiter. These will account for more than 90% of all minor planets observed. Jupiter's orbit has an eccentricity of 0.049, meaning that the aphelion is more than 10% further from the Sun than the perihelion. Consequently perihelic oppositions of Jupiter (around October) are noticeably brighter than aphelic oppositions (around April). Due to its great mass, Jupiter perturbs the orbits of the minor planets, with the effect that many of their orbits line up their perihelia in the same general direction as Jupiter's perihelion. Thus, asteroids at opposition in October tend to be brighter on average than those at opposition in April. This creates a distinct seasonal pattern.

This pattern is abundantly clear in the author's data. About 67% of all minor planets were first identified in the six-month period of August through January, leaving only 33% in the six-month period of February to July. In terms of total observations, 62% were made in August to January and 38% in February to July. These patterns are shown in Figure 3.

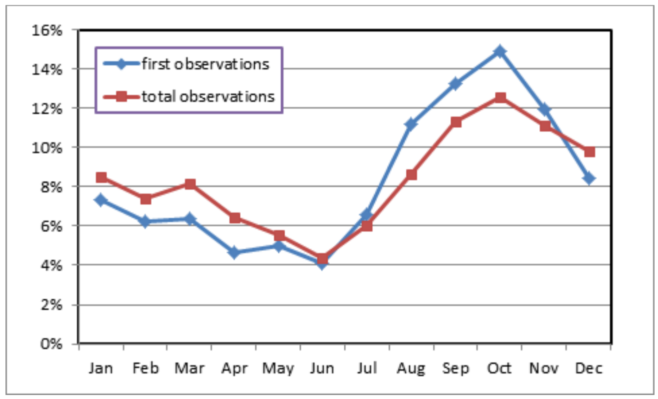

Figure 3. Monthly distribution of first sightings of each object (2,894 total) and of total observations (28,012 total) over the period 1966 to 2018.

Any observer setting out to capture minor planets in his telescope is likely to see a similar pattern. There will be far more available targets in the second half of the year than in the first half.

Although the lines of apsides of the minor planets are not randomly distributed around the ecliptic, the positions of these objects in their orbits are random. Since most main-belt asteroids have orbital periods ranging from three to six years, with most having orbital eccentricities of at least 0.10, they will have both aphelic and perihelic oppositions. A typical object will be a full magnitude or more fainter at aphelic than at perihelic opposition. Thus, many potential targets may be visible only near perihelion. Consequently, in order to capture as many objects as possible, an observer must commit to an observing program lasting up to six years. The author is nearing completion of his fifth six-year program since building his observatory in 1990.

Summary of Results

The author's lifetime totals are included in Table 1, showing the number of distinct objects, the number of oppositions, and the number of observations. Note that the recently classified dwarf planets Ceres and Pluto have been removed from the minor planet subtotal and listed separately.

Acknowledgements

The author thanks Mr. Brian Warner for his support, providing valuable help with the Minor Planet Observer website and software. He also thanks Mr. Lawrence Garrett and Mr. Gerard Faure for their support of the Magnitude Alert Program (now defunct) in which the author participated for several years. Finally, he thanks Ms. Mary Ellen Salthouse, Mr. Roger Harvey, and Mr. Frederick Pilcher for their ongoing support and encouragement.

References

Becvar, A. (1962) *Atlas of the Heavens.* Sky Publishing Corporation, Cambridge MA.

Sinnott, R. (2006). *Pocket Sky Atlas*, Sky and Telescope Media, Cambridge MA.

Tirion, W., Sinnott, R. (1998). *Sky Atlas 2000*, Cambridge University Press, Cambridge, MA.

Warner, B.D. (2018). *Minor Planet Observer Asteroid Viewing Guide* software.
bdwpublishing.com/mpo2018asteroidviewingguide.aspx

ASTEROID NUMBER			TOTAL SEEN	TOTAL OPPNS	GROSS OBSNS
2	-	200	199	2,056	6,312
201	-	400	200	1,330	3,905
401	-	600	199	1,026	3,019
601	-	800	194	796	2,326
801	-	1000	191	593	1,749
1001	-	1300	260	642	1,955
1301	-	1600	240	504	1,580
1601	-	2000	244	457	1,474
2001	-	3000	373	585	1,949
3001	-	5000	378	539	1,866
5001	-	10000	236	293	1,054
10001	-		180	197	823
MINOR PLANETS			2,894	9,018	28,012
COMETS			58	62	416
DWARF PLANETS					
	Ceres		1	26	88
	Pluto		1	22	180
GRAND TOTAL			2,954	9,128	28,696

Table I. Lifetime total observations of minor planets, comets, and dwarf planets as of 2018 June 30. Ceres was upgraded from minor to dwarf planet in 2006 (observed from 1966 to 2018). Pluto was downgraded from major to dwarf planet in 2006 (observed from 1987 to 2008).

V-BAND PHOTOMETERIC MONITORING OF 852 WLADILENA

Louis Gonzalez, Misty C. Bentz, and Leonardo Paredes
Department of Physics and Astronomy
Georgia State University
25 Park Place, Suite 605
Atlanta, GA 30303 USA
gonzalez@astro.gsu.edu

(Received: 2018 July 26)

V-band photometry of main-belt asteroid 852 Wladilena was obtained on a single night in February 2017. From the light curve, we determined a rotational period of 4.717 ± 0.023 hours and an amplitude variability of 0.26 ± 0.03 mag.

852 Wladilena (alternatively known as 1916 S2J, A913 SB, and A924 WJ), named after Soviet revolutionary Vladimir Lenin, was first discovered by Soviet-Russian astronomer Sergey Beljavskij at Simeis Observatory on 2 April 1916 (JPL 2018). It has been previously studied by several groups, but most have not utilized filtered photometry.

V-band photometric measurements of the asteroid were made at Hard Labor Creek Observatory in Rutledge, GA. This facility is owned and maintained by Georgia State University and was used to conduct observations for the semester-long project of ASTR 4100 and ASTR 6100: Observational Methods and Instrumentation. We used the 24-inch Miller telescope, which is a f/6.8 Corrected Dall-Kirkham Astrograph. The CCD camera used was an Apogee Alta which features a 15-micron pixel size distributed in a 2048 x 2048 array, providing a 26.3’ x 26.3’ field of view and a scale of 0.77 arcsec/pixel.

The observing conditions were non-photometric throughout the night. At times, the partly cloudy skies caused gaps in the observations. Eighty-nine exposures, each 240 seconds long, were taken over the course of the night. In total, the observations covered a total duration of 10 hours.

The images were reduced in IRAF using standard procedures. The reduced images were then processed using the aperture photometry function of IRAF (phot). A 10-pixel radius, approximately 7.7 arcseconds, was adopted to minimize uncertainties from variable seeing. Differential photometry between the asteroid and five field stars was used to correct the instrumental magnitudes of the asteroid. To convert from instrumental to calibrated magnitudes, we searched the APASS database for V-band magnitudes of stars in the field. We then determined the least-squared offset between the instrumental and calibrated magnitudes and calculated the final light curve for the asteroid.

MPO Canopus was used to implement the Fourier analysis as described by Harris *et. al* (1989) to examine the final light curve for the most likely rotational period. A 7th order polynomial was used in the final analysis. The plot below shows the V-band light curve with the best fit overlaid, which is found to have a period of 4.717 ± 0.023 hours and an amplitude of 0.26 ± 0.03 mag.

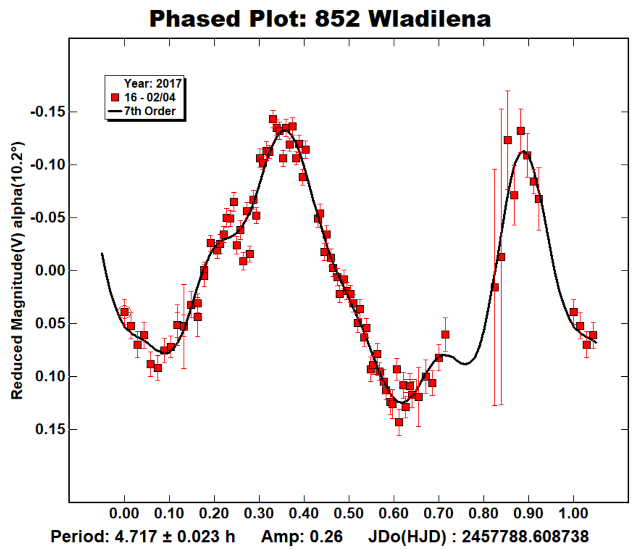

852 Wladilena has been studied by several groups over the last three decades. The following rotation periods have been reported in the literature: 4.611 hours (Di Martino and Cacciatori, 1984), 4.612 ± 0.001 hours (De Angelis and Mottola, 1995), 4.6134 ± 0.0003 hours (Harris *et. al*, 1999), 4.612 hours (Kiss *et. al*, 1999), 4.608 ± 0.002 hours (Polishook, 2012), and 4.613 ± 0.001 hours (Klinglesmith *et. al*, 2013), 4.613301 ± 0.000002 hours (Hanuš *et. al*, 2013), 4.610 ± 0.002 hours (Warner, 2014), 4.61330 ± 0.00002 hours (Hanuš *et. al*, 2018) respectively. To our knowledge, only Di Martino and Cacciatori (1984) report V-band measurements while Harris *et. al* (2013) published infrared photometry measurements using WISE, and the remaining studies largely focused on unfiltered measurements. While Di Martino and Cacciatori (1984) published V-band measurements of 852 Wladilena, this work represents a sizeable increase in the number of data points collected (89 vs. 30). Our best-fit period is slightly longer than previous measurements, but this is likely due to the gaps in time coverage caused by clouds during our observations.

Many of these previous studies also reported amplitudes of variability: 0.30 mag (Di Martino and Cacciatori, 1984), 0.30 mag (De Angelis and Mottola, 1995), 0.25 ± 0.01 mag (Harris *et. al*, 1999), 0.32 mag (Kiss *et. al*, 1999), 0.28 ± 0.01 mag (Polishook, 2012), 0.29 ± 0.05 mag (Klinglesmith *et. al*, 2013), and 0.25 ± 0.02 mag (Warner, 2014). Our calculated amplitude, 0.26 ± 0.03 mag is somewhat smaller than most of these values, but could be due to the fact that our observations were filtered, rather than unfiltered, and may also be due to the larger uncertainties in our measurements of the second peak in the light curve.

Acknowledgements

IRAF is distributed by the National Optical Astronomy Observatory, which is operated by the Association of Universities

Number	Name	2017 mm/dd	Pts	Phase	L_{PAB}	B_{PAB}	Period(h)	P.E.	Amp	A.E.	Grp
852	Wladilena	02/04	89	10.15	144.4	25.8	4.717	0.023	0.26	0.03	PHO

Table I. Observing circumstances and results. Pts is the number of data points. The phase angle is given for the first and last date. L_{PAB} and B_{PAB} are the approximate phase angle bisector longitude and latitude at mid-date range (see Harris *et al.*, 1984). Grp is the asteroid family/group (Warner *et al.*, 2009).

for Research in Astronomy (AURA) under cooperative agreement with the National Science Foundation. This research was made possible in part based on data from the AAVSO Photometric All-Sky Survey (APASS), funded by the Robert Martin Ayers Sciences Fund.

References

Di Martino, M., Cacciatori, S. (1984). "Photoelectric photometry of 14 asteroids." *Icarus* **60**, 75-82.

De Angelis, G., Mottola, S. (1995). "Lightcurves and pole determinations for the asteroids 69 Hesperia, 79 Eurynome and 852 Wladilena." *Planetary and Space Science* **43**, 1013-1017.

Hanuš, J., et al. (2013). "Asteroids' physical models from combined dense and sparse photometry and scaling of the YORP effect by the observed obliquity distribution." *Astronomy & Astrophysics* **551**, A67.

Hanuš, J., et al. (2018). "Thermophysical modeling of main-belt asteroids from WISE thermal data." *Icarus* **309**, 297-337.

Harris, A.W., Young, J.W., Scaltriti, F., Zappala, V. (1984). "Lightcurves and phase relations of the asteroids 82 Alkmene and 444 Gyptis." *Icarus* **57**, 251-258.

Harris, A.W., et al. (1989). "Photoelectric Observations of Asteroids 3, 24, 60, 261, and 863." *Icarus* **77**, 171-186.

Harris, A.W., et al. (1999). "Asteroid Lightcurve Observations from 1981 to 1983." *Icarus* **142**, 173-201.

Polishook, D. (2012). "Lightcurves for Shape Modeling: 852 Wladilena, 1089 Tama, and 1180 Rita." *Minor Planet Bulletin* **39**, 242-244.

JPL (2018). Small-Body Database Browser. *https://ssd.jpl.nasa.gov/sbdb.cgi*

Kiss, L.L., Szabo, G., Sarneczky, K. (1999). "CCD photometry and new models of 5 minor planets." *Astronomy and Astrophysics Supplement Series* **140**, 21-28.

Klinglesmith, D.A., Hanowell, J., Risley, E., Janek, T., Vargas, A., Warren, C.A. (2013). "Etscorn Observed Asteroids: Results for Size Asteroids December 2012 - March 2013." *Minor Planet Bulletin* **40**, 154-156.

Warner, B.D., Harris, A.W., Pravec, P. (2009). "The Asteroid Lightcurve Database." *Icarus* **202**, 134-146. Updated 2016 Sep. *http://www.minorplanet.info/lightcurvedatabase.html*

STAFF POSITION OPENING - ASSOCIATE PRODUCER, *MINOR PLANET BULLETIN*

The *Minor Planet Bulletin* announces the opening a new staff position of Associate Producer, with the probability of taking over the *MPB* Producer's position in about two years following a period of mentoring and collaboration. The responsibilities will be to assist the current Producer, Bob Werner, with the layout construction of each quarterly issue of the *Minor Planet Bulletin*, demonstrating proficiency for transitioning to the Producer position. For each *MPB* issue produced, the required tasks and capabilities to be demonstrated include:

- Reformatting approximately 30–40 manuscript documents from the editors.
- Responsive communication with the editorial and distribution staff.
- Able to commit to and adhere to deadlines throughout the calendar year.
- Corresponding with authors via email with article proofs.
- Handling formatting inquiries from new and seasoned authors who contribute manuscripts to the *MPB*.
- Laying out an issue's articles in a single master document, resulting in the ready-to-print and ready-to-release electronic version of each *MPB* issue.
- Constructing a full index of each annual volume.
- Maintaining a long-term electronic archive of all issues.

The skills required for the position of Associate Producer, *Minor Planet Bulletin* include:

- Proficiency with Microsoft Word 2013/2010, Portable Document Format (pdf) computer documents, and email. Production status is tracked using Excel.
- Knowledgeable expertise with asteroid astronomy sufficient for some error checking and recommending editorial corrections.
- Strong skills with written English.

The time commitment required varies from issue to issue, but typically occupies 25 or 30 hours each quarter. *The Minor Planet Bulletin* publishes four issues per year. All *MPB* staff positions, including this announced opening for Associate Producer, are volunteer positions without pay or other compensation. Materials and postage costs, as necessary, are reimbursed.

Persons wishing to be considered for the Associate Producer position should send a statement of interest, a statement on the level of available commitment, and a summary of qualifications to the Editor: rpb@mit.edu Review of applications will begin February 1, 2019. The position will remain open until filled.

ROTATION PERIOD OF ASTEROID 660 CRESCENTIA

Alberto Colognese
P.O.C. – Piccolo Osservatorio Corsionese
Corsione (AT), Italy
alberto@colognese.it

(Received: 2018 Aug 2)

Presented here are the results of a one month survey of asteroid (660) Crescentia The survey, even with incomplete coverage of the estimated period of 7.9123 ± 0.0162 h, confirms previous results.

The minor planet 660 Crescentia belongs to Maria family (also known as the Roma family) whose members have experienced substantial collisional and dynamical evolution in the main-belt (Kim et al., 2013). The asteroid is located near the 3:1 Jupiter mean motion resonance area that supplies near-Earth asteroids (NEAs) to the inner Solar System. It was discovered at Taunton by J.H. Metcalf on 1908 January 8 (Schmadel, 2003). Crescentia has a diameter of 42.3 km, an orbital semi-major axis of 2.53 AU, and eccentricity of 0.108 (JPL, 2018).

From 2018 June 23 to July 13 five sets of CCD observations were made of asteroid 660 Crescentia at P.O.C. observatory. Images were taken using a V photometric filter, Atik 314L+ b/w CCD, and 0.20-m Ritchey-Chretien. Exposures ranged from 30 to 60 seconds. The image scale after 2x2 binning was 1.66 arcsec/pixel. All images were corrected with dark frame, bias, and flat field images.

A spreadsheet was developed to estimate the coverage of the rotation period when assuming the reported value of 7.9116 h in the asteorid lightcurve database (LCDB; Warner et al., 2009a). We also use a three color ruler to indicate a missing coverage (red), poor coverage of one observation (yellow), and good coverage (green) with two more observations.

A total of 668 observations covering about 10.5 hours are presented in Table I. Two portions of the lightcurve (rotation phase 0.14-0.17 and 0.69-0.85) were predicted not to have observations. This potentially leads to incomplete or incorrect results since it is better to collect two times the rotation period to obtain a correct lightcurve.

The method of predicting the coverage of the rotation period assuming 0 at the time of the first observation was validated. In this case, it was expected to find two gaps, which was confirmed by the phased plot. This spreadsheet will be a common tool at P.O.C observatory to plan future sessions.

Despite it being derived with incomplete coverage of the lightcurve, the period of 7.9123 ± 0.0162 h agrees well with that of 7.91 h (Warner, 2009b) and 7.911 h (Stephens 2014) reported in literature.

References

Harris, A.W., Young, J.W., Scaltriti, F., Zappala, V. (1984). "Lightcurves and phase relations of the asteroids 82 Alkmene and 444 Gyptis." *Icarus* **57**, 251-258.

Kim, M.-J., Choi, Y., Moon, H., Byun, Y., Brosch, N., Kaplan, M., Kaynar, S., Uysal, O., Guzel, E., Behrend, R., and 6 coauthors (2013). "Rotational properties of Maria asteroid family." *Astron. J.* **147**, A56.

Lutz D. Schmadel (2003) *Dictionary of Minor Planet Names.* Fifth ed. Springer Verlag.

MPC (2018). JPL Database Search. *https://www.minorplanetcenter.net/db_search/show_object?utf8=%E2%9C%93&object_id=crescentia (accessed July 25, 2018)*

Stephens, R.D. (2014). "Asteroids Observed from CS3: 2014 April-June." *Minor Planet Bull.* **41**, 226-230.

Warner, B.D., Harris, A.W., Pravec, P. (2009a). "The Asteroid Lightcurve Database." *Icarus* **202**, 134-146. Updated 2018 June. *http://www.minorplanet.info/lightcurvedatabase.html*

Warner, B.D. (2009b). "Asteroid Lightcurve Analysis at the Palmer Divide Observatory: 2008 December - 2009 March." *Minor Planet Bull.* **36**, 109-116.

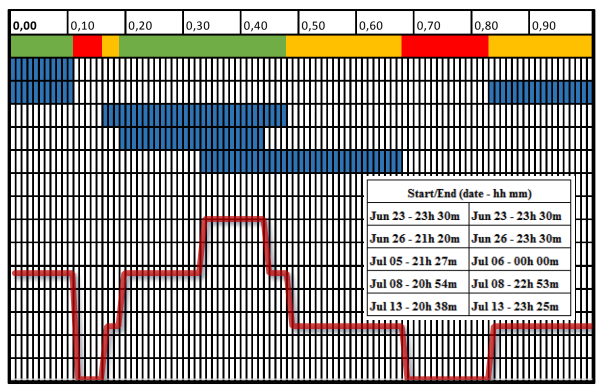

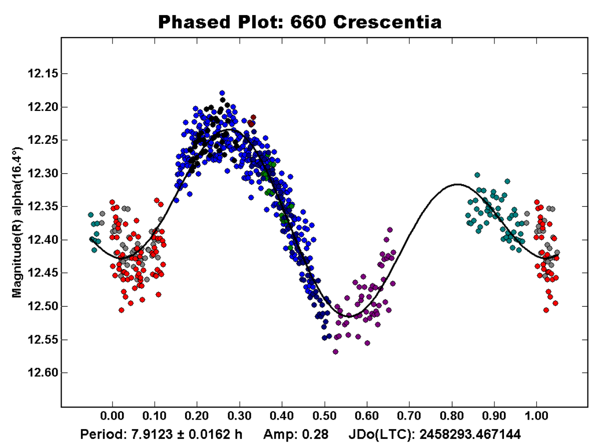

Number	Name	2018 mm/dd	Pts	Phase	L_{PAB}	B_{PAB}	Period(h)	P.E.	Amp	A.E.	Grp
660	Crescentia	06/23-07/13	668	15.6,20.8	252	19	7.9123	0.0162	0.25	0.03	Maria

Table I. Observing circumstances and results. Pts is the number of data points. The phase angle is given for the first and last date. L_{PAB} and B_{PAB} are the approximate phase angle bisector longitude and latitude at mid-date range (see Harris *et al.*, 1984). Grp is the asteroid family/group (Warner et al., 2009a).

CCD PHOTOMETRIC OBSERVATIONS OF ASTEROIDS 2746 HISSAO, 2884 REDDISH, AND 3394 BANNO

Kenneth Zeigler
George West High School
1013 Houston Street, George West, Texas 78022 USA
kzeigler@gwisd.esc2.net

Tyler Barnhart
George West High School, George West, Texas USA

Armand Moser
George West High School, George West, Texas USA

Nate Duval
George West High School, George West, Texas USA

(Received: 2018 Aug 5)

CCD photometric observations of asteroids 2746 Hissao, 2884 Reddish, and 3394 Banno conducted from the George West ISD Mobile Observatory are described. The rotational period of 2746 Hissao is 3.18 ± 0.01 hr, with an amplitude of 0.40 mag. The rotational period of 2884 Reddish is 38.3 ± 0.2 hr, with an amplitude of 0.80 mag. The rotational period of 3394 Banno is 7.34 ± 0.01 hr with an amplitude of 0.21 mag.

The photometric observations described in this paper were conducted from the George West ISD Mobile Observatory, which is located at a dark sky site 19 kilometers south of George West, Texas. This research was conducted as part of an educational program of the George West Independent School District, and was conducted during the late fall and spring semester of the 2017-2018 school year.

Throughout this research program, a Meade 0.35-meter LX600 Schmidt Cassegrain telescope was used. It is housed within a converted eight by sixteen foot Wells Cargo trailer with a hinged roof that sets on concrete blocks supported by a thick concrete slab to minimize vibrations. An SBIG STXL-6303 camera thermoelectrically cooled to –35°C was used to make the observations. The exposures ranged from 60 to 120 seconds. The raw images were dark subtracted and flat fielded. To preserve the maximum light intensity of the objects observed, no filters were placed in the optical path during the observations.

The brightness of the asteroid was compared to that of a comparison star in the same CCD frame. Two additional stars were also measured in each frame to act as check stars to assess the precision of the observations and confirm that the comparison star was not variable. Target brightness was determined by measuring a 169 (13x13) pixel sample surrounding the asteroid or star in question. This corresponds to an 8.45 by 8.45 arcsec box. When possible, the same comparison star and check stars were used during consecutive nights of observation. The coordinates of the asteroid were obtained from the online *MinorPlanet.info* website. To compensate for the effect of the asteroid's ever-changing distance from the Sun and Earth on its visual magnitude, the following equation was used in vertically aligning the photometric data points from different nights in the construction of a composite lightcurve:

$$\Delta m = -2.5 \log_{10}((e_2^2/e_1^2)(r_2^2/r_1^2))$$

where Δm is the magnitude correction between night 1 and 2, e_1 and e_2 are the earth-asteroid distances on nights 1 and 2, r_1 and r_2 are the sun-asteroid distances on nights 1 and 2.

The asteroids were chosen from the photometry opportunity list that appears regularly in the *Minor Planet Bulletin* (Warner et al., 2017; Warner et al., 2018a; 2018b).

2746 Hissao was discovered on 1979 September 22 by N. Chernykh at the Crimean Astrophysical Observatory (JPL, 2018). It is located in the inner region of the main belt with a semi-major axis of 2.248 astronomical units and an eccentricity of 0.08424. This asteroid was observed at the George West ISD Mobile Observatory on the nights of 2018 March 20 and 21. A composite lightcurve with a period of 3.18 ± 0.01 hr best fits the available data. The lightcurve amplitude is 0.40 mag, and displays two maxima and two minima per rotational cycle.

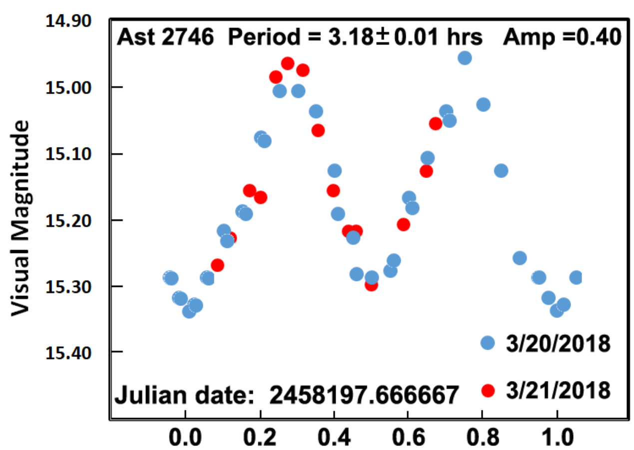

The two maxima appear to be of equal magnitude. However, the data suggests that one minimum is approximately 0.04 magnitudes fainter than the other. A search of the asteroid lightcurve database (LCDB; Warner et al., 2009) revealed that this asteroid did not have a published rotational period.

2884 Reddish was discovered on 1981 March 2 by S.J. Bus at Siding Spring Observatory, New South Wales, Australia (JPL, 2018). It is located near the middle of the main belt with a semi-major axis of 3.109 AU and an eccentricity of 0.1781. According to the LCDB, Reddish was observed during 2017 November by Owings, who reported a rotational period of 14.310 hr with an amplitude of 0.90 mag. This asteroid was observed at the George West ISD Mobile Observatory on the nights of 2017 November 23-25. On all three nights, which were exceptionally clear, the

Number	Name	20yy/mm/dd	Pts	Phase	L_{PAB}	B_{PAB}	Period(h)	P.E.	Amp	A.E.	Grp
2746	Hissao	18/03/20-03/21	46	1.4,2.0	177	0	3.18	0.01	0.40	0.02	FLOR
2884	Reddish	17/10/23-10/25	122	1.6,0.7	33	0	38.3	0.30	0.80	0.05	THM
3394	Banno	18/04/14-04/15	66	1.9,1.7	205	+2	7.34	0.01	0.21	0.02	FLOR

Table I. Observing circumstances and results. Pts is the number of data points. The phase angle is given for the first and last date. L_{PAB} and B_{PAB} are the approximate phase angle bisector longitude and latitude at mid-date range (see Harris *et al.*, 1984). Grp is the asteroid family/group (Warner *et al.*, 2009). FLOR: Flora; THM: Themis.

asteroid was observed for a minimum of seven hours and the same comparison and check stars were used. As the observing progressed, it became clear that the asteroid had a very large lightcurve amplitude and a long period. No single night of observation displayed both a maximum and minimum brightness event.

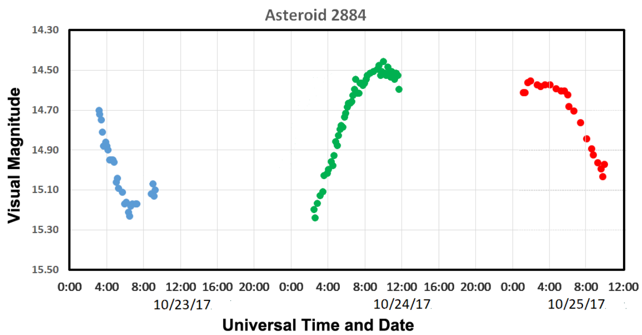

A rotational period of 38.30 ± 0.20 hr best fits the data. The asteroid's lightcurve is characterized by two maxima and two minima per rotational cycle.

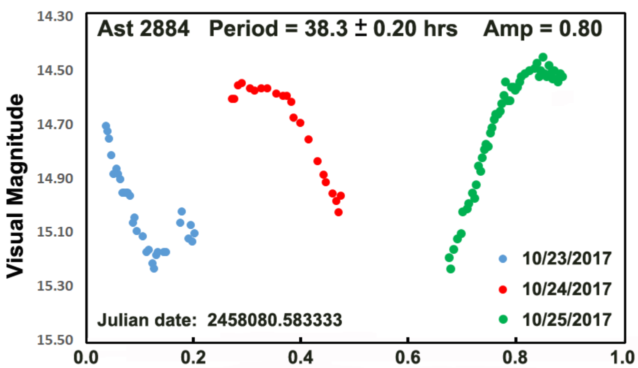

<u>3394 Banno</u> was discovered by S. Inoda and T. Urata on 1986 February 6 at Karasuyama, Japan, and was named in memory of the astronomer Yoshiaki Banno, one of Japan's pioneering amateur astronomers. The orbital eccentricity is more than 0.19 and the semi-major axis is 2.317 AU (JPL, 2018).

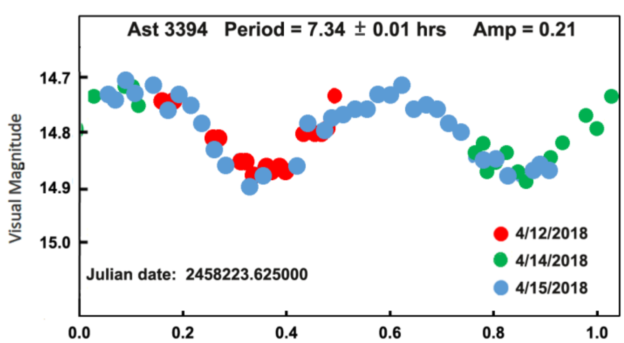

Banno was observed on 2018 April 12, 14, and 15. A rotational period of 7.34 ± 0.01 hr was determined. The lightcurve displays two maxima and minima per rotational cycle and amplitude of 0.21 mag. The LCDB showed that this asteroid was also observed by Marchini during 2018. He reported a rotational period of 7.324 hr with a lightcurve amplitude of 0.22 mag, which is in good agreement with our findings.

Acknowledgments

This research effort represents an effort to introduce high school level students to real astronomical research. Our thanks go to the McCarthey Dressman Educational Foundation and the George West Education Foundation for their continuing support.

References

Harris, A.W., Young, J.W., Scaltriti, F., Zappala, V. (1984). "Lightcurves and phase relations of the asteroids 82 Alkmene and 444 Gyptis." *Icarus* **57**, 251-258.

JPL (2018). Small Body Database Browser. *http://ssd.jpl.nasa.gov/sbdb.cgi*

Warner, B.D., Harris, A.W., Pravec, P. (2009). "The Asteroid Lightcurve Database." *Icarus* **202**, 134-146. Updated 2018 June. *http://www.minorplanet.info/lightcurvedatabase.html*

Warner, B., Harris, A.W., Durech, J., Benner, L.A.M. (2017). "Lightcurve Photometric Opportunities 2017 October-December." *Minor Planet Bull.* **44**, 355-361.

Warner, B., Harris, A.W., Durech, J., Benner, L.A.M. (2018a). "Lightcurve Photometric Opportunities 2018 January – March." *Minor Planet Bull.* **45**, 103–108.

Warner, B., Harris, A.W., Durech, J., Benner, L.A.M. (2018b). "Lightcurve Photometric Opportunities 2018 April-June." *Minor Planet Bull.* **45**, 208-213.

ROTATION PERIOD FOR 2326 TOLOLO

Stephen C. Percy
The Studios Observatory (Z52)
31 Ipswich Gardens, Grantham, NG31 8SE, U.K.
mail@opussoftware.co.uk

(Received: 2018 August 12)

CCD photometric observations of the main-belt asteroid 2326 Tololo performed by the author over seven nights from 2018 July 23 to 2018 August 10. The rotation period was found to be 9.488 ± 0.001 h with an amplitude of 0.33 ± 0.03 mag.

2326 Tololo (= 1931 RZ = 1936 SF = 1941 SF2 = 1965 QC = 1969 MB = 1973 GH1 = 1979 MB) is a main-belt asteroid discovered at Brooklyn on 1965 August 29 by the Indiana University. The asteroid was named to commemorate the founding of the Cerro Tololo Inter-American Observatory (CTIO) in northern Chile on 1962 November 23. CTIO is funded by the National Science Foundation and operated by AURA. The asteroid's name was proposed by F. K. Edmondson. [Ref: Minor Planet Circ. 9079].

CCD photometric observations were performed by the author over seven nights between 2018 July 23 and 2018 August 10. Over 30 hours of observation produced 1366 data points for analysis. The rotation period was found to be 9.488 ± 0.001 h with an amplitude of 0.33 ± 0.03 mag.

Previous Published Results

A search of the asteroid lightcurve database (LCDB, Warner *et al*, 2018) indicates no previous reported rotation period for this asteroid.

Equipment

All observations were performed at The Studios Observatory, Grantham, U.K. (Z52) using a Meade 14" (0.36 m) LX200 ACF OTA operating at f/7. The OTA was mounted on a Paramount MEII robotic mount and equipped with Moonlite CSL motorized focuser, Astro Physics AP CCDT67 focal reducer, and a QSI 683 cooled CCD camera (binned 2x2). An Astrodon Clear (UV blocking only) filter was used for all observations. The CCD is based on an 8.3 mp (3326x2504) Kodak KAF-8300 sensor with square 5.4 µm pixels. The image scale after 2x2 binning was 0.86 arcsecs/pixel.

Observations

TheSkyX Professional software by Software Bisque was used for all telescope, focuser, and camera control. This software was also later used to calibrate all science images using dark, dark-for-flat, and flat field frames. All flat field images were taken at the end of the observing sessions using a wall-mounted whiteboard illuminated by an A4-size electroluminescent (EL) panel. A recent library of dark and dark-for-flat frames was used in the calibration process, and no scaling of dark frames was necessary.

All data processing of the calibrated images and subsequent period analysis was performed using MPO Canopus (BDW Publishing 2018). Differential photometry measurements were performed using the Comp Star Selector (CSS) and Star-B-Gone procedures of MPO Canopus. The asteroid and five solar-like stars were used for all photometric comparisons. The KAF-8300 sensor has a peak spectral response in the green visual band so V band magnitudes and V-R colour indexes were used throughout the data processing. As the target declination remained below +20 deg (ranging from around -5 to -8 deg) the APASS catalog (Henden *et al*. 2009) was used for all plate solving (auto-match) and photometric reductions. The asteroid's magnitude ranged from 15.1 V to 14.7 V during the observing period.

Period analysis was performed using the Fourier analysis algorithm (FALC) of MPO Canopus developed by Alan Harris (Harris *et al.* 1989). All likely periods from 2 hours onwards were examined.

The observing schedule for this project and calibrated data are summarized in the sections and Table OS1 below. Table 1 provides an overview of the observed results. All new data are deposited in the ALCDEF database.

Number	Date 2018	Duration	Pts	Phase	L_{PAB}	B_{PAB}
2326	07/23	3 h 31	171	9.06	321.8	6.1
2326	07/31	4 h 44	165	6.19	321.8	5.7
2326	08/02	4 h 52	235	5.45	321.8	5.6
2326	08/04	2 h 48	115	4.73	321.8	5.5
2326	08/05	5 h 27	264	4.36	321.8	5.4
2326	08/06	3 h 09	137	4.02	321.8	5.3
2326	08/10	5 h 43	279	2.73	321.8	5.1

Table OSI. Observing Schedule for asteroid 2326 Tololo. Date is in month/day format. Pts is the number of data points. The phase angle is given for mid-session. L_{PAB} and B_{PAB} are the approximate phase angle bisector longitude and latitude at mid-session range (see Harris *et al.* 1984).

Fourier Analysis

The period spectrum for (2326) Tololo is shown below. All likely solutions from 2 hours onwards were examined. The Fourier analysis consistently indicated an optimum and most convincing rotation period of 9.488 h.

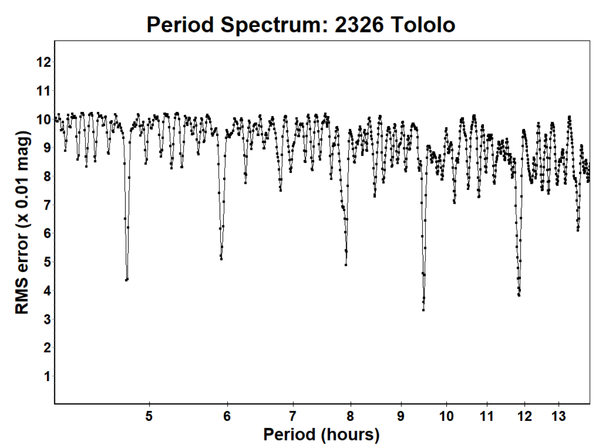

The final phased plot for 2326 Tololo showing the matched 9.488 h rotation period with amplitude 0.33 is shown below.

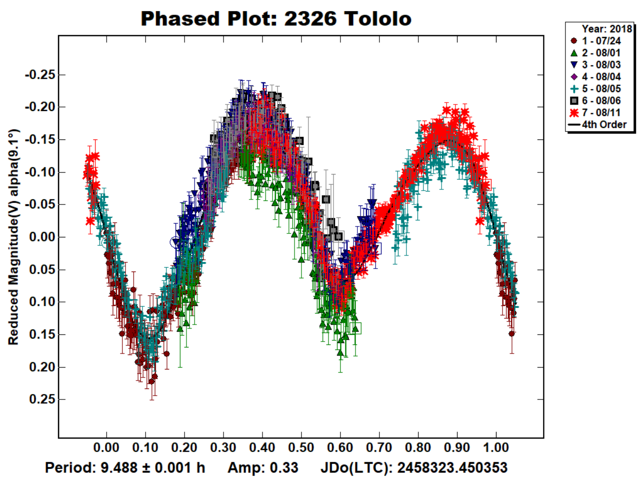

Acknowledgements

This research has made use of data and services provided by the International Astronomical Union's Minor Planet Center.

https://www.minorplanetcenter.net/iau/mpc.html

This research was made possible in part based on data from the MPCOSC3-2MASS catalog (a product of the Two Micron All Sky Survey), UCAC4 (the fourth U.S. Naval Observatory CCD Astrograph Catalog), and the AAVSO Photometric All-Sky Survey (APASS), funded by the Robert Martin Ayers Sciences Fund. The author would like to express his gratitude to Brian D. Warner for his MPO Canopus software and support, along with the 2nd edition of his book 'A Practical Guide to Lightcurve Photometry and Analysis'. Both have been invaluable in this research.

References

Minor Planet Circulars (MPCs) are published by the International Astronomical Union's Minor Planet Center. Minor Planet Circular 9079 is available from the Minor Planet Centre MPC/MPO/MPS Archive. *https://www.minorplanetcenter.net/iau/ECS/MPCArchive/MPCArchive_TBL.html*

Henden, A.A., Terrell, D., Levine, S.E., Templeton, M., Smith,T.C., Welch, D.L. (2009). "The AAVSO Photometric All-Sky Survey (APASS)." *http://www.aavso.org/apass*

Harris, A.W., Young, J.W., Scaltriti, F., Zappala, V. (1984). "Lightcurves and phase relations of the asteroids 82 Alkmene and 444 Gyptis." Icarus 57, 251-258.

Harris, A.W., Young, J.W., Bowel, E., Martin, L.J., Millis, R.L., Poutanen, M., Scaltriti, F., Zappala, V., Schober, H.J., Debehogne, H., Zeigler, K.W. (1989). "Photoelectric observations of asteroids 3, 24, 60, 261, and 863. Icarus 77, 171-186.

Software Bisque TheSkyX Professional software website. *http://www.bisque.com/sc/pages/TheSkyX-Professional-Edition.aspx*

Warner, B.D. (2006). "A Practical Guide to Lightcurve Photometry and Analysis (2nd edition)." Springer, New York.

Warner, B.D., Harris, A.W., Pravec, P. (2009). "The Asteroid Lightcurve Database." *Icarus* **202**, 134-146. Updated 2016 Sep. *http://www.minorplanet.info/lightcurvedatabase.html*

Warner, B.D. (2018). Asteroid Lightcurve Photometry Database (ALCDEF) website. *http://www.minorplanet.info/alcdef.html*

Warner, B.D. (2018). Collaborative Asteroid Lightcurve Link website. *http://www.minorplanet.info/call.html*

Warner, B.D. (2018). MPO Software, MPO Canopus v10.7.11.3. BDW Publishing *http://www.minorplanetobserver.com/MPOSoftware/MPOCanopus.htm*

Number	Name	2018 mm/dd	Pts	Phase	L_{PAB}	B_{PAB}	Period(h)	P.E.	Amp	A.E.	Grp
2326	Tololo	07/23-08/10	1366	9.1,2.7	321.8	5.6	9.488	0.001	0.33	0.03	MB-O

Table I. Observing circumstances and results. Pts is the number of data points. The phase angle is given for the first and last date. L_{PAB} and B_{PAB} are the approximate phase angle bisector longitude and latitude at mid-date range (see Harris *et al.*, 1984). Grp is the asteroid family/group (Warner *et al.*, 2009).

PHOTOMETRIC OBSERVATIONS FOR 8 MAIN-BELT ASTEROIDS: 2017 APRIL - MAY

Michael Fauerbach
Florida Gulf Coast University
10501 FGCU Blvd.
Ft. Myers, FL33965-6565
mfauerba@fgcu.edu

(Received: 2018 September 21)

Photometric observations of 8 main-belt asteroids from 2017 April and 2017 May, using the three telescopes of the SARA consortium are reported. Rotational periods for 1549 Mikko, 1939 Loretta, 5405 Neverland, 8419 Terumikazumi, 11099 Sonodamasaki, 13679 Shinanogawa, 17938 Tamsendrew, (27395) 2000 EX94 were obtained.

The three remote telescopes of the Southeastern Association for Research in Astronomy (SARA) consortium were used in the 2017 April and May timeframe to observe 8 main-belt asteroids. SARA operates a 0.9-m telescope at Kitt Peak National Observatory (KPNO), the 1-m Jacobus Kapteyn Telescope at Roque de los Muchachos Observatory (ORM) on the island of La Palma, and a 0.6-m telescope located at Cerro Tololo Inter-American Observatory (CTIO) in Chile. A detailed description of the instrumentation and setup can be found in the paper by Keel et al. (2017). As this was the first time the author utilized any of the telescopes, the operation was not as efficient as it could have been and several of the targets reported on here would have benefitted from additional data. The data was calibrated using MaximDL and photometric analysis was performed using MPO Canopus (Warner, 2017). Utilizing the asteroid lightcurve database (LCDB; Warner et al., 2009a) we searched for asteroids that had a high uncertainty in their rotational periods associated with previous observations.

Location	Date (2017)
CTIO	4-5, 4-26, 5-29
KPNO	4-26, 4-27, 4-29, 4-30, 5-21, 5-31
ORM	4-7, 4-20, 4-25, 5-26, 5-27, 5-29

Table I. observing locations for the different nights presented in the figures.

1549 Mikko. This member of the Florina family of asteroid was observed over a period of four nights from 2017 April 26 to 2017 May 21. All observations were performed with the 0.9-m telescope at KPNO. The only prior period determination is by Behrend (2007). The derived period of 11.49 ± 0.1 h with a small amplitude of only 0.03 mag was based on a partial lightcurve with large error bars on the data points and was therefore rated U = 1+. The current analysis yields a best fit rotational period of 13.74 ± 0.02 h with an amplitude of 0.10 mag. Unfortunately, there is a lot of scatter in the data and with a period close to 12 h the data only covers part of the lightcurve. A look at the period spectrum shows that two distinct groups of solutions are favored. One clustered around 13.73 h and the other clustered around 8.74 h. As can be seen the lightcurve with a period of 8.74 ± 0.01 h fits the data almost equally well and even provides better coverage of (almost) the entire lightcurve. Harris et al. (2014), showed that low amplitude lightcurves can be of almost any modality and hence the usual assumption of a (preferred) bimodal lightcurve is not necessarily valid. Accordingly, an attempt was made to fit the data with more complex curves, but this led to very similar results without any real improvements. Consequently, the simpler bimodal curves presented here are preferred. Additional observations are required to rule out the ambiguity in the data. For now, it is assumed that the best fit for the 13.74 h lightcurve is the correct period.

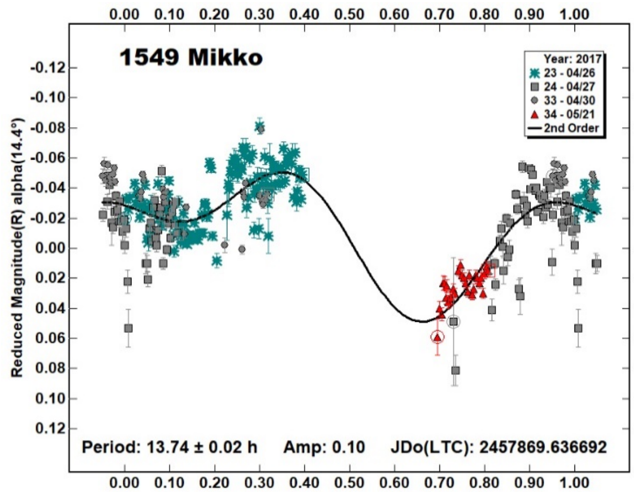

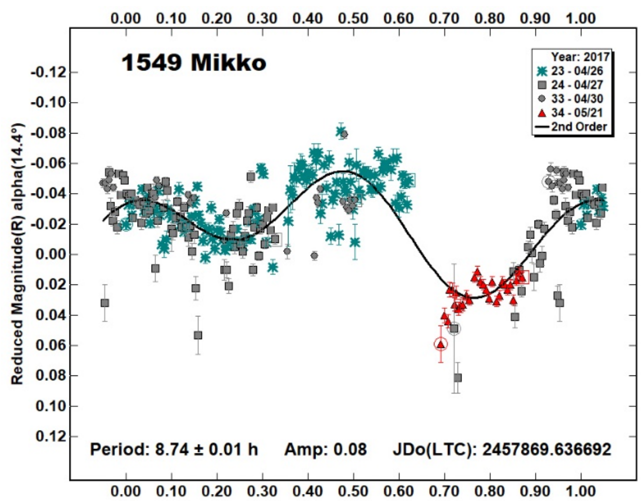

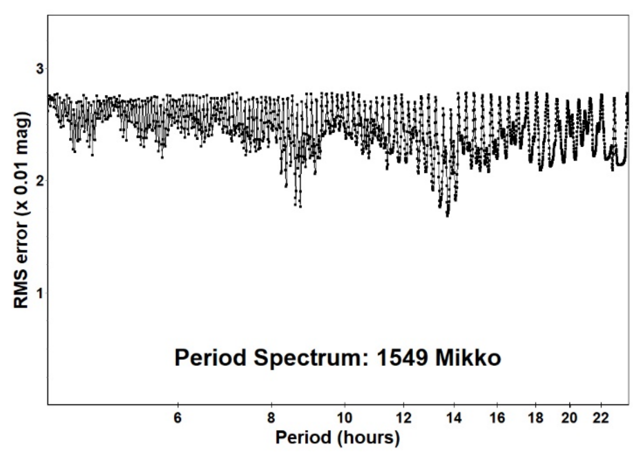

1939 Loretta. This asteroid is a member of the Themis family of asteroids. The only previous period determination is by Behrend (2011) who found a possible period of ~25 h, based on a partial lightcurve and was therefore rated U = 1. The asteroid was observed on 6 nights over a ten-day period. A look at the period spectrum shows that there are two distinct solutions - one with a period of 11.94 h and one with twice that value. We report a mono-modal solution with a period of 11.94 ± 0.01 h and a bimodal solution with a period of 23.88 ± 0.02 h and an amplitude of 0.20 mag. With a period so close two 12/24 h the data only covers a partial lightcurve and additional observations will be needed to ultimately decide which period is correct. For this paper it is assumed that the bimodal solution with a period of 23.88 ± 0.02 h is the preferred solution.

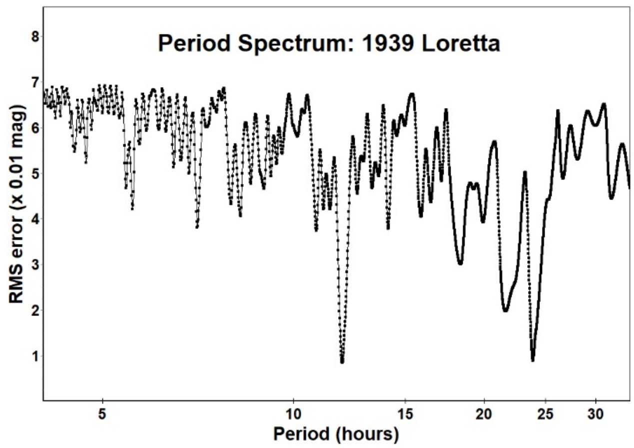

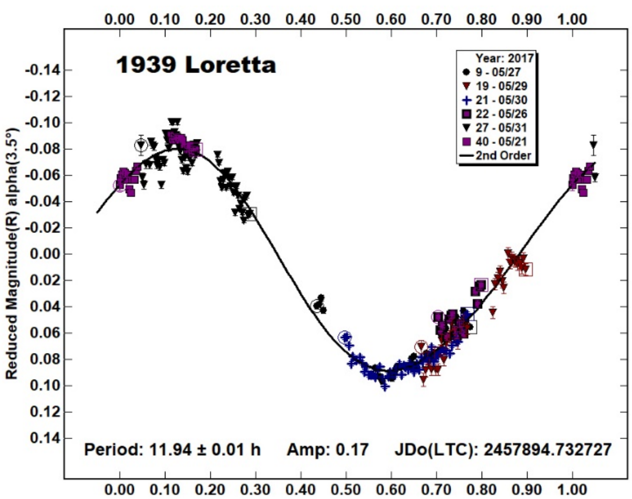

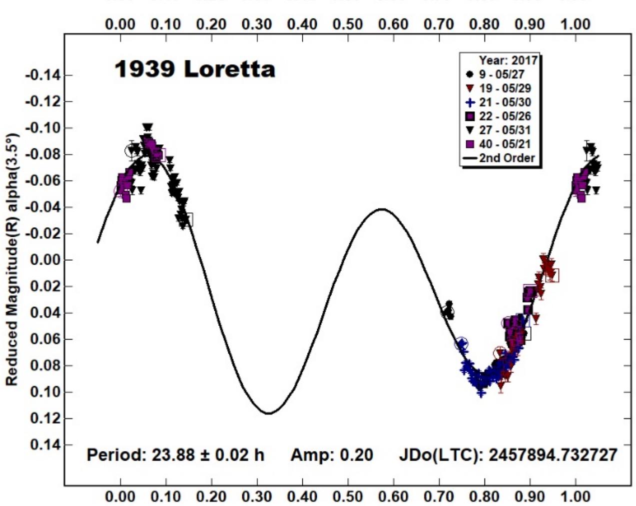

5405 Neverland. By the time of the observations presented here, there was only one prior period determinations for 5405 Neverland. Waszczak et al. (2015) reported a period of 3.181 ± 0.0012 h with an amplitude of 0.20 mag, Unbeknownst to the author, a couple of other observers also worked the asteroid during April 2017. Behrend (2017) reports a period of 7.1414 ± 0.0002 h based on a solution with four maxima per period. Mas et al. (2018) report a period of 3.149 ± 0.025 h based on a bimodal curve obtained over two successive nights. The current data is based on observations over a period of four nights from 2017 April 5 to 2017 April 29. Our result of 3.181 ± 0.001 h is in excellent agreement with Waszczak et al. (2015). The present data cannot reproduce the results by Behrend (2017). The result by Mas et al. (2018) is closer to the one reported here and therefore validates a closer look. For an asteroid with a relatively short period like 5405 Neverland even small differences in the determined period will add to large phase difference in the lightcurve when measured over several nights. The data by Mas et al. (2018) was taken on two consecutive nights. The observations reported here cover a period of over three weeks, and therefore even relatively small differences in the period will add up to big changes. We display our data below phased to the period of 3.149 h determined by Mas et al. (2018). As can be seen over the many rotations the asteroid made during this time frame the observations are out of phase, and therefore we cannot fit the current data to this period.

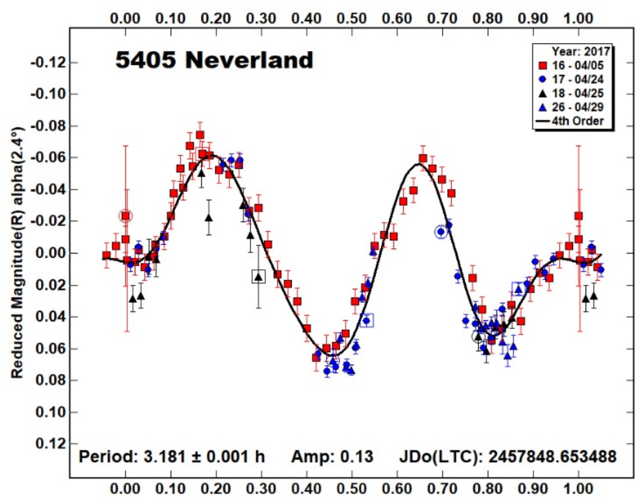

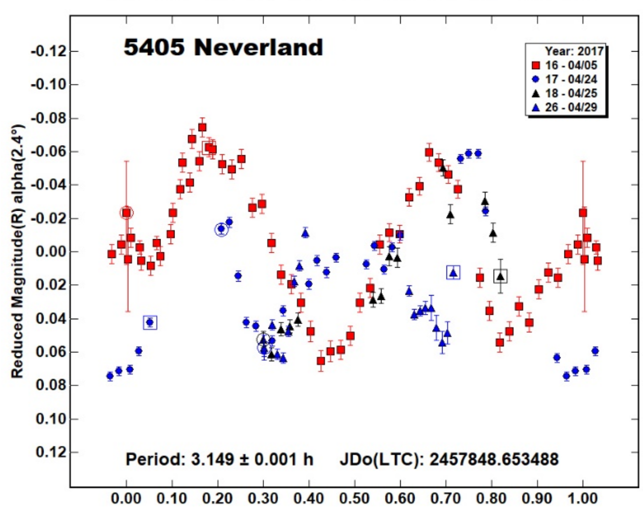

Number	Name	2017 mm/dd	Pts	Phase	L_{PAB}	B_{PAB}	Period(h)	P.E.	Amp	A.E.	Grp
1549	Mikko	04/26-05/21	272	14.4,22.0	191.1	6.5	13.74	0.02	0.10	0.02	FLOR
1939	Loretta	05/21-05/31	230	1.3,5.5	237.0	-0.3	23.88	0.02	0.20	0.02	THM
5405	Neverland	04/05-04/29	112	2.3,14.4	191.3	-0.1	3.181	0.001	0.13	0.02	MB-M
8419	Terumikazumi	04/28-05/26	125	6.7,8.9	228.7	8.7	4.49	0.01	0.21	0.02	MB-O
11099	Sonodamasaki	04/07-04/26	118	12.2,3.3	219.5	4.4	7.251	0.001	0.37	0.02	MB-I
13679	Shinanogawa	04/20-05/27	150	12.4,13.3	226.7	19.1	2.806	0.001	0.17	0.02	EUN
17938	Tamsendrew	04/07-04/25	69	3.8,14.2	192.7	-1.2	2.642	0.001	0.17	0.02	MB-I
(27395)	2000 EX94	04/29,04/30	55	14.7,15.0	191.8	-11.2	3.45	0.01	0.27	0.02	EUN

Table II. Observing circumstances and results. Pts is the number of data points. The phase angle is given for the first and last date. L_{PAB} and B_{PAB} are the approximate phase angle bisector longitude and latitude at mid-date range (see Harris *et al.*, 1984). Grp is the asteroid family/group (Warner *et al.*, 2009).

8419 Terumikazumi. The only previous period determination is by Behrend (2006) who found a possible period of 4.6 ± 0.1 h. It is listed as such in the LCDB, however, a look at Behrend's website reveals the comment: "Low amplitude, large error bars; period is meaningless." We observed the asteroid over a period of three nights and report a best fit to our data of 4.49 ± 0.01 h with an amplitude of 0.21 mag. This is in reasonable agreement with the result by Behrend. However, Like Behrend's data the current data shows large scatter and additional observations in the future will be needed to further refine the period.

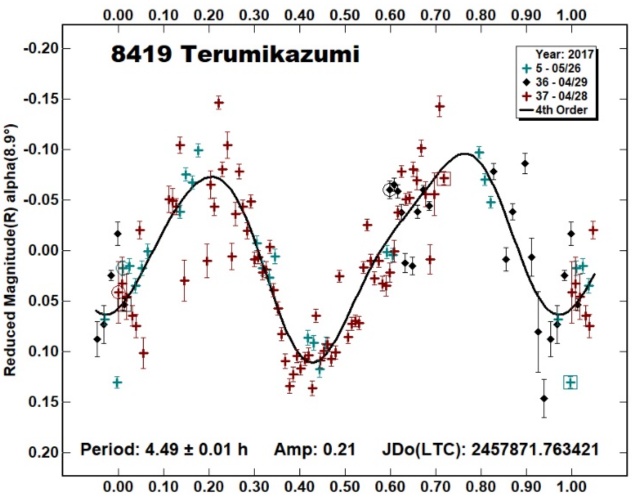

11099 Sonodamasaki. The asteroid was observed on five nights from 2017 April 7 to 2017 April 26. The asteroid was rated U = 1 based on one reported period by Waszczak et al. (2015) of 7.248 ± 0.0040 h with a small amplitude of 0.09 mag. Meanwhile Nugent et al. (2015, 2016) - using NEOWISE data -reported larger amplitudes of 0.16 mag and 0.61 mag respectively. We obtained a rotational period of 7.251 ± 0.001 h with an amplitude of 0.37 mag. This is in good agreement with the previously reported period. It should be noted, that as the lightcurve is very symmetrical a monomodal curve with half the period cannot be dismissed. A look at the split-halves plot indicates just how symmetric the lightcurve is.

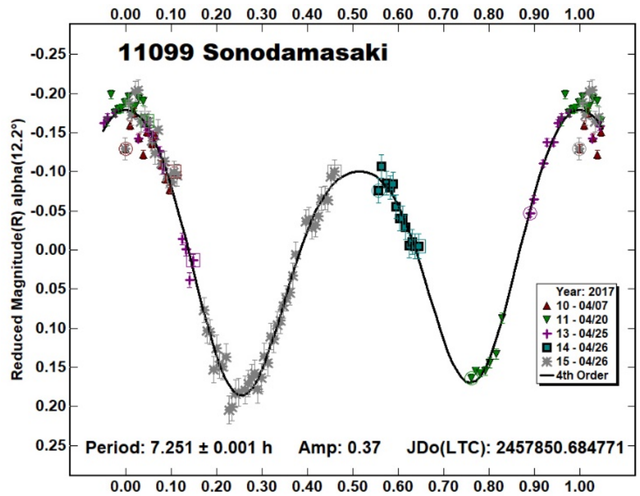

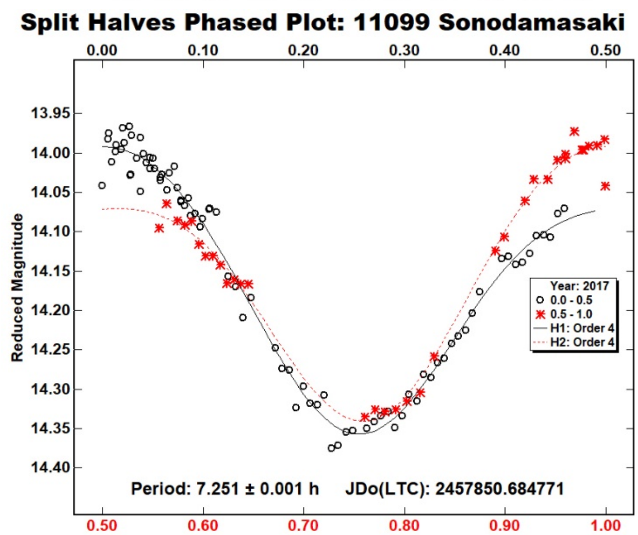

13679 Shinanogawa. This member of the Eunomia family of asteroids was observed for six nights from 2017 April 20 to 2017 May 27. Kim et al. (2014) report a period of larger than 8 h. The current data gives a rotational period of 2.806 ± 001 h with an amplitude of 0.17 mag. The solution is unique and should therefore be adopted.

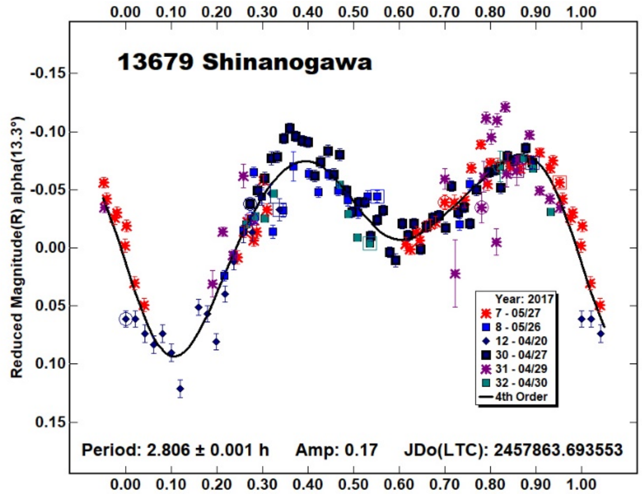

17938 Tamsendrew. Pravec et al. (2012) report a period of 2.53 h with a magnitude of 0.17 mag. The best fit to the data presented here is 2.642 ± 001 h with an amplitude of 0.17 mag. A look at the period spectrum clearly indicates that a group of possible solutions around 2.6 h exists, each with similar good fits to the data. Additional data is required to conclusively decide on the period.

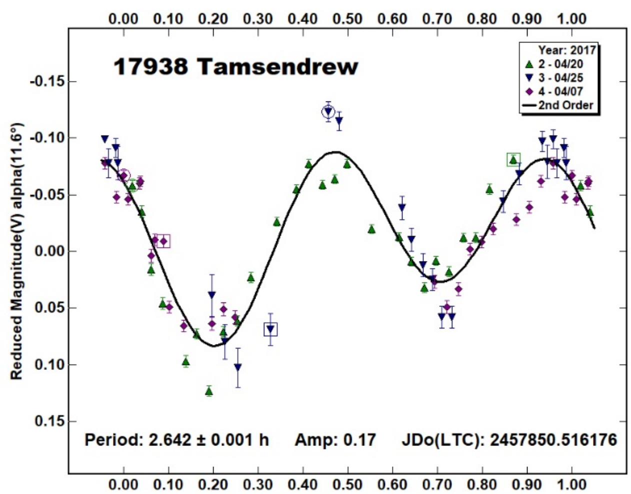

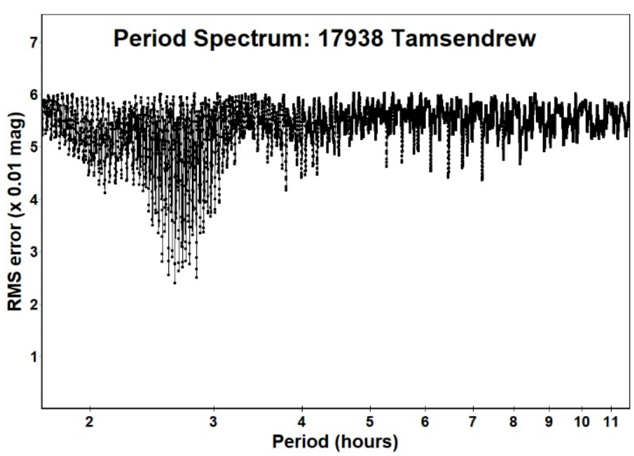

(27395) 2000 EX94. This member of the Eunomia family of asteroids was unfortunately only observed for two nights. As can be seen by the lightcurve below additional nights would have been beneficial for determining the rotational period. Waszczak et al. (2015) reported a period of 3.714 ± 0.0006 h with an amplitude of 0.24 mag, based on sparse data. The best fit to the current data shows a slightly shorter period of 3.45 ± 0.01 h with an amplitude of 0.27 mag.

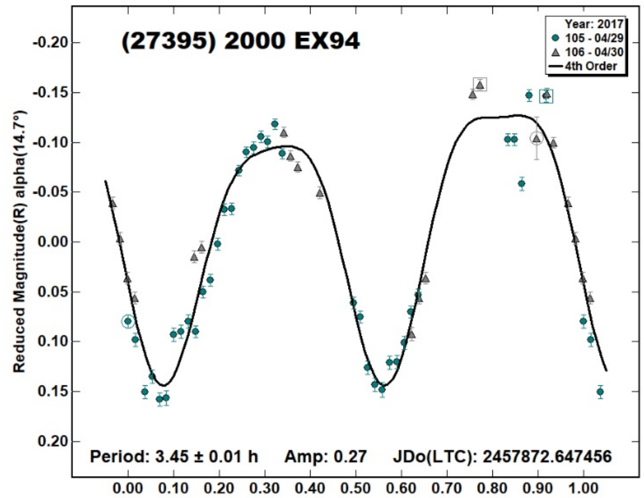

References

Behrend, R. (2006, 2007, 2011, 2017). Observatoire de Geneve web site. *http://obswww.unige.ch/~behrend/page_cou.html*

Harris, A.W., Young, J.W., Scaltriti, F., Zappala, V. (1984). "Lightcurves and phase relations of the asteroids 82 Alkmene and 444 Gyptis." *Icarus* **57**, 251-258.

Harris, A.W., Pravec, P., Galad, A., Skiff, B.A., Warner, B.D., Vilagi, J., Gajdos, S., Carbognani, A., Hornoch, K., Kusnirak, P., Cooney, W.R., Gross, J., Terrell, D., Higgins, D., Bowell, E., Koehn, B.W. (2014). "On the maximum amplitude of harmonics on an asteroid lightcurve." *Icarus* **235**, 55-59.

Keel, W.C., Oswalt, T., Mack, P., Henson, G., Hillwig, T., Batcheldor, D., Berrington, R., De Pree, C., Hartmann, D., Leake, M., Licandro, J., Murphy, B., Webb, J., Wood, M.A. (2017). "The Remote Observatories of the Southeastern Association for Research in Astronomy (SARA)." Publications of the Astronomical Society of the Pacific, 129:015002 (12pp). *http://iopscience.iop.org/article/10.1088/1538-3873/129/971/015002/pdf*

Kim, M.-J., Choi, Y.-J., Moon, H.-K., Byun, Y.-I., Brosch, N., Kaplan, M., Kaynar, S., Uysal, Ö., Güzel, E., Behrend, R., Yoon, J.-N., Mottola, S., Hellmich, S., Hinse, T.C., Eker, Z., Park, J.-H. (2014). "Rotational Properties of the Maria Asteroid Family." *The Astronomical Journal*, Volume 147, Issue 3, article id. 56, 15 pp.

Mas, V., Fornas, G., Lozano, J., Rodrigo, O., Fornas, A., Carreño, A., Arce, E., Brines, P., Herrero, D. (2018). "Twenty-one Asteroid Lightcurves at Asteroids Observers (OBAS) - MPPD: Nov 2016 - May 2017." *The Minor Planet Bulletin*, Vol. 45, No. 1, pp. 76-82.

Nugent, C. R., Mainzer, A., Masiero, J., Bauer, J., Cutri, R.M., Grav, T., Kramer, E., Sonnett, S., Stevenson, R., Wright, E.L. (2015). "NEOWISE Reactivation Mission Year One: Preliminary Asteroid Diameters and Albedos." *The Astrophysical Journal*, Volume 814, Issue 2, article id. 117, 13 pp.

Nugent, C.R., Mainzer, A., Bauer, J., Cutri, R.M., Kramer, E.A., Grav, T., Masiero, J., Sonnett, S., Wright, E.L. (2016). "NEOWISE Reactivation Mission Year Two: Asteroid Diameters and Albedos." *The Astronomical Journal*, Volume 152, Issue 3, article id. 63, 12 pp.

Pravec, P., Wolf, M., Sarounova, L. (2012). *http://www.asu.cas.cz/~ppravec/neo.htm*

Warner, B.D., Harris, A.W., Pravec, P. (2009). "The Asteroid Lightcurve Database." *Icarus* **202**, 134-146. Updated 2018 Jun. *http://www.minorplanet.info/lightcurvedatabase.html*

Warner, B.D. (2017). MPO Canopus software version 10.7.10.0. *http://www.bdwpublishing.com*

Waszczak, A., Chang, C.-K., Ofek, E.O., Laher, R., Masci, F., Levitan, D., Surace, J., Cheng, Y.-C., Ip, W.-H., Kinoshita, D., Helou, G., Prince, T.A., Kulkarni, S. (2015). "Asteroid Light Curves from the Palomar Transient Factory Survey: Rotation Periods and Phase Functions from Sparse Photometry." *The Astronomical Journal*, Volume 150, Issue 3, article id. 75, 35 pp.

ROTATIONAL PERIOD DETERMINATION FOR ASTEROIDS 2498 TSESEVICH, (16024) 1999 CT101, (46304) 2001 OZ62

Michael Fauerbach
Austin Brown
Florida Gulf Coast University
10501 FGCU Blvd.
Ft. Myers, FL33965-6565
mfauerba@fgcu.edu

(Received: 2018 August 13)

Photometric observations of 3 main-belt asteroids were obtained during three nights from 2017 September 26 to 2017 October 07, using the Jacobus Kapteyn Telescope at the Observatorio del Roque de los Muchachos.

We report on the results of photometric observations obtained with the Southeastern Association for Research in Astronomy (SARA) consortium 1m Jacobus Kapteyn Telescope at the Observatorio del Roque de los Muchachos on the Spanish island of La Palma. The telescope is coupled with an Andor iKon-L series CCD. The data was calibrated using MaximDL and photometric analysis was performed using MPO Canopus (Warner, 2017). Utilizing the asteroid lightcurve database (LCDB; Warner et al., 2009a) we searched for asteroids that had a high uncertainty in their rotational periods associated with previous observations. All three selected asteroids had only one prior publication of their period, and all three results were based on sparse data. As our observations were made on either side of the Full Moon, we also had to take the placement of the asteroids with respect to the Moon into account.

<u>2498 Tsesevich.</u> We observed 2498 Tsesevich for approximately six hours. We derived a rotational period of 2.864 ± 0.019 h with an amplitude of 0.18 mag. Thus, we covered 2 full rotations of the asteroid during a single night, which gives us strong confidence in our result. The only previously reported rotational period is by Waszczak et al. (2015) based on a fit to sparse data. They reported a period of 3.059 ± 0.0038 h with an amplitude of 0.15 mag.

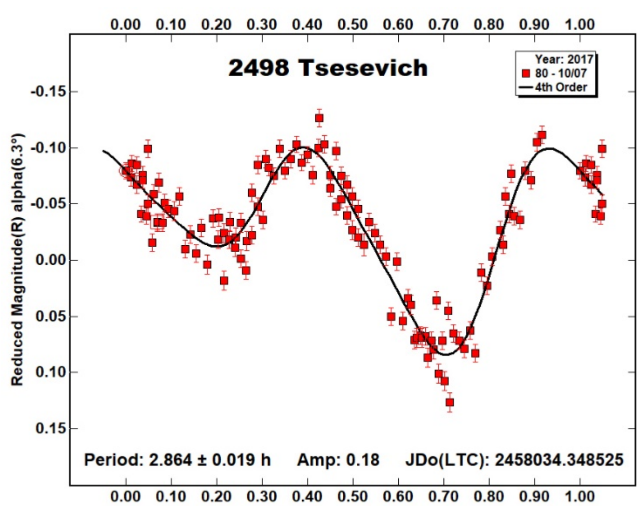

<u>(16024) 1999 CT101.</u> This is a member of the Eunomia family. We observed (16024) 1999 CT101 for approximately 4 h. Only one prior measurement, based on a fit to sparse data, of the rotational period exists. Waszczak et al. (2015) report a period of

Number	Name	2017 mm/dd	Pts	Phase	L_{PAB}	B_{PAB}	Period(h)	P.E.	Amp	A.E.	Grp
2498	Tsesevich	10/07	112	6.5	359.7	0.8	2.864	0.019	0.18	0.02	MB-O
(16024)	1999 CT101	10/07	64	4.5	5.7	0.4	2.786	0.027	0.17	0.02	EUN
(46304)	2001 OZ62	09/26,09/30	135	7.6,5.2	15.0	0.8	2.73	0.01	0.09	0.02	MB-I

Table I. Observing circumstances and results. Pts is the number of data points. The phase angle is given for the first and last date. L_{PAB} and B_{PAB} are the approximate phase angle bisector longitude and latitude at mid-date range (see Harris *et al.*, 1984). Grp is the asteroid family/group (Warner *et al.*, 2009).

2.804 ± 0.0008 h. We obtained a rotational period of 2.786 ± 0.027 h with an amplitude of 0.17 mag in good agreement with the previous measurement.

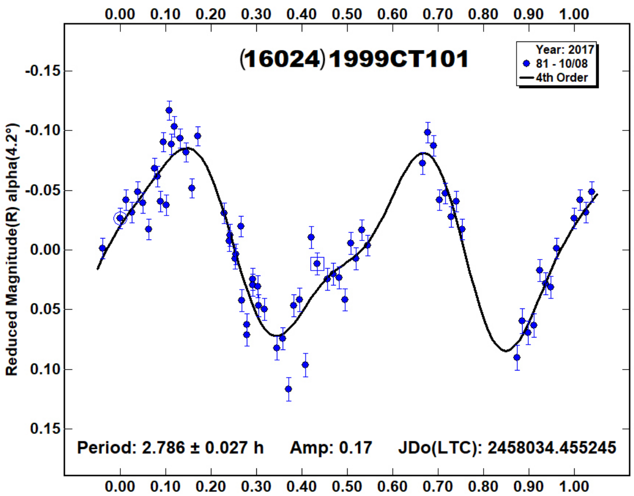

(46304) 2001 OZ62. We observed (46304) 2001 OZ62 on two nights. Unfortunately, the almost Full Moon and intermittent clouds provided less than ideal observing conditions as can be seen in the scatter of our data. We derived a rotational period of 2.73 ± 0.01 h with an amplitude of 0.09 mag. The only previously reported rotational period is by Waszczak et al. (2015) based on a fit to sparse data. They reported a period of 2.655 ± 0.0006 h with an amplitude of 0.10 mag. Their result is in fair agreement with our result.

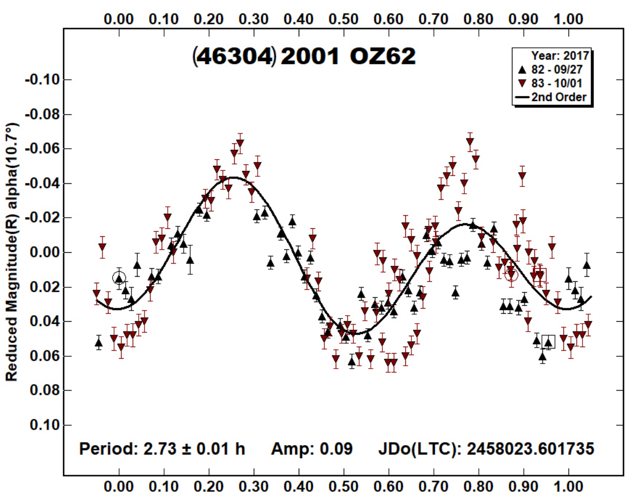

Acknowledgements

One of the authors (A.B.) would like to acknowledge support from the NASA/Florida Space Grant Consortium Summer Research Scholarship program.

References

Harris, A.W., Young, J.W., Scaltriti, F., Zappala, V. (1984). "Lightcurves and phase relations of the asteroids 82 Alkmene and 444 Gyptis." *Icarus* **57**, 251-258.

Warner, B.D., Harris, A.W., Pravec, P. (2009). "The Asteroid Lightcurve Database." *Icarus* **202**, 134-146. Updated 2017 Nov. *http://www.minorplanet.info/lightcurvedatabase.html*

Warner, B.D. (2017). MPO Canopus software version 10.7.10.0. http://www.bdwpublishing.com

Waszczak, A., Chang, C.-K., Ofek, E. O., Laher, R., Masci, F., Levitan, D., Surace, J., Cheng, Y.-C., Ip, W.-H., Kinoshita, D., Helou, G., Prince, T. A., Kulkarni, S. (2015). "Asteroid Light Curves from the Palomar Transient Factory Survey: Rotation Periods and Phase Functions from Sparse Photometry," The Astronomical Journal, Volume 150, Issue 3, article id. 75, 35 pp.

PHOTOMETRIC OBSERVATIONS OF 1007 PAWLOWIA, 1774 KULIKOV, 2764 MOELLER, 5110 BELGIRATE, (8505) 1990 YK, AND (34459) 2000 SC91

Michael Fauerbach
Kaitlyn M. Nelson
Florida Gulf Coast University
10501 FGCU Blvd.
Ft. Myers, FL33965-6565
mfauerba@fgcu.edu

(Received: 2018 September 7)

Photometric observations of 6 main-belt asteroids were obtained during five nights from 2018 January 10 to 2018 January 20, with the Jacobus Kapteyn Telescope at the Observatorio del Roque de los Muchachos, Spain.

We report on the results of photometric observations obtained with the Southeastern Association for Research in Astronomy (SARA) consortium 1m Jacobus Kapteyn Telescope at the Observatorio del Roque de los Muchachos on the Spanish island of La Palma. The telescope is coupled with an Andor iKon-L series CCD. The data was calibrated using MaximDL and photometric analysis was performed using MPO Canopus (Warner, 2017). Utilizing the asteroid lightcurve database (LCDB; Warner et al., 2009a) we searched for target asteroids that had a high uncertainty in their rotational periods. We observed for five nights from 2018 January 10 to 2018 January 20. Two additional nights scheduled for early February 2018 unfortunately were cancelled as the entire mountain was closed due to ice and snow.

1007 Pawlowia. The only previous period determination by Clark (2006) gave a value of ~8.23 h. This was based on noisy data with a low amplitude (0.02 mag) and was therefore rated U = 1. Meanwhile Nugent et al. (2015, 2016) - using NEOWISE data - reported large amplitudes of 0.35 mag and 0.49 mag respectively. We observed 1007 Pawlowia for about 7 h on our first night. Analyzing the data, we realized that it showed a continuous downward slope indicating a very long period. Therefore, we made 1007 Pawlowia the focus of our observation campaign and observed it every night. We determine a rotation period of 60.64 ± 0.04 h with a magnitude of 0.51 mag. The two additional nights scheduled for early February would have been very useful in filling in our partial lightcurve and in refining the period. Unfortunately, the weather did not cooperate.

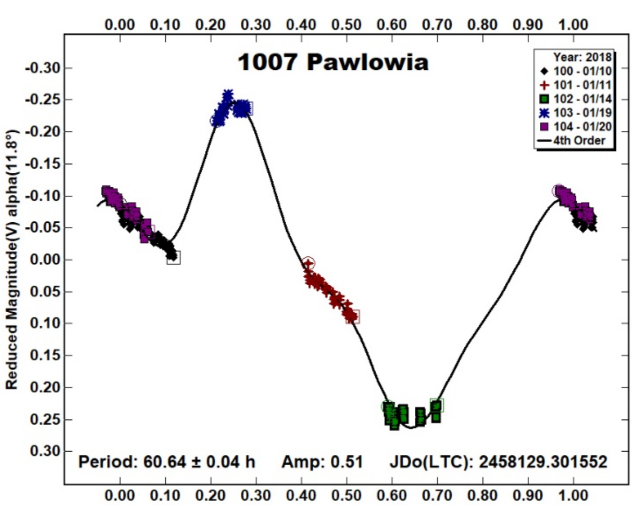

1774 Kulikov. A member of the Koronis family. We observed 1774 Kulikov for two nights for approximately 6 h and 5 h respectively, covering more than one rotational period during each night. We determined a rotational period of 3.832 ± 0.001 h with an amplitude of 0.38 mag. This is in excellent agreement with the result reported by Ďurech (2016) of 3.830791 ± 0.000001 h. It would be interesting to see, if our dense lightcurve could provide an enhancement to the shape model by Ďurech (2016) based on sparse data.

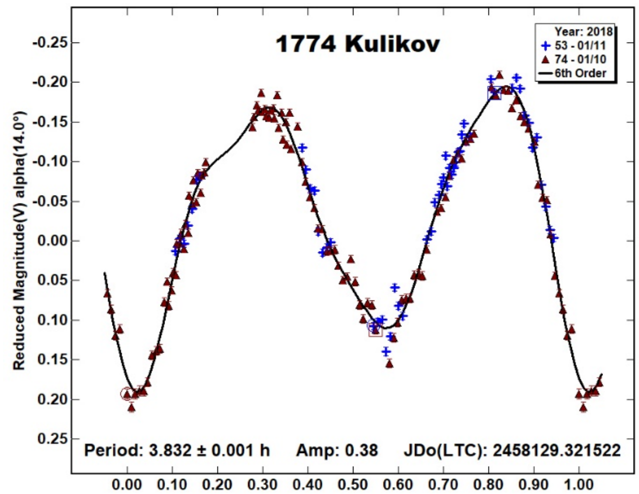

2764 Moeller. A member of the Flora family of asteroids. We observed 2764 Moeller for two nights for approximately 3 h and 7 h. We derived a rotational period of 5.952 ± 0.003 h in excellent agreement with the prior results by Waszczak (2015, 5.954 h) and Pravec (2018, 5.953 h).

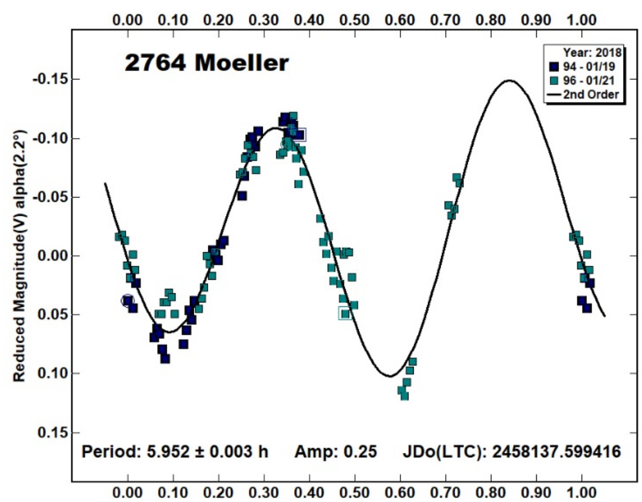

5110 Belgirate. We chose to observe 5110 Belgirate, as it had three prior period determinations with vastly different results. Behrend (2006) reported a period of 11.04 h with an amplitude of 0.08 mag. Waszczak (2015) reported a period of 4.123 ± 0.0013 h with an amplitude of 0.05 mag. The adopted value for the rotational period of 8.26 ± 0.02 h with an amplitude of 0.12 mag was derived by Hayes-Gehrke et al. (2014). We observed 5110 Belgirate over two nights. The best fit to our data gives a rotational period of 7.57 ± 0.02 h with an amplitude of 0.08 mag. Unfortunately, a look at the period/frequency spectrum quickly reveals that numerous other solutions provide similar good fits to our rather noisy data. As can be seen from the period plot a solution with a period of 8.20 ± 0.02 h - in better agreement with the currently accepted value - is also possible and has only a slightly worse fit. According to Harris et al. (2014), low amplitude lightcurves can be of almost any modality and therefore the usual assumption of a (preferred) bimodal lightcurve is not necessarily valid. Assuming more complex curves - higher order Fourier fits - leads to a better fit to the data, but still does not provide a clearly defined solution. We display a fourth order fit to our data below, and the inset shows the frequency spectrum for this fit. Out of the two solutions presented here, we prefer the more complex one with a period of 7.02 ± 0.01 h and an amplitude of 0.11 mag. This is not in agreement with any of the previous publications and as can be seen in the frequency plots our confidence in the result is not very high. More data on this asteroid is clearly needed to further define the period of 5110 Belgirate.

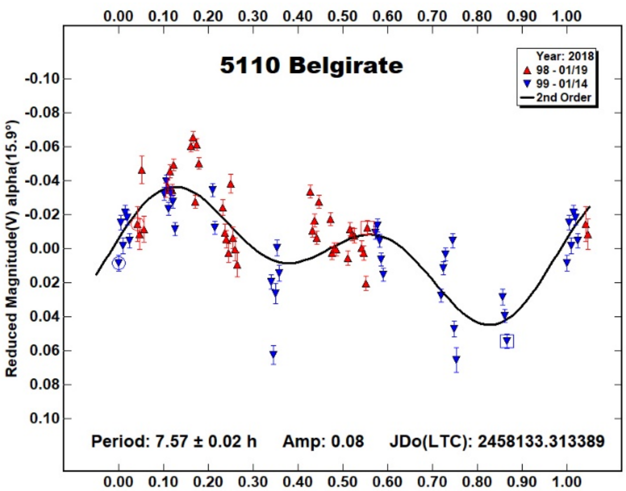

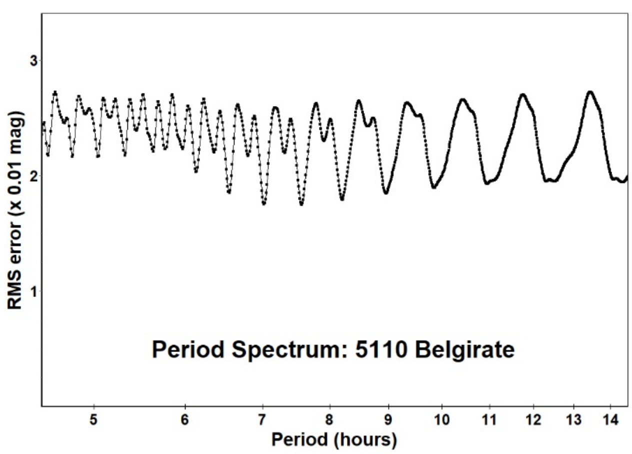

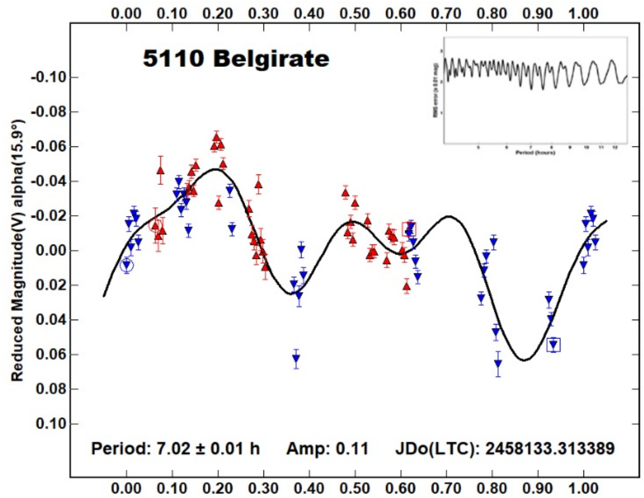

(8505) 1990 YK. A member of the Flora family of asteroids. We observed (8505) 1990 YK on three nights. Only one prior measurement of the rotational period exists. Waszczak (2015) report a period of 3.133 ± 0.0014 h based on sparse data. Forcing our data to fit a bimodal lightcurve, we obtained a rotational period of 3.133 ± 0.001 h with an amplitude of 0.06 mag. This seems to be in perfect agreement with the prior publication. However as can be seen, the fit is not very convincing. Harris et al. (2014) pointed out that for lightcurves with low amplitudes more complex curves with multiple extrema cannot be excluded. Indeed, a solution with four extrema fits our data very well. We therefore propose a period of 7.004 ± 0.002 h with an amplitude of 0.09 mag.

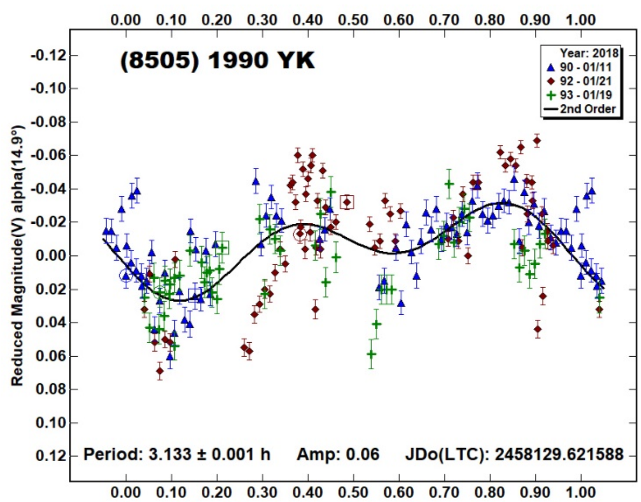

Number	Name	2018 mm/dd	Pts	Phase	L_{PAB}	B_{PAB}	Period(h)	P.E.	Amp	A.E.	Grp
1007	Pawlowia	01/10-01/20	253	11.8,15.2	83.6	1.9	60.64	0.04	0.51	0.04	MB-O
1774	Kulikov	01/10,01/11	164	13.6,14.0	73.6	-2.2	3.832	0.001	0.38	0.02	KOR
2764	Moeller	01/19,01/21	100	2.2,1.1	122.2	-0.8	5.952	0.003	0.25	0.04	FLOR
5110	Belgirate	01/14,01/19	70	14.2,15.9	86.8	3.1	7.02	0.01	0.11	0.02	MB-I
(8505)	1990 YK	01/11-01/21	192	14.9,9.2	133.1	-2.4	7.004	0.002	0.09	0.02	FLOR
(34459)	2000 SC91	01/11-01/14	126	2.5,3.9	106.5	1.7	2.781	0.001	0.14	0.02	EUN

Table I. Observing circumstances and results. Pts is the number of data points. The phase angle is given for the first and last date. L_{PAB} and B_{PAB} are the approximate phase angle bisector longitude and latitude at mid-date range (see Harris *et al.*, 1984). Grp is the asteroid family/group (Warner *et al.*, 2009).

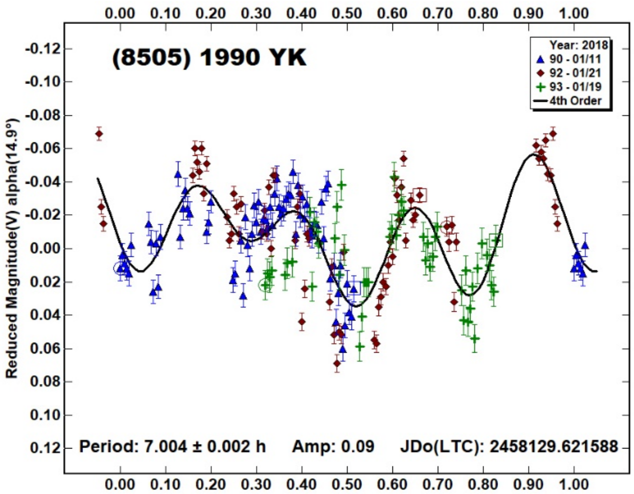

(34459) 2000 SC91. This is a member of the Eunomia family. We observed (34459) 2000 SC91 over a three-night period and measured a rotational period of 2.781 ± 0.001 h with an amplitude of 0.14 mag. The only previously reported rotational period is by Albers et al. (2010). They reported a period of 2.7791± 0.0006 h in good agreement with our result.

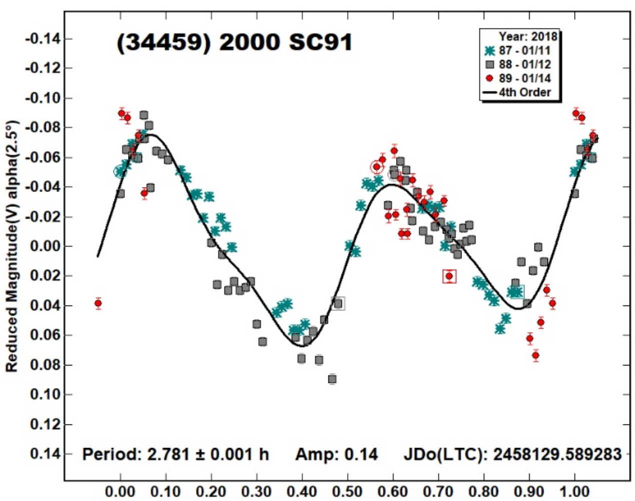

References

Albers, K., Kragh, K., Monnier, A., Pligge, Z., Stolze, K., West, J., Yim, A., Ditteon, R. (2010). “Asteroid Lightcurve Analysis at the Oakley Southern Sky Observatory: 2009 October thru 2010 April,” Minor Planet Bulletin **37**, 152-158.

Behrend, R. (2006). Observatoire de Geneve web site. *http://obswww.unige.ch/~behrend/page_cou.html*

Clark, M. (2006). “Lightcurve results for 383 Janina, 899 Jokaste, 1825 Klare, 2525 O'Steen 5064 Tanchozuru, and (17939) 1999 HH8,” Minor Planet Bulletin **33**, 53-56.

Ďurech, J., Hanuš, J., Oszkiewicz, D., Vančo, R. (2016). “Asteroid models from the Lowell photometric database.” Astronomy & Astrophysics, Volume 587, id.A48, 6 pp.

Harris, A.W., Young, J.W., Scaltriti, F., Zappala, V. (1984). “Lightcurves and phase relations of the asteroids 82 Alkmene and 444 Gyptis.” *Icarus* **57**, 251-258.

Harris, A.W., Pravec, P., Galad, A., Skiff, B.A., Warner, B.D., Vilagi, J., Gajdos, S., Carbognani, A., Hornoch, K., Kusnirak, P., Cooney, W.R., Gross, J., Terrell, D., Higgins, D., Bowell, E., Koehn, B.W. (2014). “On the maximum amplitude of harmonics on an asteroid lightcurve.” Icarus **235**, 55-59.

Hayes-Gehrke, M., Koester, K., Snyder, C., Johnson, A., Gibson, A., Greenberg, E., Mehta, S., Wells-Weitzner, C., Leung, L., (2014). “Rotation Period for 5110 Belgirate,” Minor Planet Bulletin **41**, 78.

Nugent, C.R., Mainzer, A., Masiero, J., Bauer, J., Cutri, R.M., Grav, T., Kramer, E., Sonnett, S., Stevenson, R., Wright, E.L. (2015). “NEOWISE Reactivation Mission Year One: Preliminary Asteroid Diameters and Albedos.” The Astrophysical Journal, Volume 814, Issue 2, article id. 117, 13 pp.

Nugent, C.R., Mainzer, A., Bauer, J., Cutri, R.M., Kramer, E.A., Grav, T., Masiero, J., Sonnett, S., Wright, E.L. (2016). “NEOWISE Reactivation Mission Year Two: Asteroid Diameters and Albedos.” The Astronomical Journal, Volume 152, Issue 3, article id. 63, 12 pp.

Pravec, P., Wolf, M., Sarounova, L. (2018). *http://www.asu.cas.cz/~ppravec/neo.htm*

Warner, B.D., Harris, A.W., Pravec, P. (2009). “The Asteroid Lightcurve Database.” *Icarus* **202**, 134-146. Updated 2017 Nov. *http://www.minorplanet.info/lightcurvedatabase.html*

Warner, B.D. (2017). MPO Canopus software version 10.7.10.0. *http://www.bdwpublishing.com*

Waszczak, A., Chang, C.-K., Ofek, E.O., Laher, R., Masci, F., Levitan, D., Surace, J., Cheng, Y.-C., Ip, W.-H., Kinoshita, D., Helou, G., Prince, T.A., Kulkarni, S. (2015). “Asteroid Light Curves from the Palomar Transient Factory Survey: Rotation Periods and Phase Functions from Sparse Photometry,” The Astronomical Journal, Volume 150, Issue 3, article id. 75, 35 pp.

LIGHTCURVE ANALYSIS AND ROTATION PERIOD FOR 19911 RIGAUX

Alfonso Noschese
AstroCampania Associazione
via Servio Tullio 101, 80126 Naples ITALY
and
Osservatorio Astronomico 'Salvatore Di Giacomo'
Agerola (Na) ITALY
a.noschese@astrocampania.it

Antonio Catapano
AstroCampania Associazione, Naples ITALY

Antonio Vecchione
AstroCampania Associazione, Naples ITALY

(Received: 2018 Sep 10)

From 2018 March 14 to April 6, CCD images were taken with the aim of measuring the rotation period of the minor planet 19911 Rigaux. The data analysis gives a lightcurve with a rotation period of 2.3274 ± 0.0001 hr.

The main-belt asteroid 19911 Rigaux was discovered on 1933 March 26 by Fernand Rigaux at Royal Observatory, Uccle. The diameter of this object is about 18.3 km while the orbital period is approximately 1945 days. The geometric albedo is 0.076 (JPL, 2018).

CCD photometric observations of 19911 Rigaux were performed from 2018 March 14 to April 6 to measure its lightcurve and rotation period. There were no entries in the asteroid lightcurve database (LCDB; Warner et al., 2009) for this asteroid at the time of the observations. Photometric measurements were carried out with a 0.5-m *f*/8 Ritchen-Chretien telescope using a FLI-PL4240 CCD camera with a 2048x2048 array of 13.5-micron pixels and a clear filter.

A total of 382 lightcurve data points were collected in 8 observing sessions. Exposure times were 180 s. All images were astrometrically aligned and dark and flat-field corrected. *MPO Canopus* (Warner, 2016) was used to measure the magnitudes, perform Fourier analysis, and produce the final lightcurve.

In particular, data were reduced in *MPO Canopus* using differential photometry. Night-to-night zero point calibration was accomplished by selecting up to five comparison stars with near-solar colors using the "Comp Star Selector" feature. The CMC-15 star catalog was used for determining the comparison star magnitudes. The "StarBGone" routine within *MPO Canopus* was used to subtract stars that occasionally merged with the asteroid during the observations.

MPO Canopus was also used for rotation period analysis. The software employs the FALC Fourier analysis algorithm developed by Harris (Harris et al., 1989).

After accumulating eight sessions, we found a period of 2.3274 ± 0.0001 hr. The data produced a lightcurve with an asymmetrical shape and amplitude of 0.13 mag. Table I gives the observing circumstances and results.

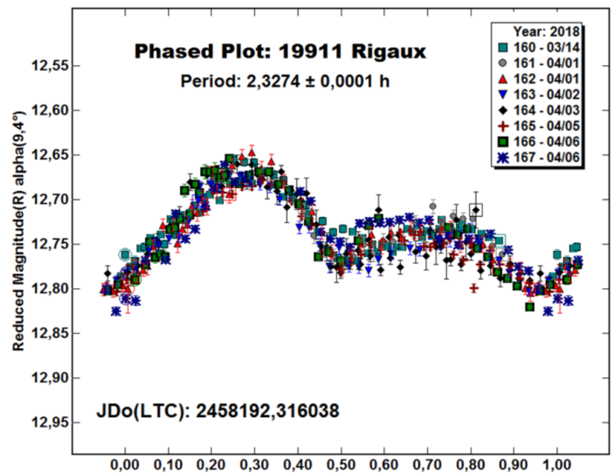

References

Harris, A.W., Young, J.W., Scaltriti, F., Zappala, V. (1984). "Lightcurves and phase relations of the asteroids 82 Alkmene and 444 Gyptis." *Icarus* **57**, 251-258.

Harris, A.W., Young, J.W., Bowell, E., Martin, L.J., Millis, R.L., Poutanen, M., Scaltriti, F., Zappala, V., Schober, H.J., Debehogne, H., Zeigler, K.W. (1989). "Photoelectric Observations of Asteroids" 3, 24, 60, 261, and 863." *Icarus* **77**, 171-186.

JPL (2018). Small-Body Database Browser. *http://ssd.jpl.nasa.gov/sbdb.cgi#top*

Warner, B.D., Harris, A.W., Pravec, P. (2009). "The Asteroid Lightcurve Database." *Icarus* **202**, 134-146. Updated 2018 June. *http://www.minorplanet.info/lightcurvedatabase.html*

Warner, B.D. (2016). MPO Software, *MPO Canopus* version 10.7.7.0. Bdw Publishing. *http://minorplanetobserver.com*

Number	Name	2018 mm/dd	Pts	Phase	L_{PAB}	B_{PAB}	Period(h)	P.E.	Amp	A.E.	Exp
19911	Rigaux	03/14-04/06	382	9.4,11.8	180	14	2.3274	0.0004	0.13	0.01	180

Table I. Observing circumstances and results. The phase angle is given for the first and last date. L_{PAB} and B_{PAB} are the approximate phase angle bisector longitude and latitude at mid-date range (see Harris *et al.*, 1984). Exp is exposure range, seconds.

LIGHTCURVE ANALYSIS AND ROTATION PERIOD FOR 4262 DEVORKIN

Alfonso Noschese
AstroCampania Associazione
and
Osservatorio Elianto (K68)
via V. Emanuele III, 95, 84098
Pontecagnano (SA) Italy
a.noschese@astrocampania.it

Antonio Vecchione
AstroCampania Associazione, Naples ITALY

(Received: 2018 Sep 15)

From 2018 July 6-16, CCD images were taken for the purpose of measuring the rotation period of 4262 DeVorkin. The data analysis gives a lightcurve with a rotation period of 6.1619 ± 0.0006 hr.

The main-belt asteroid 4262 DeVorkin discovered on 1989 February 5 by M. Arai and H. Mori at Yorii, Japan. The diameter of this asteroid is about 6.4 km and its orbital period is approximately 1276 days. The geometric albedo is 0.36 (JPL, 2018).

CCD photometric observations of 4262 DeVorkin were performed from 2018 July 6-16 to measure its lightcurve and rotation period. There were no entries in the asteroid lightcurve database (LCDB; (Warner et al., 2009) for this asteroid at the time of the observations. The observations were made with a 0.3-m *f*/4 Newtonian reflector using a Moravian KAF1603 ME CCD camera with a 1536x1024 array of 9-micron pixels and a clear filter.

A total of 535 lightcurve data points were collected in 14 observing sessions; exposures were 180 s. All images were astrometrically aligned and dark and flat-field corrected. *MPO Canopus* (Warner, 2016) was used to measure the magnitudes, perform Fourier analysis, and produce the final lightcurve.

In particular, data were reduced in *MPO Canopus* using differential photometry. Night-to-night zero point calibration was accomplished by selecting up to five comparison stars with near-solar colors using the "Comp Star Selector" feature. The CMC-15 star catalog was used for determining the comparison star magnitudes. The "StarBGone" routine within *MPO Canopus* was used to subtract stars that occasionally merged with the asteroid during the observations. *MPO Canopus* was also used for rotation period analysis, employing the FALC Fourier analysis algorithm developed by Harris (Harris et al., 1989).

After accumulating eight sessions, we found a period of 6.1619 ± 0.0006 hr. The data fully covered the lightcurve, which has two maxima and two minima and amplitude of 0.40 mag. Table I gives the observing circumstances and results.

References

Harris, A.W., Young, J.W., Scaltriti, F., Zappala, V. (1984). "Lightcurves and phase relations of the asteroids 82 Alkmene and 444 Gyptis." *Icarus* **57**, 251-258.

Harris, A.W., Young, J.W., Bowell, E., Martin, L.J., Millis, R.L., Poutanen, M., Scaltriti, F., Zappala, V., Schober, H.J., Debehogne, H., Zeigler, K.W. (1989). "Photoelectric Observations of Asteroids" 3, 24, 60, 261, and 863." *Icarus* **77**, 171-186.

JPL (2018). Small-Body Database Browser. *http://ssd.jpl.nasa.gov/sbdb.cgi#top*

Warner, B.D., Harris, A.W., Pravec, P. (2009). "The Asteroid Lightcurve Database." *Icarus* **202**, 134-146. Updated 2018 June. *http://www.minorplanet.info/lightcurvedatabase.html*

Warner, B.D. (2016). MPO Software, *MPO Canopus* version 10.7.7.0. Bdw Publishing. *http://minorplanetobserver.com*

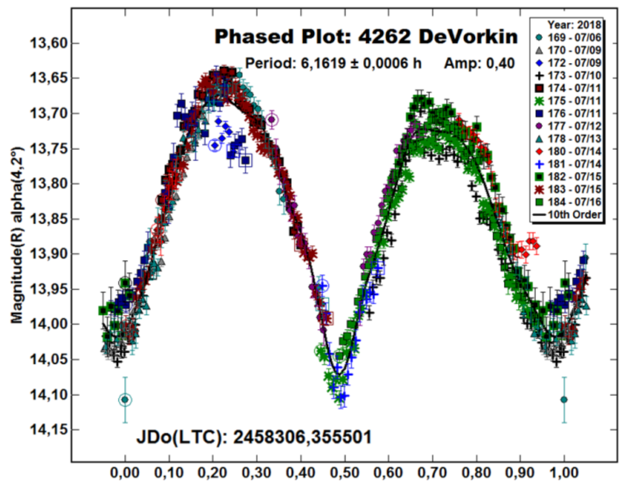

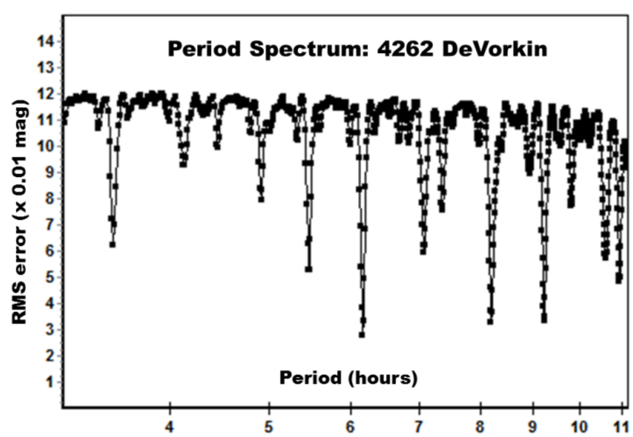

Number	Name	2018 mm/dd	Pts	Phase	L_{PAB}	B_{PAB}	Period(h)	P.E.	Amp	A.E.	Exp
4262	DeVorkin	07/06-07/16	535	4.2,4.7	288	4	6.1619	0.0001	0.40	0.01	180

Table I. Observing circumstances and results. The phase angle is given for the first and last date. L_{PAB} and B_{PAB} are the approximate phase angle bisector longitude and latitude at mid-date range (see Harris *et al.*, 1984). Exp is exposure range, seconds.

LIGHTCURVE ANALYSIS AND ROTATION PERIOD FOR (28281) 1999 CT29

Alfonso Noschese
AstroCampania Associazione
and
Osservatorio Elianto (K68)
via V. Emanuele III, 95, 84098
Pontecagnano (SA) Italy
a.noschese@astrocampania.it

Antonio Vecchione
AstroCampania Associazione, Naples ITALY

(Received: 2018 Sep 25)

From 2018 August 30 to September 13, CCD images were taken for the purpose of measuring the rotation period of (28281) 1999 CT29. The data analysis gives a lightcurve with a rotation period of 19.5275 ± 0.0067 hr.

The main-belt asteroid (28281) 1999 CT29 was discovered on 1999 February 10 by LINEAR at Socorro. The absolute magnitude is H = 12.5; with a geometric albedo is 0.167, the estimated diameter is 10.1 km (JPL, 2018). We started an observing campaign aimed at estimating the rotation period since there were no entries in the asteroid lightcurve database (LCDB; Warner et al., 2009) for this asteroid. CCD photometric observations of (28281) 1999 CT29 were performed from 2018 August 30 to September 13 to search the lightcurve and rotation period. Observations were made with a 0.3-m *f*/4 Newtonian reflector using a Moravian KAF1603 ME CCD camera with a 1536x1024 array of 9-micron pixels and a clear filter.

A total of 711 lightcurve data points were collected in 18 observing sessions; exposure times were 240 s. All images were astrometrically aligned and dark and flat-field corrected. *MPO Canopus* (Warner, 2017) was used to measure the magnitudes, perform Fourier analysis, and produce the final lightcurve. In particular, data were reduced in *MPO Canopus* using differential photometry. Night-to-night zero point calibration was accomplished by selecting up to five comparison stars with near-solar colors using the “Comp Star Selector” feature. The CMC-15 star catalog was used for determining the comparison star magnitudes. The “StarBGone” routine within *MPO Canopus* was used to subtract stars that occasionally merged with the asteroid during the observations.

MPO Canopus implements the FALC Fourier analysis algorithm developed by Harris (Harris et al., 1989) for period analysis. After accumulating 18 sessions, we found a period of 19.5275 ± 0.0067 hr. The lightcurve has an asymmetrical shape and amplitude of 0.19 mag. Table I gives the observing circumstances and results.

The phased lightcurve covers the adopted period and so the result appears to be unambiguous. The period spectrum shows that the best solution (with the lowest RMS) is the one adopted here.

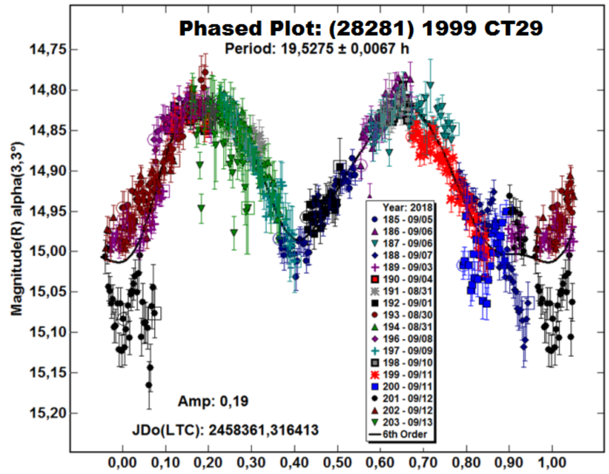

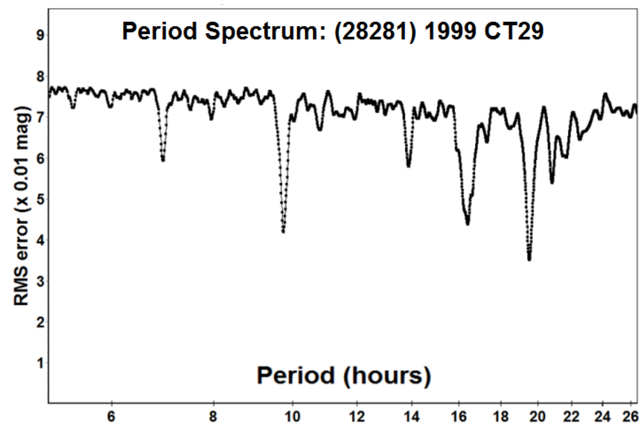

References

Harris, A.W., Young, J.W., Scaltriti, F., Zappala, V. (1984). “Lightcurves and phase relations of the asteroids 82 Alkmene and 444 Gyptis.” *Icarus* **57**, 251-258.

Harris, A.W., Young, J.W., Bowell, E., Martin, L.J., Millis, R.L., Poutanen, M., Scaltriti, F., Zappala, V., Schober, H.J., Debehogne, H., Zeigler, K.W. (1989). “Photoelectric Observations of Asteroids 3, 24, 60, 261, and 863.” *Icarus* **77**, 171-186.

JPL (2018). Small-Body Database Browser. *http://ssd.jpl.nasa.gov/sbdb.cgi#top*

Warner, B.D., Harris, A.W., Pravec, P. (2009). “The Asteroid Lightcurve Database.” Icarus 202, 134-146. Updated 2018 June. http://www.minorplanet.info/lightcurvedatabase.html

Warner, B.D. (2017). MPO Software, *MPO Canopus* version 10.7.11.1. Bdw Publishing. *http://minorplanetobserver.com*

Number	Name	2018 mm/dd	Pts	Phase	L_{PAB}	B_{PAB}	Period(h)	P.E.	Amp	A.E.	Exp
28281	1999 CT29	08/30-09/13	711	2.8,6.4	340	5	19.5275	0.0067	0.19	0.02	240

Table I. Observing circumstances and results. The phase angle is given for the first and last date. L_{PAB} and B_{PAB} are the approximate phase angle bisector longitude and latitude at mid-date range (see Harris *et al.*, 1984). Exp is exposure range, seconds.

NEAR-EARTH ASTEROID LIGHTCURVE ANALYSIS AT THE CENTER FOR SOLAR SYSTEM STUDIES: 2018 JULY-SEPTEMBER

Brian D. Warner
Center for Solar System Studies / MoreData!
446 Sycamore Ave.
Eaton, CO 80615 USA
brian@MinorPlanetObserver.com

Robert D. Stephens
Center for Solar System Studies / MoreData!
Rancho Cucamonga, CA 91730

(Received: 2018 October 6)

Lightcurves for 45 Near-Earth asteroids (NEAs) obtained at the Center for Solar System Studies (CS3) from 2018 July-September were analyzed for rotation period and signs of satellites or tumbling. NEA 13553 Massakikoyama appears to be in non-principal axis rotation, i.e., tumbling. 2011 UA (D = 0.6 km) is a super-fast rotator with a period of 0.316391 ± 0.000007 h. The period and size place it well above the spin barrier. The period for 2018 RQ2 is multiply ambiguous, with possible solutions of 4.28 h or 5.17 h (monomdal lightcurve) and 8.58 h or 10.60 h (bimodal lightcurve). 2018 KE3 may be a binary asteroid.

CCD photometric observations of 45 near-Earth asteroids (NEAs) were made at the Center for Solar System Studies (CS3) from 2018 July-September.

Table I lists the telescopes and CCD cameras that are combined to make observations. Up to nine telescopes can be used for the campaign, although seven is more common. All the cameras use CCD chips from the KAF blue-enhanced family and so have essentially the same response. The pixel scales ranged from 1.24-1.60 arcsec/pixel.

Telescopes	Cameras
0.30-m *f*/6.3 Schmidt-Cass	FLI Microline 1001E
0.35-m *f*/9.1 Schmidt-Cass	FLI Proline 1001E
0.35-m *f*/11 Schmidt-Cass	SBIG STL-1001E
0.40-m f/10 Schmidt-Cass	
0.50-m *f*/8.1 Ritchey-Chrétien	

Table I. List of available telescopes and CCD cameras at CS3. The exact combination for each telescope/camera pair can vary due to maintenance or specific needs.

All lightcurve observations were unfiltered since a clear filter can cause a 0.1-0.3 mag loss. The exposure duration varied depending on the asteroid's brightness and sky motion. Guiding on a field star sometimes resulted in a trailed image for the asteroid.

Measurements were made using *MPO Canopus*. The Comp Star Selector utility in *MPO Canopus* found up to five comparison stars of near solar-color for differential photometry. Catalog magnitudes were taken from the APASS (Henden et al., 2009) or CMC-15 (Munos, 2017) catalogs.

The nightly zero points for the APASS and CMC-15 catalogs are generally consistent to about ±0.05 mag or better, but occasionally reach >0.1 mag. There is a systematic offset between the two catalogs and so, whenever possible, the same catalog is used for all observations of a given asteroid. Period analysis is done with *MPO Canopus*, which implements the FALC algorithm by Harris (Harris *et al.,* 1989). The same algorithm is used in an iterative fashion if it appears there is more than one period. This works well for binary asteroids but not for tumbling asteroids.

In the plots below, the "Reduced Magnitude" is Johnson V as indicated in the Y-axis title. These are values that have been converted from sky magnitudes to unity distances by applying –5*log (rΔ) to the measured sky magnitudes with r and Δ being, respectively, the Sun-asteroid and Earth-asteroid distances in AU. Unless otherwise stated, the magnitudes were normalized to the phase angle in parentheses using G = 0.15. The X-axis is the rotational phase, ranging from –0.05 to +1.05.

If the plot includes an amplitude, e.g., "Amp: 0.65", this is the amplitude of the Fourier model curve and *not necessarily the adopted amplitude for the lightcurve*.

For the sake of brevity, only some of the previously reported results may be referenced in the discussions on a specific asteroid. For a more complete listing, the reader is directed to the asteroid lightcurve database (LCDB; Warner *et al.,* 2009). The on-line version at *http://www.minorplanet.info/lightcurvedatabase.html* allows direct queries that can be filtered a number of ways and the results saved to a text file. A set of text files of the main LCDB tables, including the references with bibcode, is also available for download. Readers are strongly encouraged, when possible, to cross-check with the original references listed in the LCDB.

433 Eros. The rotation period of Eros had long been determined to be about 5.27 h by numerous observers prior to the visit of the NEAR-Shoemaker spacecraft, e.g., Warner (2017a). The data from 2018 were obtained to help find a more exact value for the change in rotation rate, if any, due to the YORP (Yarkovsky–O'Keefe–Radzievskii–Paddack) thermal effect (Rubincam, 2000).

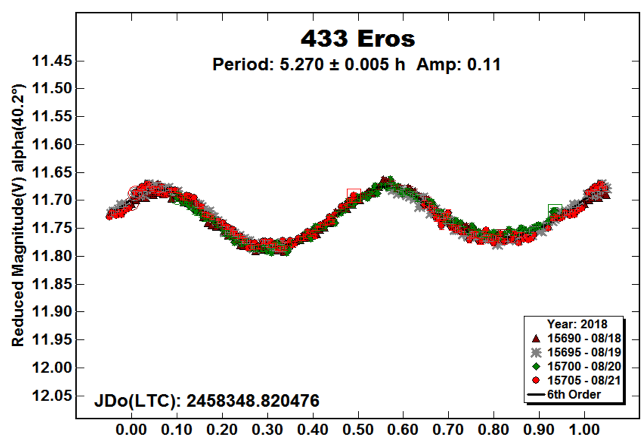

719 Albert. Recovered in 2001 after being lost for several decades, this 2.5 km NEA was observed by Pravec et al. (2001), who found a period of 5.8011 h. However, the 2001 observations were the last to be reported in the LCDB until the results given here.

The amplitude in 2018 was 0.52 mag compared to 0.94 mag found by Pravec et al. (2001) at the time of maximum amplitude in their observations (2001 Aug 23). The phase angle bisector longitude (see Harris et al., 2004) was about 2° and the phase angle was 46°. In 2018, the values were 257° and 17°, respectively. From this a rough estimate of the longitude for the asteroid's pole is 250° (or 70°) ± 20°.

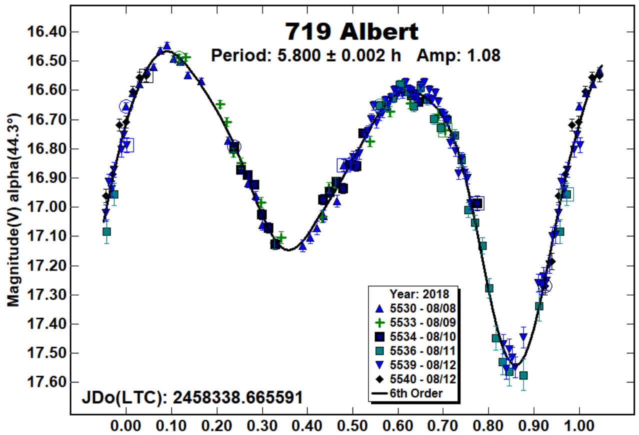

1865 Cerberus. Among some of the previous synodic period results for Ceberus are Pravec et al. (2008; 6.8039 h) and Skiff (2012; 6.804 h). Our results are in good agreement.

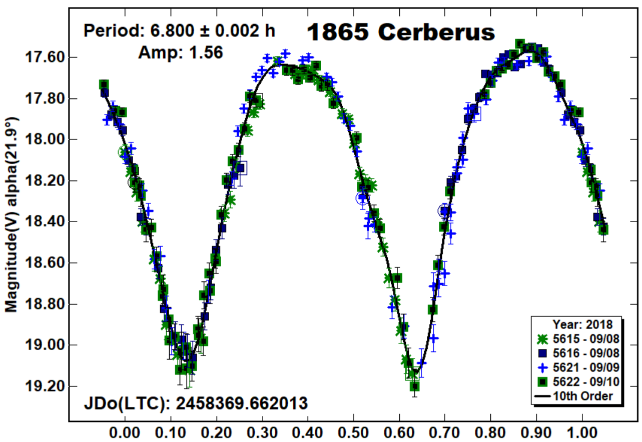

3552 Don Quixote. This NEA has an orbit that is very "comet-like" and it appears that it really is one. Mommert et al. (2018) reported seeing a tail in visible wavelengths for the first time. There were no obvious signs of cometary activity in our observations and the object did not appear "fuzzier" than nearby stars.

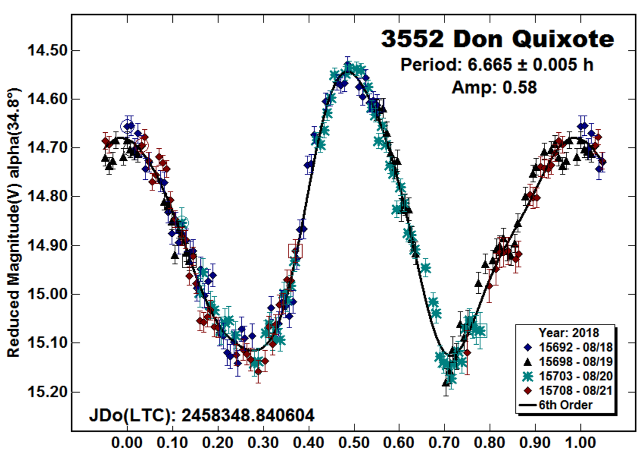

4183 Cuno. Pravec et al. (1997, 2000) reported a period of about 3.56 h. Warner (2015a) found a similar result. These earlier results were obtained when the lightcurve amplitude was at least 0.47 mag. In 2018, the amplitude was only 0.09 mag and the data errors were almost the same level. As a result, there were several possible solutions. We forced a period near the earlier results and found 3.58 h.

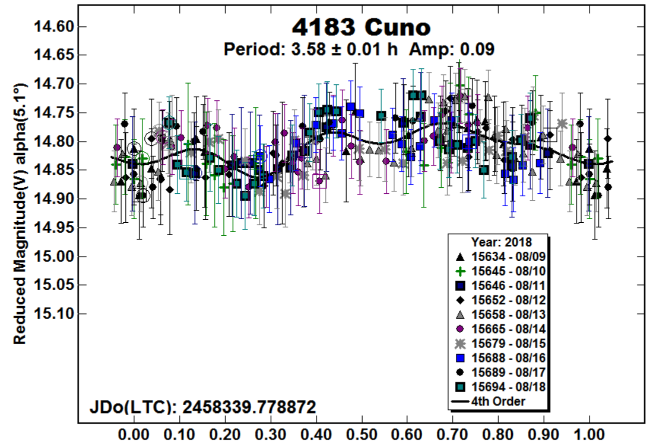

6456 Golombek. Previous results include Pravec et al. (2005, 2.5013 h; 2018, 2.5016 h). Our results are in good agreement.

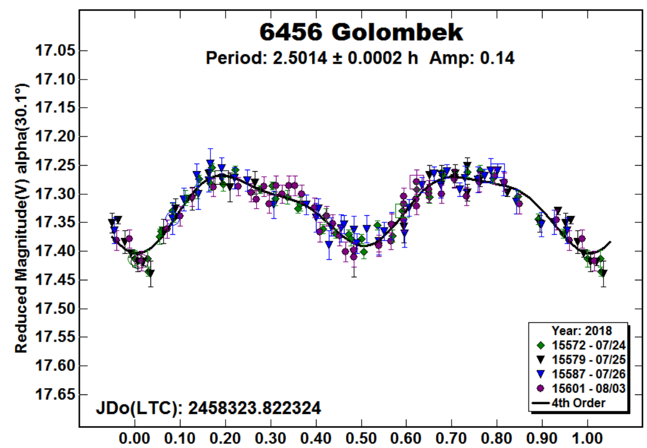

(9856) 1991 EE. Wisniewski et al. (1997) reported $P = 3.045$ h for 1991 EE. Warner (2018) observed it in 2018 May and found $P = 3.0416$ h, $A = 0.28$ mag. We observed it again in September and found $P = 3.048$ h, $A = 0.19$ mag.

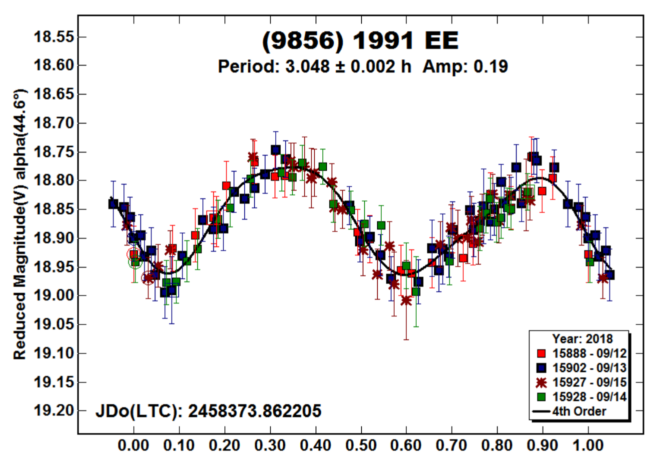

13553 Masaakikoyama. Pravec et al. (2005) found this to be a tumbler, i.e., in non-principal axis rotation. They found a dominant period at about 38 h. Our 2018 data confirm the tumbling state. The data set was insufficient to find the two rotation frequencies even with Pravec's custom software. *MPO Canopus* does not allow simultaneous dual period searches and so we provide two lightcurves, each phased to a period that dominated the period spectrum.

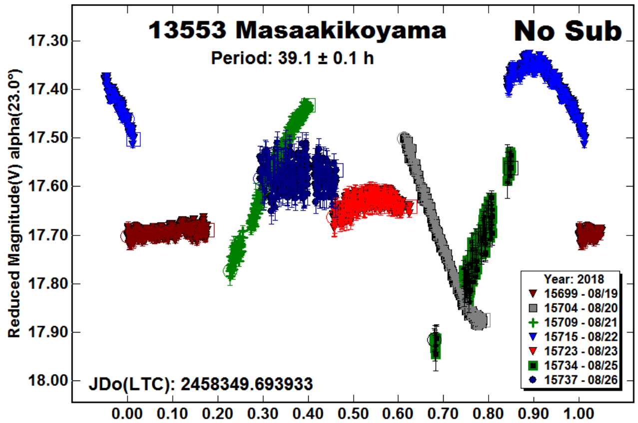

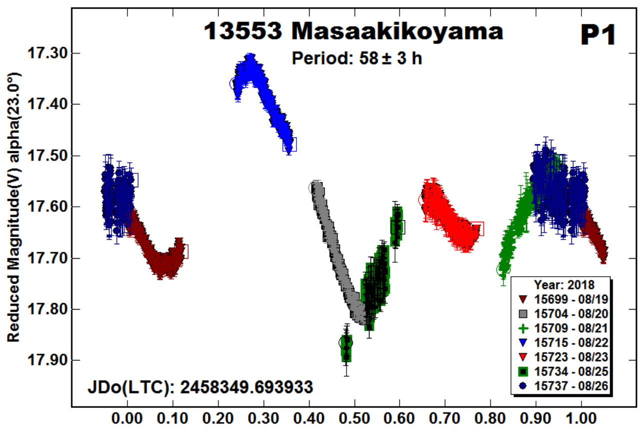

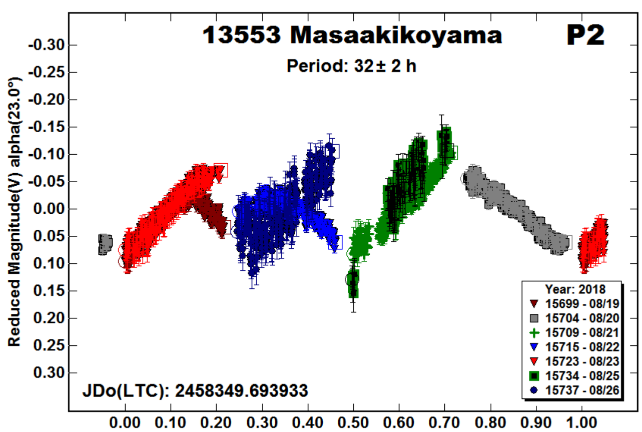

(16834) 1997 WU22. Earlier results include Pravec et al. (2000; 9.345 h), Stephens (2013; 9.374 h), and Warner (2017a; 9.343 h). The Stephens lightcurve is given here since it was not previously published except on the CS3 web site.

Our 2018 data led to a period of 9.348 h, which is within the formal errors of the previous results.

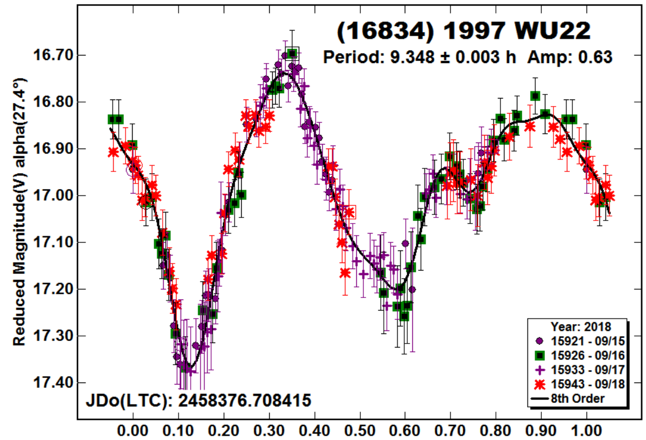

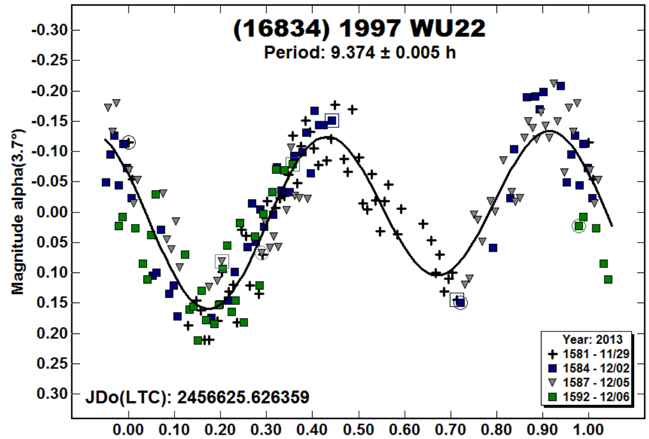

(17274) 2000 LC16. Our result of 16.50 ± 0.02 h agrees with that reported by Pravec et al. (2000). The amplitude of 0.23 mag is in a "gray area" between small amplitudes where multimodal lightcurves are easily possible and larger amplitude lightcurves where, at low phase angles, a bimodal lightcurve is virtually assured (Harris et al., 2014).

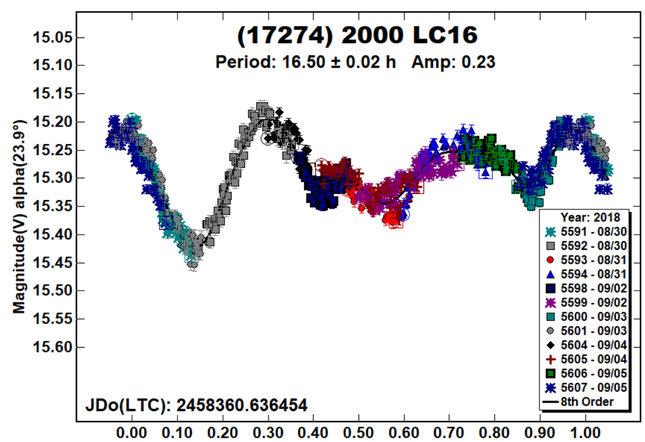

(18109) 2000 NG11. This is one of the relatively few NEAs observed by two recent Palomar Transient Factory groups: Waszczak et al. (2015) and Chang et al. (2016). They reported periods of, respectively, 4.258 h and 4.25 h. Previous dense lightcurve results include Pravec et al. (2000; P = 4.2534 h, A = 1.13 mag) and Warner (2014a; P = 4.255 h, A = 0.89 mag).

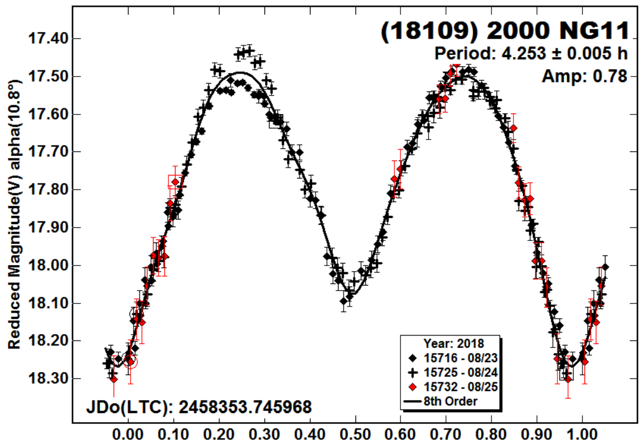

(86324) 1999 WA2. The period spectrum shows a strong preference for the adopted period of 7.161 h. The lightcurve shape is somewhat asymmetrical but, at larger phase angles, shadowing effects can likely explain some of the anomalies in the expected lightcurve shape.

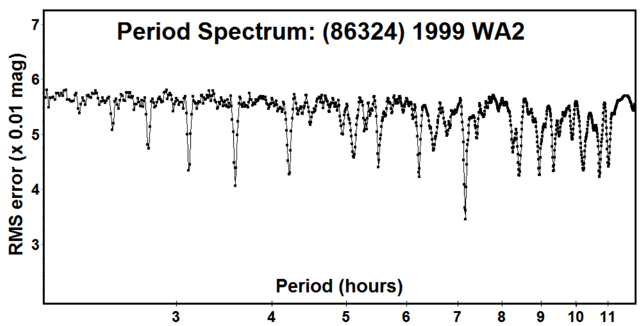

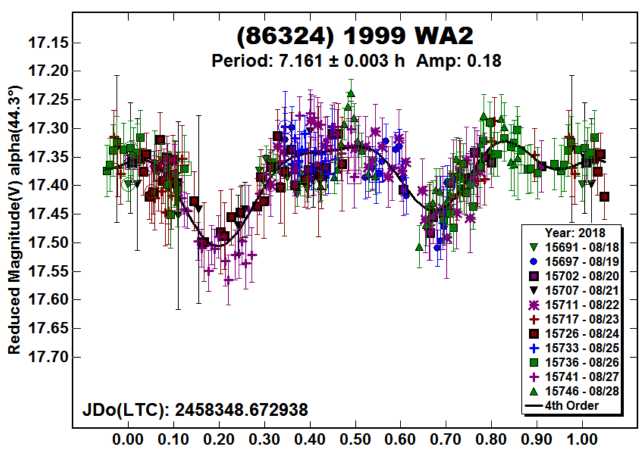

(86878) 2000 HD24. This 900-meter NEA was observed by Warner (2014b), who found a period of 23.1 ± 0.5 h. The 2018 data set was of higher-quality, but it was still not possible to get a precise period solution. Our result of P = 15.72 h represents the best fit in the period spectrum, which also includes a nearly equal RMS minimum at about 23 hours. The 2014 data set was reviewed; a reasonable fit of P = 15.65 h was found.

It's worth noting that the two periods are very close to an integer ratio of 3:2. This usually indicates a *rotational alias*, which is caused by a miscount of the actual number of rotations over the time span of the data. A rotational alias often occurs with nearly symmetrical lightcurves, where the "wrong half" of a lightcurve is matched to other half.

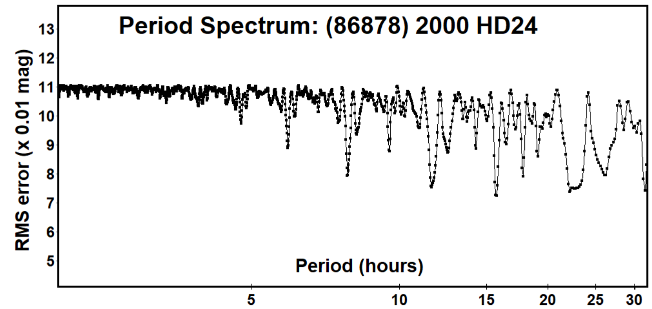

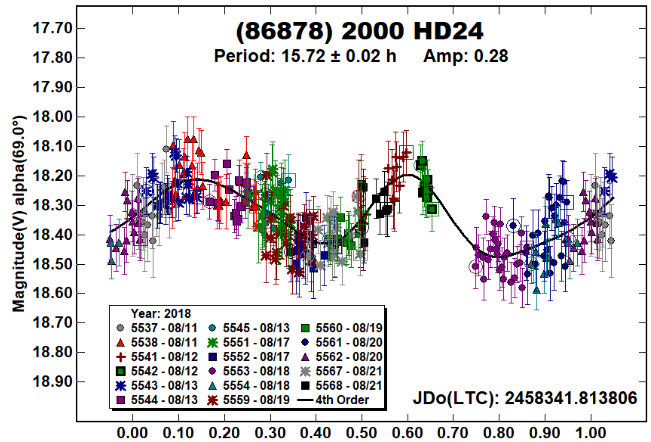

(115052) 2003 RD6. This appears to be the first reported rotation period for 2003 RD6. Unfortunately, it's an ambiguous one. The period spectrum favors two results: 12.08 h and 24.23 h. The lightcurve has been phased to the shorter period. Even a second-order fit for the longer period produced a Fourier model with an amplitude of several magnitudes.

We adopt the shorter period for this paper, but the double period of 24.23 h should be given equal weight.

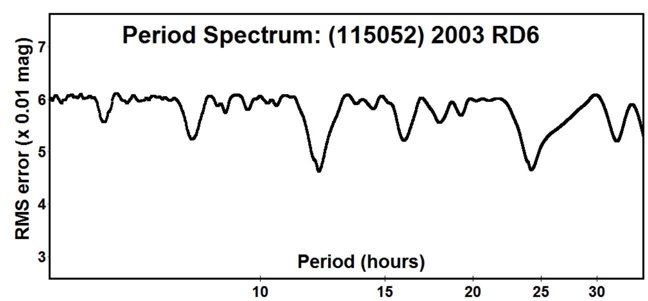

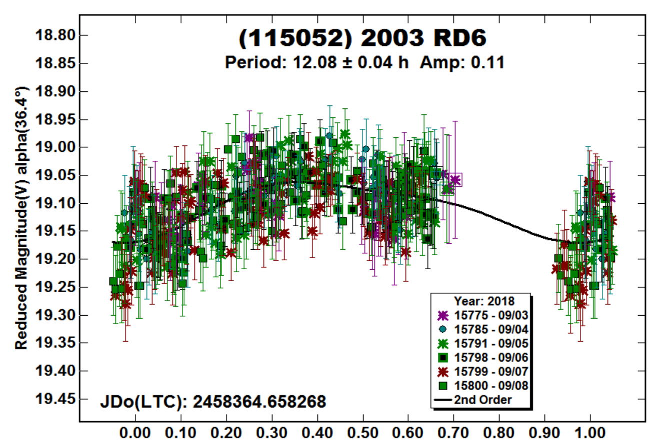

(141527) 2002 FG7. The phase angle longitude in 2018 differed from the one in 2015 (Warner, 2015b) by 175°, meaning that the 2018 view was of the opposite pole. The gap in coverage and only three nights of data in 2018 allowed only 0.02 h precision for the result. This is statistically the same as the earlier result of 6.306 h.

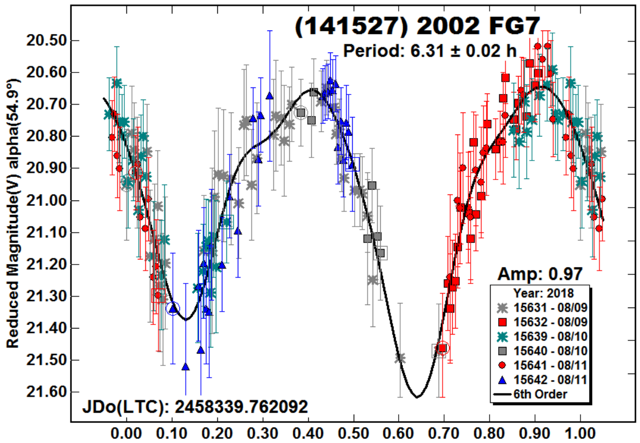

(283729) 2002 UX, (333889) 1998 SV4, (337248) 2000 RH60. These appear to be the first reported rotation periods for these three NEAs. The solutions for 2002 UX and 1998 SV4 are considered secure (at least U = 2+ in the LCDB). The solution for 2000 RH60 suffers the fate of being nearly commensurate with an Earth day. Despite this, we consider P = 25.2 h to be more likely correct than not because of the lightcurve amplitude and low phase angle (Harris et al., 2014).

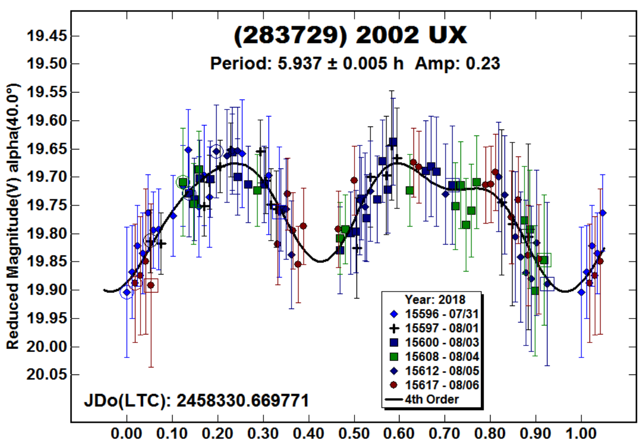

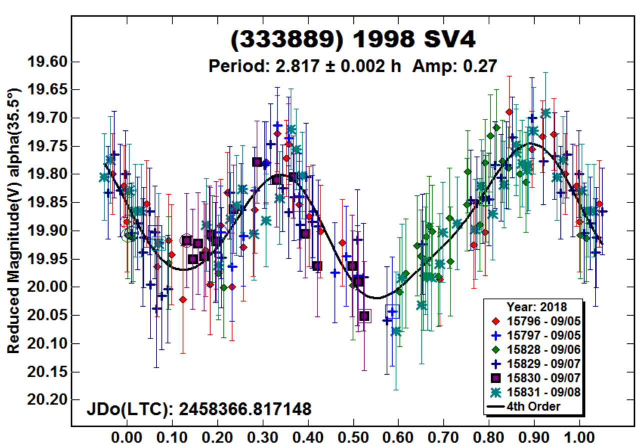

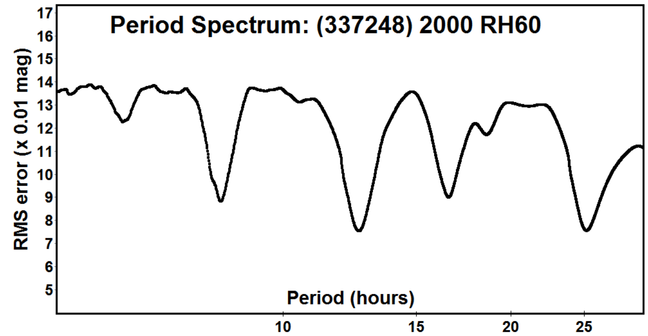

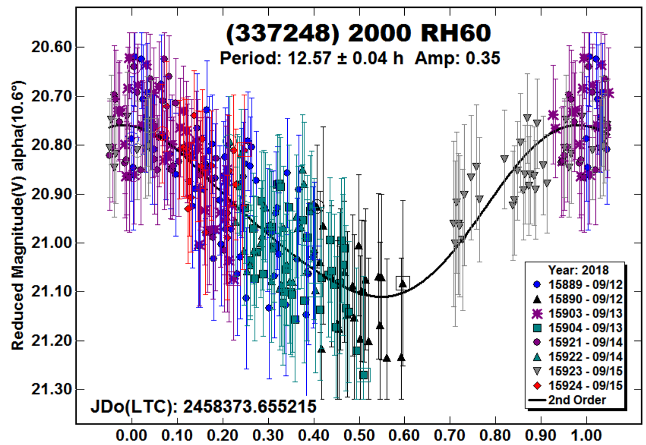

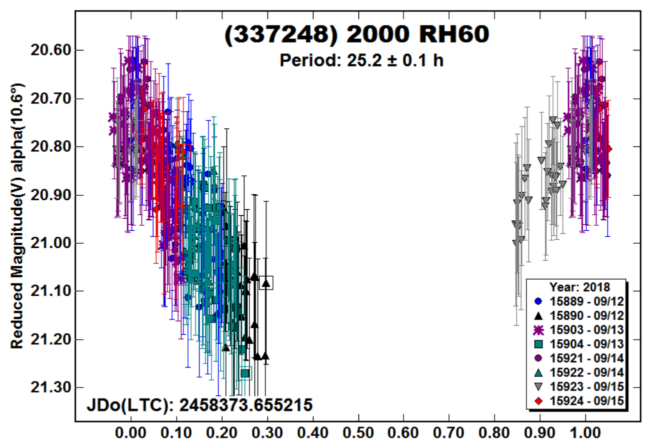

(418929) 2009 DM1. There were no previous rotation period entries in the LCDB. We consider the solution secure.

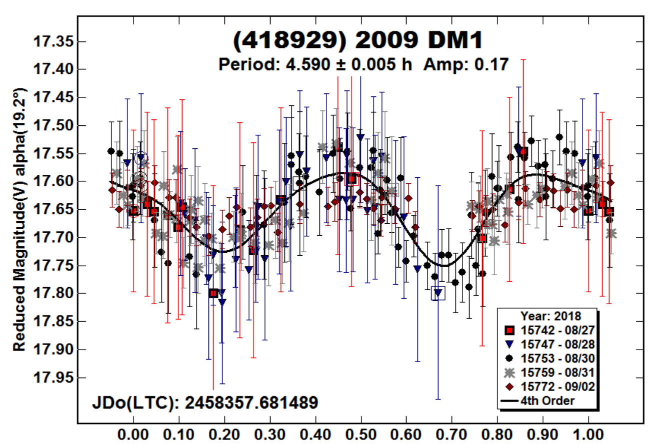

(438429) 2006 WN1. The LCDB had no previous entries of any kind for 2006 WN1.

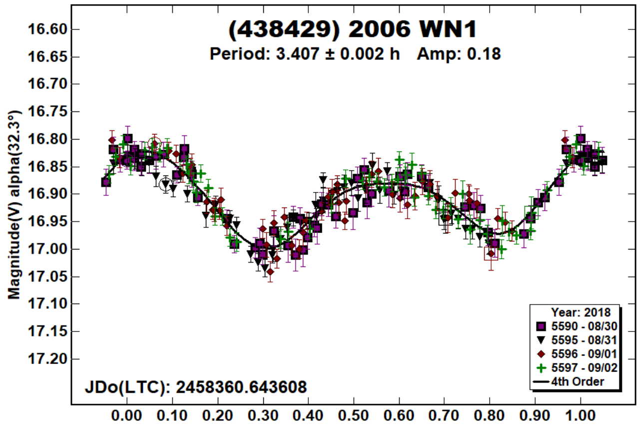

(441987) 2010 NY65. Two previous results are from Warner (2016b, 4.979 h; 2017b, 4.973 h). The period spectrum using the 2018 data strongly favors a period of 5.541 h. When forcing the data to a period near 4.97 h, there was a clear mismatch on two nights that could not be corrected by zero point adjustments.

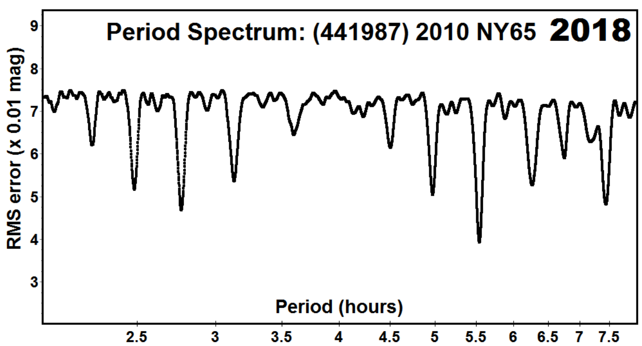

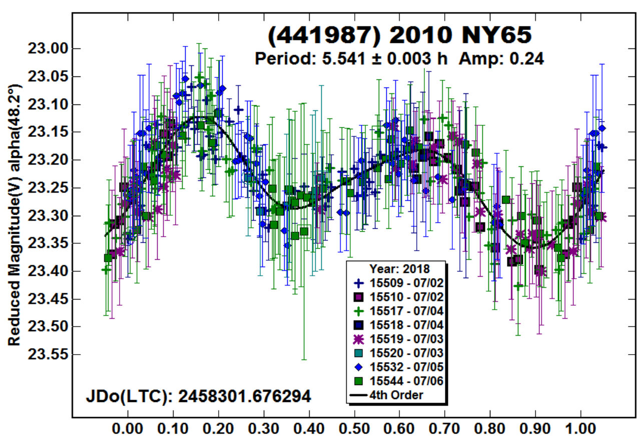

The two periods do not have a simple integer ratio, which helps eliminate a rotational alias. So does the strong asymmetry of the 2018 lightcurve. To see if the discrepancy in periods could be resolved, we took another look at the data from 2016 and 2017. The results did not fully resolve the question.

Forcing the 2016 data to near 5.5 h led to a period of 5.593 h while the 2017 data had a best fit at 5.518 h. These are well outside the limits set by the formal and conservative "10°" errors. The latter is the period difference that results in a 10° rotation difference over the time span of the data set.

The argument for the longer period is reinforced by noting that the two earlier data sets had data from only three consecutive nights. On the other hand, the 2018 data set had five consecutive nights, covering about nine more rotations.

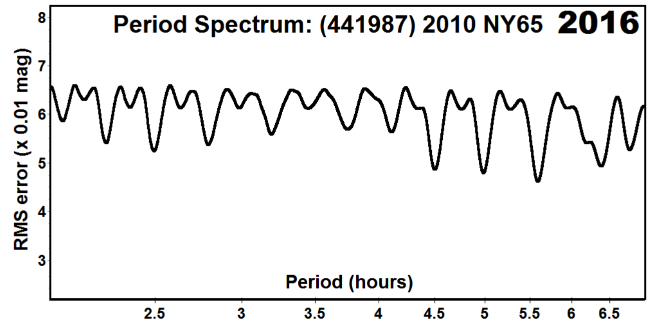

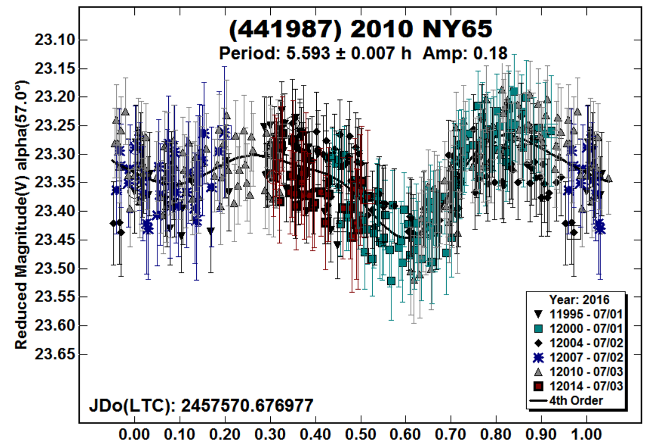

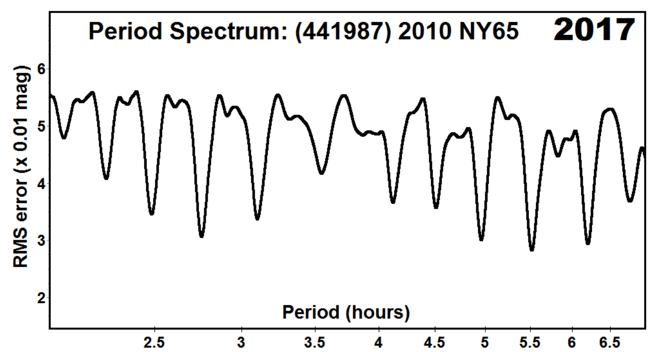

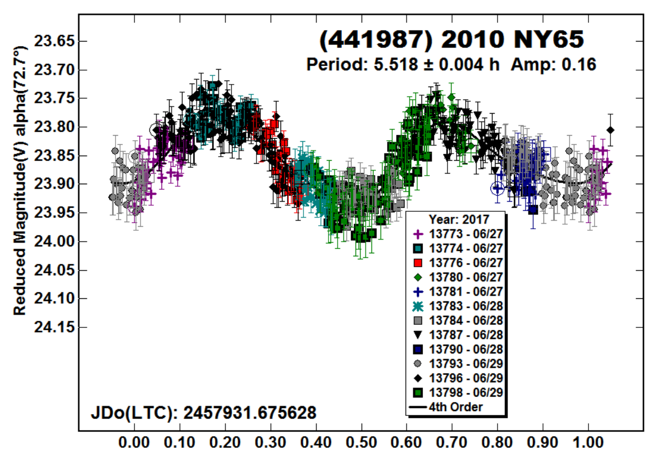

(457260) 2008 RY24. The 2018 data set produced yet another object with a period that was nearly commensurate with an Earth day. The low amplitude and SNR compounded the problem of finding the correct period. The period spectrum favored the longer period of 8.19 h. However this left a gap in the lightcurve at about 0.7 rotation phase. Such gaps are sometimes caused by the Fourier algorithm finding a period that minimizes the number of overlapping data points. The half-period (4.09 h) lightcurve has no gaps and is monomodal. While we have adopted P = 8.19 h; this is another case where an alternate period should be given equal weight.

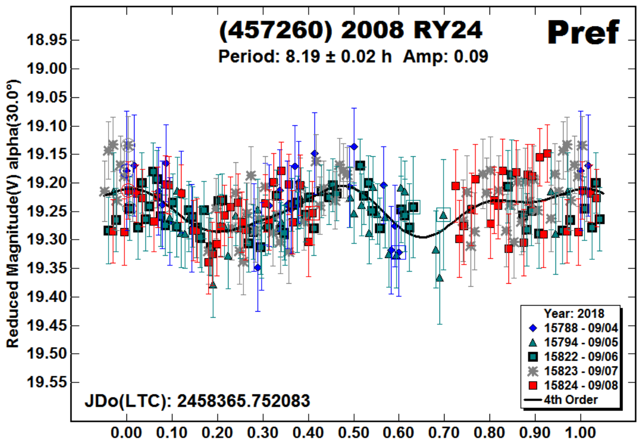

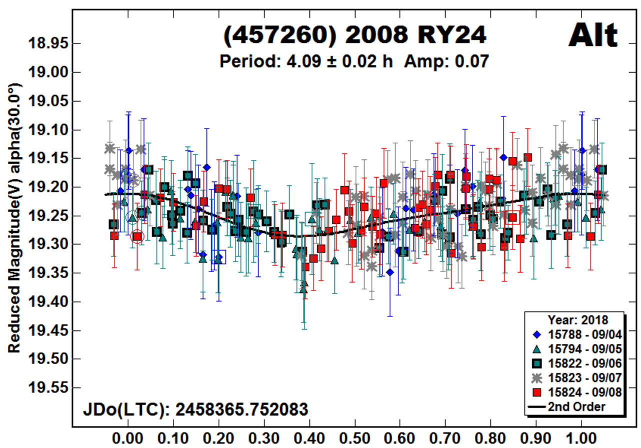

(481394) 2006 SF6, 1999 RB32. Neither of these NEAs had a previous entry of any kind in the LCDB. The period for 2006 SF6 is considered secure. This is not so for 199 RB32.

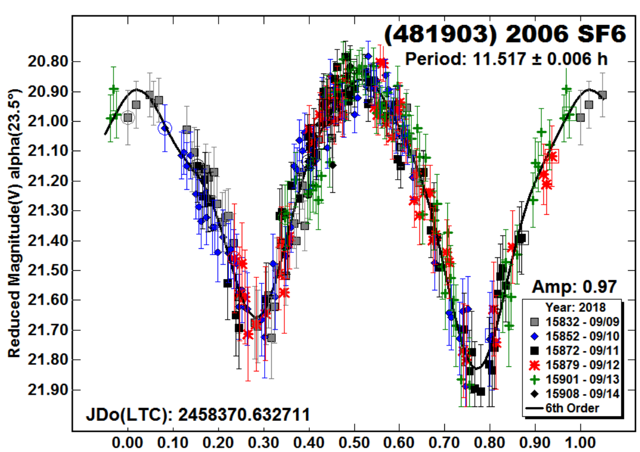

There are significant gaps in the lightcurve and the error bars are nearly the amplitude of the lightcurve. Furthermore, the period is nearly commensurate with an Earth day. A period near 24 hours produced a monomodal lightcurve. Given the apparent amplitude of at least 0.27 mag, the longer, bimodal solution was favored.

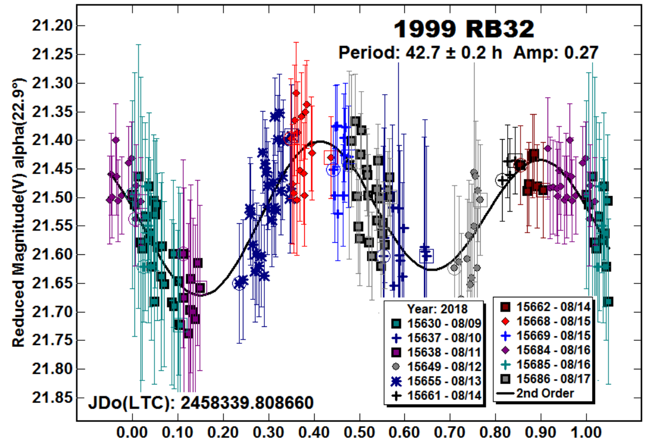

1999 VQ11. The period spectrum gave strong preference to the period of 32.21 h. This could be correct or the result of minimizing the number of overlapping data points. The former theory was adopted but the solution is by no means secure.

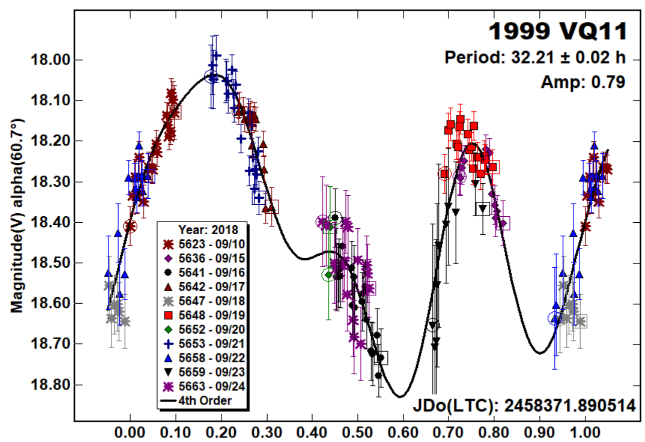

2001 QA143. The amplitude of 0.25 mag gave high confidence in the bimodal solution of 11.78 h (Harris et al., 2014) despite missing more than 25% lightcurve.

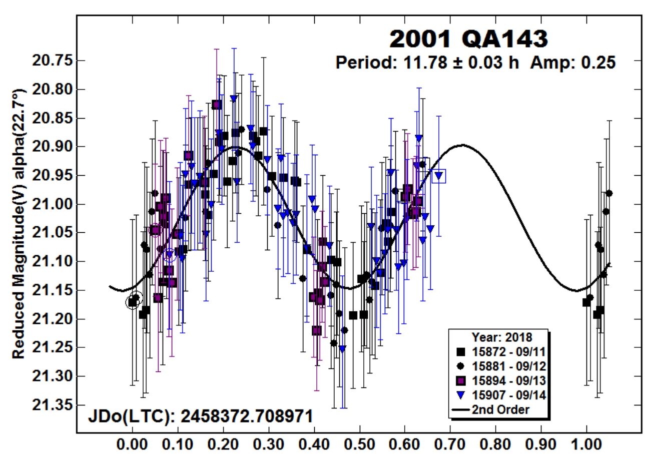

2005 RB, 2007 RX19. The two NEAs had no previous entries of any kind in the LCDB. The solutions are considered secure.

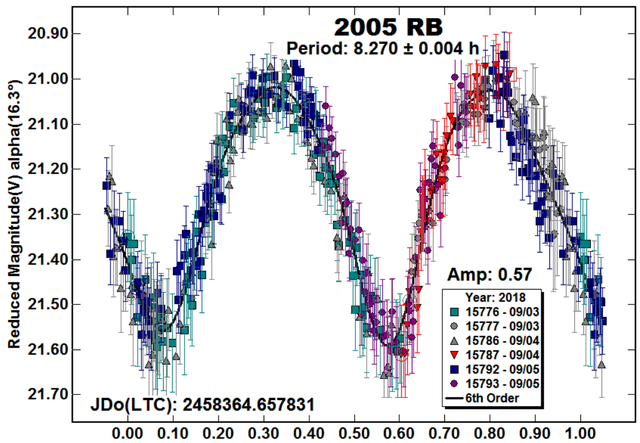

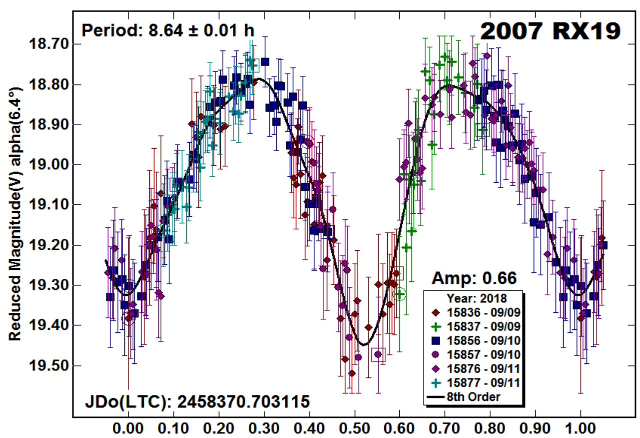

2011 UA. As the period spectrum shows, there are three very strong solutions. Narrowing down the preferred period relied mostly on the symmetry or asymmetry of the lightcurves.

The shortest solution of about 0.15 h produced a monomodal lightcurve. The low amplitude allowed that possibility (Harris et al., 2014), but the slight asymmetry of the bimodal solution at 0.316391 h eliminated the monomodal solution. This meant that either the bimodal or a quadramodal one with a doubled-period was more likely correct.

A "split-halves" plot was made for the longer period of 0.63280 h. This is where the second half of a lightcurve is superimposed on the first half (see Harris et al., 2014). If this results in the two halves being essentially the same, there is a reasonable chance that the half-period is the correct solution. Based on this, a period of 0.316391 h is adopted here.

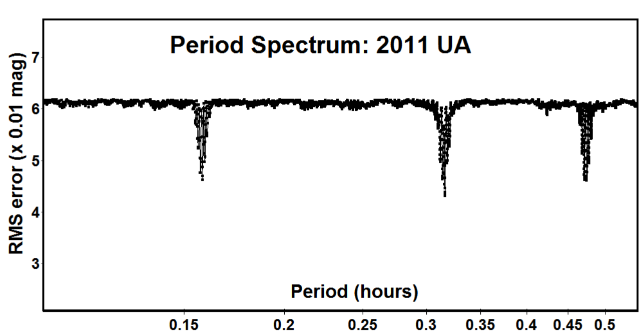

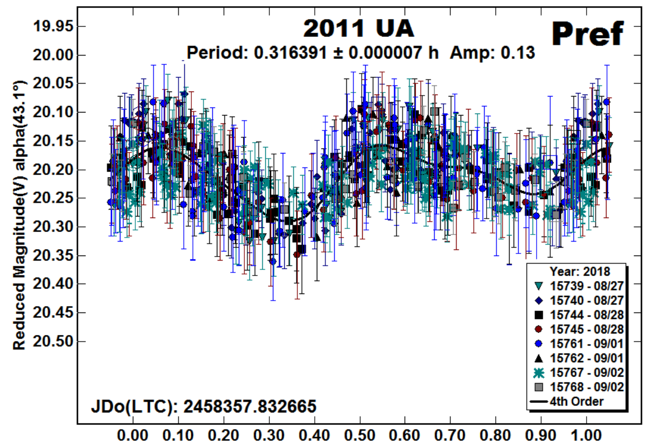

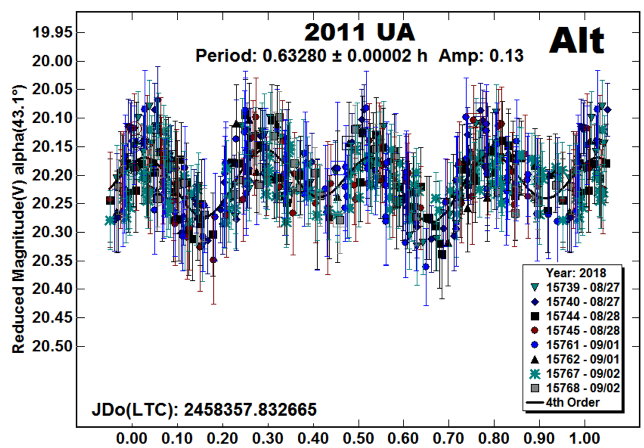

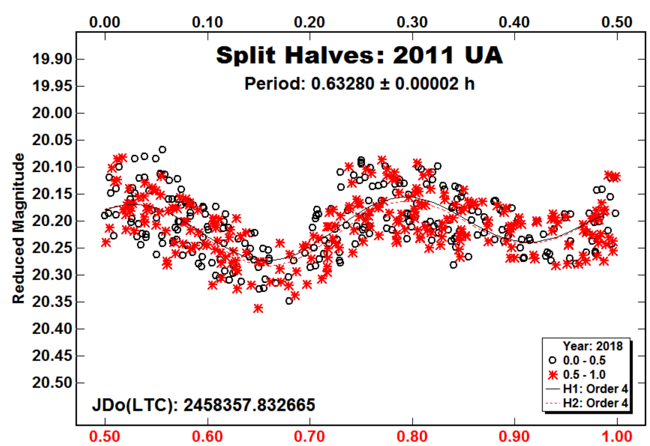

Even if the period of 0.15 h or 0.63 h is correct, this still makes the asteroid somewhat unusual. The frequency-diameter plot based on data from the LCDB shows that the asteroid is well above the spin barrier. It is also to the right of the "ascending branch" which starts at about 0.2 km diameter and *roughly* defines a point where tumbling becomes more possible.

The location on the frequency-diameter plot is very close to the first object discovered (Pravec et al., 2002) in what might be called the "forbidden zone" (the term is ours and not one formally or even informally adopted within the planetary science community). Polishook et al. (2017) did an extensive analysis of the asteroid, including the constraints on the internal structure that would help keep the asteroid from breaking apart given its size and rotation period.

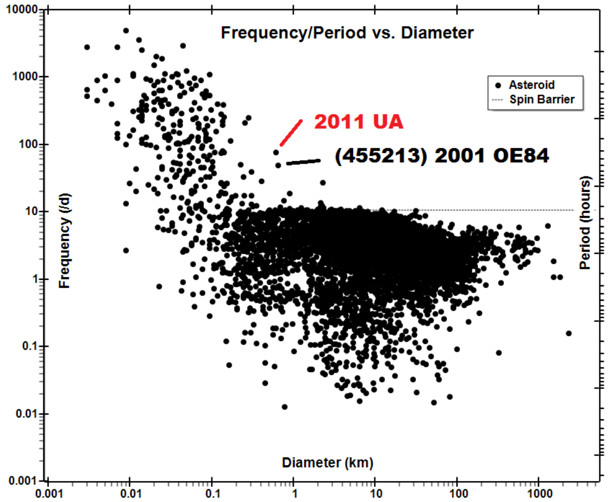

2011 GA62, 2012 OD1. There were no previous rotation periods in the LCDB for 2011 GA62 or 2012 OD1. The solution for 2011 GA 62 is considered fully secure.

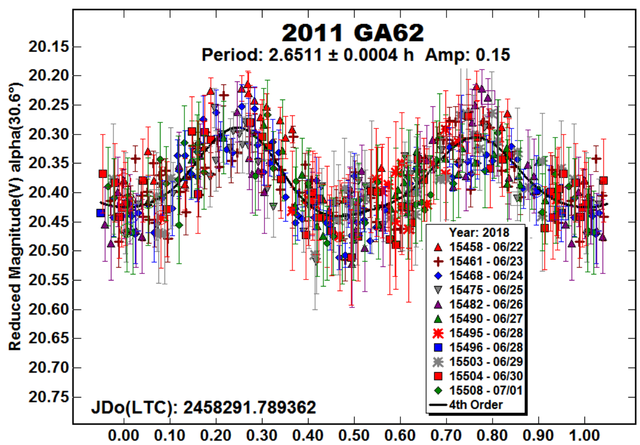

The period for 2012 is not as secure but it is very likely to be close to the correct solution. The large amplitude made this possible despite the large error bars.

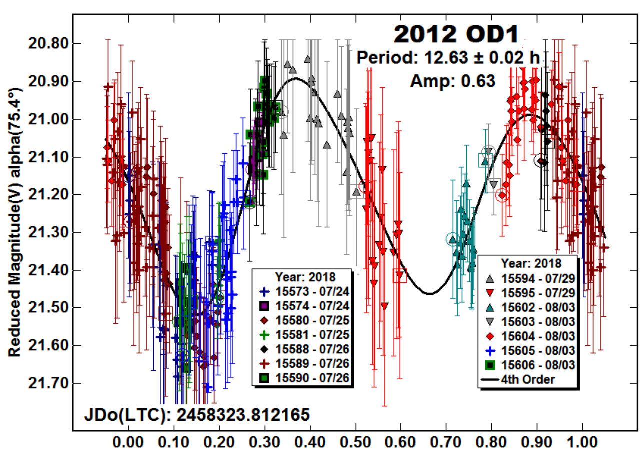

2013 EP41, 2015 AX16, 2015 RJ83, 2015 FP118. These four NEAs are new additions to the LCDB. Of the four, the solution for 2013 EP41 might be the least secure because of the low amplitude and large error bars.

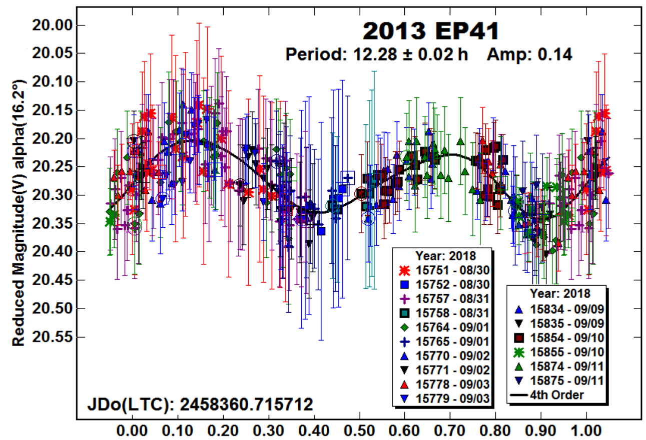

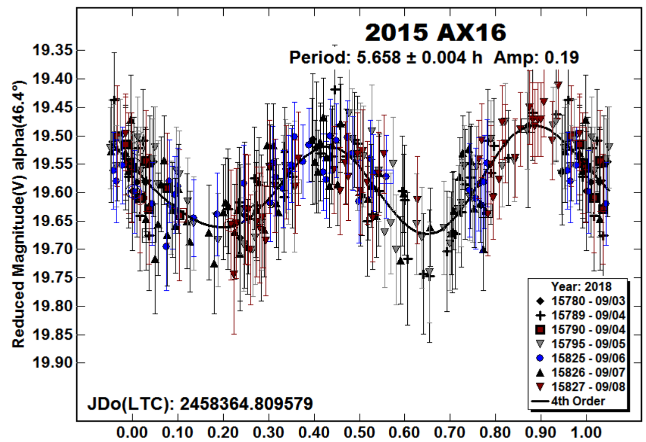

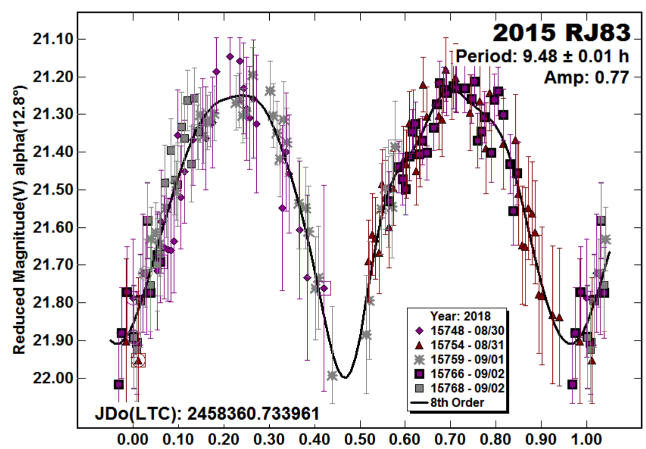

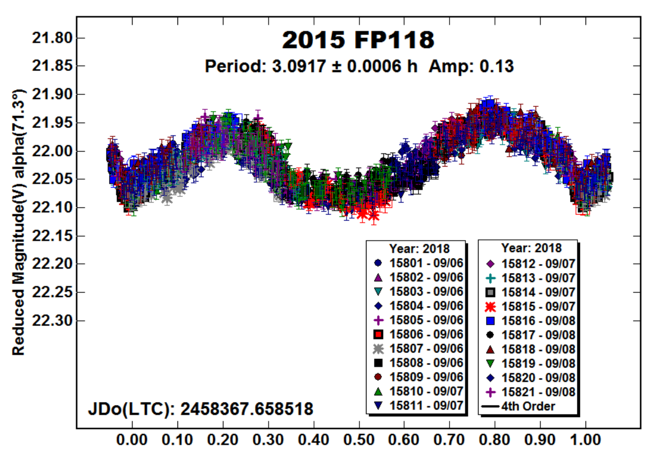

2016 NF23. The adopted period of 17.1 h was the best fit in the period spectrum. The result is supported by the slopes of the lightcurve data and model and an amplitude that makes anything other than a bimodal solution unlikely (Harris et al., 2014)

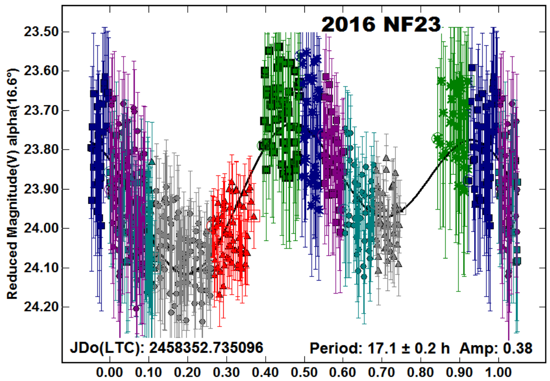

2018 NB. The period spectrum strongly favored the adopted period of 50.2 h. The half-period, with a monomodal lightcurve, was not considered likely because of the apparent amplitude.

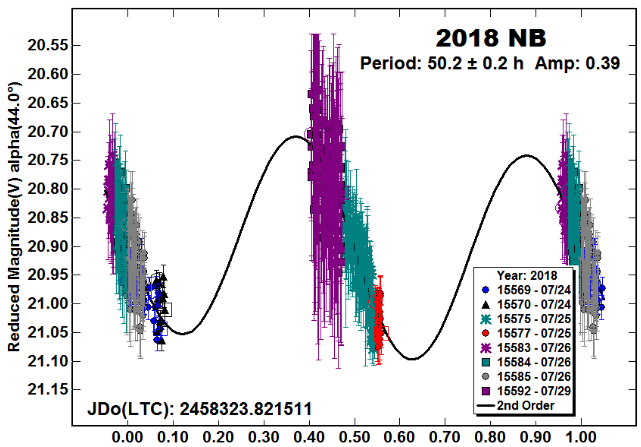

2018 QU1. There were no previous entries of any kind in the LCDB. Despite the large error bars, the solution is considered secure since the scatter in the data is relatively low and, therefore, the data closely follow the Fourier curve.

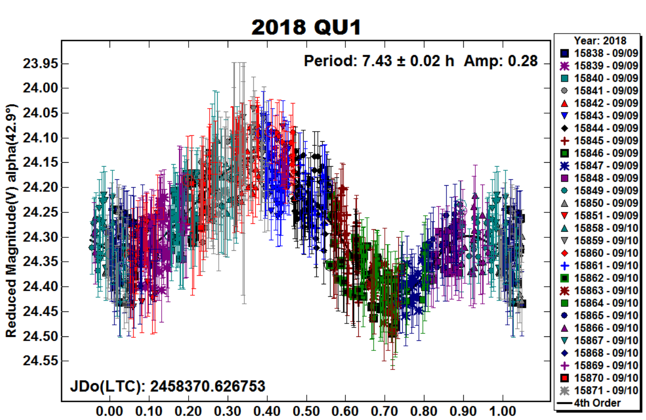

2018 QV1. The period spectrum favored 67.9 h. To be more certain about this, the data were forced to alternates of 34.1 h and 17.84 h. The lightcurve forced to 17.84 h, shown below, is an improbable result. This reinforces the conclusion that 34.1 h is the approximate half-period of the adopted period of 67.9 h. Unfortunately, confirming observations are not coming any time soon. The 2018 apparition is the only one between 1995 and 2050 where the asteroid is brighter than V = 18. The brightest apparition from 2019-2050 is V ~ 21.3 in 2049.

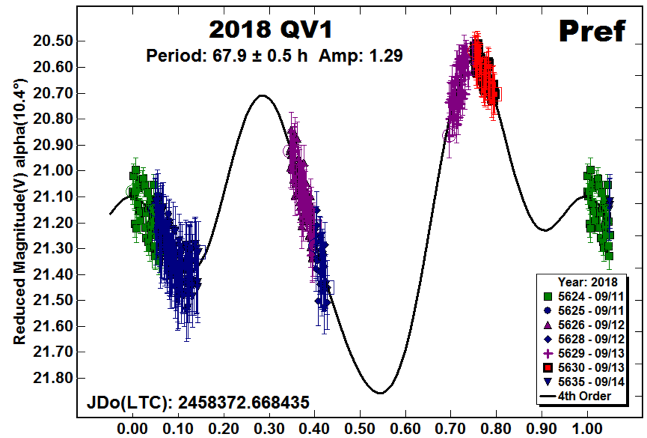

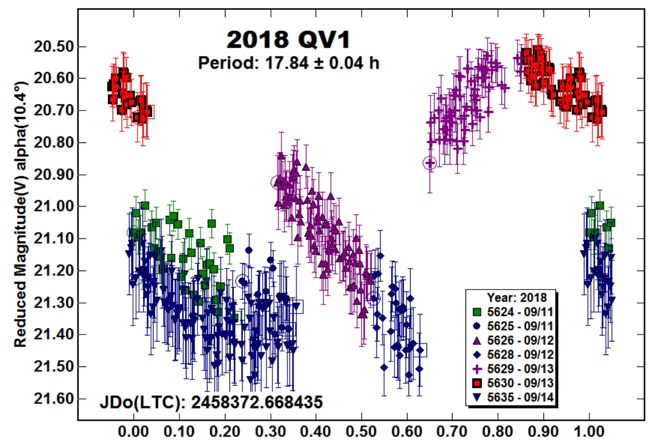

2018 LQ2. There were no previous entries of any kind in the LCDB. The estimated diameter, assuming an albedo of 0.2, is only 30 meters. At such a small size, it was a good candidate for tumbling. There were no signs of that.

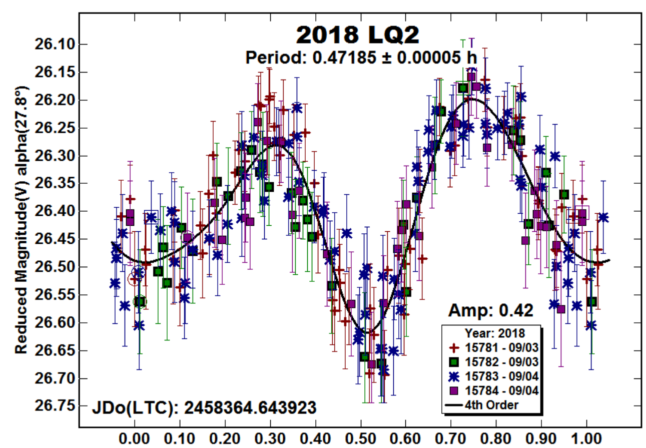

2018 RQ2. Finding a single period for this 80-meter NEA, and new addition to the LCDB, wasn't enough. The data fit four nearly likely results. The period spectrum favored 8.58 h (#3), but this had a gap in the bimodal lightcurve that raised concerns that this was a "fit by exclusion" solution, one where the number of overlapping data points is minimized by the Fourier algorithm.

The second more-likely period was the half-period at 4.28 h (#1). However, given the low amplitude and large error bars, a solution of 5.17 h (#2) was examined. This one was chosen over one near 3.8 h because the double period of 10.80 h (#4) produced a bimodal lightcurve with no gaps and had nearly the same RMS fit as the one at 8.58 h. We have adopted P = 8.58 h, mostly because it's the most favored in the period spectrum.

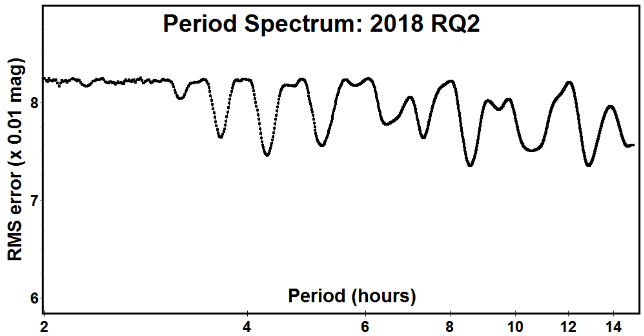

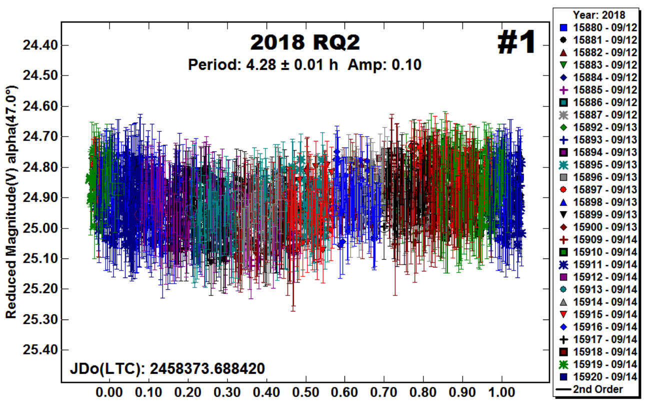

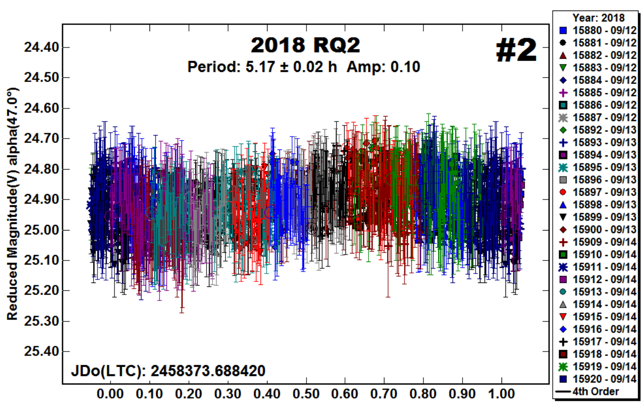

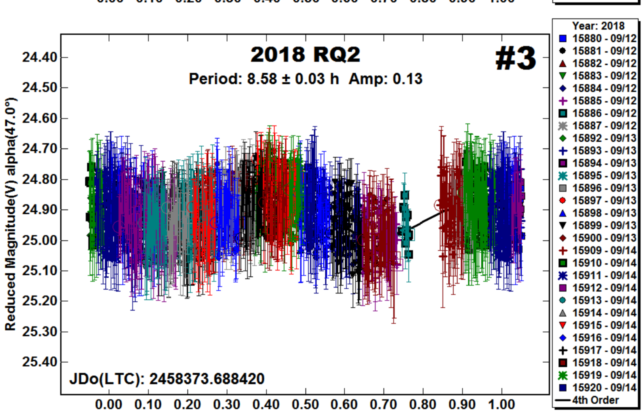

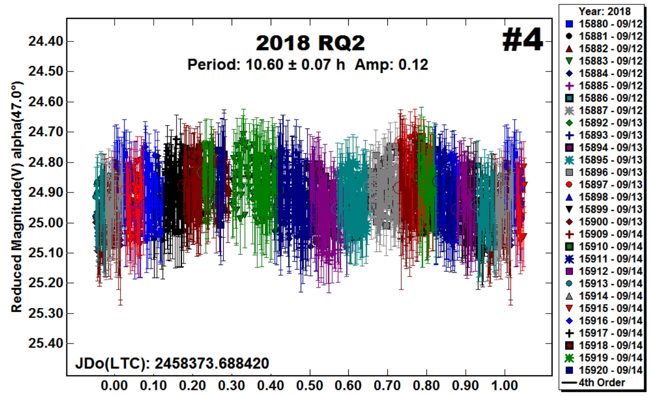

Looking ahead, the only apparition brighter than V = 19 is in 2028. As is the case for so many other NEAs, the observations in 2018 were a once-in-a-lifetime opportunity for those with modest telescopes.

2018 KE3. The initial observations were made in 2018 mid-August. These led to a period of 4.158 h with no obvious signs of a second period. The follow-up observations three weeks later told a different story.

Those new data indicated the possibility of two periods. One was very similar to the earlier result, P_1 = 4.168 h. However, this was superimposed on a longer period, P_2 = 47.08 h. Shorter periods for P_2 were tried, e.g., ≈24 h. That produced a convincing second-order fit to a monomodal lightcurve. We have adopted 47.08 h for P_2.

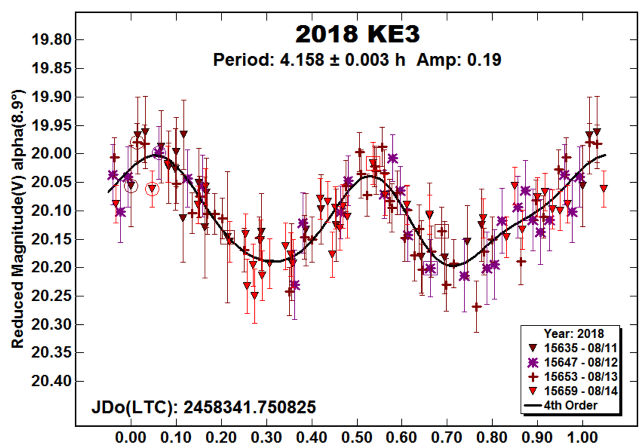

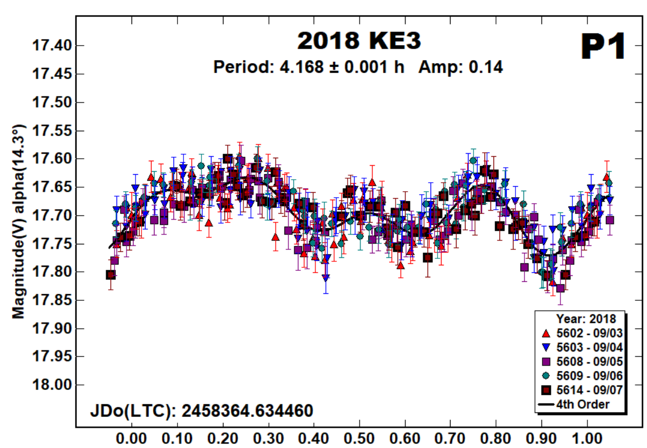

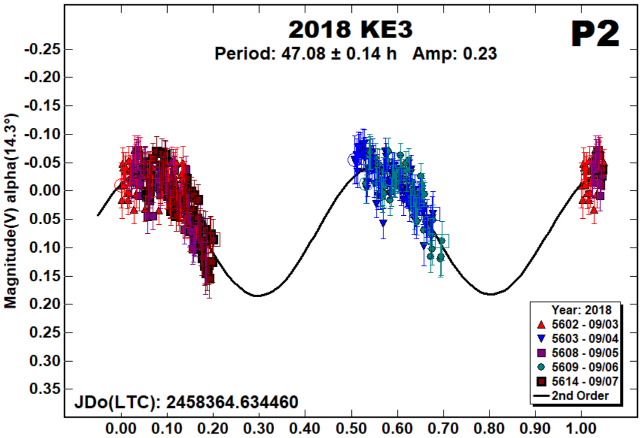

This makes 2018 KE3 a potential new member of the rare class of very wide binaries (see Warner, 2016a).

2018 GA5. There were no previous entries in the LCDB for this NEA. The solution is weak because of the large error bars.

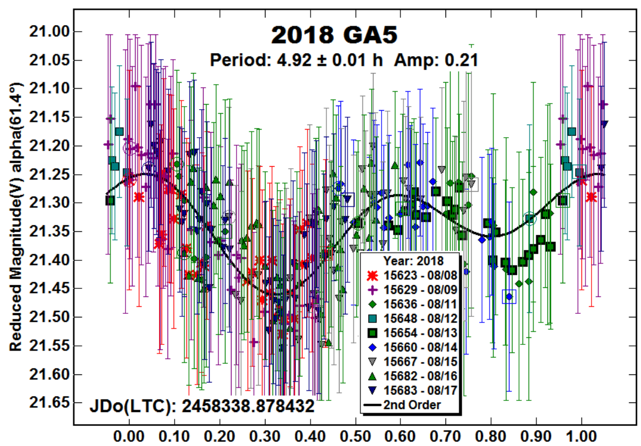

2018 MM8. The period spectrum for 2018 MM8 showed several distinct solutions. We used the split-halves plot to try to remove doubt about a period of 5.048 h over one between 2.5-2.9 h. The result showed two distinct halves. Combined with the amplitude of 0.27 mag, P = 5.048 h is considered reasonably secure.

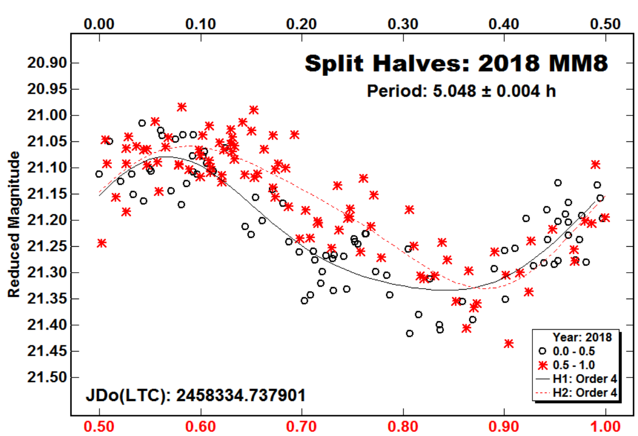

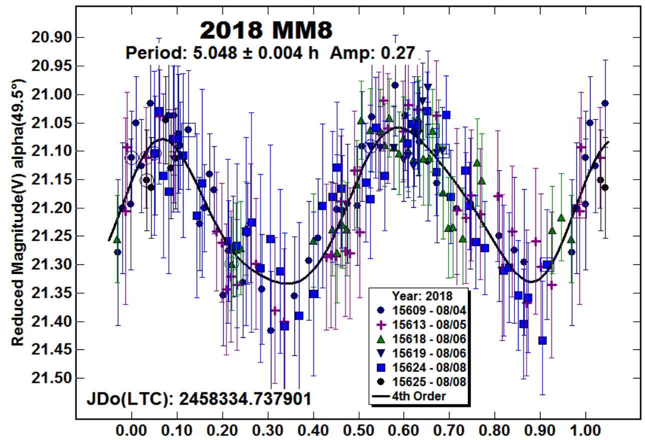

2018 PJ10. The period spectrum favored 1.75 or 3.5 h. The shorter period produced a bimodal lightcurve with an amplitude of 0.27 mag. This seemed more likely than a quadramodal solution at 3.5 hours. P = 1.75 h puts the asteroid just above the spin barrier in the frequency-diameter plot, but far enough left to be in the ascending branch, making it an "ordinary" and not particularly unusual asteroid.

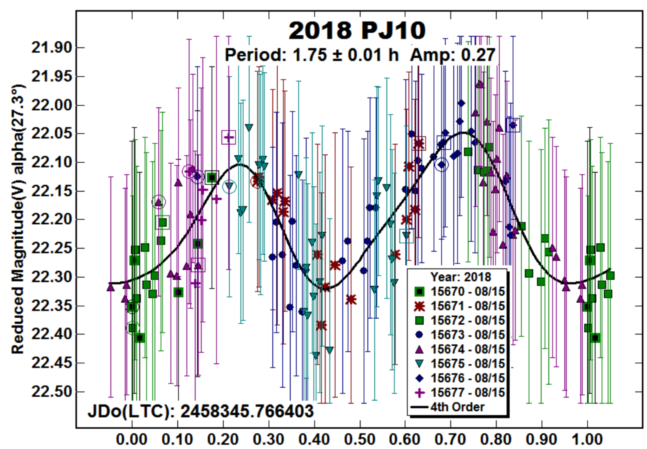

Acknowledgements

Observations at CS3 and continued support of the asteroid lightcurve database (LCDB; Warner et al., 2009) are supported by NASA grant 80NSSC18K0851. Work on the asteroid lightcurve database (LCDB) was also partially funded by National Science Foundation grant AST-1507535.

This research was made possible through the use of the AAVSO Photometric All-Sky Survey (APASS), funded by the Robert Martin Ayers Sciences Fund, and by data from CMC15 Data Access Service at CAB (INTA-CSIC) (*http://svo2.cab.inta-csic.es/vocats/cmc15/*).

The authors gratefully acknowledge Shoemaker NEO Grants from the Planetary Society (2007, 2013). These were used to purchase some of the telescopes and CCD cameras used in this research.

References

References from web sites should be considered transitory, unless from an agency with a long lifetime expectancy. Sites run by private individuals, even if on an institutional web site, do not necessarily fall into this category.

Number	Name	2018 mm/dd	Pts	Phase	L_{PAB}	B_{PAB}	Period(h)	P.E.	Amp	A.E.
433	Eros	08/18-08/21	525	40.2,40.3	26	13	5.270	0.005	0.11	0.01
719	Albert	08/08-08/12	151	44.3,46.0	276	20	5.800	0.002	1.08	0.02
1865	Cerberus	09/08-09/10	211	21.9,20.6	3	18	6.800	0.002	1.56	0.02
3552	Don Quixote	08/18-08/21	219	34.8,34.2	35	18	6.665	0.005	0.58	0.02
4183	Cuno	08/09-08/18	223	5.1,2.0	326	4	3.58	0.01	0.09	0.02
6456	Golombek	07/24-08/03	152	30.1,24.7	328	0	2.5014	0.0002	0.14	0.01
9856	1991 EE	09/12-09/15	124	44.7,41.7	32	-7	3.048	0.002	0.19	0.01
13553	Masaakikoyama	08/19-08/26	2098	23.0,18.2	337	13	58	3	0.75	0.10
16834	1997 WU22	09/15-09/18	189	27.4,26.0	27	21	9.349	0.004	0.63	0.03
17274	2000 LC16	08/30-09/05	665	24.0,25.3	323	8	16.50	0.02	0.23	0.02
18109	2000 NG11	08/23-08/25	200	10.8,9.7	339	-2	4.253	0.005	0.78	0.02
86324	1999 WA2	08/18-08/28	279	44.4,51.0	287	20	7.161	0.003	0.18	0.02
86878	2000 HD24	08/11-08/21	277	68.9,89.1	16	27	15.72	0.02	0.28	0.05
115052	2003 RD6	09/03-09/08	413	36.4,31.1	360	26	12.08	0.04	0.11	0.02
141527	2002 FG7	08/09-08/10	163	54.8,56.4	353	18	6.31	0.02	0.97	0.05
283729	2002 UX	07/31-08/06	110	40.1,43.3	286	28	5.937	0.005	0.23	0.02
333889	1998 SV4	09/05-09/08	169	35.6,32.3	15	-2	2.817	0.002	0.27	0.03
337248	2000 RH60	09/12-09/15	288	10.5,8.9	351	7	25.2	0.1	0.35	0.04
418929	2009 DM1	08/27-09/02	204	19.2,3.5,18.4	343	15	4.590	0.005	0.17	0.03
438429	2006 WN1	08/30-09/02	208	32.3,32.1	323	16	3.407	0.002	0.18	0.02
441987	2010 NY65	[16]07/01-07/03	511	56.6,51.9	259	21	5.593	0.007	0.18	0.03
441987	2010 NY65	[17]06/27-06/29	593	71.2,58.3	257	29	5.518	0.004	0.16	0.02
441987	2010 NY65	07/02-07/06	292	48.2,43.3	268	22	5.541	0.003	0.24	0.03
457260	2008 RY24	09/04-09/05	214	30.0,29.9	10	8	8.19	0.02	0.09	0.02
481394	2006 SF6	09/09-09/13	246	23.5,22.8	348	17	11.517	0.006	0.97	0.04
	1999 RB32	08/09-08/17	170	22.9,26.5	337	-1	42.7	0.2	0.27	0.03
	1999 VQ11	09/10-09/24	152	60.6,61.5	47	-3	32.21	0.02	0.79	0.10
	2001 QA143	09/11-09/14	135	22.8,22.9	2	13	11.78	0.03	0.25	0.03
	2005 RB	09/03-09/05	415	16.2,13.7	345	10	8.270	0.004	0.57	0.03
	2007 RX19	09/09-09/11	237	6.4,4.4	353	1	8.64	0.01	0.68	0.04
	2011 UA	08/27-09/02	375	43.2,35.9	179	-6	0.316391	0.000007	0.13	0.03
	2011 GA62	06/22-07/01	419	30.6,34.5	293	11	2.6511	0.0004	0.15	0.02
	2012 OD1	07/24-08/03	274	75.5,60.9	340	29	12.63	0.02	0.63	0.05
	2013 EP41	08/30-09/11	300	16.2,2.8,3.1	348	3	12.28	0.02	0.14	0.02
	2015 AX16	09/03-09/08	266	46.4,48.5	22	1	5.658	0.004	0.19	0.03
	2015 RJ83	08/30-09/01	162	12.8,10.9	344	5	9.48	0.01	0.76	0.04
	2015 FP118	09/06-09/08	1304	70.6,59.0	6	27	3.0917	0.0006	0.13	0.01
	2016 NF23	08/22-08/24	572	16.4,5.7	336	0	17.1	0.2	0.39	0.05
	2018 NB	07/24-07/29	396	43.9,52.2	330	0	50.2	0.2	0.39	0.04
	2018 QU1	09/09-09/10	721	44.9,57.4	355	26	7.43	0.02	0.28	0.04
	2018 QV1	09/11-09/14	397	10.4,13.4	342	4	67.9	0.5	0.85	0.10
	2018 LQ2	09/03-09/04	208	30.2,28.6	338	15	0.47185	0.00005	0.42	0.03
	2018 RQ2	09/12-09/14	1470	47.2,56.7	15	9	8.58	0.03	0.13	0.03
	2018 KE3	08/11-08/14	124	8.9,7.8	326	0	4.158	0.003	0.19	0.01
	2018 KE3	09/03-09/07	326	14.3,16.1	341	11	[P]4.168	0.001	0.14	0.02
	2018 KE3						47.08	0.14	0.23	0.02
	2018 GA5	08/08-08/17	276	61.5,54.7	81	-10	4.92	0.02	0.21	0.04
	2018 MM8	12/31-12/31	180	30.2,0.0,28.6	0	0	5.048	0.004	0.27	0.03
	2018 PJ10	08/15-08/15	137	27.1,27.1	338	4	1.75	0.01	0.27	0.04

Table II. Observing circumstances. [yy] indicates the data are from 20yy. [P] indicates the period for the primary in a binary system. The phase iangle (α) is given at the start and end of each date range, unless it reached a minimum, which is then the second of three values. L_{PAB} and B_{PAB} are, respectively the average phase angle bisector longitude and latitude.

Chang, C.-K., Ip, W.-H., Lin, H.-W., Cheng, Y.-C., Ngeow, C.-C., Yang, T.-C., Waszczak, A., Kulkarni, S.R., Levitan, D., Sesar, B., Laher, R., Surace, J., Prince, T.A. (2015). "Asteroid Spin-rate Study Using the Intermediate Palomar Transient Factory." *Ap. J. Suppl. Ser.* **219**, A27.

Harris, A.W., Young, J.W., Scaltriti, F., Zappala, V. (1984). "Lightcurves and phase relations of the asteroids 82 Alkmene and 444 Gyptis." *Icarus* **57**, 251-258.

Harris, A.W., Young, J.W., Bowell, E., Martin, L.J., Millis, R.L., Poutanen, M., Scaltriti, F., Zappala, V., Schober, H.J., Debehogne, H., Zeigler, K.W. (1989). "Photoelectric Observations of Asteroids 3, 24, 60, 261, and 863." *Icarus* **77**, 171-186.

Harris, A.W., Pravec, P., Galad, A., Skiff, B.A., Warner, B.D., Vilagi, J., Gajdos, S., Carbognani, A., Hornoch, K., Kusnirak, P., Cooney, W.R., Gross, J., Terrell, D., Higgins, D., Bowell, E., Koehn, B.W. (2014). "On the maximum amplitude of harmonics on an asteroid lightcurve." *Icarus* **235**, 55-59.

Henden, A.A., Terrell, D., Levine, S.E., Templeton, M., Smith, T.C., Welch, D.L. (2009). *http://www.aavso.org/apass*

Mommert, M., Polishook, D., Moskovitz, N. (2018). *CBET* **4502**.

Munos, J.L. (2017) Carlsberg Meridian Catalog web site. *http://svo2.cab.inta-csic.es/vocats/cmc15/*

Polishook, D., Moskovitz, N., Thirouin, A., Bosh, A., Levine, S., Zuluaga, C., Tegler, S.C., Aharonson, O. (2017). "The fast spin of near-Earth asteroid (455213) 2001 OE84, revisited after 14 years: Constraints on internal structure." *Icarus* **297**, 126-133.

Pravec, P., Wolf, M., Sarounova, L. (1997, 2000, 2001, 2005, 2008, 2018). *http://www.asu.cas.cz/~ppravec/neo.htm*

Pravec, P., Kusnirak, P., Sarounova, L., Harris, A.W., Binzel, R.P., Rivkin, A.S. (2002). "Large coherent asteroid 2001 OE84." Proc. ACM 2002, ESA SP-500, 743-745.

Rubincam, D.P. (2000). "Relative Spin-up and Spin-down of Small Asteroids." *Icarus* **148**, 2-11.

Skiff, B.A., Bowell, E., Koehn, B.W., Sanborn, J.J., McLelland, K.P., Warner, B.D. (2012). *Minor Planet Bull*. **39**, 111-130.

Warner, B.D., Harris, A.W., Pravec, P. (2009). "The Asteroid Lightcurve Database." *Icarus* **202**, 134-146. Updated 2018 April. *http://www.minorplanet.info/lightcurvedatabase.html*

Warner, B.D. (2014a). *Minor Planet Bull.* **41**, 113-124.

Warner, Brian D. (2014b). "Near-Earth Asteroid Lightcurve Analysis at CS3-Palmer Divide Station: 2014 March-June." *Minor Planet Bull*. **41**, 213-224.

Warner, B.D. (2015a). "Near-Earth Asteroid Lightcurve Analysis at CS3-Palmer Divide Station: 2014 October-December." *Minor Planet Bull.* **42**, 115-127.

Warner, B.D. (2015b). "Near-Earth Asteroid Lightcurve Analysis at CS3-Palmer Divide Station: 2015 March-June." *Minor Planet Bull.* **42**, 256-266.

Warner, B.D. (2016a). "Three Additional Candidates for the Group of Very Wide Binaries." *Minor Planet Bul.* **43**, 306-309.

Warner, B.D. (2016b). "Near-Earth Asteroid Lightcurve Analysis at CS3-Palmer Divide Station: 2016 April-July." *Minor Planet Bull*. **43**, 311-319.

Warner, B.D. (2017a). "Near-Earth Asteroid Lightcurve Analysis at CS3-Palmer Divide Station: 2016 July-September." *Minor Planet Bull*. **44**, 22-36.

Warner, B.D. (2017b). "Near-Earth Asteroid Lightcurve at CS3-Palmer Divide Station: 2017 April thru June." *Minor Planet Bull.* **44**, 335-344.

Warner, B.D. (2018). "Near-Earth Asteroid Lightcurve Analysis at CS3-Palmer Divide Station: 2018 April-June." *Minor Planet Bull*. **45**, 366-379.

Waszczak, A., Chang, C.-K., Ofek, E.O., Laher, R., Masci, F., Levitan, D., Surace, J., Cheng, Y.-C., Ip, W.-H., Kinoshita, D., Helou, G., Prince, T.A., Kulkarni, S. (2015). "Asteroid Light Curves from the Palomar Transient Factory Survey: Rotation Periods and Phase Functions from Sparse Photometry." *Astron. J.* **150**, A75.

Wisniewski, W.Z., Michalowski, T.M., Harris, A.W., McMillan, R.S. (1997). "Photometric Observations of 125 Asteroids." *Icarus* **126**, 395-449.

MINOR PLANETS AT UNUSUALLY FAVORABLE ELONGATIONS IN 2019

Frederick Pilcher
4438 Organ Mesa Loop
Las Cruces, NM 88011 USA
fpilcher35@gmail.com

(Received: 2018 September 18)

A list is presented of minor planets which are much brighter than usual at their 2019 apparitions.

The minor planets in the lists which follow will be much brighter at their 2019 apparitions than at their average distances at maximum elongation. Many years may pass before these planets will be again as bright as in 2019. Observers are encouraged to give special attention to those which lie near the limit of their equipment.

These lists have been prepared by an examination of the maximum elongation circumstances of minor planets computed by the author for all years through 2060 with a full perturbation program written by Dr. John Reed, and to whom he expresses his thanks. Elements are from EMP 1992, except that for all planets for which new or improved elements have been published subsequently in the Minor Planet Circulars or in electronic form, the newer elements have been used. Planetary positions are from the JPL DE-200 ephemeris, courtesy of Dr. E. Myles Standish.

Any planets whose brightest magnitudes near the time of maximum elongation vary by at least 2.0 in this interval and in 2019 will be within 0.3 of the brightest occurring, or vary by at least 3.0 and in 2019 will be within 0.5 of the brightest occurring; and which are visual magnitude 14.5 or brighter, are included. For planets brighter than visual magnitude 13.5, which are within the range of a large number of observers, these standards have been relaxed somewhat to include a larger number of planets. Magnitudes have been computed from the updated magnitude parameters published in MPC28104-28116, on 1996 Nov. 25, or more recently in the Minor Planet Circulars.

Oppositions may be in right ascension or in celestial longitude. Here we use still a third representation, maximum elongation from the Sun, instead of opposition. Though unconventional, it has the advantage that many close approaches do not involve actual opposition to the Sun near the time of minimum distance and greatest brightness and are missed by an opposition-based program. Other data are also provided according to the following tabular listings: Minor planet number, date of maximum elongation from the Sun in format yyyy/mm/dd, maximum elongation in degrees, right ascension on date of maximum elongation, declination on date of maximum elongation, both in J2000 coordinates, date of brightest magnitude in format yyyy/mm/dd, brightest magnitude, date of minimum distance in format yyyy/mm/dd, and minimum distance in AU.

Users should note that when the maximum elongation is about 177° or greater, the brightest magnitude is sharply peaked due to enhanced brightening near zero phase angle. Even as near as 10 days before or after minimum magnitude the magnitude is generally about 0.4 greater. This effect takes place in greater time interval for smaller maximum elongations. There is some interest in very small minimum phase angles. For maximum elongations

E near 180° at Earth distance Δ, an approximate formula for the minimum phase angle φ is φ=(180°-E)/(Δ+1).

A special list of asteroids approaching the Earth more closely than 0.3 AU is provided following the list of temporal sequence of favorable elongations.

Table I. Numerical Sequence of Favorable Elongations

	Max Elong				Br Mag		Min Dist	
Planet	Date	Elong	RA	Dec	Date	Mag	Date	Dist
21	2019/09/28	174.3°	0h25m	- 3°	2019/09/27	9.4	2019/09/22	1.083
24	2019/01/14	178.7°	7h41m	+22°	2019/01/14	10.7	2019/01/16	1.801
33	2019/10/14	179.2°	1h15m	+ 8°	2019/10/14	10.1	2019/10/04	0.998
36	2019/09/15	176.0°	23h36m	- 6°	2019/09/16	10.5	2019/09/25	1.099
39	2019/08/17	176.0°	21h38m	- 9°	2019/08/17	9.2	2019/08/19	1.516
69	2019/12/30	165.9°	6h30m	+ 9°	2019/12/30	10.4	2019/12/31	1.519
77	2019/10/05	179.2°	0h42m	+ 5°	2019/10/05	11.3	2019/10/08	1.419
86	2019/12/19	179.9°	5h46m	+23°	2019/12/19	11.7	2019/12/13	1.628
97	2019/12/02	157.0°	4h43m	- 0°	2019/12/01	9.9	2019/12/01	1.037
130	2019/08/26	174.4°	22h29m	-15°	2019/08/26	10.5	2019/08/31	1.615
132	2019/12/14	176.5°	5h27m	+19°	2019/12/14	11.0	2019/12/28	0.952
135	2019/09/06	179.7°	22h57m	- 6°	2019/09/06	9.6	2019/09/01	0.934
176	2019/11/06	164.7°	3h 7m	+ 1°	2019/11/05	11.6	2019/11/03	1.685
247	2019/09/23	179.3°	23h58m	- 0°	2019/09/23	10.4	2019/09/29	1.256
265	2019/03/21	151.1°	11h50m	-28°	2019/03/26	13.2	2019/04/01	0.916
283	2019/08/13	176.3°	21h26m	-11°	2019/08/13	12.2	2019/08/16	1.670
304	2019/08/26	175.9°	22h10m	- 6°	2019/08/26	11.1	2019/08/25	0.861
333	2019/08/30	178.3°	22h36m	-10°	2019/08/30	12.9	2019/09/02	1.705
341	2019/07/22	167.1°	20h16m	-33°	2019/07/23	11.8	2019/07/26	0.791
347	2019/12/23	178.1°	6h 5m	+25°	2019/12/23	11.9	2019/12/29	1.482
380	2019/09/05	170.2°	23h 9m	-16°	2019/09/04	12.4	2019/09/03	1.378
384	2019/01/05	171.8°	7h 7m	+30°	2019/01/05	12.3	2019/01/03	1.301
385	2019/03/17	175.4°	11h40m	- 2°	2019/03/17	10.6	2019/03/18	1.510
390	2019/01/12	174.9°	7h35m	+26°	2019/01/12	13.1	2019/01/14	1.343
405	2019/04/21	162.6°	13h21m	-27°	2019/04/21	10.5	2019/04/21	0.978
410	2019/06/15	174.8°	17h30m	-18°	2019/06/15	10.3	2019/06/16	1.053
413	2019/08/17	148.7°	23h13m	-37°	2019/08/23	11.8	2019/08/27	0.798
422	2019/09/24	178.3°	0h 5m	- 1°	2019/09/24	11.6	2019/09/19	0.759
429	2019/10/30	178.9°	2h14m	+14°	2019/10/30	12.3	2019/10/28	1.295
449	2019/01/20	176.8°	8h 9m	+23°	2019/01/20	11.6	2019/01/22	1.135
459	2019/11/30	167.7°	4h20m	+33°	2019/11/30	12.7	2019/11/27	1.114
479	2019/01/01	171.1°	6h41m	+14°	2018/12/31	12.4	2018/12/25	1.313
488	2019/02/27	162.5°	11h 7m	+24°	2019/02/27	11.6	2019/02/27	1.705
504	2019/08/27	161.3°	23h 0m	-26°	2019/08/28	12.0	2019/08/29	1.172
519	2019/08/06	160.8°	21h28m	-35°	2019/08/07	12.2	2019/08/10	1.358
532	2019/02/05	166.3°	9h36m	+28°	2019/02/06	8.9	2019/02/10	1.424
540	2019/04/13	179.8°	13h24m	- 8°	2019/04/13	12.4	2019/04/12	1.031
563	2019/12/24	177.7°	6h 7m	+25°	2019/12/23	10.6	2019/12/19	1.140
675	2019/11/11	169.8°	2h50m	+26°	2019/11/11	10.5	2019/11/11	1.227
678	2019/10/30	169.1°	1h58m	+23°	2019/10/30	11.0	2019/10/30	1.027
703	2019/09/21	176.9°	23h49m	+ 2°	2019/09/22	13.5	2019/09/24	0.904
711	2019/09/22	179.4°	23h56m	+ 0°	2019/09/22	13.4	2019/09/13	0.956
746	2019/08/19	161.5°	22h14m	-30°	2019/08/18	13.2	2019/08/16	1.405
765	2019/12/19	170.4°	5h41m	+32°	2019/12/17	14.2	2019/12/08	0.975
768	2019/11/03	179.3°	2h30m	+15°	2019/11/03	13.1	2019/11/04	1.493
770	2019/11/27	176.8°	4h 9m	+24°	2019/11/27	12.3	2019/11/26	0.899
788	2019/04/22	167.0°	14h19m	- 0°	2019/04/22	12.1	2019/04/24	1.726
791	2019/07/21	174.1°	19h52m	-14°	2019/07/21	12.6	2019/07/24	1.578
817	2019/12/15	165.7°	5h26m	+ 8°	2019/12/14	13.4	2019/12/10	1.200
848	2019/09/09	178.7°	23h 5m	- 4°	2019/09/08	14.1	2019/09/06	1.605
900	2019/07/18	159.3°	19h29m	- 0°	2019/07/18	14.2	2019/07/19	1.092
914	2019/06/24	161.2°	18h30m	- 5°	2019/06/26	10.8	2019/06/29	0.977
940	2019/09/12	170.5°	23h36m	-12°	2019/09/12	13.4	2019/09/11	1.796
944	2019/02/05	112.8°	11h46m	+81°	2018/11/23	14.3	2018/11/24	1.448
953	2019/05/27	172.5°	16h12m	-28°	2019/05/28	13.2	2019/06/03	1.377
1000	2019/05/06	145.8°	13h58m	-48°	2019/05/09	13.1	2019/05/11	1.470
1003	2019/12/31	178.1°	6h39m	+21°	2019/12/31	13.5	2019/12/31	1.657
1041	2019/10/19	167.2°	1h51m	- 2°	2019/10/20	13.5	2019/10/20	1.668
1057	2019/11/15	177.3°	3h18m	+21°	2019/11/15	13.5	2019/11/08	1.291
1066	2019/08/17	176.4°	21h50m	-16°	2019/08/17	14.1	2019/08/23	0.961
1067	2019/12/26	175.2°	6h16m	+28°	2019/12/26	13.7	2019/12/20	1.470
1074	2019/12/21	178.9°	5h53m	+24°	2019/12/21	13.3	2019/12/17	1.647
1107	2019/01/06	179.0°	7h 7m	+21°	2019/01/06	12.7	2019/01/06	1.806
1136	2019/08/25	164.3°	21h49m	+ 3°	2019/08/26	13.0	2019/08/30	0.965
1165	2019/06/17	161.1°	17h48m	- 4°	2019/06/19	13.8	2019/06/22	1.550
1187	2019/11/15	159.8°	2h57m	+37°	2019/11/14	13.7	2019/11/12	1.101
1212	2019/01/17	174.0°	7h49m	+15°	2019/01/17	14.1	2019/01/19	2.253
1278	2019/08/07	162.3°	21h39m	-32°	2019/08/08	12.2	2019/08/09	0.789
1467	2019/08/20	179.7°	21h55m	-12°	2019/08/20	12.4	2019/08/18	1.943
1530	2019/10/08	170.1°	0h38m	+14°	2019/10/08	14.4	2019/10/06	0.811
1585	2019/02/06	168.5°	8h56m	+ 5°	2019/02/04	14.0	2019/01/26	1.520
1607	2019/07/17	177.4°	19h39m	-18°	2019/07/17	13.4	2019/07/30	1.017
1634	2019/06/29	178.1°	18h33m	-25°	2019/06/29	14.2	2019/06/30	0.866
1680	2019/05/13	176.0°	15h23m	-14°	2019/05/13	13.6	2019/05/15	1.223
1681	2019/12/22	179.0°	6h 0m	+22°	2019/12/22	13.6	2019/12/23	1.163
1703	2019/09/10	171.9°	23h27m	-12°	2019/09/10	13.8	2019/09/06	0.850
1761	2019/02/21	176.0°	10h23m	+14°	2019/02/21	14.5	2019/02/18	1.496
1866	2019/05/25	135.0°	18h58m	-51°	2019/06/08	13.5	2019/06/14	0.450
2006	2019/09/22	179.5°	23h55m	- 0°	2019/09/22	13.9	2019/09/25	0.907
2013	2019/06/22	178.4°	18h 3m	-21°	2019/06/22	14.1	2019/07/03	0.948
2031	2019/09/26	177.6°	0h12m	- 1°	2019/09/26	14.2	2019/09/27	0.864
2064	2019/06/26	171.7°	18h13m	-31°	2019/06/28	12.9	2019/07/10	0.486
2081	2019/06/28	176.2°	18h27m	-27°	2019/06/28	14.0	2019/06/30	1.045
2093	2019/07/10	170.4°	19h10m	-12°	2019/07/10	14.2	2019/07/08	0.886
2100	2019/09/18	171.0°	0h 5m	- 8°	2019/09/18	13.3	2019/09/21	0.180
2167	2019/01/23	171.6°	8h11m	+11°	2019/01/23	14.5	2019/01/28	1.187
2331	2019/01/05	176.2°	7h 2m	+18°	2019/01/05	13.6	2019/01/08	0.918
2389	2019/09/08	176.7°	23h 1m	- 2°	2019/09/08	14.4	2019/08/31	0.920
2397	2019/02/04	177.0°	9h 6m	+13°	2019/02/04	14.4	2019/01/31	1.703
2433	2019/05/04	168.2°	15h 2m	- 5°	2019/05/05	14.1	2019/05/11	1.092
2466	2019/09/26	176.3°	0h16m	- 2°	2019/09/26	14.4	2019/09/24	1.208
2543	2019/10/20	173.6°	1h47m	+ 4°	2019/10/20	14.1	2019/10/10	1.482
2569	2019/11/12	170.3°	3h13m	+ 7°	2019/11/11	13.8	2019/11/09	1.231
2580	2019/09/09	177.2°	23h13m	- 8°	2019/09/09	14.1	2019/09/06	0.751
2629	2019/09/07	178.4°	23h 3m	- 4°	2019/09/07	14.5	2019/08/25	0.561
2714	2019/06/28	171.2°	18h22m	-14°	2019/06/28	14.5	2019/06/29	0.772
2768	2019/11/28	177.2°	4h13m	+24°	2019/11/28	13.7	2019/11/22	0.920
3089	2019/05/29	169.3°	16h25m	-10°	2019/05/30	14.1	2019/06/02	1.417
3197	2019/12/19	167.0°	5h43m	+10°	2019/12/19	14.3	2019/12/16	1.233
3267	2019/12/23	154.8°	5h28m	- 0°	2019/12/20	14.4	2019/12/16	0.733
3628	2019/08/13	175.6°	21h24m	-10°	2019/08/14	13.7	2019/08/19	0.806
3728	2019/02/16	164.7°	9h29m	- 1°	2019/02/14	14.3	2019/02/10	1.289
3761	2019/07/12	151.4°	19h12m	+ 6°	2019/07/12	14.2	2019/07/12	1.297
3958	2019/10/20	177.4°	1h35m	+12°	2019/10/20	13.9	2019/10/21	0.967
4264	2019/09/05	177.0°	22h50m	- 4°	2019/09/05	14.4	2019/09/14	0.821
4288	2019/11/10	178.5°	3h 0m	+18°	2019/11/10	14.1	2019/11/05	1.243
4420	2019/07/20	178.6°	19h59m	-22°	2019/07/20	13.2	2019/07/22	0.810
4422	2019/10/02	173.4°	0h43m	- 2°	2019/10/02	13.9	2019/09/30	0.840
4533	2019/03/20	179.4°	11h57m	+ 0°	2019/03/20	14.5	2019/03/11	1.041
4577	2019/02/06	160.8°	9h48m	+33°	2019/02/05	14.0	2019/02/03	0.913
4711	2019/10/12	157.6°	1h41m	-13°	2019/10/09	13.8	2019/10/05	0.830
4797	2019/10/17	176.7°	1h23m	+12°	2019/10/17	14.2	2019/10/18	0.985
4820	2019/12/21	157.0°	5h44m	+46°	2019/12/18	13.4	2019/12/15	0.930
5131	2019/01/13	172.7°	7h56m	+27°	2019/01/16	14.5	2019/02/02	0.560
5391	2019/09/12	178.6°	23h16m	- 3°	2019/09/12	13.9	2019/09/04	0.739
5445	2019/06/18	178.5°	17h46m	-21°	2019/06/18	14.1	2019/06/12	1.038
5534	2019/10/01	179.6°	0h29m	+ 2°	2019/10/01	13.6	2019/10/12	1.008
5817	2019/10/21	138.1°	1h27m	+52°	2019/10/31	14.2	2019/11/02	0.745
5822	2019/12/11	179.4°	5h13m	+22°	2019/12/11	14.5	2019/12/12	0.999
6260	2019/08/08	176.1°	21h15m	-20°	2019/08/08	14.4	2019/08/10	1.219
6518	2019/02/04	169.4°	9h31m	+25°	2019/02/06	14.0	2019/02/13	0.903
6572	2019/09/29	176.2°	0h27m	- 1°	2019/09/29	13.9	2019/09/20	0.931
6649	2019/07/22	173.0°	20h 8m	-27°	2019/07/22	14.4	2019/07/25	0.888
7365	2019/09/01	179.1°	22h37m	- 7°	2019/09/01	14.5	2019/08/31	0.731
7965	2019/02/20	160.1°	9h59m	- 8°	2019/02/24	14.4	2019/03/05	1.103
9900	2019/07/21	177.4°	19h59m	-17°	2019/07/21	14.3	2019/07/12	0.743
9992	2019/06/24	174.1°	18h14m	-29°	2019/06/25	14.3	2019/06/27	0.522
10261	2019/09/29	168.6°	0h 4m	+12°	2019/09/27	14.5	2019/09/21	0.844
10936	2019/10/21	168.5°	1h16m	+20°	2019/10/21	13.8	2019/10/20	0.779
16143	2019/08/27	168.4°	22h17m	+ 1°	2019/08/27	14.4	2019/08/25	0.492
22722	2019/03/26	179.3°	12h16m	- 2°	2019/03/26	14.5	2019/04/02	1.106
23120	2019/07/16	179.6°	19h40m	-21°	2019/07/16	14.5	2019/07/24	1.305
24094	2019/05/22	157.2°	16h 3m	-43°	2019/05/23	14.4	2019/05/24	0.928
29943	2019/12/30	175.4°	6h40m	+27°	2019/12/30	13.9	2020/01/01	1.674
66146	2019/09/15	118.7°	20h34m	-52°	2019/08/31	12.1	2019/08/25	0.074
66391	2019/06/02	103.8°	12h 0m	+11°	2019/05/27	12.5	2019/05/25	0.035
68950	2019/06/11	112.2°	13h55m	+23°	2019/05/24	14.1	2019/05/20	0.088
162082	2019/10/27	178.7°	2h10m	+13°	2019/10/27	12.3	2019/10/25	0.042

Table II. Temporal Sequence of Favorable Elongations

	Max Elong				Br Mag		Min Dist	
Planet	Date	Elong	RA	Dec	Date	Mag	Date	Dist
479	2019/01/01	171.1°	6h41m	+14°	2018/12/31	12.4	2018/12/25	1.313
384	2019/01/05	171.8°	7h 7m	+30°	2019/01/05	12.3	2019/01/03	1.301
2331	2019/01/05	176.2°	7h 2m	+18°	2019/01/05	13.6	2019/01/08	0.918
1107	2019/01/06	179.0°	7h 7m	+21°	2019/01/06	12.7	2019/01/06	1.806
390	2019/01/12	174.9°	7h35m	+26°	2019/01/12	13.1	2019/01/14	1.343
5131	2019/01/13	172.7°	7h56m	+27°	2019/01/16	14.5	2019/02/02	0.560
24	2019/01/14	178.7°	7h41m	+22°	2019/01/14	10.7	2019/01/16	1.801
1212	2019/01/17	174.0°	7h49m	+15°	2019/01/17	14.1	2019/01/19	2.253
449	2019/01/20	176.8°	8h 9m	+23°	2019/01/20	11.6	2019/01/22	1.135
2167	2019/01/23	171.6°	8h11m	+11°	2019/01/23	14.5	2019/01/28	1.187
2397	2019/02/04	177.0°	9h 6m	+13°	2019/02/04	14.4	2019/01/31	1.703
6518	2019/02/04	169.4°	9h31m	+25°	2019/02/06	14.0	2019/02/13	0.903
532	2019/02/05	166.3°	9h36m	+28°	2019/02/06	8.9	2019/02/10	1.424
944	2019/02/05	112.8°	11h46m	+81°	2018/11/23	14.3	2018/11/24	1.448
1585	2019/02/06	168.5°	8h56m	+ 5°	2019/02/04	14.0	2019/01/26	1.520
4577	2019/02/06	160.8°	9h48m	+33°	2019/02/05	14.0	2019/02/03	0.913
3728	2019/02/16	164.7°	9h29m	- 1°	2019/02/14	14.3	2019/02/10	1.289
7965	2019/02/20	160.1°	9h59m	- 8°	2019/02/24	14.4	2019/03/05	1.103
1761	2019/02/21	176.0°	10h23m	+14°	2019/02/21	14.5	2019/02/18	1.496
488	2019/02/27	162.5°	11h 7m	+24°	2019/02/27	11.6	2019/02/27	1.705

Planet	Max Elong Date	Elong	RA	Dec	Br Mag Date	Mag	Min Dist Date	Dist
385	2019/03/17	175.4°	11h40m	- 2°	2019/03/17	10.6	2019/03/18	1.510
4533	2019/03/20	179.4°	11h57m	+ 0°	2019/03/20	14.5	2019/03/11	1.041
265	2019/03/21	151.1°	11h50m	-28°	2019/03/26	13.2	2019/04/01	0.916
22722	2019/03/26	179.3°	12h16m	- 2°	2019/03/26	14.5	2019/04/02	1.106
540	2019/04/13	179.8°	13h24m	- 8°	2019/04/13	12.4	2019/04/12	1.031
405	2019/04/21	162.6°	13h21m	-27°	2019/04/21	10.5	2019/04/21	0.978
788	2019/04/22	167.0°	14h19m	- 0°	2019/04/22	12.1	2019/04/24	1.726
2433	2019/05/04	168.2°	15h 2m	- 5°	2019/05/05	14.1	2019/05/11	1.092
1000	2019/05/06	145.8°	13h58m	-48°	2019/05/09	13.1	2019/05/11	1.470
1680	2019/05/13	176.0°	15h23m	-14°	2019/05/13	13.6	2019/05/15	1.223
24094	2019/05/22	157.2°	16h 3m	-43°	2019/05/23	14.4	2019/05/24	0.928
1866	2019/05/25	135.0°	18h58m	-51°	2019/06/08	13.5	2019/06/14	0.450
953	2019/05/27	172.5°	16h12m	-28°	2019/05/28	13.2	2019/06/03	1.377
3089	2019/05/29	169.3°	16h25m	-10°	2019/05/30	14.1	2019/06/02	1.417
66391	2019/06/02	103.8°	12h 0m	+11°	2019/05/27	12.5	2019/05/25	0.035
68950	2019/06/11	112.2°	13h55m	+23°	2019/05/24	14.1	2019/05/20	0.088
410	2019/06/15	174.8°	17h30m	-18°	2019/06/15	10.3	2019/06/16	1.053
1165	2019/06/17	161.1°	17h48m	- 4°	2019/06/19	13.8	2019/06/22	1.550
5445	2019/06/18	178.5°	17h46m	-21°	2019/06/18	14.1	2019/06/12	1.038
2013	2019/06/22	178.4°	18h 3m	-21°	2019/06/22	14.1	2019/07/03	0.948
914	2019/06/24	161.2°	18h30m	- 5°	2019/06/26	10.8	2019/06/29	0.977
9992	2019/06/24	174.1°	18h14m	-29°	2019/06/25	14.3	2019/06/27	0.522
2064	2019/06/26	171.7°	18h13m	-31°	2019/06/28	12.9	2019/07/10	0.486
2081	2019/06/28	176.2°	18h27m	-27°	2019/06/28	14.0	2019/06/30	1.045
2714	2019/06/28	171.2°	18h22m	-14°	2019/06/28	14.5	2019/06/29	0.772
1634	2019/06/29	178.1°	18h33m	-25°	2019/06/29	14.2	2019/06/30	0.866
2093	2019/07/10	170.4°	19h10m	-12°	2019/07/10	14.2	2019/07/08	0.886
3761	2019/07/12	151.4°	19h12m	+ 6°	2019/07/12	14.2	2019/07/12	1.297
23120	2019/07/16	179.6°	19h40m	-21°	2019/07/16	14.5	2019/07/24	1.305
1607	2019/07/17	177.4°	19h39m	-18°	2019/07/17	13.4	2019/07/30	1.017
900	2019/07/18	159.3°	19h29m	- 0°	2019/07/18	14.2	2019/07/19	1.092
4420	2019/07/20	178.6°	19h59m	-22°	2019/07/20	13.2	2019/07/22	0.810
791	2019/07/21	174.1°	19h52m	-14°	2019/07/21	12.6	2019/07/24	1.578
9900	2019/07/21	177.4°	19h59m	-17°	2019/07/21	14.3	2019/07/12	0.743
341	2019/07/22	167.1°	20h16m	-33°	2019/07/23	11.8	2019/07/26	0.791
6649	2019/07/22	173.0°	20h 8m	-27°	2019/07/22	14.4	2019/07/25	0.888
519	2019/08/06	160.8°	21h28m	-35°	2019/08/07	12.2	2019/08/10	1.358
1278	2019/08/07	162.3°	21h39m	-32°	2019/08/08	12.2	2019/08/09	0.789
6260	2019/08/08	176.1°	21h15m	-20°	2019/08/08	14.4	2019/08/10	1.219
283	2019/08/13	176.3°	21h26m	-11°	2019/08/13	12.2	2019/08/16	1.670
3628	2019/08/13	175.6°	21h24m	-10°	2019/08/14	13.7	2019/08/19	0.806
39	2019/08/17	176.0°	21h38m	- 9°	2019/08/17	9.2	2019/08/19	1.516
413	2019/08/17	148.7°	23h13m	-37°	2019/08/23	11.8	2019/08/27	0.798
1066	2019/08/17	176.4°	21h50m	-16°	2019/08/17	14.1	2019/08/23	0.961
746	2019/08/19	161.5°	22h14m	-30°	2019/08/18	13.2	2019/08/16	1.405
1467	2019/08/20	179.7°	21h55m	-12°	2019/08/20	12.4	2019/08/18	1.943
1136	2019/08/25	164.3°	21h49m	+ 3°	2019/08/26	13.0	2019/08/30	0.965
130	2019/08/26	174.4°	22h29m	-15°	2019/08/26	10.5	2019/08/31	1.615
304	2019/08/26	175.9°	22h10m	- 6°	2019/08/26	11.1	2019/08/25	0.861
504	2019/08/27	161.3°	23h 0m	-26°	2019/08/28	12.0	2019/08/29	1.172
16143	2019/08/27	168.4°	22h17m	+ 1°	2019/08/27	14.4	2019/08/25	0.492
333	2019/08/30	178.3°	22h36m	-10°	2019/08/30	12.9	2019/09/02	1.705
7365	2019/09/01	179.1°	22h37m	- 7°	2019/09/01	14.5	2019/08/31	0.731
380	2019/09/05	170.2°	23h 9m	-16°	2019/09/04	12.4	2019/09/03	1.378
4264	2019/09/05	177.0°	22h50m	- 4°	2019/09/05	14.4	2019/09/14	0.821
135	2019/09/06	179.7°	22h57m	- 6°	2019/09/06	9.6	2019/09/01	0.934
2629	2019/09/07	178.4°	23h 3m	- 4°	2019/09/07	14.5	2019/08/25	0.561
2389	2019/09/08	176.7°	23h 1m	- 2°	2019/09/08	14.4	2019/08/31	0.920
848	2019/09/09	178.7°	23h 5m	- 4°	2019/09/08	14.1	2019/09/06	1.605
2580	2019/09/09	177.2°	23h13m	- 8°	2019/09/09	14.1	2019/09/06	0.751
1703	2019/09/10	171.9°	23h27m	-12°	2019/09/10	13.8	2019/09/06	0.850
940	2019/09/12	170.5°	23h36m	-12°	2019/09/12	13.4	2019/09/11	1.796
5391	2019/09/12	178.6°	23h16m	- 3°	2019/09/12	13.9	2019/09/04	0.739
36	2019/09/15	176.0°	23h36m	- 6°	2019/09/16	10.5	2019/09/25	1.099
66146	2019/09/15	118.7°	20h34m	-52°	2019/08/31	12.1	2019/08/25	0.074
2100	2019/09/18	171.0°	0h 5m	- 8°	2019/09/18	13.3	2019/09/21	0.180
703	2019/09/21	176.9°	23h49m	+ 2°	2019/09/22	13.5	2019/09/24	0.904
711	2019/09/22	179.4°	23h56m	+ 0°	2019/09/22	13.4	2019/09/13	0.956
2006	2019/09/22	179.5°	23h55m	- 0°	2019/09/22	13.9	2019/09/25	0.907
247	2019/09/23	179.3°	23h58m	- 0°	2019/09/23	10.4	2019/09/29	1.256
422	2019/09/24	178.3°	0h 5m	- 1°	2019/09/24	11.6	2019/09/19	0.759
2031	2019/09/26	177.6°	0h12m	- 1°	2019/09/26	14.2	2019/09/27	0.864
2466	2019/09/26	176.3°	0h16m	- 2°	2019/09/26	14.4	2019/09/24	1.208
21	2019/09/28	174.3°	0h25m	- 3°	2019/09/27	9.4	2019/09/22	1.083
6572	2019/09/29	176.2°	0h27m	- 1°	2019/09/29	13.9	2019/09/20	0.931
10261	2019/09/29	168.6°	0h 4m	+12°	2019/09/27	14.5	2019/09/21	0.844
5534	2019/10/01	179.6°	0h29m	+ 2°	2019/10/01	13.6	2019/10/12	1.008
4422	2019/10/02	173.4°	0h43m	- 2°	2019/10/02	13.9	2019/09/30	0.840
77	2019/10/05	179.2°	0h42m	+ 5°	2019/10/05	11.3	2019/10/08	1.419
1530	2019/10/08	170.1°	0h38m	+14°	2019/10/08	14.4	2019/10/06	0.811
4711	2019/10/12	157.6°	1h41m	-13°	2019/10/09	13.8	2019/10/05	0.830
33	2019/10/14	179.2°	1h15m	+ 8°	2019/10/14	10.1	2019/10/04	0.998
4797	2019/10/17	176.7°	1h23m	+12°	2019/10/17	14.2	2019/10/18	0.985
1041	2019/10/19	167.2°	1h51m	- 2°	2019/10/20	13.5	2019/10/20	1.668
2543	2019/10/20	173.6°	1h47m	+ 4°	2019/10/20	14.1	2019/10/10	1.482
3958	2019/10/20	177.4°	1h35m	+12°	2019/10/20	13.9	2019/10/21	0.967
5817	2019/10/21	138.1°	1h27m	+52°	2019/10/31	14.2	2019/11/02	0.745
10936	2019/10/21	168.5°	1h16m	+20°	2019/10/21	13.8	2019/10/20	0.779
162082	2019/10/27	178.7°	2h10m	+13°	2019/10/27	12.3	2019/10/25	0.042
429	2019/10/30	178.9°	2h14m	+14°	2019/10/30	12.3	2019/10/28	1.295
678	2019/10/30	169.1°	1h58m	+23°	2019/10/30	11.0	2019/10/30	1.027
768	2019/11/03	179.3°	2h30m	+15°	2019/11/03	13.1	2019/11/04	1.493
176	2019/11/06	164.7°	3h 7m	+ 1°	2019/11/05	11.6	2019/11/03	1.685
4288	2019/11/10	178.5°	3h 0m	+18°	2019/11/10	14.1	2019/11/05	1.243
675	2019/11/11	169.8°	2h50m	+26°	2019/11/11	10.5	2019/11/11	1.227
2569	2019/11/12	170.3°	3h13m	+ 7°	2019/11/11	13.8	2019/11/09	1.231
1057	2019/11/15	177.3°	3h18m	+21°	2019/11/15	13.5	2019/11/08	1.291
1187	2019/11/15	159.8°	2h57m	+37°	2019/11/14	13.7	2019/11/12	1.101
770	2019/11/27	176.8°	4h 9m	+24°	2019/11/27	12.3	2019/11/26	0.899
2768	2019/11/28	177.2°	4h13m	+24°	2019/11/28	13.7	2019/11/22	0.920
459	2019/11/30	167.7°	4h20m	+33°	2019/11/30	12.7	2019/11/27	1.114
97	2019/12/02	157.0°	4h43m	- 0°	2019/12/01	9.9	2019/12/01	1.037
5822	2019/12/11	179.4°	5h13m	+22°	2019/12/11	14.5	2019/12/12	0.999
132	2019/12/14	176.5°	5h27m	+19°	2019/12/14	11.0	2019/12/28	0.952
817	2019/12/15	165.7°	5h26m	+ 8°	2019/12/14	13.4	2019/12/10	1.200
86	2019/12/19	179.9°	5h46m	+23°	2019/12/19	11.7	2019/12/13	1.628
765	2019/12/19	170.4°	5h41m	+32°	2019/12/17	14.2	2019/12/08	0.975
3197	2019/12/19	167.0°	5h43m	+10°	2019/12/19	14.3	2019/12/16	1.233
1074	2019/12/21	178.9°	5h53m	+24°	2019/12/21	13.3	2019/12/17	1.647
4820	2019/12/21	157.0°	5h44m	+46°	2019/12/18	13.4	2019/12/15	0.930
1681	2019/12/22	179.0°	6h 0m	+22°	2019/12/22	13.6	2019/12/23	1.163
347	2019/12/23	178.1°	6h 5m	+25°	2019/12/23	11.9	2019/12/29	1.482
3267	2019/12/23	154.8°	5h28m	- 0°	2019/12/20	14.4	2019/12/16	0.733
563	2019/12/24	177.7°	6h 7m	+25°	2019/12/23	10.6	2019/12/19	1.140
1067	2019/12/26	175.2°	6h16m	+28°	2019/12/26	13.7	2019/12/20	1.470
69	2019/12/30	165.9°	6h30m	+ 9°	2019/12/30	10.4	2019/12/31	1.519
29943	2019/12/30	175.4°	6h40m	+27°	2019/12/30	13.9	2020/01/01	1.674
1003	2019/12/31	178.1°	6h39m	+21°	2019/12/31	13.5	2019/12/31	1.657

Table III. Numerical list of approaches closer than 0.3 AU

Planet	Max Elong Date	Elong	RA	Dec	Br Mag Date	Mag	Min Dist Date	Dist
2100	2019/09/18	171.0°	0h 5m	- 8°	2019/09/18	13.3	2019/09/21	0.180
66146	2019/09/15	118.7°	20h34m	-52°	2019/08/31	12.1	2019/08/25	0.074
66391	2019/06/02	103.8°	12h 0m	+11°	2019/05/27	12.5	2019/05/25	0.035
68950	2019/06/11	112.2°	13h55m	+23°	2019/05/24	14.1	2019/05/20	0.088
162082	2019/10/27	178.7°	2h10m	+13°	2019/10/27	12.3	2019/10/25	0.042

LIGHTCURVE ANALYSIS OF HILDA ASTEROIDS AT THE CENTER FOR SOLAR SYSTEM STUDIES: 2018 JULY-SEPTEMBER

Brian D. Warner
Center for Solar System Studies / MoreData!
446 Sycamore Ave.
Eaton, CO 80615 USA
brian@MinorPlanetObserver.com

Robert D. Stephens
Center for Solar System Studies / MoreData!
Rancho Cucamonga, CA

(Received: 2018 September 30)

Lightcurves for seven Hilda asteroids were obtained at the Center for Solar System Studies (CS3) from 2018 July-September: 6124 Mecklenburg, 8550 Hesiodos, 15231 Ehdita, 15376 Martak, (15638) 2000 JA65, (23174) 2000 HM40, (73418) 2002 LK36.

CCD photometric observations of seven Hilda asteroids were made at the Center for Solar System Studies (CS3) from 2018 July-September. This is another installment of an on-going series of papers on this group of asteroids, which is located between the outer main-belt and Jupiter Trojans in a 3:2 orbital resonance with Jupiter. The goal is to determine the spin rate statistics of the group and find pole and shape models when possible. We also look to examine the degree of influence that the YORP (Yarkovsky–O'Keefe–Radzievskii–Paddack) effect (Rubincam, 2000) has on distant objects and to compare the spin rate distribution against the Jupiter Trojans, which can provide evidence that the Hildas are more "comet-like" than main-belt asteroids.

Table I lists the telescopes and CCD cameras that are combined to make observations. Up to nine telescopes can be used for the campaign, although seven is more common. All the cameras use CCD chips from the KAF blue-enhanced family and so have essentially the same response. The pixel scales ranged from 1.24-1.60 arcsec/pixel. All lightcurve observations were unfiltered since a clear filter can result in a 0.1-0.3 magnitude loss. The exposures varied depending on the asteroid's brightness and sky motion.

Telescopes	Cameras
0.30-m *f*/6.3 Schmidt-Cass	FLI Microline 1001E
0.35-m *f*/9.1 Schmidt-Cass	FLI Proline 1001E
0.35-m *f*/11 Schmidt-Cass	SBIG STL-1001E
0.40-m *f*/10 Schmidt-Cass	
0.50-m *f*/8.1 Ritchey-Chrétien	

Table I. List of available telescopes and CCD cameras at CS3. The exact combination for each telescope/camera pair can vary due to maintenance or specific needs.

Measurements were made using *MPO Canopus*. The Comp Star Selector (CSS) utility in *MPO Canopus* found up to five comparison stars of near solar-color for differential photometry. Catalog magnitudes were usually taken from the APASS (Henden et al., 2009) or CMC-15 (Munos, 2017) catalogs.

The nightly zero points for the APASS and CMC-15 catalogs are generally consistent to about ±0.05 mag or better, but occasionally reach >0.1 mag. There is a systematic offset between the two catalogs so, whenever possible, the same catalog is used for all observations of a given asteroid. Period analysis is done with *MPO Canopus*, which implements the FALC algorithm by Harris (Harris *et al.,* 1989).

In the plots below, the "Reduced Magnitude" is Johnson V as indicated in the Y-axis title. These are values that have been converted from sky magnitudes to unity distance by applying $-5*\log(r\Delta)$ to the measured sky magnitudes with r and Δ being, respectively, the Sun-asteroid and Earth-asteroid distances in AU. The magnitudes were normalized to the phase angle in the parentheses using $G = 0.15$, unless otherwise stated. The X-axis is the rotational phase ranging from –0.05 to 1.05.

If the plot includes an amplitude, *e.g.*, "Amp: 0.65", this is the amplitude of the Fourier model curve and *not necessarily the adopted amplitude for the lightcurve*.

For the sake of brevity, only some of the previously reported results may be referenced in the discussions on specific asteroids. For a more complete listing, the reader is directed to the asteroid lightcurve database (LCDB; Warner *et al.,* 2009). The on-line version at *http://www.minorplanet.info/lightcurvedatabase.html* allows direct queries that can be filtered a number of ways and the results saved to a text file. A set of text files of the main LCDB tables, including the references with bibcode, is also available for download. Readers are strongly encouraged to obtain, when possible, the original references listed in the LCDB for their work.

6124 Mecklenburg, 8550 Hesiodos. There were no previous rotation period entries in the LCDB for these two Hildas. Mainzer et al. (2016) give diameters of 19.6 km for Mecklenburg and 24.7 km for Hesidos.

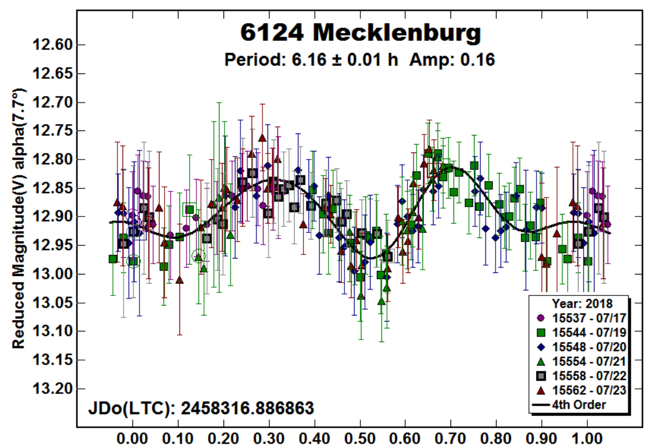

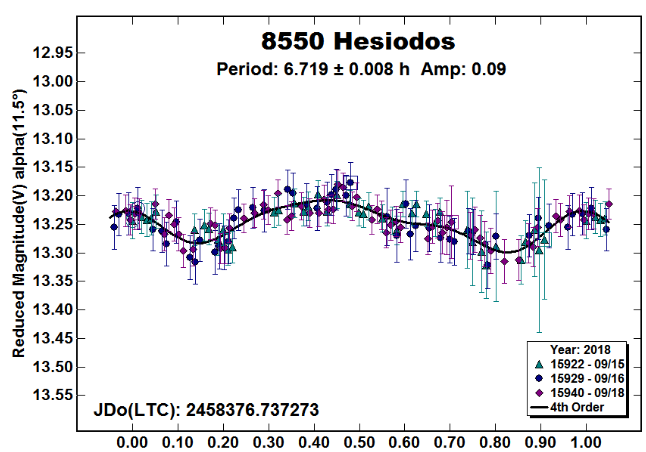

15231 Ehdita. The 23.5 km Ehdita (Mainzer et al., 2016) is another first-time rotation period entry into the LCDB. There are good indications that the asteroid is tumbling as judged by not finding a single period solution that fit all the data. The deviations from the model curve are too large to be simple zero point calibration issues.

Even for the shorter damping times to go from tumbling to single-axis rotation (see Pravec et al., 2014 and 2005), Ehdita, based on its size and distance from the Sun, is not expected to be tumbling. Further observations are needed to confirm the true rotation state of the asteroid.

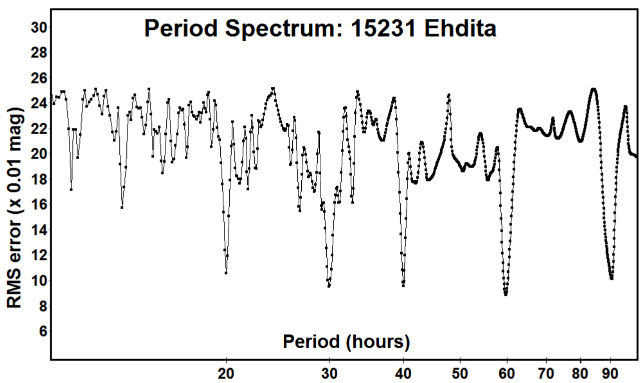

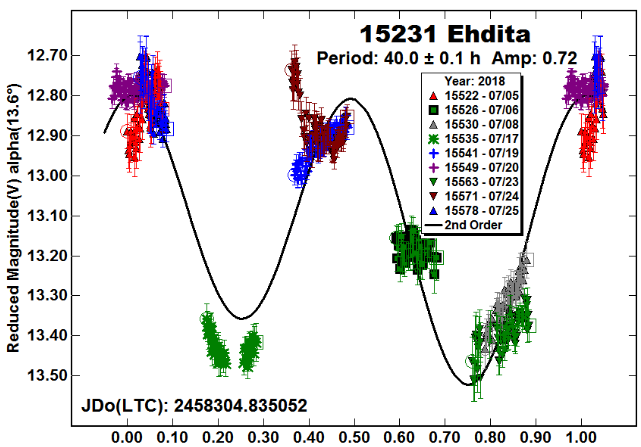

15376 Martak. Mainzer et al. (2016) give a diameter of 18.0 km for Martak, There were no previous rotation period entries in the LCDB.

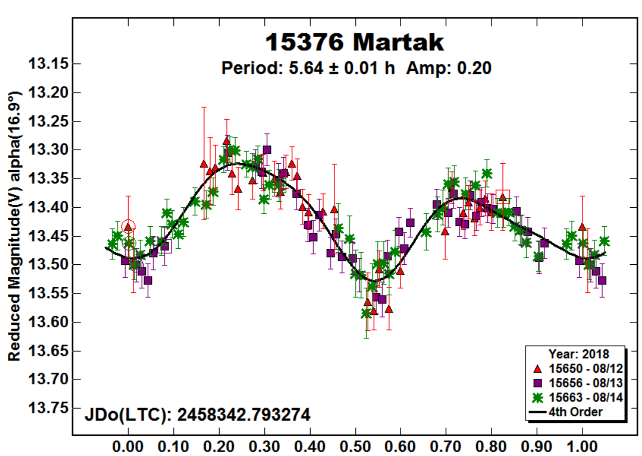

(15638) 2000 JA65. Waszczak et al. (2015) found a period of 5.914 h based on data obtained in 2010 and 2014. The denser lightcurve obtained at CS3 refined that period somewhat. Mainzer et al. (2016) reported a diameter of 32.3 km and albedo of 0.056. Such a low albedo is expected for the Hildas, which are usually taxonomic type D or P, but occasionally C.

The period is near the spin barrier for icy objects (French et al., 2015). Only four Hildas have a shorter period.

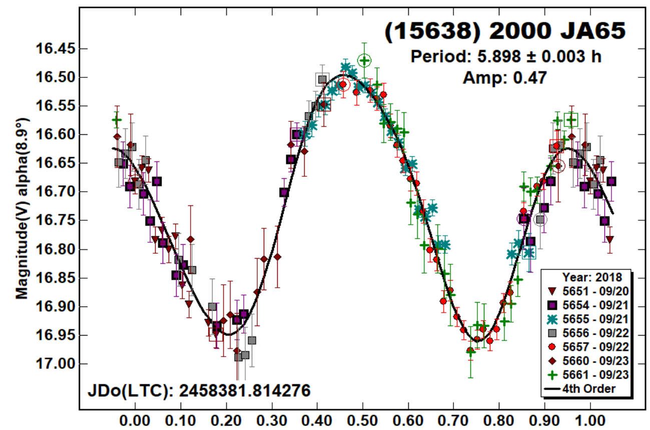

(23174) 2000 HM40, (73418) 2002 LK36. These appear to be the first reported rotation periods for the two Hildas. Mainzer et al. (2016) found D = 23.5 km and p_V = 0.073 for 2000 HM40 and, for 2002 LK36, D = 12.2 km and p_V = 0.108.

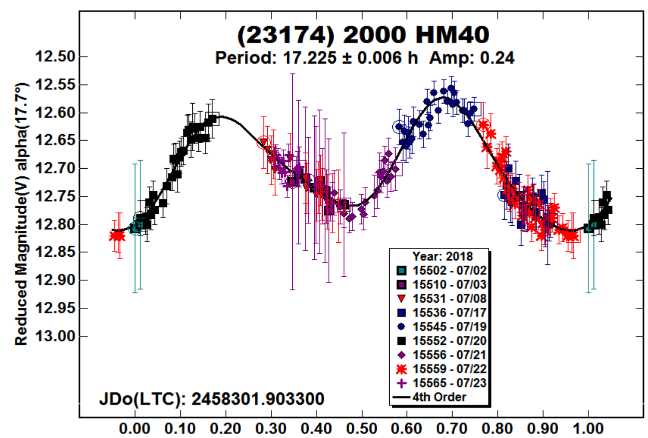

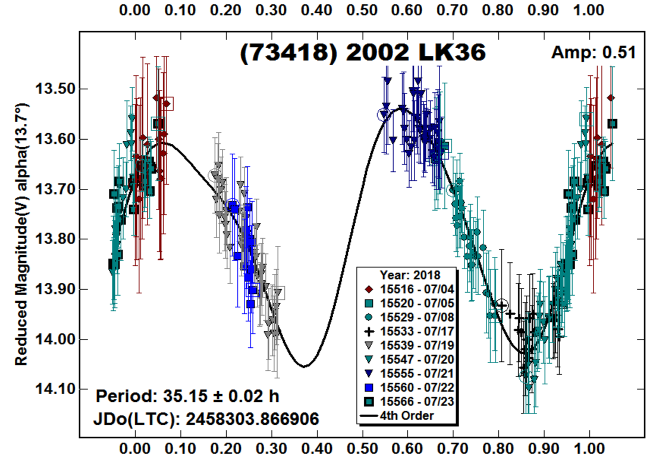

Number	Name	2018/mm/dd	Pts	Phase	L_{PAB}	B_{PAB}	Period(h)	P.E.	Amp	A.E.
6124	Mecklenburg	07/17-07/23	176	7.8,6.2	320	4	6.159	0.004	0.16	0.02
8550	Hesiodos	09/15-09/16	105	11.5,11.2	22	0	6.719	0.008	0.09	0.01
15231	Ehdita	07/05-07/24	480	13.6,8.6	323	3	40.0	0.1	0.72	0.05
15376	Martak	08/12-08/14	123	16.9,16.4	2	3	5.64	0.01	0.20	0.01
15638	2000 JA65	09/20-09/23	137	9.0,8.2	22	-11	5.898	0.003	0.47	0.02
23174	2000 HM40	07/02-07/23	168	17.7,15.3	347	2	17.225	0.006	0.24	0.02
73418	2002 LK36	07/03-07/23	213	13.9,9.0	314	8	35.15	0.02	0.51	0.04

Table II. Observing circumstances. The phase angle (α) is given at the start and end of each date range. If there are three values, the middle one is the minimum phase angle over the range of observations. L_{PAB} and B_{PAB} are each the average phase angle bisector longitude and latitude (see Harris *et al.*, 1984).

Acknowledgements

Observations at CS3 and continued support of the asteroid lightcurve database (LCDB; Warner et al., 2009) are supported by NASA grant 80NSSC18K0851. Work on the asteroid lightcurve database (LCDB) was also partially funded by National Science Foundation grant AST-1507535.

This research was made possible through the use of the AAVSO Photometric All-Sky Survey (APASS), funded by the Robert Martin Ayers Sciences Fund, and by data from CMC15 Data Access Service at CAB (INTA-CSIC) (*http://svo2.cab.inta-csic.es/vocats/cmc15/)*.

The authors gratefully acknowledge Shoemaker NEO Grants from the Planetary Society (2007, 2013). These were used to purchase some of the telescopes and CCD cameras used in this research.

References

Harris, A.W., Young, J.W., Scaltriti, F., Zappala, V. (1984). "Lightcurves and phase relations of the asteroids 82 Alkmene and 444 Gyptis." *Icarus* **57**, 251-258.

Harris, A.W., Young, J.W., Bowell, E., Martin, L.J., Millis, R.L., Poutanen, M., Scaltriti, F., Zappala, V., Schober, H.J., Debehogne, H., Zeigler, K.W. (1989). "Photoelectric Observations of Asteroids 3, 24, 60, 261, and 863." *Icarus* **77**, 171-186.

Harris, A.W., Pravec, P., Galad, A., Skiff, B.A., Warner, B.D., Vilagi, J., Gajdos, S., Carbognani, A., Hornoch, K., Kusnirak, P., Cooney, W.R., Gross, J., Terrell, D., Higgins, D., Bowell, E., Koehn, B.W. (2014). "On the maximum amplitude of harmonics on an asteroid lightcurve." *Icarus* **235**, 55-59.

Henden, A.A., Terrell, D., Levine, S.E., Templeton, M., Smith, T.C., Welch, D.L. (2009). *http://www.aavso.org/apass*

French, L.M., Stephens, R.D., Coley, D., Wasserman, L.H., Sieben, J. (2015). "Rotation lightcurves of small Jovian Trojan asteroids." *Icarus* **254**, 1-17.

Mainzer, A.K., Bauer, J.M., Cutri, R.M., Grav, T., Kramer, E.A., Masiero, J.R., Nugent, C.R., Sonnett, S.M., Stevenson, R.A., Wright, E.L. (2016). "NEOWISE Diameters and Albedos V1.0." NASA Planetary Data System.
EAR-A-COMPIL-5-NEOWISEDIAM-V1.0.

Pravec, P., Harris, A.W., Scheirich, P., Kušnirák, P., Šarounová, L., Hergenrother, C.W., Mottola, S., Hicks, M.D., Masi, G., Krugly, Yu.N., Shevchenko, V.G., Nolan, M.C., Howell, E.S., Kaasalainen, M., Galád, A., Brown, P., Degraff, D.R., Lambert, J. V., Cooney, W.R., Foglia, S. (2005). "Tumbling asteroids." *Icarus* **173**, 108-131.

Pravec, P., Scheirich, P., Durech, J., Pollock, J., Kusnirak, P., Hornoch, K., Galad, A., Vokrouhlicky, D., Harris, A.W., Jehin, E., Manfroid, J., Opitom, C., Gillon, M., Colas, F., Oey, J., Vrastil, J., Reichart, D., Ivarsen, K., Haislip, J., LaCluyze, A. (2014). "The tumbling state of (99942) Apophis." *Icarus* **233**, 48-60.

Rubincam, D.P. (2000). "Relative Spin-up and Spin-down of Small Asteroids." *Icarus* **148**, 2-11.

Warner, B.D., Harris, A.W., Pravec, P. (2009). "The Asteroid Lightcurve Database." *Icarus* **202**, 134-146. Updated 2018 June. *http://www.minorplanet.info/lightcurvedatabase.html*

Waszczak, A., Chang, C.-K., Ofek, E.O., Laher, R., Masci, F., Levitan, D., Surace, J., Cheng, Y.-C., Ip, W.-H., Kinoshita, D., Helou, G., Prince, T.A., Kulkarni, S. (2015). "Asteroid Light Curves from the Palomar Transient Factory Survey: Rotation Periods and Phase Functions from Sparse Photometry." *Astron. J.* **150**, A75.

ASTEROID LIGHTCURVE ANALYSIS AT CS3-PALMER DIVIDE STATION: 2018 JULY-SEPTEMBER

Brian D. Warner
Center for Solar System Studies-Palmer Divide Station
446 Sycamore Ave.
Eaton, CO 80615 USA
brian@MinorPlanetObserver.com

(Received: 2018 September 30)

Lightcurves for 12 main-belt asteroids were obtained at the Center for Solar System Studies-Palmer Divide Station (CS3-PDS) from 2018 July-September. Analysis of a larger amplitude lightcurve in 2018 for 5175 Ables lead to new analysis and results for earlier apparitions. The Hungaria asteroid (37378) 2001 VU76 is possibly a super-fast rotator with a period and size that put it just above the so-called "spin barrier."

CCD photometric observations of 12 main-belt asteroids were made at the Center for Solar System Studies-Palmer Divide Station (CS3-PDS) from 2018 July-September. The main focus at CS3-PDS is on near-Earth and Hilda asteroids. However, when there is a full moon or a dearth of NEAs sufficiently bright and placed, members of other groups or families are targeted. Any Hungaria members were observed to provide additional data for spin axis modeling. The other objects were chosen because they had no reported period, were bright enough to work despite the moon, and/or were in the same field as a planned target.

Table I lists the telescope/CCD camera combinations that were used. All the cameras use the KAF-1001E blue-enhanced CCD chip and so have essentially the same response. The pixel scales for the combinations range from 1.24-1.60 arcsec/pixel.

Desig	Telescope	Camera
Squirt	0.30-m f/6.3 Schmidt-Cass	STL-1001E
Borealis	0.35-m f/9.1 Schmidt-Cass	ML-1001E
Eclipticalis	0.35-m f/9.1 Schmidt-Cass	ML-1001E
Australius	0.35-m f/9.1 Schmidt-Cass	STL-1001E
Zephyr	0.50-m f/8.1 R-C	FLI-1001E

Table I. List of CS3-PDS telescope/CCD camera combinations.

All lightcurve observations were unfiltered since a clear filter can cause a 0.1-0.3 mag loss. The exposure duration varied depending on the asteroid's brightness and sky motion. Guiding on a field star sometimes resulted in a trailed image for the asteroid.

Measurements were made using *MPO Canopus*. The Comp Star Selector utility in *MPO Canopus* found up to five comparison stars of near solar-color for differential photometry. Catalog magnitudes were taken from the APASS (Henden et al., 2009) or CMC-15 (Munos, 2017) catalogs.

The nightly zero points for the APASS and CMC-15 catalogs are generally consistent to about ±0.05 mag or better, but occasionally reach >0.1 mag. There is a systematic offset between the two catalogs and so, whenever possible, the same catalog was used for all observations of a given asteroid. Period analysis was done with *MPO Canopus*, which implements the FALC algorithm by Harris (Harris *et al.,* 1989).

In the lightcurves below, the "Reduced Magnitude" is Johnson V as indicated in the Y-axis title. These are values that have been converted from sky magnitudes to unity distance by applying $-5*\log(r\Delta)$ to the measured sky magnitudes with r and Δ being, respectively, the Sun-asteroid and Earth-asteroid distances in AU. The magnitudes were normalized to the phase angle in the parentheses using $G = 0.15$, unless otherwise stated.

The X-axis is the rotational phase ranging from –0.05 to 1.05. If the plot includes an amplitude, *e.g.*, "Amp: 0.65", this is the amplitude of the Fourier model curve and *not necessarily the adopted amplitude for the lightcurve*.

For the sake of brevity, only some of the previously reported results may be referenced in the discussions on specific asteroids. For a more complete listing, the reader is directed to the asteroid lightcurve database (LCDB; Warner et al., 2009a). The on-line version at *http://www.minorplanet.info/lightcurvedatabase.html* allows direct queries that can be filtered a number of ways and the results saved to a text file. A set of text files of the main LCDB tables, including the references with Bibcode, is also available for download. Readers are strongly encouraged, when possible, to cross-check with the original references listed in the LCDB.

4019 Klavetter. This is a 3.4-km (Mainzer et al., 2016) member of the Flora group of asteroids. There was no previous rotation period result in the LCDB.

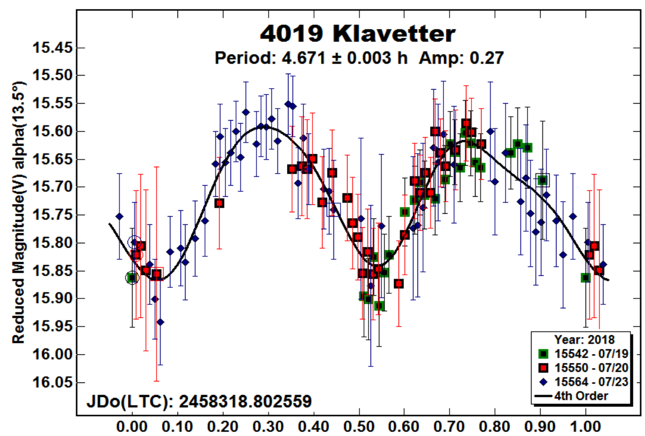

4483 Petofi is a Hungaria asteroid (5.85 km; Mainzer et al., 2016) that has been worked numerous times by the author (Warner 2008; 2009b; 2012; and 2015). In all cases, the period was found to be close to P = 4.333 h. A preliminary shape model shows the asteroid to be highly elongated, which is supported by the large amplitude seen at every apparition.

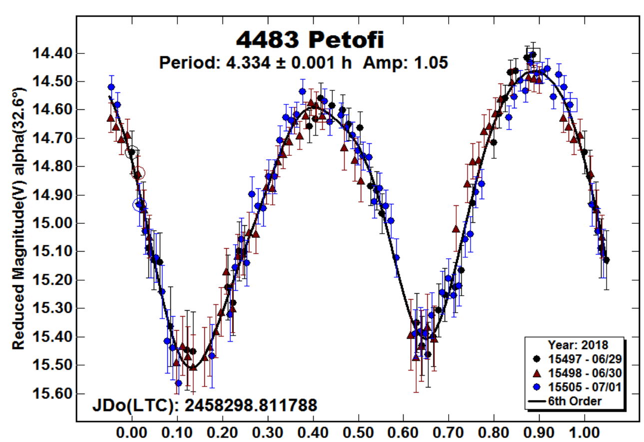

5175 Ables. Mainzer et al. (2016) found D = 4.49 km and p_V = 0.042. This low albedo is not usually compatible with the type Q/Sq taxonomic type found by Lucas et al. (2017).

In previous work by the author (Warner, 2011; Warner 2014), the amplitude was always ≤ 0.1 mag. At such low amplitudes, it is not safe to assume a bimodal lightcurve (Harris et al., 2014). Even so, that assumption was made when reporting a period of about 2.798 h in the earlier works (Warner, 2011; Warner 2014).

With the lightcurve amplitude of 0.33 mag, the 2018 data removed *almost* all doubt about the lightcurve shape. However, they *added* doubt about the true period.

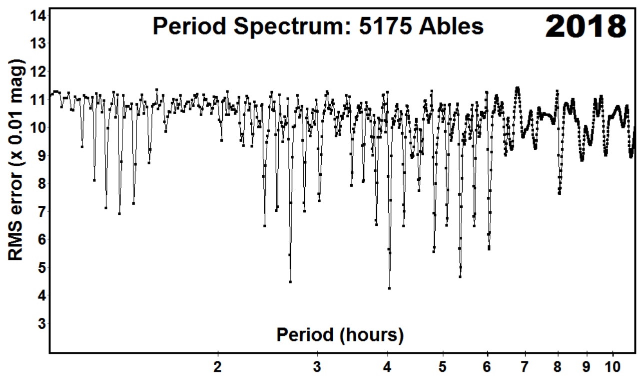

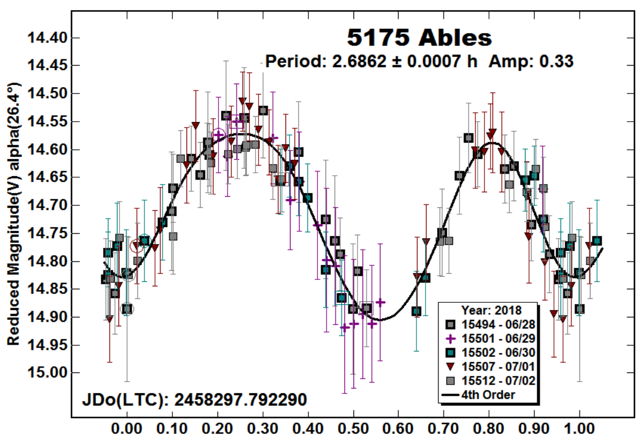

The data set in 2018 was not as extensive as in earlier years, but it was still sufficient to find a reliable solution of 2.6862 h, or about 0.11 h faster than the earlier results (Warner, 2011; Warner 2014). This prompted a revisit to the original data used in those works.

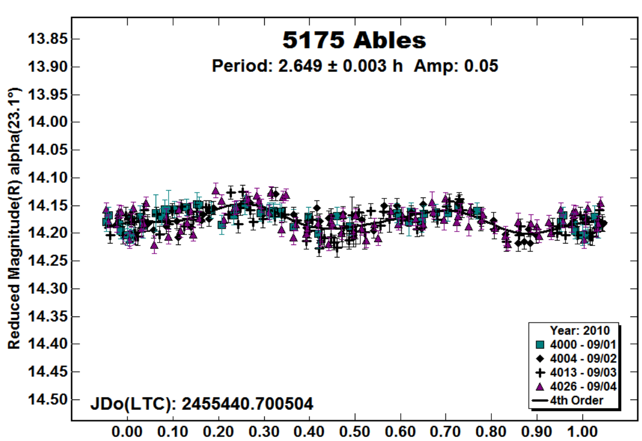

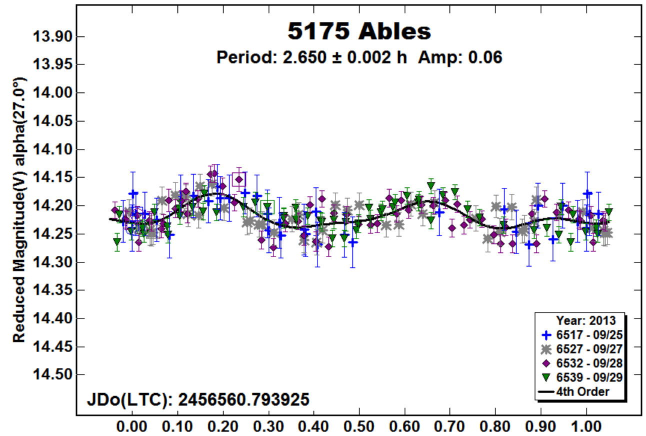

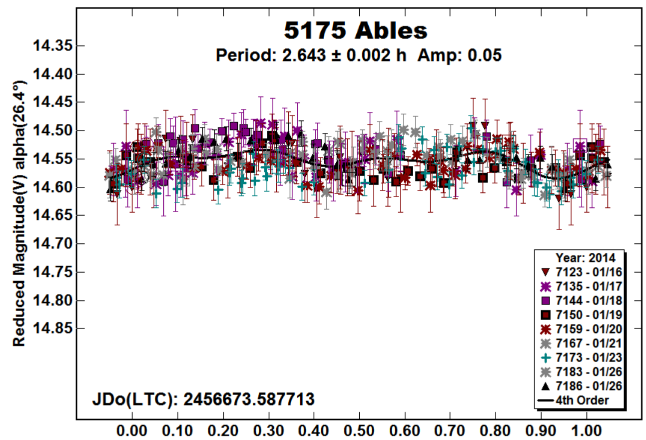

On the presumption that the new, shorter period was correct, the zero points on the earlier data were adjusted by very small amounts of <0.01-0.02 mag. After numerous iterations through each set, it was possible to get a reasonable fit near the shorter period. However, the average is 2.647 ± 0.005 h, or 0.04 h faster than the 2018 result. The 2018 period is adopted here, but with the realization that a definitive period has yet to be found.

5998 Sitensky, 17408 McAdams. There were no previously reported rotation periods in the LCDB for either asteroid. The result for 5998 Sitensky is considered secure given the amplitude, even though the shape is somewhat irregular. A double-period of 13 h was considered, but the two halves of the lightcurve were essentially identical, which helped exclude the longer solution.

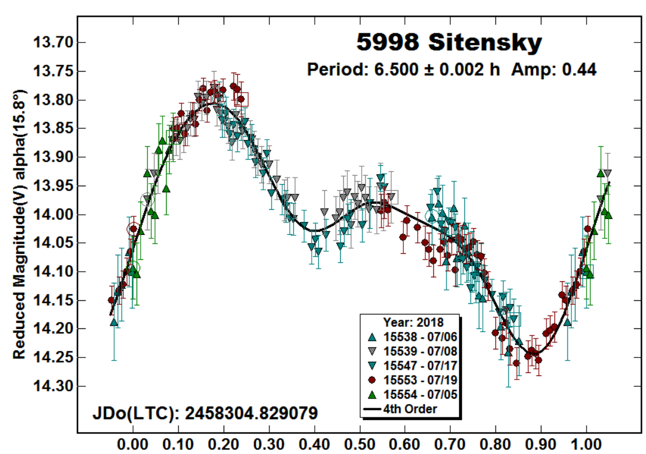

The solution for McAdams is not so secure. Unfortunately, there were no previous results to help guide the analysis. The period spectrum shows several “more likely than not” solutions. In the end, P = 18.42 h was adopted since it gave a bimodal lightcurve, which is almost certain given the 0.48 mag amplitude (Harris et al., 2014). The strength of the half-period was also a factor in choosing the longest period in the spectrum. Further observations are encouraged.

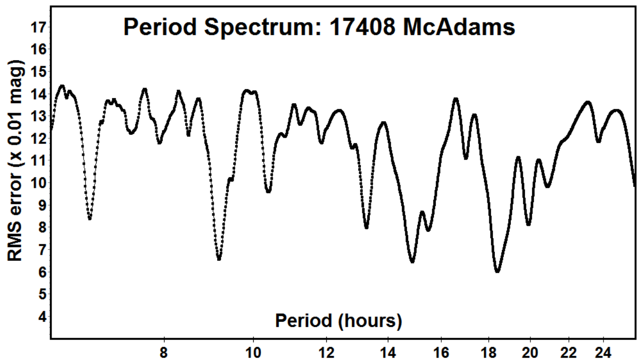

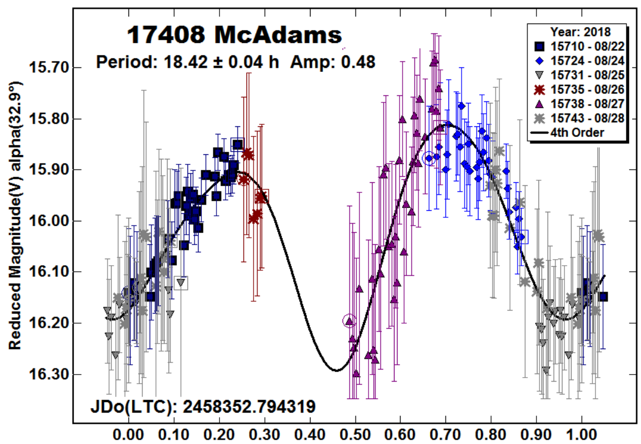

(25059) 1998 QA69, 26578 Cellinekim. This appears to be the first reported rotation period for 1998 QA69, which, according to Mainzer et al. (2016), has a diameter of 3.6 km. They also found p_V = 0.286 ± 0.096, which is consistent with many other inner main-belt asteroids.

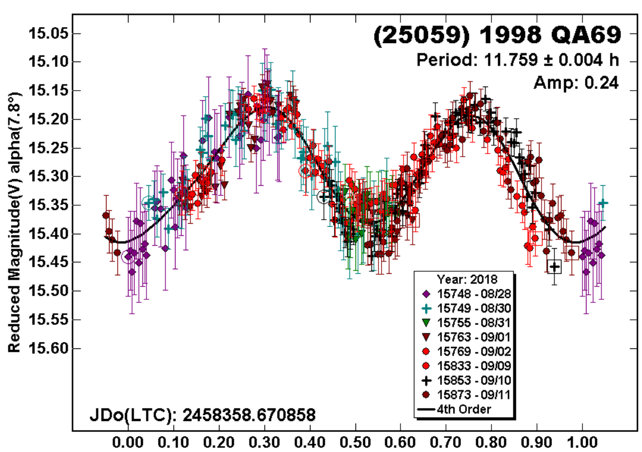

It also appears that this is the first reported period for 26578 Cellinekim. Mainzer et al. (2016) found D = 5.75 km and p_V= 0.048, the latter is expected for outer main-belt asteroids.

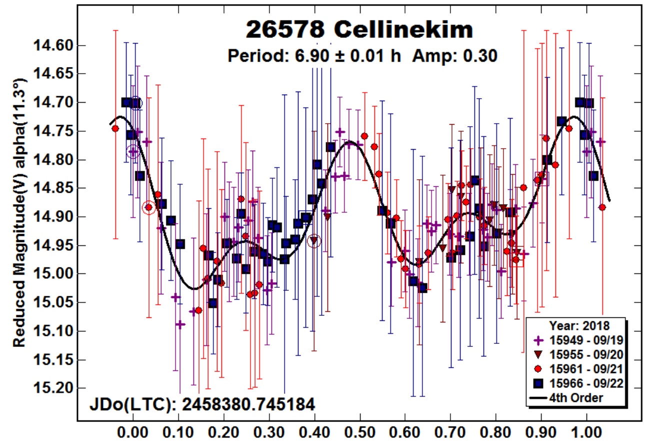

(37378) 2001 VU76. The first observations of this 2.2 km Hungaria were made in 2018 late June. At that time, the best solution appeared to be a bimodal lightcurve with a period of 1.780 h. This put the asteroid above the spin barrier of about 2.2 hours. For that reason, the double period of 3.56 h was considered.

This gave a quadramodal lightcurve that was highly symmetric about the two halves, which is a suspicious result since it requires extraordinary symmetry in the asteroid shape. In the end, the 1.780 hour period was adopted.

Such extraordinary results required verification and so the asteroid was re-observed two months later. The phase angle bisector longitude and latitude (see Harris et al., 2004) did not change significantly over that time but the phase angle doubled to 36°.

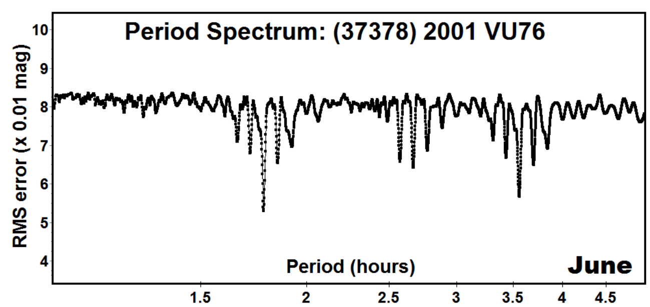

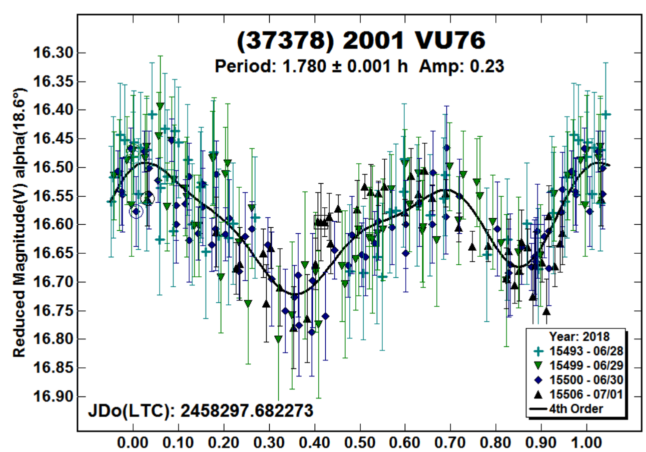

Lightcurve amplitudes generally increase with larger phase angles (Zappala et al., 1990). In this case, the opposite was true when working with later data set, making it even more difficult to determine the correct period. Since the viewing aspect did not change significantly, the best guess for the unexpected behavior is deeper shadowing effects at the higher phase angle. That, in turn, lends some credibility to a "strange" shape that might result in a quadramodal lightcurve despite the larger amplitude at the lower phase angle.

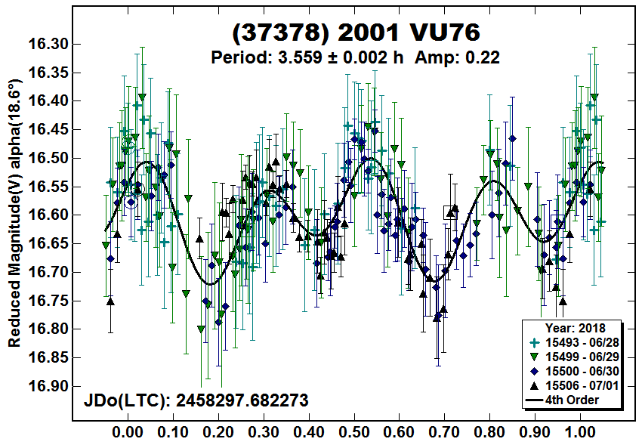

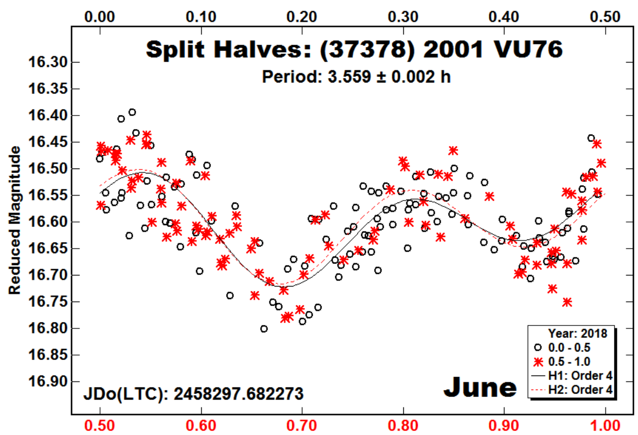

The mid-August data were fit to P = 1.792 ± 0.001 h, a little longer than the period found in June. This gave a low-amplitude bimodal lightcurve. The fit to a period near 3.5 h, however, gave a lightcurve that could be only loosely interpreted to be showing alternating maximums of different heights, which was the case for the June lightcurve. The asymmetry of the mid-August 3.5-hour lightcurve may justify adopting the longer period but, for now, a period of 1.780 h is considered to be the more probable solution.

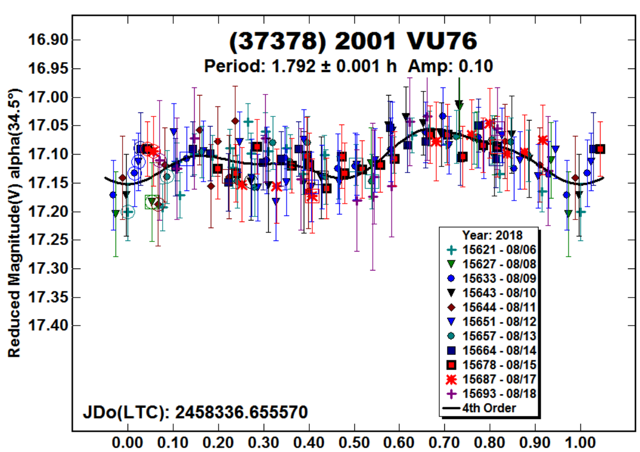

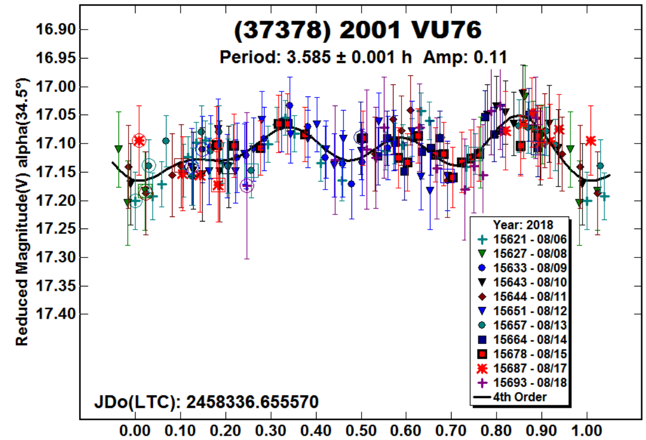

The location of the two periods is shown in the frequency-diameter plot based on the LCDB. The shorter period is above the spin barrier, but only by a small amount, i.e., the solution is not unreasonable. The longer period puts 2001 VU76 in the league of ordinary asteroids. Further observations are encouraged.

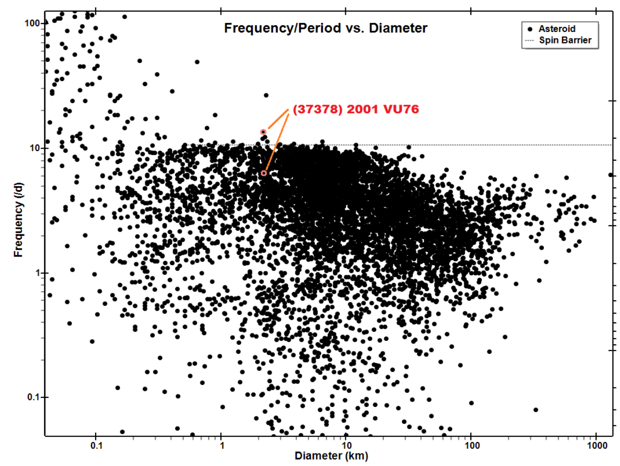

(56213) 1999 GW50. There were no previous rotation periods found in the LCDB. The asteroid was not observed by the recent IR surveys and so its estimated size of 6.1 km is based on using an albedo of 0.1, which is assumed for middle main-belt asteroids.

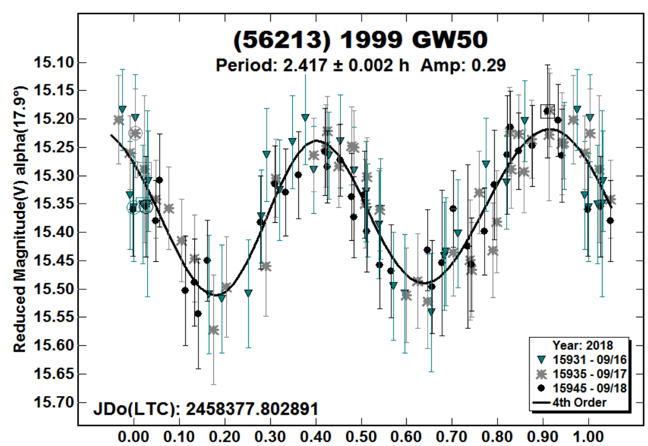

(186035) 2001 RX80. Circumstances did not allow following this 2.5 km middle main-belt asteroid long enough to get a reliable solution. A waxing moon and fading asteroid is not a good combination.

Number	Name	2018 mm/dd	Pts	Phase	L_{PAB}	B_{PAB}	Period(h)	P.E.	Amp	A.E.	Group
4019	Klavetter	07/23-07/23	106	11.8,11.8	322	3	4.671	0.003	0.27	0.03	FLOR
4483	Petofi	06/29-07/01	152	32.6,32.5	333	26	4.334	0.001	1.05	0.03	H
5175	Ables	06/28-07/02	108	26.4,25.6	321	21	2.6862	0.0007	0.33	0.02	H
5998	Sitensky	07/05-07/19	187	16.1,11.8	322	3	6.500	0.001	0.44	0.02	MB-O
17408	McAdams	08/22-08/28	146	32.9,32.2	27	19	18.42	0.04	0.51	0.05	H
25059	1998 QA69	08/28-09/11	356	7.8,13.6	327	9	11.759	0.004	0.24	0.02	MB-I
26578	Cellinekim	09/19-09/22	136	11.3,10.2	22	0	6.90	0.01	0.3	0.03	MB-O
37378	2001 VU76	06/28-07/01	195	18.6,20.3	261	17	1.78	0.001	0.23	0.03	H
37378	2001 VU76	08/06-08/18	157	34.5,36.7	271	24	1.792	0.001	0.1	0.02	H
56213	1999 GW50	09/16-09/18	108	18.0,17.5	36	-5	2.417	0.002	0.29	0.03	MB-M
186035	2001 RX80	09/16-09/18	87	22.2,21.6	34	-5	21.4	0.5	0.65	0.1	MB-M
282505	2004 PA102	07/23-07/23	155	15.0,15.0	320	2	7.092	0.003	0.69	0.04	MB-I

Table II. Observing circumstances and results. The phase angle (α) is given at the start and end of each date range. L_{PAB} and B_{PAB} are, respectively, the average phase angle bisector longitude and latitude (see Harris *et al.*, 1984). The Group column gives the orbital group to which the asteroid belongs. The definitions are those used in the LCDB (Warner et al., 2009a). FLOR: Flora, H: Hungaria, MB-I/M/O: Main-belt inner/middle/outer.

As a result, the solution is not fully secure. The period spectrum shows two more likely than not solutions. The shorter one of 10.7 hours shows a bimodal lightcurve of 0.59 mag amplitude. However, the shape is not symmetrical: the fall from the first maximum to the minimum takes only 0.35 of the period. Regardless, it was the best fit achieved without extraordinary zero point adjustments.

Given the amplitude, a bimodal solution seemed inevitable (Harris et al., 2014). However, when using a second order Fourier search a period of about 20.4 hours was found, not the double period of 21.4 hours. The data can be fit to both periods. It's almost certain that the period is about 21 hours. It will take more data to prove that assertion.

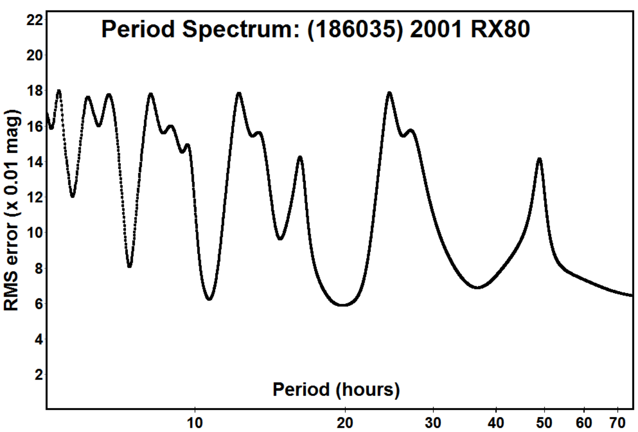

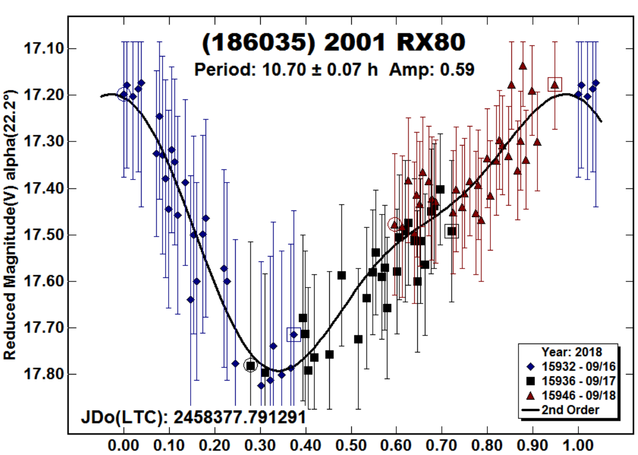

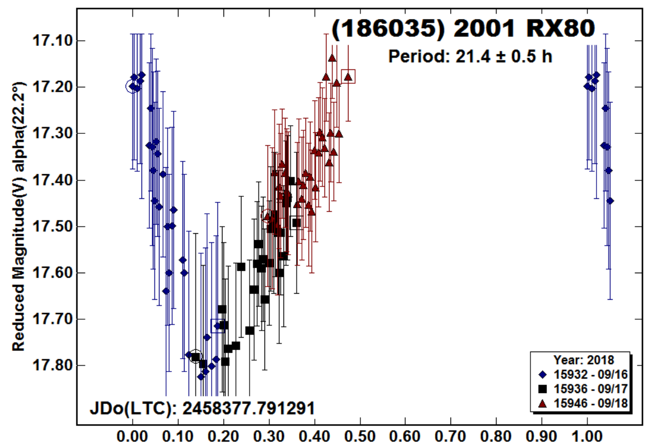

<u>(282505) 2004 PA102</u>. A good data set and large amplitude led to a very reliable solution for this inner main-belt asteroid. The estimated diameter is 1.5 km.

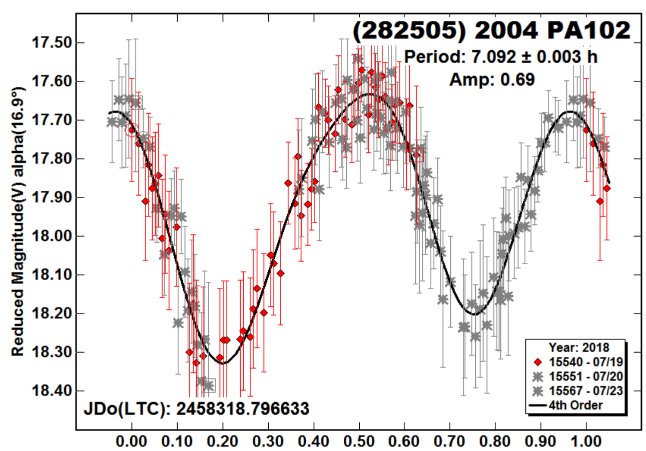

Acknowledgements

Observations at CS3 and continued support of the asteroid lightcurve database (LCDB; Warner et al., 2009a) are supported by NASA grant 80NSSC18K0851. Work on the asteroid lightcurve database (LCDB) was also partially funded by National Science Foundation grant AST-1507535.

This research was made possible through the use of the AAVSO Photometric All-Sky Survey (APASS), funded by the Robert

Martin Ayers Sciences Fund, and by data from CMC15 Data Access Service at CAB (INTA-CSIC) (*http://svo2.cab.inta-csic.es/vocats/cmc15/)*.

The author gratefully acknowledges a Shoemaker NEO Grant from the Planetary Society (2007), which was used to purchase some of the equipment used in this research.

References

References from web sites should be considered transitory, unless from an agency with a long lifetime expectancy. Sites run by private individuals, even if on an institutional web site, do not necessarily fall into this category.

Harris, A.W., Young, J.W., Scaltriti, F., Zappala, V. (1984). “Lightcurves and phase relations of the asteroids 82 Alkmene and 444 Gyptis.” *Icarus* **57**, 251-258.

Harris, A.W., Young, J.W., Bowell, E., Martin, L.J., Millis, R.L., Poutanen, M., Scaltriti, F., Zappala, V., Schober, H.J., Debehogne, H., Zeigler, K.W. (1989). “Photoelectric Observations of Asteroids 3, 24, 60, 261, and 863.” *Icarus* **77**, 171-186.

Harris, A.W., Pravec, P., Galad, A., Skiff, B.A., Warner, B.D., Vilagi, J., Gajdos, S., Carbognani, A., Hornoch, K., Kusnirak, P., Cooney, W.R., Gross, J., Terrell, D., Higgins, D., Bowell, E., Koehn, B.W. (2014). “On the maximum amplitude of harmonics on an asteroid lightcurve.” *Icarus* **235**, 55-59.

Henden, A.A., Terrell, D., Levine, S.E., Templeton, M., Smith, T.C., Welch, D.L. (2009). *http://www.aavso.org/apass*

Lucas, M.P., Emery, J.P., Pinilla-Alonso, N., Lindsay, S.S., Lorenzi, V. (2017). “Hungaria asteroid region telescopic spectral survey (HARTSS) I: Stony asteroids abundant in the Hungaria background population.” *Icarus* **291**, 268-287.

Mainzer, A.K., Bauer, J.M., Cutri, R.M., Grav, T., Kramer, E.A., Masiero, J.R., Nugent, C.R., Sonnett, S.M., Stevenson, R.A., Wright, E.L. (2016). “NEOWISE Diameters and Albedos V1.0.” NASA Planetary Data System.
EAR-A-COMPIL-5-NEOWISEDIAM-V1.0.

Warner, B.D. (2008). “Asteroid Lightcurve Analysis at the Palmer Divide Observatory - June - October 2007.” *Minor Planet Bull.* **35**, 56-60.

Warner, B.D., Harris, A.W., Pravec, P. (2009a). “The Asteroid Lightcurve Database.” *Icarus* **202**, 134-146. Updated 2018 June. *http://www.minorplanet.info/lightcurvedatabase.html*

Warner, B.D. (2009b). “Asteroid Lightcurve Analysis at the Palmer Divide Observatory: 2009 March-June.” *Minor Planet Bull.* **36**, 172-176.

Warner, B.D (2011). “Lightcurve Analysis at the Palmer Divide Observatory: 2010 June-September.” *Minor Planet Bull.* **38**, 25-31.

Warner, B.D. (2012). “Asteroid Lightcurve Analysis at the Palmer Divide Observatory: 2012 March - June.” *Minor Planet Bull.* **39**, 245-252.

Warner, B.D. (2014). “Asteroid Lightcurve Analysis at CS3-Palmer Divide Station: 2013 September-December.” *Minor Planet Bull.* **41**, 102-112.

Warner, B.D. (2015). “Asteroid Lightcurve Analysis at CS3-Palmer Divide Station: 2015 March-June.” *Minor Planet Bull.* **42**, 267-276.

Waszczak, A., Chang, C.-K., Ofek, E.O., Laher, R., Masci, F., Levitan, D., Surace, J., Cheng, Y.-C., Ip, W.-H., Kinoshita, D., Helou, G., Prince, T.A., Kulkarni, S. (2015). “Asteroid Light Curves from the Palomar Transient Factory Survey: Rotation Periods and Phase Functions from Sparse Photometry.” *Astron. J.* **150**, A75.

Zappala, V., Cellini, A., Barucci, A.M., Fulchignoni, M., Lupishko, D.E. (1990). “An analysis of the amplitude-phase relationship among asteroids.” *Astron. Astrophys*. **231**, 548-560.

ASTEROID-DEEPSKY APPULSES IN 2019

Brian D. Warner
Center for Solar System Studies
446 Sycamore Ave.
Eaton, CO 80615
brian@MinorPlanetObserver.com

(Received: 2018 September 29)

The following list is a *very small* subset of the results of a search for asteroid-deepsky appulses for 2019, presenting only the highlights for the year based on close approaches of brighter asteroids to brighter DSOs. For the complete set visit

http://www.minorplanet.info/ObsGuides/Appulses/DSOAppulses.htm

For any event not covered, the Minor Planet Center's web site at *https://www.minorplanetcenter.net/cgi-bin/checkmp.cgi* allows you to enter the location of a suspected asteroid or supernova and check if there are any known targets in the area.

The table gives the following data:

Date/Time	Universal Date (MM DD) and Time of closest approach
#/Name	The number and name of the asteroid
RA/Dec	The J2000 position of the asteroid
AM	The approximate visual magnitude of the asteroid
Sep/PA	The separation in arcseconds and the position angle from the DSO to the asteroid
DSO	The DSO name or catalog designation
DM	The approximate total magnitude of the DSO
DT	DSO Type: OC = Open Cluster; GC = Globular Cluster; G = Galaxy
SE/ME	The elongation in degrees from the sun and moon, respectively
MP	The phase of the moon: 0 = New, 1.0 = Full. Positive = waxing; Negative = waning

Date	UT	#	Name	RA	Dec	AM	Sep	PA	DSO	DM	DT	SE	ME	MP
01 02	**14:43**	**151**	**Abundantia**	**12 22.07**	**+04 32.5**	**14.0**	**219**	**17**	**M61**	**9.6**	**G**	**98**	**60**	**-0.11**
01 04	22:34	337	Devosa	12 08.28	+02 55.1	12.8	146	31	NGC 4123	11.4	G	103	91	-0.01
01 13	15:48	92	Undina	10 47.28	+17 17.6	12.2	179	58	NGC 3370	11.6	G	136	141	0.44
01 31	14:37	224	Oceana	08 27.11	+25 59.3	12.4	81	7	NGC 2592	12.3	G	169	141	-0.15
02 04	19:18	216	Kleopatra	06 52.17	+02 55.3	11.1	48	215	Biur 10	10.4	OC	143	143	0.00
02 05	23:14	110	Lydia	12 19.41	+06 07.1	12.6	11	41	NGC 4260	11.8	G	134	146	0.01
02 07	**19:44**	**388**	**Charybdis**	**10 44.08**	**+11 45.9**	**13.4**	**246**	**17**	**M95**	**9.7**	**G**	**160**	**167**	**0.08**
03 01	08:13	236	Honoria	09 29.31	+07 40.7	13.0	157	210	NGC 2894	12.4	G	161	140	-0.23
03 02	20:38	92	Undina	10 18.47	+21 56.4	11.8	156	24	NGC 3193	10.9	G	163	151	-0.12
03 03	08:45	433	Eros	06 34.97	+05 22.3	10.3	46	211	NGC 2252	7.7	OC	116	147	-0.09
03 05	04:21	7	Iris	13 09.07	-15 26.5	9.9	275	13	NGC 4984	11.3	G	142	126	-0.02
03 06	08:47	151	Abundantia	12 23.14	+05 13.3	12.7	173	200	NGC 4324	11.6	G	161	159	0.00
03 06	13:42	136	Austria	10 12.55	+03 05.0	13.0	223	217	NGC 3156	12.3	G	166	164	0.00
03 09	03:41	405	Thia	13 41.21	-29 56.8	11.3	230	258	NGC 5264	12.0	G	131	151	0.06
03 09	16:51	151	Abundantia	12 20.47	+05 27.0	12.6	193	19	NGC 4281	11.3	G	164	160	0.09
03 10	08:20	1304	Arosa	11 39.83	+31 58.1	13.8	212	27	NGC 3786	12.3	G	152	129	0.13
03 10	08:28	151	Abundantia	12 19.92	+05 29.7	12.6	47	18	NGC 4270	12.2	G	165	152	0.13
03 28	13:05	665	Sabine	13 31.93	-33 16.2	12.9	136	171	NGC 5193	11.6	G	146	70	-0.46
04 01	06:13	326	Tamara	13 00.15	+12 24.6	12.0	270	170	NGC 4880	11.4	G	163	135	-0.15
04 02	17:36	191	Kolga	12 47.86	+04 22.3	13.5	92	34	NGC 4688	11.9	G	171	154	-0.06
04 03	04:34	57	Mnemosyne	13 05.63	-08 02.3	11.9	99	217	NGC 4958	10.7	G	175	150	-0.04
04 03	06:33	532	Herculina	09 09.73	+33 11.0	9.8	208	29	NGC 2770	12.2	G	116	139	-0.04
04 08	15:18	787	Moskva	12 45.18	+00 27.3	13.2	26	223	NGC 4666	10.7	G	171	134	0.11
04 29	00:46	212	Medea	18 03.38	-27 53.4	13.9	36	339	NGC 6520	7.6	OC	127	60	-0.30
04 11	20:15	787	Moskva	12 42.69	+00 06.6	13.3	125	41	NGC 4632	11.7	G	168	90	0.40
04 28	23:39	490	Veritas	14 11.44	-05 04.8	13.2	118	206	NGC 5493	11.4	G	170	119	-0.31
04 29	00:46	212	Medea	18 03.38	-27 53.4	13.9	36	339	NGC 6520	7.6	OC	127	60	-0.30
04 29	08:04	326	Tamara	12 22.25	+09 00.0	12.4	222	144	NGC 4307	12.0	G	142	153	-0.28
04 30	18:35	349	Dembowska	10 25.18	+17 10.3	11.2	68	72	NGC 3239	11.3	G	112	160	-0.17
05 07	18:07	44	Nysa	14 03.46	-05 57.6	10.1	211	16	NGC 5427	11.4	G	163	129	0.09
06 04	07:16	1166	Sakuntala	17 27.58	-05 01.8	12.8	217	331	NGC 6366	10.0	GC	160	164	0.01
07 05	00:32	33	Polyhymnia	00 39.33	+03 00.9	12.1	75	156	NGC 194	12.2	G	92	123	0.07
07 05	13:48	221	Eos	14 22.58	+00 22.7	13.1	177	63	NGC 5584	11.4	G	110	72	0.11
07 06	11:36	702	Alauda	23 50.85	+20 10.4	13.0	225	293	NGC 7769	12.0	G	97	141	0.18
07 07	08:26	323	Brucia	18 31.06	-25 33.3	12.7	239	146	NGC 6638	9.2	GC	172	110	0.27
08 25	01:33	410	Chloris	17 23.95	-26 23.0	12.0	126	200	NGC 6355	9.6	GC	111	174	-0.35
09 04	22:59	679	Pax	17 21.26	-19 34.3	13.6	64	49	NGC 6342	9.9	GC	99	23	0.38
09 05	18:51	21	Lutetia	00 42.72	-01 32.6	10.0	44	150	NGC 227	12.1	G	153	121	0.47
09 23	05:00	1186	Turnera	01 53.16	+04 15.0	13.4	243	352	NGC 718	11.7	G	151	76	-0.38
10 25	18:02	162082	1998 HL1	01 50.33	+27 38.7	12.9	110	67	NGC 684	12.4	G	164	138	-0.08
10 28	00:13	773	Irmintraud	02 35.39	+40 57.7	13.6	41	354	NGC 982	12.5	G	151	146	0.00
10 29	11:58	162082	1998 HL1	02 27.63	-01 09.3	13.2	69	252	NGC 936	10.1	G	165	158	0.03
11 02	11:21	1186	Turnera	01 20.10	+03 27.0	13.3	119	360	NGC 474	11.5	G	160	92	0.32
11 02	20:45	1186	Turnera	01 19.80	+03 27.0	13.3	119	0	NGC 470	11.8	G	159	87	0.35
11 24	22:52	139	Juewa	09 14.99	+29 45.2	12.3	70	353	NGC 2789	12.2	G	110	87	-0.04
11 28	01:32	41	Daphne	02 30.60	-01 05.8	12.6	11	345	NGC 955	12.0	G	147	130	0.03
12 03	**14:57**	**1074**	**Beljawskya**	**06 08.90**	**+24 19.5**	**14.0**	**27**	**184**	**M35**	**5.1**	**OC**	**159**	**118**	**0.44**

7002 BRONSHTEN: A NEW MARS-CROSSING BINARY

Brian D. Warner
Center for Solar System Studies / MoreData!
446 Sycamore Ave.
Eaton, CO 80615 USA
brian@MinorPlanetObserver.com

Robert D. Stephens
Center for Solar System Studies / MoreData!
Rancho Cucamonga, CA USA

(Received: 2018 September 30)

CCD photometric observations of the Mars-crosser asteroid 7002 Bronshten show it to be a binary system. The primary period is P_1 = 2.67025 ± 0.00007 h. The orbital period of the satellite, which is also its rotation period, is P_{ORB} = 13.323 ± 0.003 h. The mutual event attenuations in the satellite lightcurve are 0.06-0.11 mag. This establishes a lower limit of the secondary-to-primary mean diameter ratio of 0.24 ± 0.02.

The minor planet 7002 Bronshten is a member of the Mars-crossing group of asteroids. Carry et al. (2016) used Sloan photometry data to determine the asteroid is type S in the Bus-DeMeo taxonomic system. The estimated diameter is 3.4 km. The only previously reported period for Bronshten was by Skiff (2011), who found a period of 2.671 ± 0.001 h. He did not report any indications of a satellite.

Warner began observations of the asteroid 2018 July 5 when it was at –9° Declination. After a couple of nights, it seemed apparent that the asteroid was likely a binary. The southerly position reduced the potential number of hours for each night's run since the 0.5-m telescope is restricted to objects with an altitude *A* > 40°. On the other hand, Stephens could observe down to 30° altitude, which could add almost another two hours to each night's observing run, and so he took over observations starting July 21. This proved vital to completing the lightcurve for the satellite and finding the correct orbital period.

Table I lists the equipment that was used at CS3. The cameras have KAF blue-enhanced CCD chips and so have essentially the same response. The pixel scales ranged from 1.24-1.60 arcsec/pixel. All lightcurve observations were unfiltered since a clear filter can result in a 0.1-0.3 magnitude loss.

Telescopes	Cameras
0.40-m f/10 Schmidt-Cass	FLI Proline 1001E
0.50-m *f*/8.1 Ritchey-Chrétien	FLI Proline 1001E

Table I. List of telescopes and cameras used.

Observer	Dates	Sessions	Scope
Warner	2018 07/05-07/20	1-6	0.5-m R-C
Stephens	2018 07/21-07/23	7-9	0.4-m SCT

Table II. Dates of observation for each person.

Tables II and III shows observational details and the final results of period analysis.

Measurements were made using *MPO Canopus*. The Comp Star Selector utility in *MPO Canopus* found up to five comparison stars of near solar-color for differential photometry. Catalog magnitudes were usually taken from the APASS (Henden et al., 2009) or CMC-15 (Munos, 2017) catalogs.

Period analysis was done with *MPO Canopus*, which implements the FALC algorithm by Harris (Harris *et al.,* 1989). The dual-period feature in *MPO Canopus* uses an iterative instead of simultaneous algorithm to find more than one period.

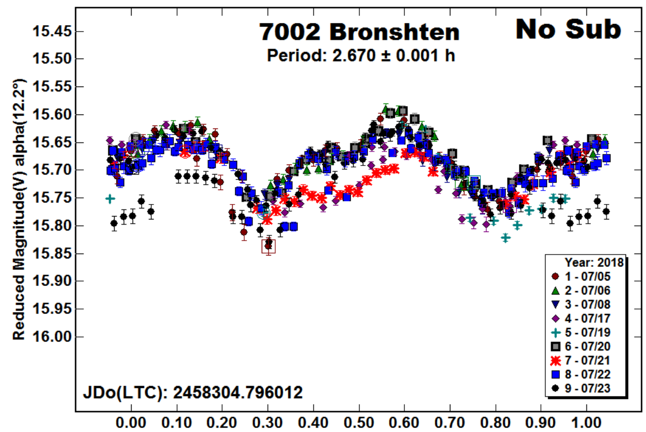

The "No Sub" plot shows a single period solution using the entire data set. The prolonged deviations of lower magnitude are a good indication of occultations and/or eclipses due to a satellite.

A good estimate of the primary period was easily established after only a couple of nights. However, the orbital period proved to be more difficult. Through July 22, the period seemed to be about 18.4 h, but the mutual events were not symmetrically spaced, i.e., there were not close to 0.5 orbital period apart. This is not impossible if the satellite orbit is significantly eccentric, but it's rare.

Additional data from Stephens on July 23 solved the mystery by leading to an orbital period of 13.323 h ("Porb") with symmetrically-spaced events. The "P_1" and "P_{ORB}" plots show the final results: P_1 = 2.67025 ± 0.00007 h, A_1 = 0.13 mag and P_{ORB} = 13.323 ± 0.003 h, A_{EVENTS} = 0.06-0.11 mag. Note that the lightcurve in P_{ORB} is not flat between the events. This likely indicates that the satellite is somewhat elongated.

Using the lesser amplitude of the two events gives the estimated size ratio of the two bodies:

$$\frac{Ds}{Dp} = \sqrt{(10^{0.4\Delta m} - 1.0)}$$

$$\geq 0.24 \pm 0.02$$

Number	Name	2018 mm/dd	Pts	Phase	L_{PAB}	B_{PAB}	Period(h)	P.E.	Amp	A.E.
7002	Bronshten	07/05-07/23	363	12.3,6.3	296	+8	2.67025	0.00007	0.13	0.01
	Orbital period						13.323	0.003	0.06-0.11	0.01

Table III. Observing circumstances and results. The phase angle (α) is given at the start and end of each date range. L_{PAB} and B_{PAB} are, respectively, the average phase angle bisector longitude and latitude (see Harris *et al.*, 1984). The first line gives the results for the primary in the binary system. The second line gives the orbital period of the satellite and the amplitude range of mutual events.

where D_S and D_P are, respectively, the effective diameters of the satellite and primary. The value is a minimum since no total eclipses were seen.

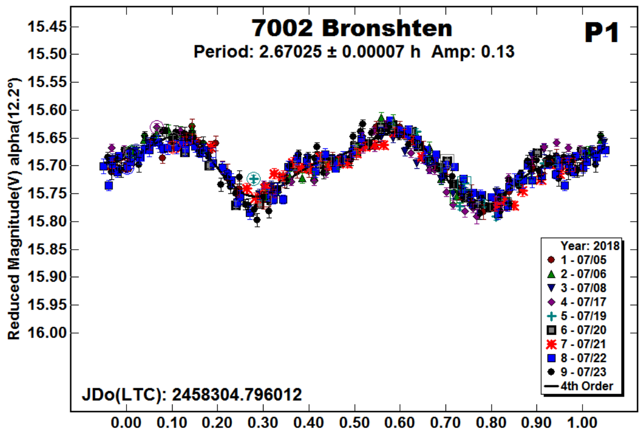

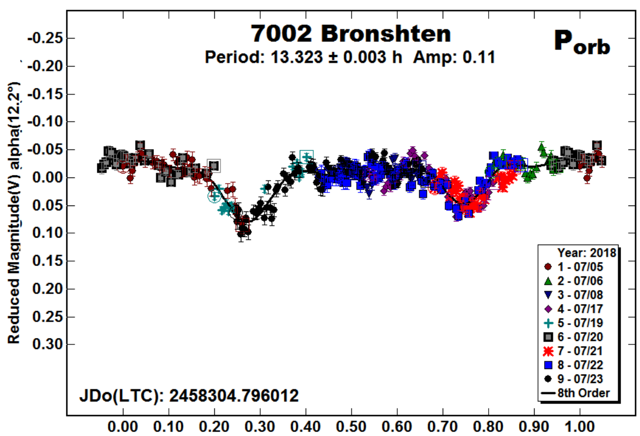

Acknowledgements

Observations at CS3 and continued support of the asteroid lightcurve database (LCDB; Warner et al., 2009) are supported by NASA grant 80NSSC18K0851. Work on the asteroid lightcurve database (LCDB) was also funded in-part by National Science Foundation grant AST-1507535.

This research was made possible through the use of the AAVSO Photometric All-Sky Survey (APASS), funded by the Robert Martin Ayers Sciences Fund, and by data from CMC15 Data Access Service at CAB (INTA-CSIC) (*http://svo2.cab.inta-csic.es/vocats/cmc15/)*.

The authors gratefully acknowledge Shoemaker NEO Grants from the Planetary Society (2007, 2013). These were used to purchase some of the telescopes and CCD cameras used in this research.

References

Carry, B., Solano, E., Eggl, S., DeMeo, F.E. (2016). “Spectral properties of near-Earth and Mars-crossing asteroids using Sloan photometry.” *Icarus* **268**, 340-354.

Harris, A.W., Young, J.W., Scaltriti, F., Zappala, V. (1984). “Lightcurves and phase relations of the asteroids 82 Alkmene and 444 Gyptis.” *Icarus* **57**, 251-258.

Harris, A.W., Young, J.W., Bowell, E., Martin, L.J., Millis, R.L., Poutanen, M., Scaltriti, F., Zappala, V., Schober, H.J., Debehogne, H., Zeigler, K.W. (1989). “Photoelectric Observations of Asteroids 3, 24, 60, 261, and 863.” *Icarus* **77**, 171-186.

Henden, A.A., Terrell, D., Levine, S.E., Templeton, M., Smith, T.C., Welch, D.L. (2009). *http://www.aavso.org/apass*

Munos, J.L. (2017) Carlsberg Meridian Catalog web site. *http://svo2.cab.inta-csic.es/vocats/cmc15/*

Skiff, B.A. (2011). Posting on CALL web site. *http://www.minorplanet.info/call.html*

Warner, B.D., Harris, A.W., Pravec, P. (2009). “The Asteroid Lightcurve Database.” *Icarus* **202**, 134-146. Updated 2018 June. *http://www.minorplanet.info/lightcurvedatabase.html*

(31345) 1998 PG: A BINARY NEAR-EARTH ASTEROID?

Brian D. Warner
Center for Solar System Studies
446 Sycamore Ave.
Eaton, CO 80615 USA
brian@MinorPlanetObserver.com

Petr Pravec
Astronomical Institute
Academy of Sciences of the Czech Republic
Fricova, CZ-25165 Ondřejov, CZECH REPUBLIC
ppravec@asu.cas.cz

Amadeo Aznar Macías
APT Observatory Group
EURONEAR
Valencia, SPAIN

Vladimir Benishek
Belgrade Astronomical Observatory
Volgina 7, 11060 Belgrade 38, SERBIA

Victor Casanova
Observatorio de Sierra Nevada
Instituto de Astrofisica de Andalucia-CSIC
SPAIN

Julian Oey
Blue Mountains Observatory (MPC Q68)
Leura, NSW AUSTRALIA

Donald P. Pray
Sugarloaf Mountain Observatory
South Deerfield, MA USA

(Received: 2018 October 12)

Photometric observations of the near-Earth asteroid (31345) 1998 PG by Pravec et al. (2000) found a rotation period of 2.51620 h. Also found was a secondary period of 7.0035 h, or the double-period of 14.007 h, possibly indicating an additional body in the system. An extended campaign by the authors in 2018 lead to a similar primary period of 2.5168 h. However, instead of a 7-hour secondary period, one of about 16 hours was found with the lightcurve showing apparent mutual events (occultations and/or eclipses). The data sets from 1998 and 2018 could not be fit to a secondary period near the one found at the opposing apparition. The conclusion is that the asteroid is very likely binary, but – other than the primary rotation period – the system's parameters are ill-defined and only future observations will sufficiently refine them.

(31345) 1998 PG is a near-Earth asteroid (NEA) with an estimated diameter of 0.9 km (LCDB; Warner et al., 2009). The first reported rotation period came from Kiss et al. (1999), who found a period of 2.5 hours based on a sparse data set. Pravec et al. (2000) performed an extensive campaign in 1998, shortly after the asteroid's discovery.

Analysis of their data found a primary rotation period of P_1 = 2.51620 ± 0.00003 h and lightcurve amplitude of 0.11 mag. They also found a secondary period with a period of P_2 = 7.0035 ± 0.0007 h (A = 0.09 mag) that produced a monomodal lightcurve. This was interpreted as indicating a second body in the system. Allowing for the possibility that P_2 was actually the half-period and that the putative satellite's rotation period was tidally locked to its orbital period, they suggested that the double-period was the correct solution, i.e., P_2 = 14.007 ± 0.0014 h. A check for a third period found a very weak solution that was not considered reliable since its amplitude rivaled the scatter in the data.

In 2018, a new campaign involving observers in North America, Europe, and Australia lead to essentially the same results for P_1 but not for P_2. Table I shows the list of observers and the instrument used by each one.

OBS	Telescope	Camera
Warner (BW)	0.50m R-C 0.35m SCT	FLI PL-1001E FLI ML-1001E
Aznar (AA)	1.50m N-C	Andor iKon-L 936
Benishek (VB)	0.35m SCT	SBIG ST-8/10XME
Oey (JO)	0.61m CDK	Apogee U16M
Pray (DP)	0.50m NWT	ST-10XME

Table I. The instrumentation used by the observers. SCT: Schmidt-Cassegrain; R-C: Ritchey-Chretien; N-C: Nasmyth-Cassegrain; CDK: Corrected Dall-Kirkham; NWT: Newtonian reflector.

All observations were unfiltered with exposures based on the telescope used and asteroid magnitude. Each observer measured his own images, which were flat-field and dark frame corrected, using *MPO Canopus*. The Comp Star Selector utility was used to find up to five near solar-color stars for ensemble differential photometry. Catalog magnitudes were taken from the APASS (Henden et al., 2009), CMC-15 (Munos, 2017), or MPOSC3 catalogs.

All observers used V magnitudes, except Pray, who used R. The V magnitudes are native only to the APASS catalog. The R magnitudes are not native to any of the three. For CMC-15, conversion formulae by Jester (2005) were used to get V magnitudes. For the MPOSC3, which is a hybrid based on the 2MASS catalog, formulae by Warner (2007) were used for the R magnitudes.

The initial observations were made by Warner. When it became apparent that a single station could not determine the system parameters because the second period was nearly commensurate with an Earth day, the other observers joined in a collaboration effort. Table II lists the observers, the dates of their observations, and the session numbers (those given in the lightcurve legends).

OBS	Dates (2018 mm/dd)	Sess
BW	07/25-08/06 08-09 30-31	1-15 20 23 28 31
AA	21, 27-28, 31	24-27 30
VB	08/06-08 30	16 19 22 29
JO	08/07-08	18 21
DP	08/08	17

Table II. The observer codes are given in Table I. The Sess column gives the session numbers in the data set. These are listed in the legend for each lightcurve.

Initial Period Analysis

The initial period analysis was done by Warner using *MPO Canopus*, which incorporates the FALC period search algorithm (Harris et al., 1989). *MPO Canopus* does an iterative dual period search, i.e., finds a dominant period and subtracts it to find the second period; it then subtracts the second period to find the first period again. The process is repeated until the two periods stabilize. This usually works for additive lightcurves such as with 1998 PG. It does not work on complex periods such as those for tumbling asteroids. In that case, and for a better solution for additive lightcurves, custom software by Pravec uses a simultaneous period search (see, e.g., Pravec et al., 2000).

It was apparent that there was a long period component in the data after only the first few observing runs. However, the short period was not very strong and, in fact, almost not existent. When doing the initial dual period analysis with *MPO Canopus*, the short period search was be forced to a range of 2.5-2.56 h, i.e., to include P_1 found by Pravec et al. (2000) since it was considered secure.

Using the initial value for P_1 from the 2018 data, a secondary period of about 16 hours emerged and, with each additional data set, became more definitive. The same applied to the primary period, although – as seen in the period spectrum for the combined data set (PS1-C) – the solution was weak and stayed that way to the end of the campaign.

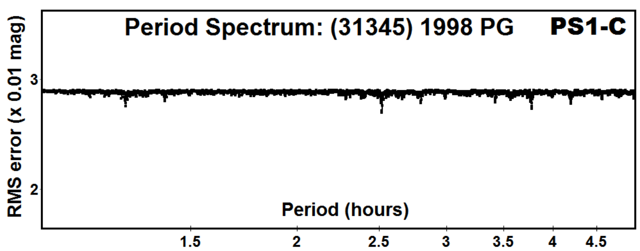

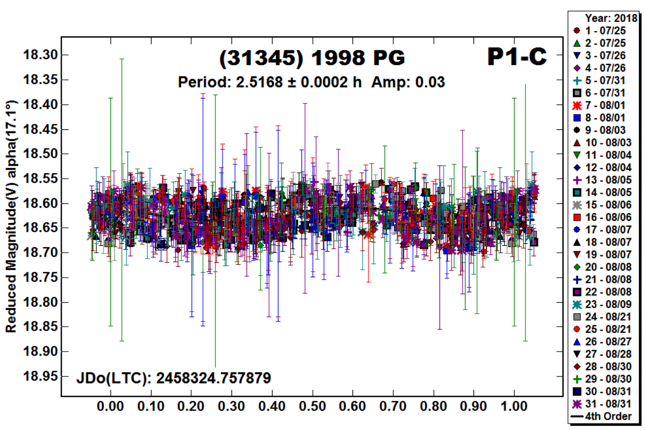

The period for the secondary lightcurve for the combined data set was clearly defined (PS2-C). On first glance, it appeared to show mutual events (occultations and/or eclipses), which would secure the claim of the asteroid being binary. If so, then the presumed satellite rotation was tidally locked to the orbital period. Questions remain, however, about the secondary period solution.

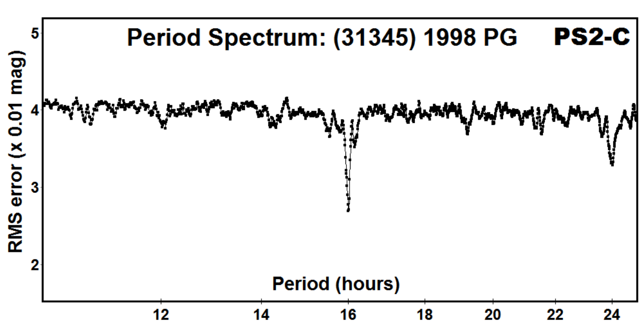

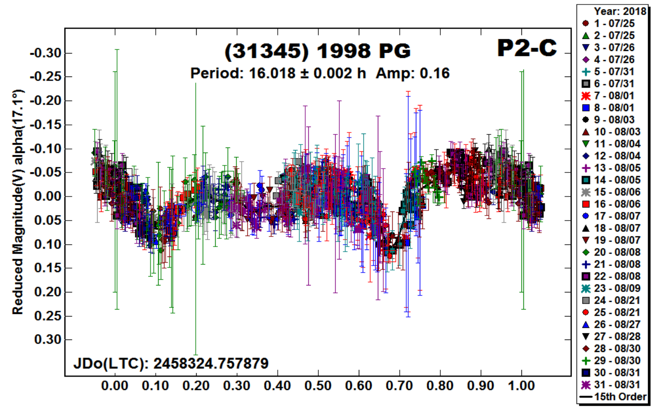

First, the mutual events are not evenly spaced in the orbit. Instead of being 0.5 rotation phase apart, the events are spaced about 0.6 (or 0.4) rotation phase apart. This is possible with the right viewing geometry and if the satellite orbit is sufficiently eccentric, which is very rare. Numerous other periods were tried to see if they would produce a symmetric secondary lightcurve. None did and, as seen in the period spectrum, no solution other than $P_2 = 16.018 \pm 0.002$ h was remotely possible.

The greatest concern is that Pravec could not get the 1998 data set to fit the 16-hour solution, only those periods originally reported. He was given the 2018 data set and found that the 16-hour solution was very likely. Compounding the problem was that when the 2018 data set was broken into two parts, one before and one after interference from the moon, Pravec found that the lightcurve components had changed. Separate solutions are shown for the "early" (E) and "late" (L) lightcurve plot pairs.

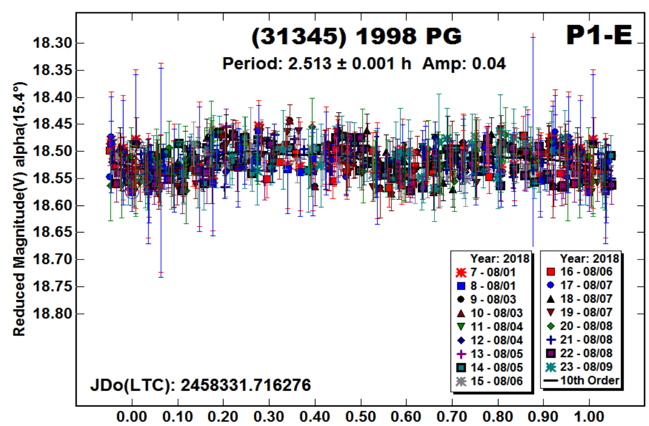

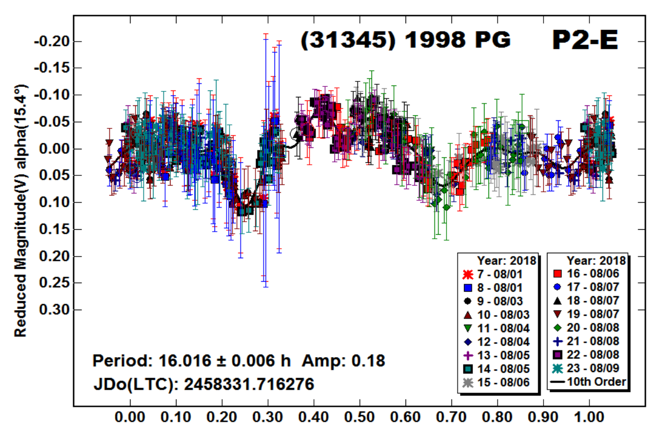

Number	Name	2018 mm/dd	Pts	Phase	L_{PAB}	B_{PAB}	Period(h)	P.E.	Amp	A.E.
31345	1998 PG	07/25-08/31	927	17.2,14.8,22.7	319	+13	2.5168	0.0002	0.03	0.01
							16.018	0.002	0.16	0.02
31345	1998 PG	07/25-08/31	696				2.513	0.001	0.04	0.01
							16.016	0.006	0.18	0.02
31345	1998 PG	07/25-08/31	231				2.5139	0.0005	0.06	0.01
							16.014	0.017	0.11	0.02

Table I. Observing circumstances. The three sets of solutions are based on, from top to bottom, the combined data set, the set before the full moon break, and the set after the break. For each pair, the first line gives the results for the primary and the observing aspects. The second line gives the period and amplitude range of the secondary lightcurve. The end phase angle (α) values are for the start and end of the combined data set. The middle value is the lowest phase angle during the period. L_{PAB} and B_{PAB} are each the average phase angle bisector longitude and latitude (see Harris *et al.*, 1984).

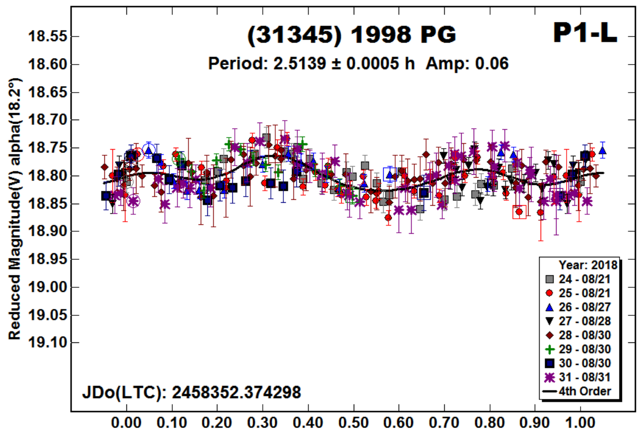

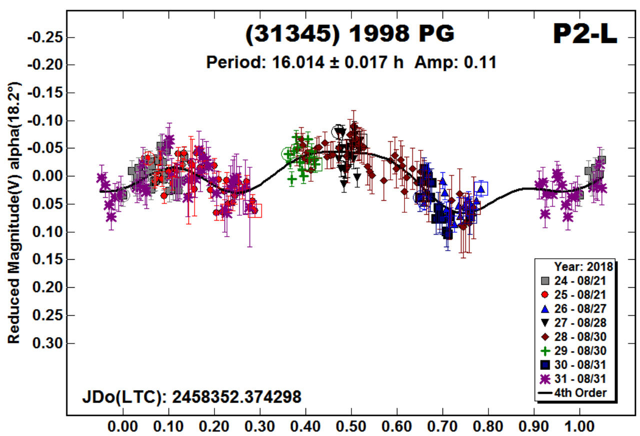

In particular, the change in the P_2 lightcurve, the less dense data set notwithstanding, makes it possible that it does not actually include mutual events but, instead, is simply due to the rotation of an elongated second body. There just aren't enough high-quality data to say for certain.

Conclusion

The lower primary amplitude in 2018, which was seen at about the same phase angle as in 1998, suggests that the viewing aspect in 2018 was at a higher asteroidcentric latitude, i.e., it was more "pole on" and less "equatorial."

It may be possible that the solutions for P_2 in 1998 and 2018 are both correct. If the changing value of P_2 is due to the rotation of a satellite, 1998 PG could be an example of a system with an asynchronous satellite with unstable rotation. Pravec et al. (2016) found similar behavior for (35107) 1991 VH, which had a different rotation period for the satellite at two different apparitions.

At this time, with the available data, it is not possible to say definitively which secondary period, the one from Pravec et al. (2000) or from this work, is correct or, as just mentioned, both are. It seems very likely that there are at least two bodies in the system. It will take high-quality data from future observations to try to finding secure system parameters.

Looking ahead, the next apparition that is V < 18 is in 2021 December (V ≈ 17.8) but it's not favorable because the galactic latitude will be near 0°. After that, the only apparition through 2050 with V < 18 is in 2041 December (V ≈ 17.1), but that is also at very low galactic latitudes. Anyone with data from the 2018 apparition is encouraged to contact Petr Pravec at the email address in the author's list.

Acknowledgements

Observations at CS3 and continued support of the asteroid lightcurve database (LCDB; Warner et al., 2009) are supported by NASA grant 80NSSC18K0851. Work on the asteroid lightcurve database (LCDB) was also funded in part by National Science Foundation grant AST-1507535.

This research was made possible through the use of the AAVSO Photometric All-Sky Survey (APASS), funded by the Robert Martin Ayers Sciences Fund, and by data from CMC15 Data Access Service at CAB (INTA-CSIC) (*http://svo2.cab.inta-csic.es/vocats/cmc15/*).

BW gratefully acknowledges a 2007Shoemaker NEO Grant from the Planetary Society, which was used to purchase some of the equipment used in this research.

Observational work at the Sopot Astronomical Observatory by Vladimir Benishek is supported by a 2018 Gene Shoemaker NEO Grant from the Planetary Society.

Operations at Sugarloaf Mountain Observatory were supported by Gene Shoemaker NEO Grants from the Planetary Society.

This publication makes use of data products from the Two Micron All Sky Survey, which is a joint project of the University of Massachusetts and the Infrared Processing and Analysis Center/California Institute of Technology, funded by the National Aeronautics and Space Administration and the National Science Foundation. (*http://www.ipac.caltech.edu/2mass/*)

References

Harris, A.W., Young, J.W., Scaltriti, F., Zappala, V. (1984). "Lightcurves and phase relations of the asteroids 82 Alkmene and 444 Gyptis." *Icarus* **57**, 251-258.

Harris, A.W., Young, J.W., Bowell, E., Martin, L.J., Millis, R.L., Poutanen, M., Scaltriti, F., Zappala, V., Schober, H.J., Debehogne, H., Zeigler, K.W. (1989). "Photoelectric Observations of Asteroids 3, 24, 60, 261, and 863." *Icarus* **77**, 171-186.

Henden, A.A., Terrell, D., Levine, S.E., Templeton, M., Smith, T.C., Welch, D.L. (2009). *http://www.aavso.org/apass*

Jester, S., Schneider, D.P., Richards, G.T., Green, R.F., Schmidt, M., Hall, P.B., Strauss, M.A., Vanden Berk, D.E., Stoughton, C., Gunn, J.E., Brinkmann, J., Kent, S.M., Smith, J.A., Tucker, D.L, Yanny, B. (2005). "The Sloan Digital Sky Survey View of the Palomar-Green Bright Quasar Survey." *Astron. J.* **130**, 873-895.

Kiss, L.L., Szabo, G., Sarneczky, K. (1999). "CCD photometry and new models of 5 minor planets." *Astron. Astrophys. Suppl. Ser.* **140**, 21-28.

Munos, J.L. (2017) Carlsberg Meridian Catalog web site. *http://svo2.cab.inta-csic.es/vocats/cmc15/*

Pravec, P., Sarounova, L., Rabinowitz, D.L., Hicks, M.D., Wolf, M., Krugly, Y.N., Velichko, F.P., Shevchenko, V.G., Chiorny, V.G., Gaftonyuk, N.M., Genevier, G. (2000). "Two-Period Lightcurves of 1996 FG 3, 1998 PG, and (5407) 1992 AX: One Probable and Two Possible Binary Asteroids." *Icarus* **146**, 190-203.

Pravec, P. Scheirich, P., KuŠnirák, P., Hornoch, K., Galad, A., Naidu, S.P., Pray, D.P., Vilargi, J., Gajdoš, Š., Kornoš, L., and 39 coauthors. (2016). "Binary asteroid population. 3. Secondary rotations and elongations." *Icarus* **267**, 267-295.

Warner, B.D. (2007). "Initial Results of a Dedicated H-G Program." *Minor Planet Bull.* **34**, 113-119.

Warner, B.D., Harris, A.W., Pravec, P. (2009). "The Asteroid Lightcurve Database." *Icarus* **202**, 134-146. Updated 2018 March. *http://www.minorplanet.info/lightcurvedatabase.html*

NEW LIGHTCURVES OF 156 XANTHIPPE, 445 EDNA, AND 676 MELITTA

Frederick Pilcher
Organ Mesa Observatory (G50)
4438 Organ Mesa Loop
Las Cruces, NM 88011 USA
fpilcher35@gmail.com

(Received: 2018 October 3)

Synodic rotation periods and amplitudes are found for 156 Xanthippe 22.132 ± 0.002 hours, 0.22 ± 0.01 magnitudes; 445 Edna 19.974 ± 0.002 hours, 0.27 ± 0.01 magnitudes; 676 Melitta 16.743 ± 0.001 hours, 0.16 ± 0.01 magnitudes.

Observations to obtain the data used in this paper were made at the Organ Mesa Observatory with a 0.35-meter Meade LX200 GPS Schmidt-Cassegrain (SCT) and SBIG STL-1001E CCD. Exposures were 60 seconds, unguided, with a clear filter except where otherwise stated. Photometric measurement and lightcurve construction is with *MPO Canopus* software. To reduce the number of points on the lightcurves and make them easier to read, data points have been binned in sets of 3 with a maximum time difference of 5 minutes.

156 Xanthippe. Previously published rotation periods and amplitudes for 156 Xanthippe are by Debehogne et al. (1982), 22.5 hours, 0.12 magnitudes; Harris and Young (1989), 22.37 hours, 0.12 magnitudes; Behrend (2005), 22.104 hours, 0.10 magnitudes; and Behrend (2006), 22 hours, 0.05 magnitudes in a very sparse lightcurve. New observations on 11 nights 2018 Aug. 28 – Sept. 18 provide a good fit to a lightcurve (Figure 1) with period 22.132 ± 0.002 hours, amplitude 0.22 ± 0.01 magnitudes. This period is broadly compatible with several previous measurements. The amplitude is larger than has been reported previously, suggesting that at 310 degrees celestial longitude the object is in near equatorial presentation. A split halves plot (Figure 2) of the double period 44.294 hours shows that the two halves are nearly identical and rules out the double period.

445 Edna. Two previously published rotation periods for 445 Edna are by Behrend (2001), 9.12 hours in a very sparse lightcurve; and Malcolm, (2002), 19.97 hours with a dense lightcurve at almost the same position in the sky as the current study. Sessions on seven consecutive nights 2018 June 17-23 provide a good fit to a period 19.959 ± 0.003 hours, amplitude 0.27 ± 0.01 magnitudes (Figure 3). Nearly two months before opposition, only about 4.5 hours could be sampled each night. With a period almost exactly 5/6 of Earth's rotation period, nearly half of the double period could not be sampled from a single observatory. Seven more sessions were obtained 2018 Aug. 5-27. These seven sessions provide a good fit to a lightcurve (Figure 4) with period 19.977 ± 0.002 hours, amplitude 0.27 ± 0.01 magnitudes, and a shape as well as period significantly changed from June. With sessions of 6 to 7.5 hours obtained, nearly all of

Number	Name	2018/mm/dd	Pts	Phase	LPAB	BPAB	Period(h)	P.E	Amp	A.E.
156	Xanthippe	08/28-09/18	2219	12.4, 17.6	310	12	22.132	0.002	0.22	0.01
445	Edna	06/17-06/23	1369	15.8, 14.4	309	4	19.959	0.003	0.27	0.01
445	Edna	08/05-08/27	1827	4.1, 10.9	310	10	19.977	0.002	0.27	0.01
767	Melitta	08/30-10/01	1604	8.8, 18.2	318	1	16.743	0.001	0.16	0.01

Table I. Observing circumstances and results. Pts is the number of data points. The phase angle is given for the first and last dates. LPAB and BPAB are the approximate phase angle bisector longitude and latitude at mid-date range (see Harris *et al.*, 1984).

the double period was also sampled. A split halves plot (Figure 5) of the double period 39.965 hours for the interval 2018 Aug. 5-27 shows that the two halves are nearly identical and rules out the double period. A lightcurve including all observations 2018 June 17-Aug. 27 (Figure 6) provides a fit to a period 19.974 ± 0.002 hours, amplitude also 0.27 ± 0.01 hours, in which the change of shape of the lightcurve is especially notable near phase 0.9.

676 Melitta. Several rotation periods near 7.87 hours were published in the first decade of the 21st century: Behrend (2002), 7.87 hours; Clark and Joyce (2003), 7.870 hours; Behrend (2006, 7.87 hours; Behrend (2012), 7.8 hours. Violante and Leake (2012) published a conflicting period of 8.35 hours. More recently Ferrero (2013) obtained 16.757 hours and Benishek obtained 16.740 hours, much longer and not even commensurable with the early measurements. This study, with sessions on 8 nights 2018 Aug. 30 – Oct. 1, provides a good fit to a lightcurve with period 16.743 ± 0.001 hours, amplitude 0.16 ± 0.01 magnitudes (Figure 7), and is compatible with Ferrero (2013) and Benishek (2018). About ¾ of a split halves plot of the double period 33.486 hours (Figure 8) includes data from both halves that fit well. This is strong additional evidence that the double period can be rejected. A high peak in the Fourier series representation at phases 0.33-0.43 is an artifact constructed by the numerical Fourier series algorithm in the absence of data at these phases. The amplitude of 0.26 magnitudes implied by this peak is again an artifact and should be rejected.

References

Behrend, R. (2001, 2002, 2005, 2006, 2012). Observatoire de Geneve web site. *http://*obswww.unige.ch/*~behrend/page_cou.html*.

Benishek, V. (2018). "Lightcurve and rotation period determinations for 29 asteroids." *Minor Planet Bull.* **45**, 82-91.

Clark, M., Joyce, B. (2003). "Asteroid Lightcurve Photometry from Goodsell Observatory." *Minor Planet Bull.* **30**, 4-7.

Debehogne, H., De Sanctis, G., Zappala, V. (1982). "Photoelectric photometry of three dark asteroids." *Astron. Astrophys.* **108**, 197-200.

Ferrero, A. (2013). "Rotational period of five asteroids." *Minor Planet Bull.* **40**, 31-32.

Harris, A.W., Young, J.W., Scaltriti, F., Zappala, V. (1984). "Lightcurves and phase relations of the asteroids 82 Alkmene and 444 Gyptis." *Icarus* **57**, 251-258.

Harris, A.W., Young, J.W. (1989). "Asteroid lightcurve observations from 1979-1981." *Icarus* **81**, 314-364.

Malcolm, G. (2002). "Rotational periods and lightcurves of 445 Edna, 1817 Katanga, and 1847 Stobbe." *Minor Planet Bull.* **29**, 28-29.

Violante, R., Leake, M.A. (2012). "Photometry and lightcurve analysis of 7 main-belt asteroids." *J SE Assoc. Research in Astronomy* **7**, 41-44.

Waszczak, A., Chang, C.-K., Ofek, E.O., Laher, R., Masci, F., Levitan, D., Surace, J., Cheng, Y.-C., Ip, W.H., Kinoshita, D., Helou, G., Prince, T.A., Kulkarni, S. (2015). "Asteroid Light Curves from the Palomar Transient Factory Survey: Rotation Periods and Phase Function from Sparse Photometry." *Astron. J.* **150**, A75.

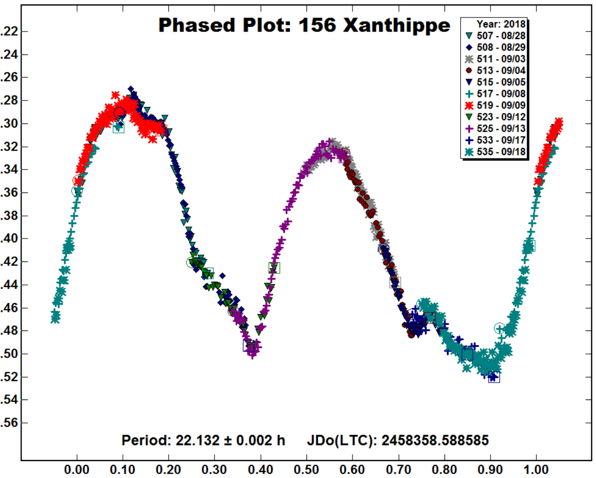

Figure 1. Phased lightcurve of 156 Xanthippe.

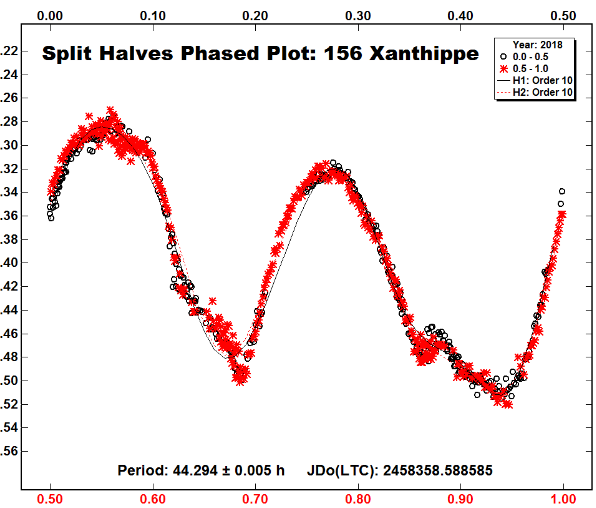

Figure 2. Split halves lightcurve of 156 Xanthippe phased to the double period 44.294 hours.

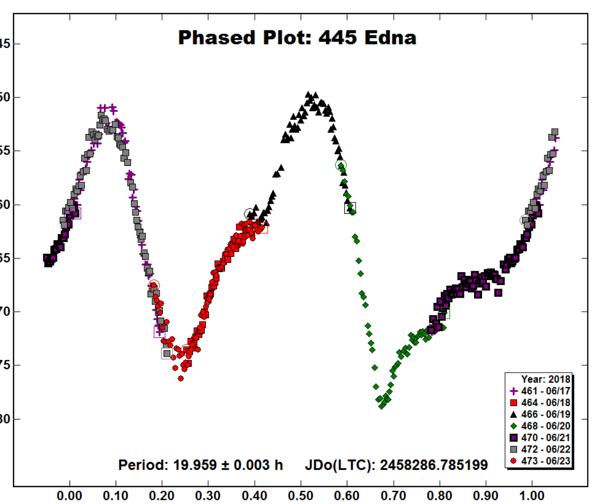

Figure 3. Phased lightcurve of 445 Edna for the interval 2018/06/17 through 2018/06/23.

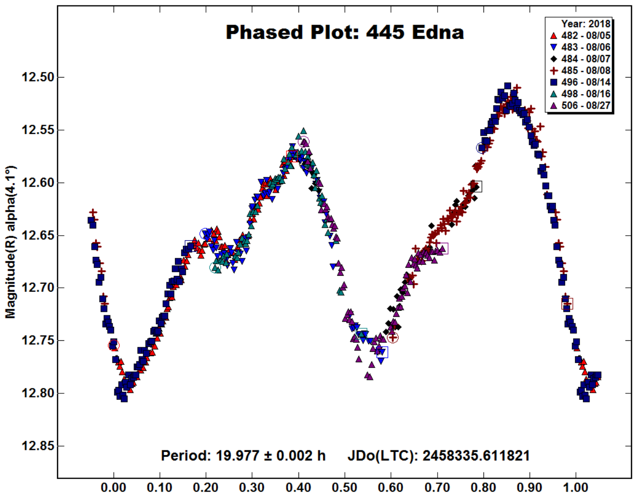

Figure 4. Phased lightcurve of 445 Edna for the interval 2018/08/05 through 2018/08/27.

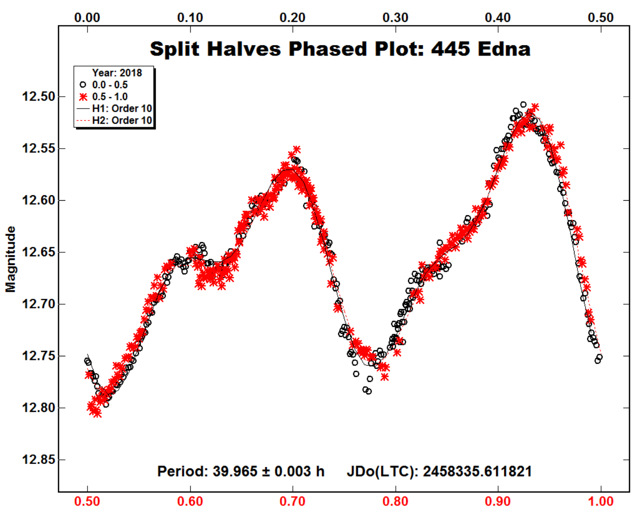

Figure 5. Split halves lightcurve of 445 Edna phased to the double period 39.965 hours for the interval 2018/08/05 through 2018/08/27.

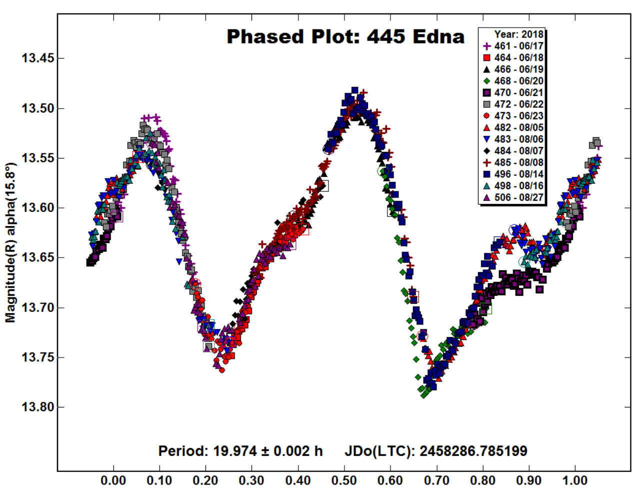

Figure 6. Phased lightcurve of 445 Edna for the interval 2018/06/17 through 2018/08/27.

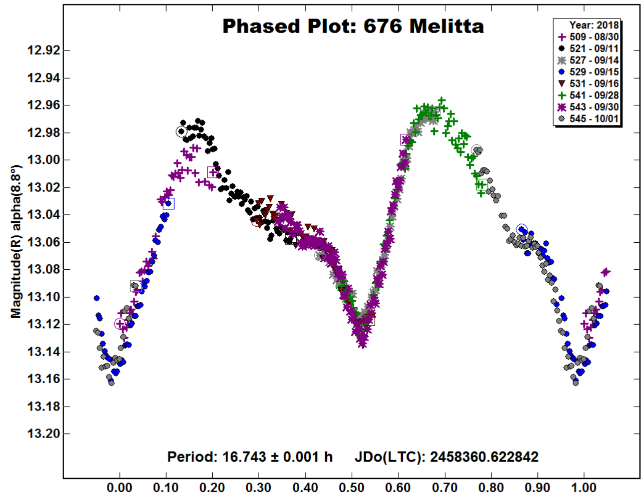

Figure 7. Phased lightcurve of 676 Melitta.

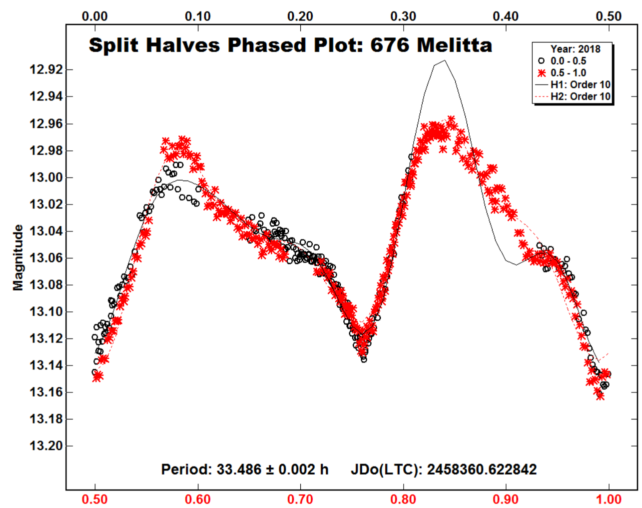

Figure 8. Split halves lightcurve of 676 Melitta phased to the double period 33.486 hours.

PHOTOMETRIC OBSERVATIONS OF MAIN-BELT ASTEROIDS 232 RUSSIA, 1117 REGINITA, AND (11200) 1999 CV121.

Charles Galdies
Znith Observatory
Armonie, E. Bradford Street,
Naxxar NXR 2217, MALTA
charles.galdies@um.edu.mt

Stephen M. Brincat
Flarestar Observatory (MPC 171)
San Gwann SGN 3160, MALTA

Winston Grech
Antares Observatory
Fgura FGR 1555, MALTA

(Received: 2018 Oct 1)

Photometric observations of three main-belt asteroids were obtained from 2018 April-July from Malta in order to determine their synodic rotation periods. We provide lightcurves for 232 Russia and 1117 Reginita that were obtained from the Spin/Shape Modeling Opportunities list by Warner et al. (2018). The asteroid (11200) 1999 CV121 did not have a referenced period in the LCDB database (Warner et al., 2009).

Photometric observations of three main-belt asteroids were carried out from three observatories located in Malta (Europe). Observations of asteroids 232 Russia, 1117 Reginita, and (11200) 1999 CV121 were obtained from 2018 April-July. Znith Observatory employed a 0.20-m Schmidt-Cassegrain (SCT) equipped with a Moravian G2-1600 CCD camera at 1x1 binning; Flarestar Observatory used the same CCD model coupled with a 0.25-m SCT, also at 1x1 binning; Antares Observatory used an SBIG STL-11000 CCD camera binned 2x2 attached to a 0.28-m SCT. All cameras were cooled to –15°C. The science images were dark subtracted and flat-fielded.

All telescopes and cameras were controlled remotely from a location near each telescope via *Sequence Generator Pro* (Binary Star Software). Photometric reduction, lightcurve construction, and analyses were done using *MPO Canopus* (Warner, 2017) and differential aperture photometry. The Comparison Star Selector (CSS) feature of *MPO Canopus* was used to select comparison stars of near-solar color. Measurements were based on the CMC-15 catalogue with magnitudes converted from J-K to BVRI (Warner, 2007).

(232) Russia is a large main-belt asteroid that was discovered on 1883 January 31 by Johann Palisa in Vienna; it was suggested as a possible target in order to derive spin/shape models (Warner et al., 2018). It orbits the Sun with a semi-major axis of 2.553 AU, eccentricity 0.175, and period of 4.08 years (JPL, 2018). The diameter is 49.863 ± 0.975 km based on an absolute magnitude $H = 10.25$ (JPL, 2018).

Observations at all three observatories were made on 11 nights from 2018 May 6 to July 12. We obtained a synodic period of 21.901 ± 0.001 hr and amplitude of 0.14 ± 0.02 mag. These results are consistent with previously published results from Ruthroff (2009), Pilcher (2014), and Stephens (2014).

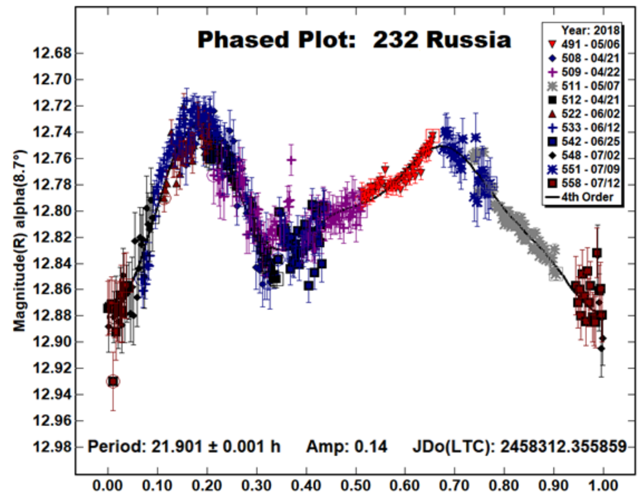

1117 Reginita is a main-belt asteroid discovered on 1972 May 24 by J. Comas Sola in Barcelona, Spain. This 10.193 ± 0.250 km diameter asteroid has an absolute magnitude $H = 11.7$ and orbits the Sun with a semi-major axis of 2.248, eccentricity of 0.198, and period of 3.37 years (JPL, 2018).

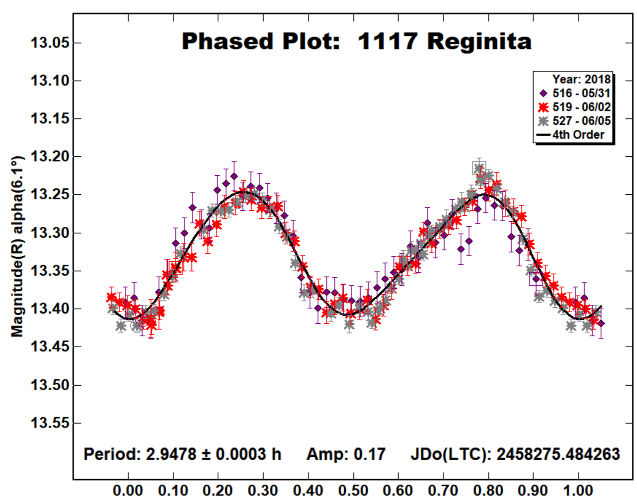

Observations were made on three nights from 2018 May 31 to June 6. Each observatory contributed one session. Our results indicate a synodic period of 2.9478 ± 0.0003 hr and amplitude of 0.17 ± 0.02 mag. These are consistent with previously published

Number	Name	2018 mm/dd	Pts	Phase	L_{PAB}	B_{PAB}	Period(h)	P.E.	Amp	A.E.	Grp
232	Russia	05/06-07/12	554	8.2,27.1	220	+8	21.901	0.001	0.14	0.02	MB-I
1117	Reginita	05/31-06/06	170	5.7,8.4	245	+7	2.9478	0.0003	0.17	0.02	FLOR
11200	1999 CV121	04/23-07/12	286	4.9,26.7	220	+1	6.792	0.001	0.29	0.05	MB-M

Table I. Observing circumstances and results. Pts is the number of data points. The phase angle is given for the first and last date. L_{PAB} and B_{PAB} are the approximate phase angle bisector longitude and latitude at mid-date range (see Harris *et al.*, 1984). Grp is the asteroid family/group (Warner *et al.*, 2009). MB-I/M: main-belt inner/middle; FLOR: Flora.

periods from Wisniewski et al. (1997), Behrend (2007), Kryszczynska et al. (2012), Chang et al. (2015). Waszczak et al. (2015), and Tan et al. (2017).

(11200) 1999 CV121 is a main-belt asteroid discovered on 1999 February 11 in Socorro (New Mexico) as part of the LINEAR (Lincoln Near-Earth Asteroid Research) project conducted in collaboration with the US Air Force, NASA, and the Laboratory Lincoln of the Massachusetts Institute of Technology.

This asteroid orbits the Sun with a semi-major axis of 2.738 AU, eccentricity 0.215, and period of 4.53 years (JPL, 2018). JPL (2018) lists the diameter as 9.137 ± 0.081 km based on an absolute magnitude $H = 12.2$.

1999 CV121 was observed at all observatories from 2018 April 23 through June 18. Our results include a synodic period of 6.792 ± 0.001 hr and amplitude of 0.29 ± 0.05 mag. The lightcurve database (LCDB; Warner et al., 2009) did not contain any references with a rotation period for this asteroid.

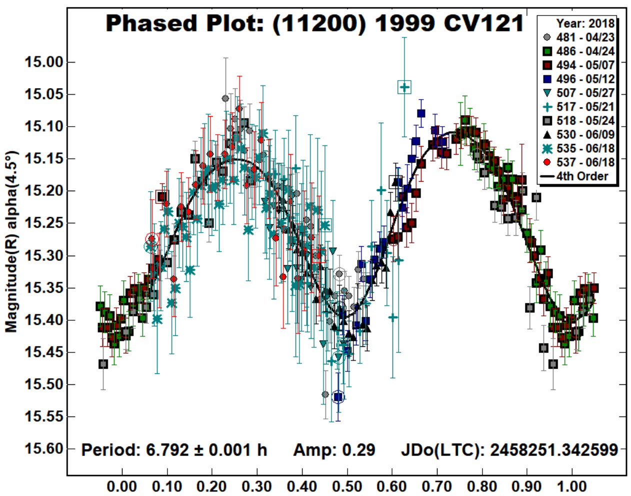

Acknowledgements

We would like to thank Brian Warner for his work in the development of *MPO Canopus* and for his efforts in maintaining the CALL website (Warner, 2016).

This research has made use of the JPL's Small-Body Database.

References

Behrend, R. (2007). CdL Observatoire de Geneve web site: *http://obswww.unige.ch/~behrend/page_cou.html* Accessed: 2018 September 26.

Chang, C.-K., Ip, W.-H., Lin, H.-W., Cheng, Y.-C., Ngeow, C.-C., Yang, T.-C., Waszczak, A., Kulkarni, S.R., Levitan, D., Sesar, B., Laher, R., Surace, J., Prince, T.A. (2015). "Asteroid Spin-rate Study Using the Intermediate Palomar Transient Factory." *Ap. J. Suppl. Ser.* **219**, A27.

Harris, A.W., Young, J.W., Scaltriti, F., Zappala, V. (1984). "Lightcurves and phase relations of the asteroids 82 Alkmene and 444 Gyptis." *Icarus* **57**, 251-258.

JPL (2018). Small-Body Database Browser - JPL Solar System. Dynamics web site. *http://ssd.jpl.nasa.gov/sbdb.cgi* Accessed: 2018 September 26.

Kryszczynska, A., Colas, F., Polinska, M., Hirsch, R., Ivanova, V., Apostolovska, G., Bilkina, B., Velichko, F.P., Kwiatkowski, T., Kankiewicz, P. and 20 coauthors. (2012). "Do Slivan states exist in the Flora family? I. Photometric survey of the Flora region." *Astron. Astrophys.* **546**, A72.

Pilcher, F. (2014). "Another Asteroid with a Changing Lightcurve: 232 Russia." *Minor Planet Bull.* **41**, 205.

Ruthroff J.C. (2009). "Photometric Observations and Lightcurve Analysis of Asteroids 129 Antigone, 174 Phaedra, 232 Russia, 291 Alice, and 343 Ostara." *Minor Planet Bull.* **36**, 121-122.

Stephens, R.D. (2014). "Asteroids Observed from CS3: 2014 April-June." *Minor Planet Bull*. **41**, 226-230.

Tan, H., Li, B., Gao, X. (2017). "The Rotation Period of 1117 Reginita." *Minor Planet Bull*. **44**, 307.

Warner, B.D. (2007). "Initial Results of a Dedicated H-G Program." *Minor Planet Bull*. **34**, 113-119.

Warner, B.D., Harris, A.W., Pravec, P. (2009). "The asteroid lightcurve database." *Icarus* **202**, 134-146. Updated 2018 June 23. *http://www.MinorPlanet.info/lightcurvedatabase.html*

Warner, B.D. (2016). Collaborative Asteroid Lightcurve Link website. *http://www.minorplanet.info/call.html* Accessed: 2018 September 26.

Warner, B.D. (2017). MPO Software, *MPO Canopus* version 10.7.10.0. Bdw Publishing. *http://www.minorplanetobserver.com/*

Warner, B.D., Harris A.W., Durech J., Benner L.A.M. (2018). "Lightcurve photometry opportunities: 2018 April-June." *Minor Planet Bull*. **45**, 208-213.

Waszczak, A., Chang, C.-K., Ofek, E.O., Laher, R., Masci, F., Levitan, D., Surace, J., Cheng, Y.-C., Ip, W.-H., Kinoshita, D., Helou, G., Prince, T.A., Kulkarni, S. (2015). "Asteroid Light Curves from the Palomar Transient Factory Survey: Rotation Periods and Phase Functions from Sparse Photometry." *Astron. J.* **150**, A75.

Wisniewski, W.Z., Michalowski, T.M., Harris, A.W., McMillan, R.S. (1997). "Photometric Observations of 125 Asteroids." *Icarus* **126**, 395-449.

OSIRIS-REX TARGET ASTEROIDS! PHOTOMETRY OF NEAR-EARTH ASTEROID (276049) 2002 CE26

Jessica Forelli[1], Carl W. Hergenrother[1], Dolores H. Hill[1], John Briol[2], Patrick Wiggins[3], Alberto Betzler[4], Alessandro Odasso[5], Dante S. Lauretta[1]

[1]Lunar and Planetary Laboratory
University of Arizona
Tucson, AZ 85721 USA
jessicaforelli@email.arizona.edu

[2]Spirit Marsh Observatory
Sauk Centre, MN 56378 USA

[3]Tooele, UT 84074 USA

[4]Centro de Ciência e Tecnologia em Energia e Sustentabilidade,
Universidade Federal do Recôncavo da Bahia,
Feira de Santana,
44085-132, Bahia, Brazil

[5]Via Francesco Anzani 3,
20135, Milano, Italy

(Received: 2018 October 3)

Broadband BVRI photometry of near-Earth asteroid (276049) 2002 CE26 was collected by several participants of the OSIRIS-REx *Target Asteroids!* program. A range of phase angles were observed in each filter to obtain color dependent phase functions. Measurements of 2002 CE26's V-R and V-I color indices are most consistent with a C-type taxonomy and, to a lesser extent, an X-type taxonomy.

Target Asteroids! is a program conducted by the OSIRIS-REx asteroid sample return mission to encourage astronomers from around the world to observe asteroids through small aperture telescopes (Hergenrother and Hill, 2013). One such asteroid that was the focus of a *Target Asteroids!* observing campaign was near-Earth asteroid (276049) 2002 CE26 (Hergenrother and Hill, 2014). Analysis of these data was conducted in the spring of 2017 as part of a First Year Undergraduate Honors Project for the University of Arizona.

2002 CE26 was discovered on 2002 February 10 by the LINEAR near-Earth asteroid survey. It is an Apollo near-Earth asteroid with a semi-major axis of 2.23 AU, eccentricity of 0.56 and inclination of 47.3°. Visible, near-IR and radar observations found it to be a low-albedo, C-type binary with a rotation period of 3.293 hours (Pravec et al., 2006; Shepard et al., 2006; Warner, 2015). The radar observations detected one satellite and contained evidence of a possible third satellite.

Target Asteroids! observations of 2002 CE26 were obtained on twelve nights between 2014 September 1 and 19 using telescopes from multiple observers. Photometric observations by Betzler were obtained with a 0.43-m f/6.8 Corrected Dall-Kirkham Astrograph and SBIG STL-11000M CCD Camera as well as a 0.32-m f/7 Ritchey-Chrétien with a SBIG ST-8XME CCD Camera. Both telescopes are part of the iTelescopes network. Photometry from Briol was obtained with a 0.20-m reflector and Canon 1000d DSLR CCD camera. Observations from Hergenrother and Odasso were obtained with a 0.51-m f/6.8 Corrected Dall-Kirkham Astrograph and SBIG STL6303E CCD Camera operated by the Sierra Stars Observatory Network. Photometry from Wiggins was acquired with a 0.35-m Schmidt-Cassegrain and SBIG ST-10XME CCD Camera.

Phase Function Observations and Analysis

The dataset for 2002 CE26 consists of broadband BVRI photometry covering phase angles from 32.2° to 69.4° (see Table 1). Using a linear trend line, the data display a trend of decreasing brightness with increasing phase angle. At phase angles larger than 60º, there is a larger than expected deviation, or drop-off, from the linear trend in the B-, V-, and R- filters (see Figure 1). Linear phase function regression fits were determined for all of the phase angles per filter and for only those phase angles less than 60º per filter (see Table 2). The drop-off could be due to an oblong or other abnormal shape that resulted in the object being viewed down the horizontal side. However, based on the radar derived shape model of Shepard et al. (2006), the object is expected to have a more spherical shape, so this is likely not the explanation behind this observation.

An attempt was made to identify confirming photometry in the Minor Planet Center (MPC) archives during the period when 2002 CE26 was at a phase angle greater than 60º. Surprisingly, no photometry for dates when the phase angles was greater than 55º was reported to the MPC in 2014 or any other year. The object was located at far southern declinations (<-60º) at those times, possibly explaining the lack of observations.

Table 2. Linear fit parameters to BVRI photometry obtained at phase angles < 60°.

	For phase angles < 60°		For all phase angles	
Filt	**H(1,1,0)**	**Slope**	**H(1,1,0)**	**Slope**
B	16.80±0.19	0.040±0.004	16.36±0.18	0.050±0.003
V	16.66±0.03	0.027±0.001	16.39±0.12	0.035±0.002
R	16.25±0.07	0.028±0.002	16.03±0.11	0.034±0.002
I	15.63±0.11	0.034±0.002	No phase angles > 60°	

Table 3. IAU H-G fit parameters to BVRI photometry for all phase angles..

	For phase angles < 60°		For all phase angles	
Filter	**H(1,1,0)**	**G**	**H(1,1,0)**	**G**
B	16.52±0.28	-0.01±0.09	15.68±0.14	-0.21±0.02
V	16.26±0.06	0.20±0.04	15.84±0.17	-0.03±0.06
R	15.86±0.14	0.20±0.08	15.50±0.15	0.00±0.06
I	15.00±0.15	-0.03±0.05	No phase angles > 60°	

Filter	2014 mm/dd	Pts	Phase	H(1,1,α)	Magnitude
B	09/09-09/19	11	32.21,69.34	17.96-19.97	13.63-16.60
V	09/03-09/19	15	23.94,69.34	17.28-19.14	13.15-15.77
R	09/01-09/19	14	22.43,69.44	16.84-18.59	13.02-15.46
I	09/09-09/14	5	32.21,55.06	16.75-17.56	12.43-13.56

Table I. Observing circumstances and results in the four filters. Pts is the number of data points. The phase angle is given for the first and last date. H(1,1,α) represents how bright the object would be 1 AU from the observer at 0° phase angle.

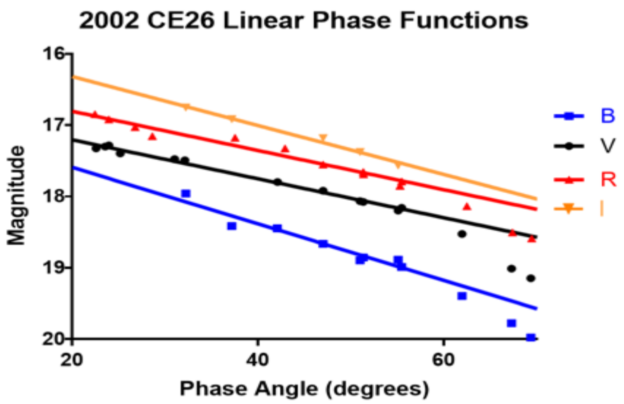

Figure 1. Linear BVRI phase functions for 2002 CE26. The phase functions are fit to phase angles < 60°.

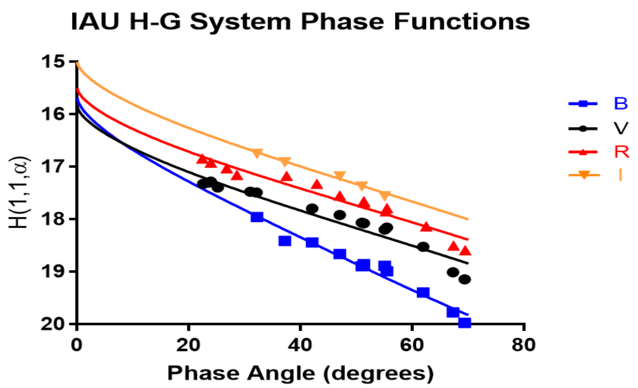

Figure 2. IAU H-G phase functions for 2002 CE26 in B, V, R and I bands.

Solving within the IAU H-G system in the BVRI bands produces the values shown in Table 3 (Bowell et al., 1989). The phase function photometry and phase function solutions for all phase angles are shown in Figure 2.

Albedo from the Phase Function

The slope of the linear part of the phase function is directly correlated with albedo (Belskaya and Shevchenko, 2000; Hergenrother *et al.,* 2013). The R-band linear slope from phase angles less than 60° of 0.028 ± 0.002 magnitude per degree of phase angle suggests a moderate albedo between 0.1 and 0.3. The R-band linear slope for all phase angles of 0.034 ± 0.002 suggests a dark object with an albedo of 0.04 to 0.12 which is consistent with the dark albedo found by Shepard et al. (2006) and Mainzer et al. (2011). Figure 3 presents the phase function slope to albedo relationship for near-Earth asteroids as analyzed in Hergenrother *et al.* (2013). The upper grey area covers the range of phase angle slopes determined for all phase angles while the lower grey area covers only phase angles less than 60°.

Taxonomic Classification

BVRI filter photometry was obtained on multiple dates. The average color indices of B-V = +0.77, V-R = +0.39 and V-I = +0.70 are most consistent with a C-type taxonomy and to a lesser extent an X-type taxonomy, though the B-V value is low for both taxonomies (see Figures 4 and 5). An alternate approach to determining colors was also used by calculating the colors from the difference between the IAU H-G phase function. The V-R and V-I indices are consistent with C- and X-types. However, the B-V filter is only consistent with C- and X-types at phase angles near 50º. The data become unreliable at higher and lower phase angles resulting in atypical B-V values for an asteroid.

Future Observing Opportunities

The next good opportunity to characterize 2002 CE26 will be in September 2024 when it will approach to within 0.18 AU of Earth. This apparition will be similar to the one in 2014. Peak brightness will be V = 15.1 and observable phase angles will range from 39º to 77º. As in 2014, the asteroid will be located at far southern declinations (from -41º to -83º) when its phase angle is greater than 60º.

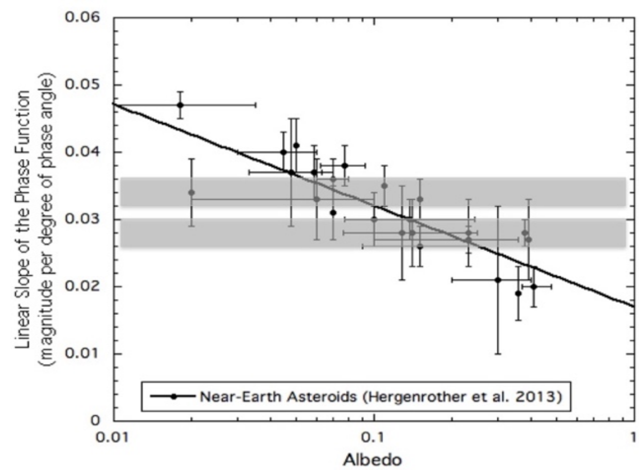

Figure 3. Relationship between the R-band slope of the phase function and albedo for near-Earth asteroids. The grey area covers the range of phase function slope measured for 2002 CE26. The upper band corresponds to the linear fit to only data with phase angles less than 60°. The lower band corresponds to a linear fit to all phase angles. NEA data are from Hergenrother et al. (2013).

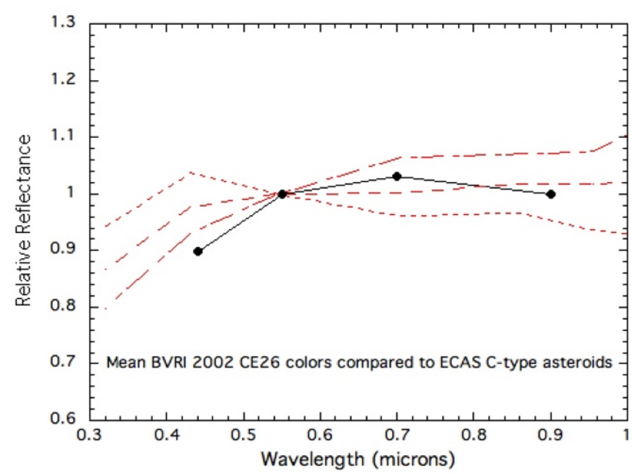

Figure 4. BVRI colors for 2002 CE26 are converted to relative reflectance and compared with low, median and high ECAS color values for C-type asteroids from Zellner et al. (2009).

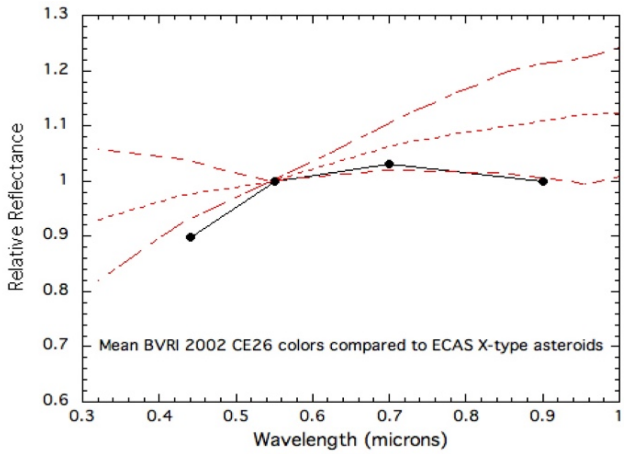

Figure 5. BVRI colors for 2002 CE26 are converted to relative reflectance and compared with low, median and high ECAS color values for X-type asteroids from Zellner et al. (2009).

Acknowledgements

First, we would like to thank all staff members of OSIRIS-REx and volunteers for *Target Asteroids!* for their contributions to our mission. We would especially like to thank our families for providing us with endless support and encouragement along our journey.

References

Belskaya, I.N., Shevchenko, V.G. (2000). "Opposition Effect of Asteroids." *Icarus* **147**, 94-105.

Bowell, E., Hapke, B., Domingue, D., Lumme, K., Peltoniemi, J., Harris, A.W. (1989). Application of Photometric Models to Asteroids. In *Asteroids II*, 524–556.

Hergenrother, C.W., Nolan, M.C., Binzel, R.P., Cloutis, E.A., Barucci, M.A., Michel, P., Scheeres, D., d'Aubigny, C.D., Lazzaro, D., Pinilla-Alonso, N., Campins, H., Licandro, J., Clark, B.E., Rizk, B., Beshore, E.C., Lauretta, L.S. (2013). "Lightcurve, Color and Phase Function Photometry of the OSIRIS-REx Target Asteroid (101955) Bennu." *Icarus* **226**, 663-670.

Hergenrother, C., Hill, D. (2013). "The OSIRIS-REx Target Asteroids Project: A Small Telescope Initiative to Characterize Potential Spacecraft Mission Targets." *Minor Planet Bulletin* **40**, 164-166.

Hergenrother, C., Hill, D. (2014). "Target Asteroids! Observing Targets for July Through September 2014." *Minor Planet Bulletin* **41**, 191-193.

Mainzer, A., Grav, T., Bauer, J., Masiero, J., McMillan, R.S., Cutri, R.M., Walker, R., Wright, E., Eisenhardt, P., Tholen, D.J., Spahr, T., Jedicke, R., Denneau, L., DeBaun, E., Elsbury, D., Gautier, T., Gomillion, S., Hand, E., Mo, W., Watkins, J., Wilkins, A., Bryngelson, G.L., Del Pino Molina, A., Desai, S., Gómez Camus, M., Hidalgo, S.L., Konstantopoulos, I., Larsen, J.A., Maleszewski, C., Malkan, M.A., Mauduit, J.-C., Mullan, B.L., Olszewski, E.W., Pforr, J., Saro, A., Scotti, J.V., Wasserman, L.H. (2011). "NEOWISE Observations of Near-Earth Objects: Preliminary Results." *Astrophysical Journal* **743**, id. 156.

Pravec, P., Scheirich, P., Kušnirák, P., Šarounová, L., Mottola, S., Hahn, G., Brown, P., Esquerdo, G., Kaiser, N., Krzeminski, Z., Pray, D.P., Warner, B.D., Harris, A.W., Nolan, M.C., Howell, E. S., Benner, L.A.M., Margot, J.-L., Galád, A., Holliday, W., Hicks, M.D., Krugly, Yu.N., Tholen, D., Whiteley, R., Marchis, F., DeGraff, D.R., Grauer, A., Larson, S., Velichko, F.P., Cooney, W. R., Stephens, R., Zhu, J., Kirsch, K., Dyvig, R., Snyder, L., Reddy, V., Moore, S., Gajdoš, Š., Világi, J., Masi, G., Higgins, D., Funkhouser, G., Knight, B., Slivan, S., Behrend, R., Grenon, M., Burki, G., Roy, R., Demeautis, C., Matter, D., Waelchli, N., Revaz, Y., Klotz, A., Rieugné, M., Thierry, P., Cotrez, V., Brunetto, L., Kober, G. (2006). "Photometric Survey of Binary Near-Earth Asteroids." *Icarus* **181**, 63-93.

Shepard, M.K., Margot, J.-L., Magri, C., Nolan, M.C., Schlieder, J., Estes, B., Bus, S.J., Volquardsen, E.L., Rivkin, A.S., Benner, L.A.M., Giorgini, J.D., Ostro, S.J., Busch, M.W. (2006). "Radar and Infrared Observations of Binary Near-Earth Asteroid 2002 CE26." *Icarus* **184**, 198-210.

Warner, B.D. (2015). "A Quartet of Near-Earth Asteroid Binary Candidates." *Minor Planet Bulletin* **42**, 79-83.

Zellner, B., Tholen, D.J., Tedesco, E.F., (2009). "Eight Color Asteroid Survey." EAR-A-2CP-3-RDR-ECAS-V4.0. NASA Planetary Data System

ASTEROIDS OBSERVED FROM CS3: 2018 JULY - SEPTEMBER

Robert D. Stephens
Center for Solar System Studies (CS3)/MoreData!
11355 Mount Johnson Ct., Rancho Cucamonga, CA 91737 USA
rstephens@foxandstephens.com

(Received: 2018 October 8)

CCD photometric observations of 10 main-belt asteroids were obtained from the Center for Solar System Studies from 2018 July to September.

The Center for Solar System Studies “Trojan Station” (CS3, MPC U81) has two telescopes which are normally used in program asteroid family studies such as NEAs, Jovian Trojans and Hildas. During the 3rd quarter of 2018 the targets which are normally studied were either out of season, or the Moon was too close. In these cases, targets of opportunity amongst the main-belt families were selected.

All images were made with a 0.4-m or a 0.35-m SCT using an FLI ML-Proline 1001E or FLI ML-Microline 1001E CCD camera. Images were unbinned with no filter and had master flats and darks applied. Image processing, measurement, and period analysis were done using *MPO Canopus* (Bdw Publishing), which incorporates the Fourier analysis algorithm (FALC) developed by Harris (Harris et al., 1989). Night-to-night calibration (generally < ±0.05 mag) was done using field stars from the CMC-15 or APASS (Henden *et al*., 2009) catalogs. The Comp Star Selector feature in *MPO Canopus* was used to limit the comparison stars to near solar color.

In the lightcurve plots, the “Reduced Magnitude” is Johnson V corrected to a unity distance by applying -5*log (rΔ) to the measured sky magnitudes with r and Δ being, respectively, the Sun-asteroid and the Earth-asteroid distances in AU. The magnitudes were normalized to the phase angle given in parentheses using G = 0.15. The X-axis rotational phase ranges from -0.05 to 1.05.

The amplitude indicated in the plots (e.g. Amp. 0.20) is the amplitude of the Fourier model curve and not necessarily the adopted amplitude of the lightcurve.

For brevity, only some of the previously reported rotational periods may be referenced. A complete list is available at the lightcurve database (LCDB; Warner et al., 2009).

<u>1026 Ingrid</u>. Szekely et al. (2005) found a 5.3 h period for this Flora family member from a single lightcurve covering less than the entire period. This year’s period spectrum shows aliases at 5.4 and 10.8 h and a low amplitude. When combined with the large amplitude Szekely result, the 5.437 h as the rotational period is adopted for this paper.

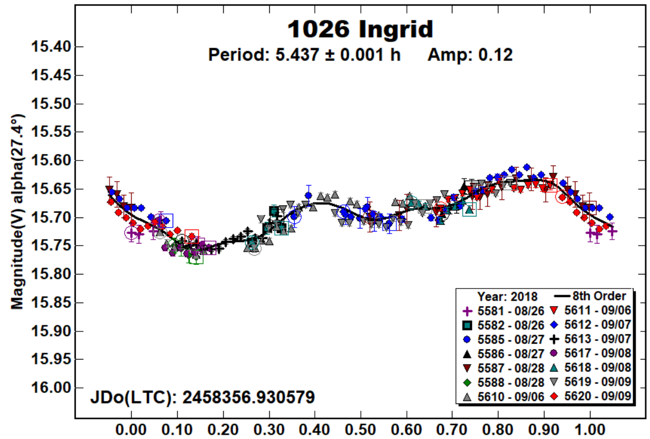

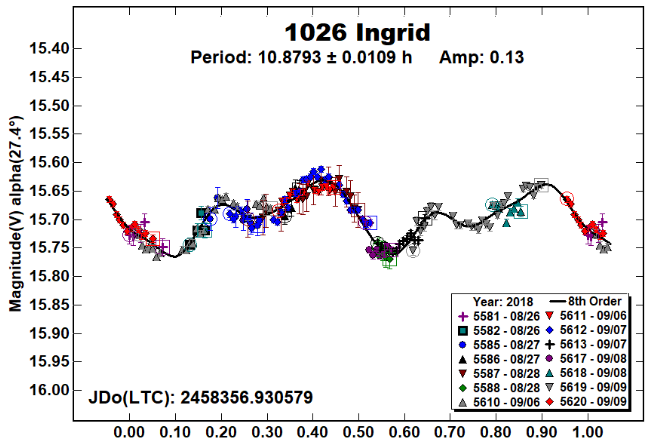

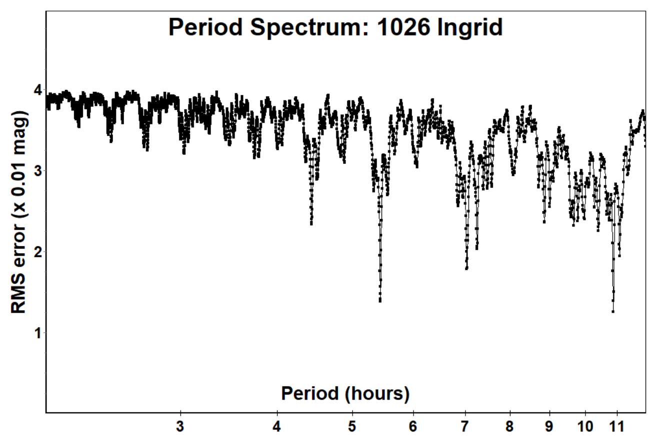

<u>1523 Pieksamaki</u>. This member of the Flora family has been studied several times in the past (Lagerkvist, 1979; Kryszczynska et al., 2012; Behrend, 2018) each time finding a rotational period near 5.32 h. The result found this year is consistent with those findings.

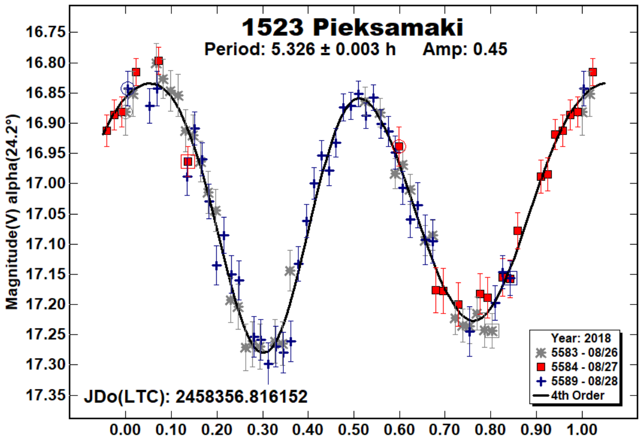

1991 Darwin. Wisniewski et al. (1979) found a rotational period near 4.7 h with a low amplitude of 0.08 mag for this Flora family member. Due to the extremely low amplitude, a number of aliases were present in the period spectrum. These include periods near 5 h, 6 h and 8 h. The 5.92 period creates a lightcurve that is a better fit to the data, although the 4.73 h period cannot be formally ruled out.

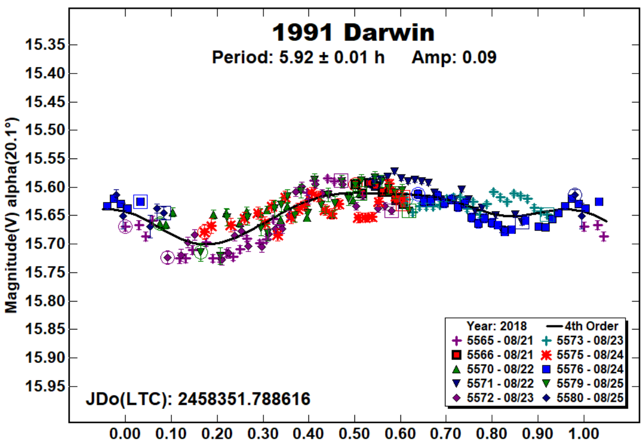

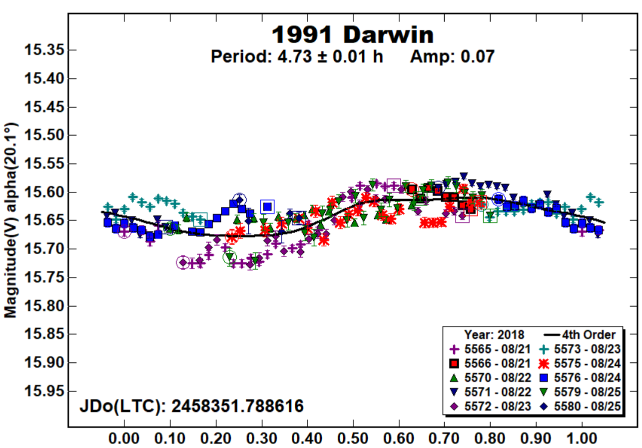

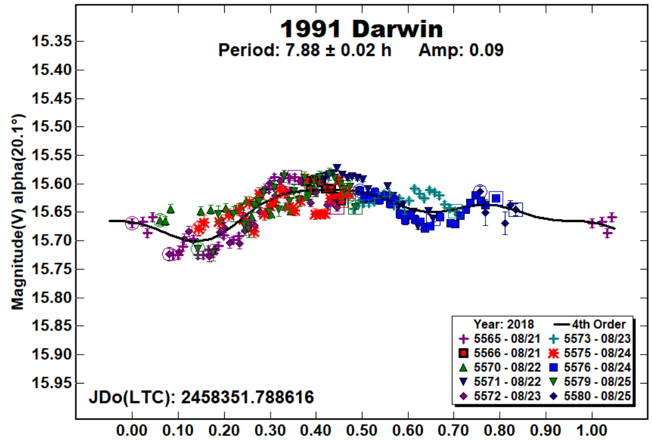

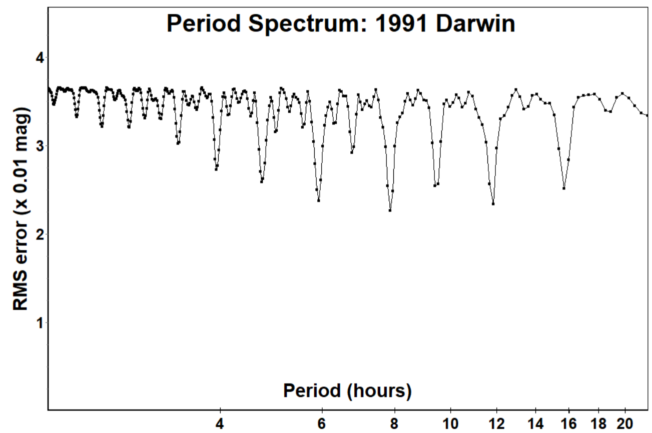

2017 Wesson. Behrend (2018) and Kryszczynska et al. (2012) reported periods near 3.415 h for this Flora family member. This year's finding is in good agreement with those results.

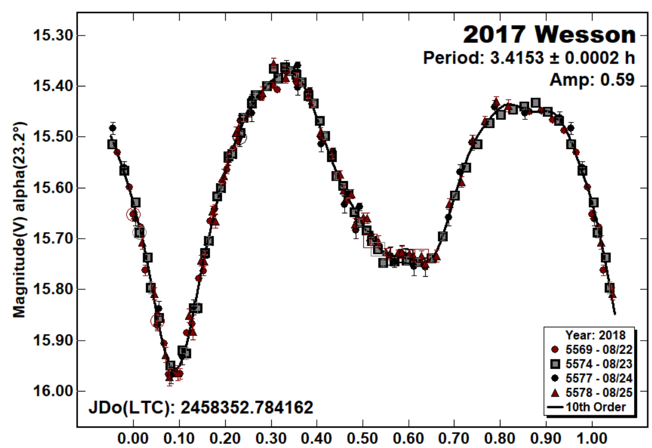

3562 Ignatius. Previous results found in the lightcurve database (LCDB; Warner et al., 2009) are from Falese et al. (2014) and Stephens (2016) each reporting a periods near 2.73 h. The initial observations ("No Sub" plot) showed what appeared to be a second frequency indicating a binary asteroid. The dual period analysis found a primary lightcurve of $P_1 = 2.832 \pm 0.001$ h, $A_1 = 0.09 \pm 0.01$ mag ("P1" plot). As suspected, subtracting this lightcurve from the data set and doing a period search found a solution that showed what appears to be an *orbital period* due to a satellite ("P2" plot). A number of aliases can be seen in the period spectrum. The most likely period of $P_2 = 16.00 \pm 0.02$ h, $A_2 = 0.18$ mag shows a classic bimodal lightcurve. Since the asteroid was well past opposition when observations commenced, and because P_2 is so close to three quarters of an Earth day, the secondary lightcurve could not be completed and it remains a suspected binary. A good opportunity for follow up is in 2020 March.

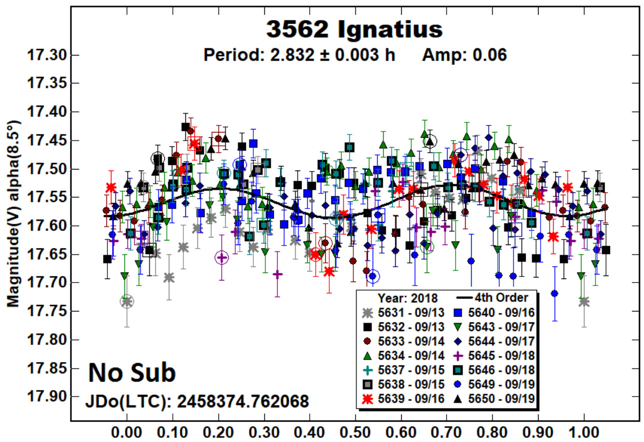

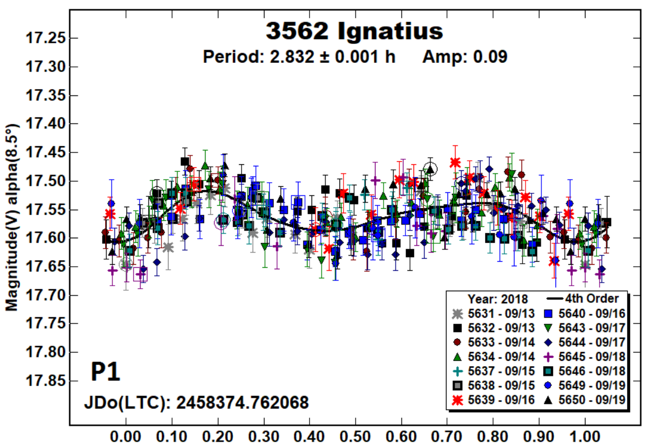

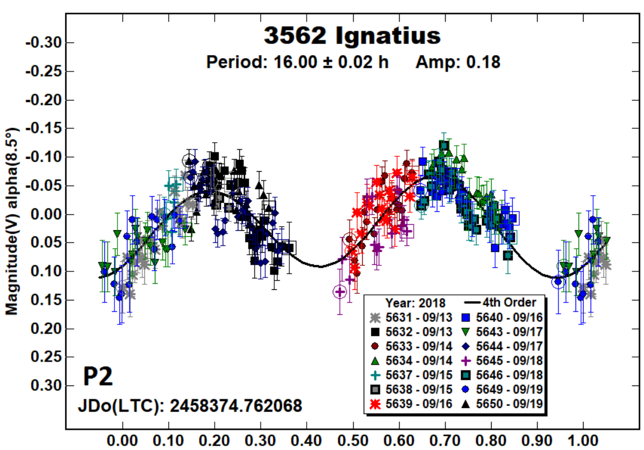

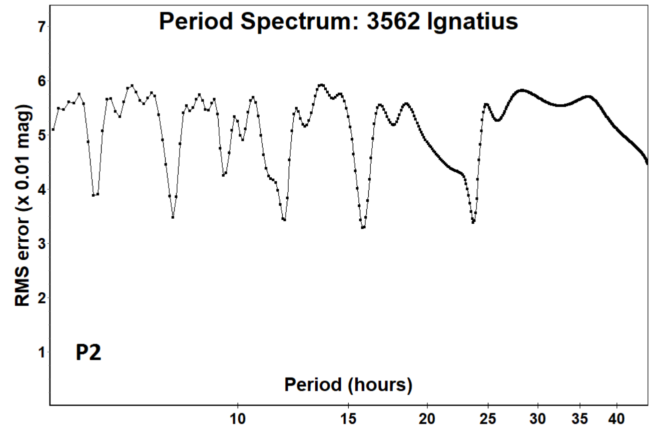

3890 Bunin. No entry was found in the lightcurve database (LCDB; Warner et al., 2009) for this Vestoid.

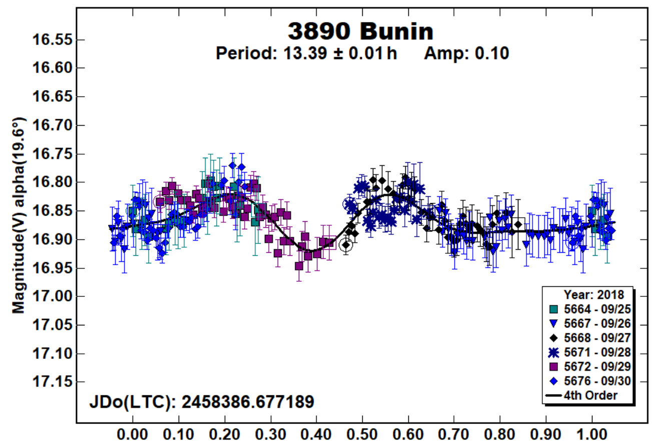

3893 DeLaeter. This Phocaea family member has been studied twice in past with differing results. A previous rotational period of 13.84 h was found in 2003 (Stephens 2004). Warner (2014) found a period of 5.633 h. The Warner result had an asymmetric lightcurve with an amplitude of only 0.13 mag. The analysis of this year's data does not support either of those periods. The period spectrum for 2018 shows several aliases at 6 h, 10 h and 16 h.

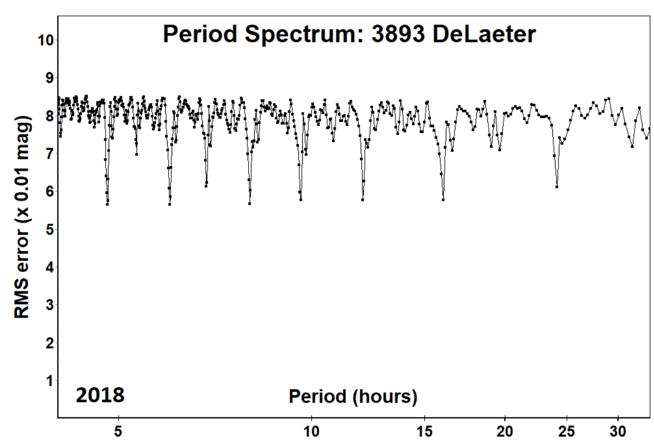

The period spectrums of the 2003 and 2018 data formally ruled out the possibility of a 5.6 h period. Because the asteroid was well past opposition when observing started, a complete lightcurve could not be obtained. However, the period spectrums for all three oppositions allow for the possibility of a 9.6 h period. Plotting the

2018 data to that period shows a classic bimodal lightcurve with an amplitude of 0.19 mag. The 2003 data results in a single modal lightcurve with a 9.73 h period. Finally, the 2014 data results in a 9.61 h period with a trimodal lightcurve. With such low amplitudes, it is possible that a lightcurve could have a single minimum/maximum pair, or three or more pairs (Harris et al., 2014). Presently, the 9.61 h period is the only one that seems to fit all three datasets and is adopted for this paper.

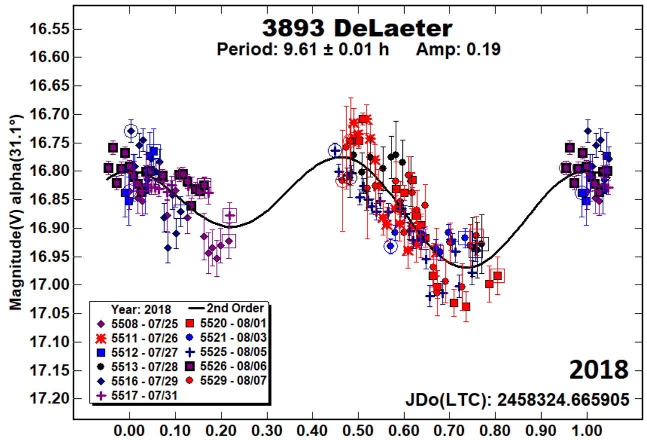

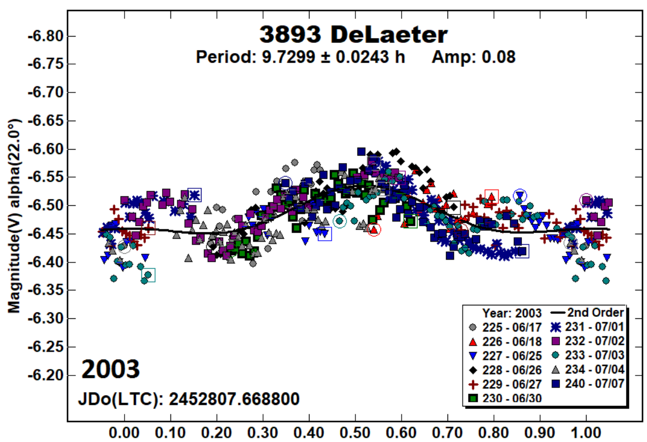

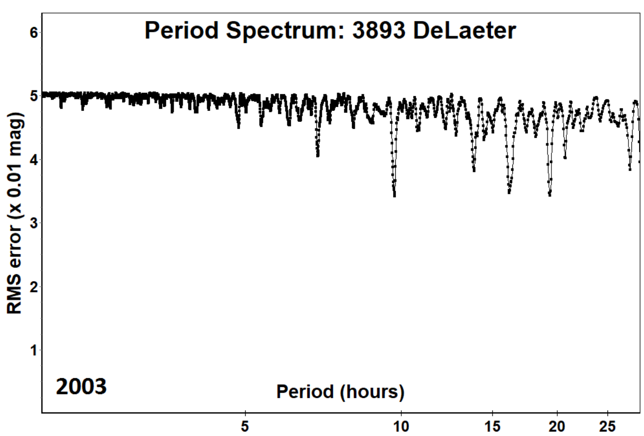

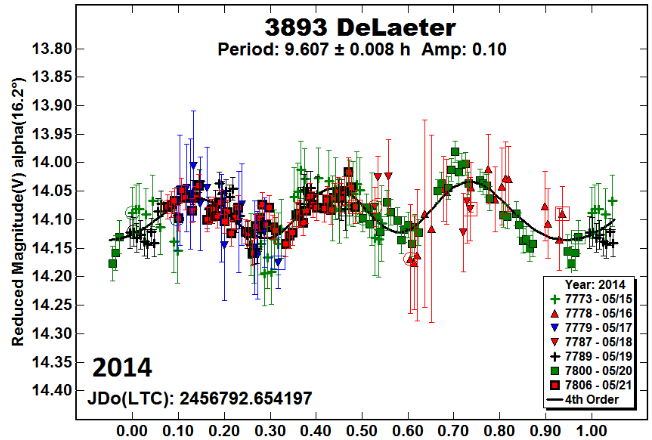

3894 Williamcooke. Macias (2015) reported this member of the Eunomia family as having a low amplitude asymmetrical curve with three nights of coverage. Behrend (2018) reported a period of 8.33 h with eight extrema with an amplitude of 0.15 mag. At the time the asteroid was in a dense star field. These observations started two weeks after the Behrend result and were carefully controlled to remove background stars from the measurements. The period spectrum showed possible periods near 2, 4, 7, and 8.5 h. Because of the bimodal shape of the lightcurve and 0.20 mag amplitude, the 4.16 h period is adopted for this paper.

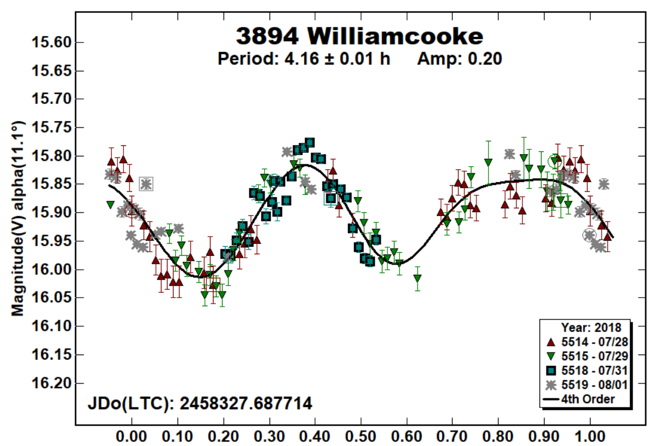

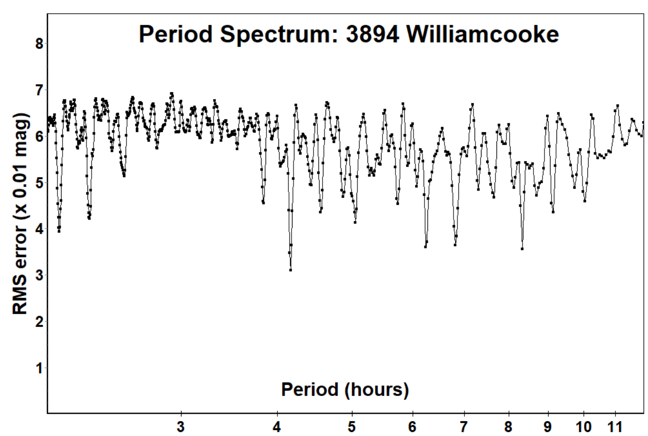

Number	Name	mm\dd	Pts	Phase	LPAB	BPAB	Period	P.E.	Amp	A.E.	Grp
1026	Ingrid	08/26-09/09	185	27.4,23.1	23	-7	5.437	0.001	0.12	0.01	FLOR
1523	Pieksamaki	08/26-08/28	90	24.2,24.0	35	5	5.326	0.003	0.45	0.02	FLOR
1991	Darwin	08/21-08/25	197	20.1,18.1	357	3	5.92	0.01	0.09	0.02	FLOR
2017	Wesson	08/22-08/25	181	23.2,22.0	6	0	3.4153	0.0002	0.59	0.01	FLOR
3562	Ignatius	09/13-09/19	271	8.5,6.2	7	-7	2.832	0.001	0.09	0.01	FLOR
3562	Ignatius						16.00	0.02	0.18	0.02	FLOR
3890	Bunin	09/25-09/30	224	19.7,21.4	331	7	13.39	0.03	0.1	0.01	V
3893	DeLaeter	07/25-08/07	162	31.1,32.8	256	29	9.61	0.01	0.19	0.04	PHO
3894	Williamcooke	07/28-08/01	131	11.1,12.4	289	14	4.16	0.01	0.2	0.03	EUN
31098	Frankhill	07/04-07/24	242	14.9,22.1	282	22	50.04	0.03	0.44	0.10	MC
44588	1999 JF124	07/02-07/03	36	11.4,11.0	287	13	4.88	0.002	0.18	0.03	H

Table I. Observing circumstances and results. Pts is the number of data points. The phase angle values are for the first and last date. LPAB and BPAB are the approximate phase angle bisector longitude and latitude at mid-date range (see Harris et al., 1984). Grp is the asteroid family/group (Warner et al., 2009).

31098 Frankhill. No entry was found in the lightcurve database (LCDB; Warner et al., 2009) for this Mars Crosser.

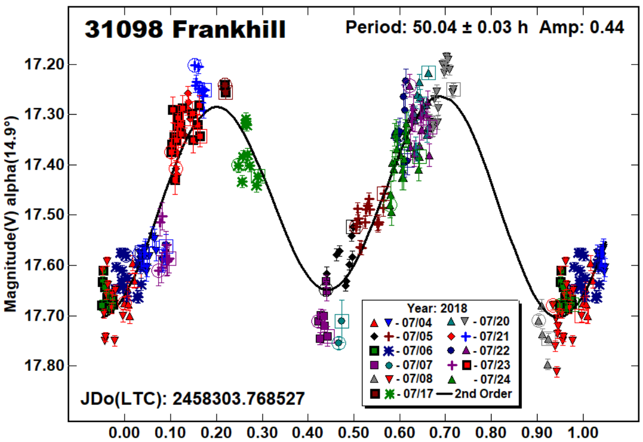

(44588) 1999 JF124. No entry was found in the lightcurve database (LCDB; Warner et al., 2009) for this Hungaria.

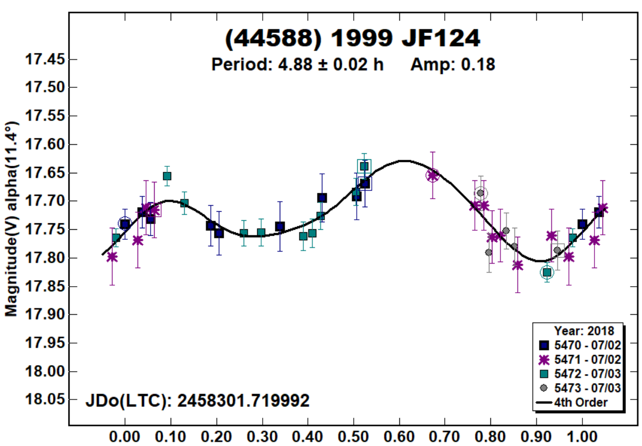

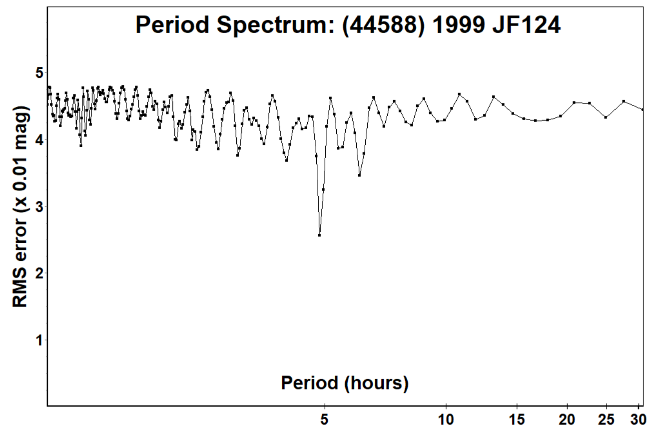

Acknowledgements

This research was made possible in part based on data from CMC15 Data Access Service at CAB (INTA-CSIC) (*http://svo2.cab.inta-csic.es/vocats/cmc15/)*. The purchase of a FLI-1001E CCD cameras was made possible by a 2013 Gene Shoemaker NEO Grants from the Planetary Society.

References

Behrend, R. (2018). Observatoire de Geneve web site, *http://obswww.unige.ch/~behrend/page_cou.html*

Falese, J., Odden, C., Prakash, P. (2014). "Lightcurve Analysis for 3562 Ignatius." *Minor Planet Bull.* **41**, 3.

Harris, A.W., Young, J.W., Bowell, E., Martin, L.J., Millis, R.L., Poutanen, M., Scaltriti, F., Zappala, V., Schober, H.J., Debehogne, H., Zeigler, K.W. (1989). "Photoelectric Observations of Asteroids 3, 24, 60, 261, and 863." *Icarus* **77**, 171-186.

Harris, A.W., Young, J.W., Scaltriti, F., Zappala, V. (1984). "Lightcurves and phase relations of the asteroids 82 Alkmene and 444 Gyptis." *Icarus* **57**, 251-258.

Harris, A.W., Pravec, P., Galád, B. Skiff, B., Warner, B., Világi, J., Gajdoš, S., Carbognani, A., Hornoch, K., Kušnirák, P., Cooney, W., Gross, J., Terrell, D., Higgins, D., Bowell, E., Koehn, B. (2014). "On the maximum amplitude of harmonics of an asteroid lightcurve." *Icarus* **235**, 55-59.

Henden, A.A., Terrell, D., Levine, S.E., Templeton, M., Smith, T.C., Welch, D.I. (2009). *http//www.aavso.org/apass*

Kryszczyńska, A., Colas, F., Polińska, M., Hirsch, R., Ivanova, V., Apostolovska, G., Bilkina, B., Velichko, F.P., Kwiatkowski, T., Kankiewicz, P., Vachier, F., Umlenski, V., Michałowski, T., Marciniak, A., Maury, A., Kamiński, K., Fagas, M., Dimitrov, W., Borczyk, W., Sobkowiak, K., Lecacheux, J., Behrend, R., Klotz, A., Bernasconi, L., Crippa, R., Manzini, F., Poncy, R., Antonini, P., Oszkiewicz, D., Santana-Ros, T. (2012). "Do Slivan states exist in the Flora family?. I. Photometric survey of the Flora region." *Astron. Astrophys.* **546**, A72.

Lagerkvist, C.I. (1979). "A lightcurve survey of asteroids with Schmidt telescopes - Observations of nine asteroids during oppositions in 1977." *Icarus* **38**, 106-114.

Macias, A.A. (2015). "Asteroid Lightcurve Analysis at Isaac Aznar Observatory Aras De Los Olmos, Valencia, Spain." *Minor Planet Bull.* **42**, 4-6.

Stephens, R.D. (2004). "Photometry of 683 Lanzia, 1101 Clematis, 1499 Pori, 1507 Vaasa, and 3893 DeLaeter." *Minor Planet Bull.* **31**, 4-6.

Stephens, R.D. (2016). "Asteroids Observed from CS3: 2016 January-March." *Minor Planet Bull.* **43**, 252-255.

Székely, P., Kiss, L.L., Szabó, Gy. M., Sárneczky, K., Csák, B., Váradi, M., Mészáros, Sz. (2005). "CCD photometry of 23 minor planets." *Icarus* **53**, 925-936.

Warner, B.D. (2014). "Asteroid Lightcurve Analysis at CS3-Palmer Divide Station: 2014 March-June." *Minor Planet Bull.* **41**, 235-241.

Warner, B.D., Harris, A.W., Pravec, P. (2009). "The Asteroid Lightcurve Database." *Icarus* **202**, 134-146. Updated 2018 July *http://www.minorplanet.info/lightcurvedatabase.html*

Wisniewski, W.Z., Michałowski, T.M., Harris, A.W., McMillan, R.S. (1979). "Photometric Observations of 125 Asteroids." *Icarus* **126**, 395-449.

ON THE ROTATION PERIOD OF 1599 GIOMUS

Luca Izzo, Heriberto Francisco Busquier Cerdan,
Miguel Angel Diaz Diaz, Joaquin Lopez Suarez,
Elena Montoro Rodriguez, Belen Moreno Megias,
Jesus Navarro Romero, Alejandra Raja De La Llave,
Irene Yoldi Vergara
IAA-CSIC, Granada, SPAIN
izzo@iaa.es

Alfonso Noschese, Maurizio Mollica, Antonio Vecchione
AstroCampania Associazione, Naples, ITALY

(Received: 2018 Oct 9 Revised: 2018 Nov 19)

We present and discuss a rotation period of P = 6.51 ± 0.01 hr for 1599 Giomus. This was the result of five observing sessions between 2017 Dec 9-24. Although this estimate is in agreement with previous measurements, other possible minima are found in the period spectrum RMS plot. We conclude that more observations are needed to confirm or reject our finding.

The main-belt asteroid 1599 Giomus has a diameter of about 39.54 km. Its orbit has semi-major axis of 3.129 AU, eccentricity of 0.14, and inclination 6.09 deg. Its rotation period, however, remains uncertain.

There are several previous results in the literature. Clark (2010) gave a period of 6.46 ± 0.05 hr based on only two observing sessions. Warner (2013) observed Giomus on five nights (four of them were consecutive). He concluded that the low amplitude of 0.04 mag made it impossible to find an accurate period. Even so, he reported a period of 29.1 hr. Linville et al. (2017) were not able to determine a period. Foylan et al. (2018) observed for seven nights, obtaining a period of 9.53 ± 0.03 hr. However, also in this case, the authors stated that their photometric errors were almost consistent with the low amplitude (0.06 mag) from the previous apparition.

We observed Giomus from the Osservatorio Salvatore di Giacomo, Agerola (MPC L07) on five nights from 2017 December 9-24. Table I gives the observing circumstances and results. Observations were made with a 0.50-m *f*/8 Ritchey-Chretien telescope equipped with a FLI PL-4240 CCD camera (2048x2048x13.5-μ), and Rc filter. Exposures were 180 s. All science images were astrometrically calibrated and corrected with dark frames and flat fields. A total of 191 lightcurve data points were collected in five nights.

This campaign was part of the PIIISA project (*http://www.piiisa.es*) sponsored by the Spanish MINECO, the Junta de Andalucia, the Universidad de Granada, and the CSIC. Its purpose is to initiate young students to astronomy through direct contact with people working in astronomical research and/or data analysis. Four groups of two students each analyzed the photometric data of Giomus in search of its rotation period. The data analysis was coordinated by astronomer L. Izzo.

Number	Name	2017 mm/dd	Pts	Phase	L_{PAB}	B_{PAB}	Period(h)	P.E.	Amp	A.E.	Exp
1599	Giomus	12/09-12/24	191	4.4	78	+4	6.51	0.01	0.08	0.03	180

Table I. Observing circumstances and results. The phase angle is given for the first and last date. LPAB and BPAB are the approximate phase angle bisector longitude and latitude at mid-date range (see Harris et al., 1984). The U rating is our estimate and not necessarily the one assigned in the asteroid lightcurve database (Warner et al., 2009). Exp is average exposure, seconds.

MPO Canopus was used for the photometry, employing up to five near-solar color stars with the "Comp Star Selector" tool, and then for the period analysis using the FALC Fourier algorithm (Harris et al., 1989). From the single power spectrum obtained by each group, we derived a final average RMS-period plot and consequently the best measurement of the period through the minimization of the RMS value. We also included in our analysis the results of an independent analysis of the period led by co-authors Izzo and Mollica. The distribution of the averaged RMS values with respect to the period, suggests a best period for Giomus of $P = 6.51 \pm 0.01$ hr (1-sigma).

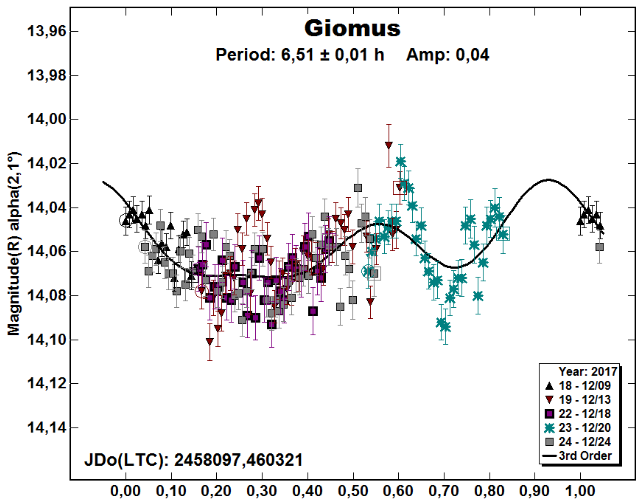

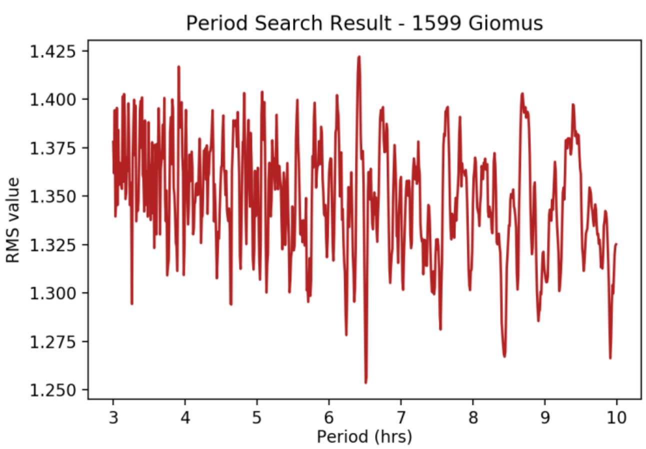

This value is in agreement with the previous estimate given by Clark (2010). However, we were not able to investigate the long-period range with much detail since our dataset was quite limited in time. This constrained the period search to a range of 3-10 hours. We also used a third-order fit function in the FALC algorithm, while Foylan et al. (2018) used a sixth-order fit function. Moreover, from the final power spectrum we note the presence of other relative minima, with only a small difference in the RMS value from the best period found in this work. For example, two possible period solutions are at 8.4 hr and 8.9 hr.

Another important consideration is that the amplitude reported in our dataset is quite low (0.08 mag), suggesting that the viewing aspect during the 2018 apparition was nearly pole-on, or that the asteroid has a nearly spheroidal shape. All of these factors imply that our final estimate cannot be considered to be the actual rotation period. More detailed observations in the future are needed in order to quantify accurately the rotation period.

References

Clark, M. (2010). "Asteroid light curves from the Chiro Observatory." *Minor Planet Bull.* **40**, 137-145.

Foylan, M., Rowe, B., Smith, K.S., (2013). "Lightcurve and Rotation Period Determinations for 1599 Giomus and 1888 Zu Chong-Zhi." *Minor Planet Bull.* **45**, 132-133.

Harris, A.W., Young, J.W., Scaltriti, F., Zappala, V. (1984). "Lightcurves and phase relations of the asteroids 82 Alkmene and 444 Gyptis." *Icarus* **57**, 251-258.

Harris, A.W., Young, J.W., Bowell, E., Martin, L.J., Millis, R.L., Poutanen, M., Scaltriti, F., Zappala, V., Schober, H.J., Debehogne, H., Zeigler, K.W. (1989). "Photoelectric Observations of Asteroids 3, 24, 60, 261, and 863." *Icarus* **77**, 171-186.

Linville, D., Jiang, H., Michalik, D., Wilson, S., Ditteon, R. (2017). "Lightcurve Analysis of Asteroids Observed at the Oakley Southern Sky Observatory: 2016 July-October." *Minor Planet Bull*. **44,** 173-176.

Warner, B.D., Harris, A.W., Pravec, P. (2009). "The Asteroid Lightcurve Database." *Icarus* **202**, 134-146. Updated 2018 June. *http://www.minorplanet.info/lightcurvedatabase.html*

Warner, B. (2013). "Asteroid light analysis at the Palmer Divide Observatory: 2013 January - March." *Minor Planet Bull.* **37**, 89-92.

Warner, B., (2016) MPO Software, *MPO Canopus* version 10.7.7.0, Bdw Publishing. *http://minorplanetobserver.com*

LIGHTCURVE ANALYSIS OF L4 TROJAN ASTERIODS AT THE CENTER FOR SOLAR SYSTEM STUDIES - 2018 JULY TO SEPTEMBER

Robert D. Stephens
Center for Solar System Studies (CS3)/MoreData!
11355 Mount Johnson Ct., Rancho Cucamonga, CA 91737 USA
rstephens@foxandstephens.com

Brian D. Warner
Center for Solar System Studies (CS3)/MoreData!
Eaton, CO

(Received: 2018 October 8)

Lightcurves for five Jovian Trojan asteroids were obtained at the Center for Solar System Studies (CS3) from 2018 July to September.

CCD Photometric observations of five Trojan asteroids from the L_4 (Greek) Lagrange point were obtained at the Center for Solar System Studies (CS3, MPC U81). For several years, CS3 has been conducting a study of Jovian Trojan asteroids. This is another in a series of papers reporting data analysis being accumulated for family pole and shape model studies. It is anticipated that for most Jovian Trojans, two to five dense lightcurves per target at oppositions well distributed in ecliptic longitudes will be needed and can be supplemented with reliable sparse data for the brighter Trojan asteroids. For all of these targets we were able to get preliminary pole positions and create shape models from sparse data and the dense lightcurves obtained to date. These preliminary models will be improved as more data are acquired at future oppositions and will be published at a later date.

Table I lists the telescopes and CCD cameras that were used to make the observations. Images were unbinned with no filter and had master flats and darks applied. The exposures depended upon various factors including magnitude of the target, sky motion, and Moon illumination.

Image processing, measurement, and period analysis were done using *MPO Canopus* (Bdw Publishing), which incorporates the Fourier analysis algorithm (FALC) developed by Harris (Harris et al., 1989). Night-to-night calibration (generally < ±0.05 mag) was done using field stars from the CMC-15 or APASS (Henden et al., 2009) catalogs. The Comp Star Selector feature in *MPO Canopus* was used to limit the comparison stars to near solar color.

Telescope	Camera
0.40-m F/10 Schmidt-Cass	FLI Proline 1001E
0.35-m F/11 Schmidt-Cass	Fli Microline 1001E

Table I. List of telescopes and CCD cameras used at CS3.

In the lightcurve plots, the "Reduced Magnitude" is Johnson V corrected to a unity distance by applying –5*log (rΔ) to the measured sky magnitudes with r and Δ being, respectively, the Sun-asteroid and the Earth-asteroid distances in AU. The magnitudes were normalized to the phase angle given in parentheses using G = 0.15. The X-axis rotational phase ranges from –0.05 to 1.05.

The amplitude indicated in the plots (e.g. Amp. 0.23) is the amplitude of the Fourier model curve and not necessarily the adopted amplitude of the lightcurve.

Targets were selected for this L_4 observing campaign based upon the availability of dense lightcurves acquired in previous years. We obtained two to four lightcurves for most of these Trojans at previous oppositions, and some data were found from the Palomar Transient Factory (Waszczak et al., 2015).

For brevity, only some of the previously reported rotational periods may be referenced. A complete list is available at the lightcurve database (LCDB; Warner et al., 2009).

To evaluate the quality of the data obtained to determine how much more data might be needed, preliminary pole and shape models were created for all of these targets. Sparse data observations were obtained from the Catalina Sky Survey and USNO-Flagstaff survey using the AstDyS-3 site (*http://hamilton.dm.unipi.it/asdys2/*). These sparse data were combined with our dense data as well as any other dense data found in the ALCDEF asteroid photometry database (*http://www.alcdef.org/*) using *MPO LCInvert*, (Bdw Publishing). This Windows-based program incorporates the algorithms developed by Kassalainen *et al* (2001a, 2001b) and converted by Josef Durech from the original FORTRAN to C. A period search was made over a sufficiently wide range to assure finding a global minimum in χ^2 values.

1583 Antilochus. We observed Antilochus three times in the past. Lightcurves obtained in 2009, 2016 and 2017 (Stephens 2010), Stephens et al. (2016), Stephens and Warner (2018) all had low amplitudes between 0.05 and 0.12 mag. With such low amplitudes, it is possible that a lightcurve could have a single minimum/maximum pair, or three or more pairs (Harris et al., 2014). For the 2017 observations, only a 15.89 h period resulted in a bimodal lightcurve. The 2009 and 2016 data were rephased to this period with a single modal lightcurve. The observations obtained in 2018 confirmed the 2017 period with a large amplitude ruling out the 31.5 h period found in the 2009 and 2016 data. The data collected this year, when combined with our previous data and available sparse data, were used to create a preliminary shape model with a sidereal rotational period of 15.76149 ± 0.00001 h.

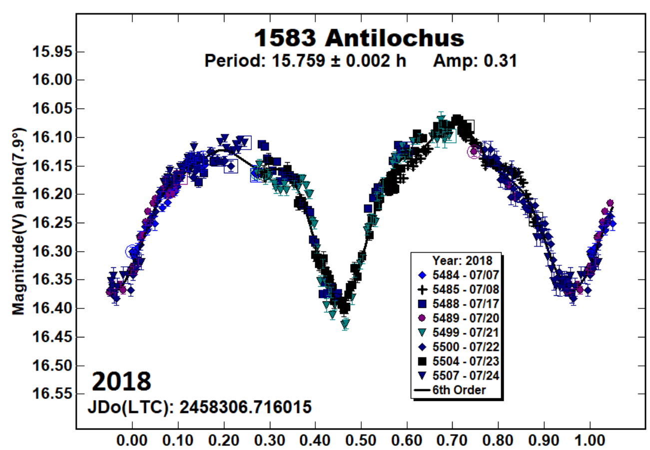

2920 Automedon. The synodic period found in 2018 using CS3 data agrees with previous synodic results (Molnar et al., 2008; Mottola et al., 2011; Stephens and Warner (2017) near 10.22 h. The data analysis in 2018 is in good agreement and when combined with our previous data and available sparse data, were used to create a preliminary shape model with a sidereal rotational period of 10.22368 ± 0.00001 h.

Number	Name	2018 mm/dd	Pts	Phase	L_{PAB}	B_{PAB}	Period(h)	P.E.	Amp	A.E.
1583	Antilochus	07/07-07/24	386	7.9,6.7	311	32	15.759	0.002	0.31	0.02
2920	Automedon	09/24-09/30	122	10.6,10.9	296	21	10.22	0.01	0.25	0.03
3709	Polypoites	08/05-08/10	202	6.9,7.5	281	21	10.07	0.02	0.12	0.02
3793	Leonteus	07/24-08/04	202	4.4,4.3,4.4	306	22	5.621	0.001	0.31	0.02
4060	Deipylos	08/13-08/19	97	5.2,6.0	293	14	9.22	0.03	0.10	0.02

Table II. Observing circumstances and results. ^{P} in the period column indicates the period of the primary in a binary system. Pts is the number of data points. Phase is the solar phase angle for the first and last date. If there are three values, the middle value is the minimum phase angle. L_{PAB} and B_{PAB} are, respectively, the approximate phase angle bisector longitude and latitude at mid-date range (see Harris et al., 1984).

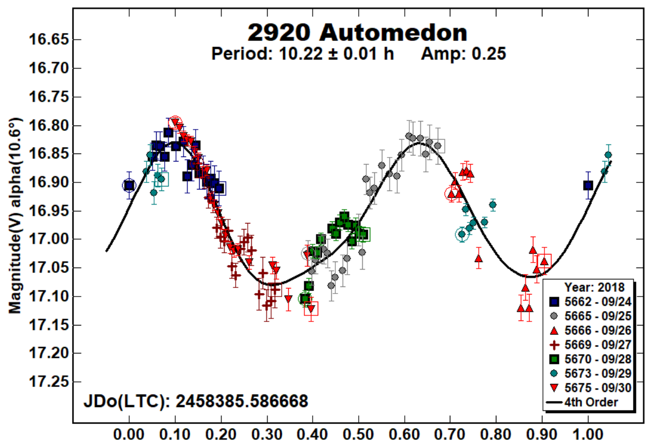

3709 Polypoites. We observed this Trojan four times in the past (French et al., 2011, Stephens et al., 2016a, Stephens et al., 2016b and 2017), each time finding a period near 10.04 h. The 2018 analysis results are in good agreement and were used to create a preliminary shape model with a sidereal rotational period of 10.04745 ± 0.00001 h.

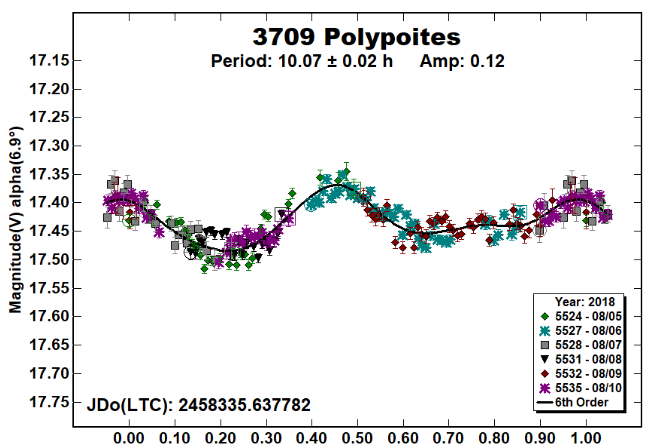

3793 Leonteus. This large Trojan has been well studied in the past. Mottola et al., (2011) observed it in 1994 and 1997. We found periods in 2009, 2015 and 2016 (Stephens et al., 2016a and 2016b). Each of these periods was found to be close to 5.62 h. This year's data analysis result is in good agreement. We were able to create a preliminary shape model with a sidereal rotational period of 5.62192 ± 0.00001 h.

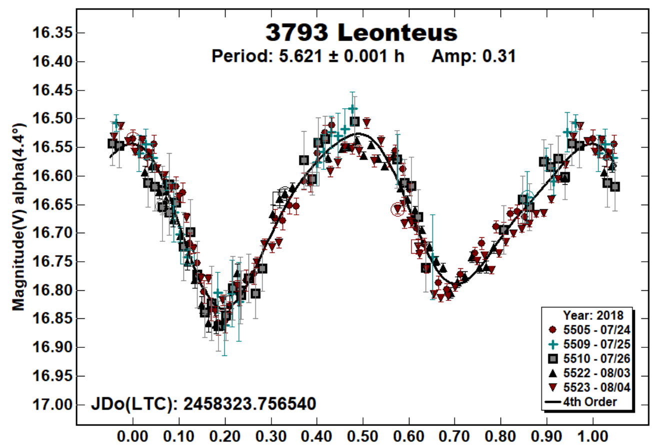

4060 Deipylos. Using sparse photometry from the Palomar Transient Factory, Waszczak et al. (2015) reported a period of 11.4905 h for Deipylos. We observed it three times (Stephens et al 2016a, 2016b and 2017) finding periods near 9.3 h. That period appears to be a 5:4 alias of the Waszczak period of rotation. The 2018 result of 9.38 h is in good agreement with our prior results, but the 11.5 h alias was still present as seen in the ChiSq versus Period plot. The sharper minimum in that plot as well as the synodic periods found in each of the four oppositions cause us to adopt the sidereal rotational period of 9.3316 ± 0.00001 h.

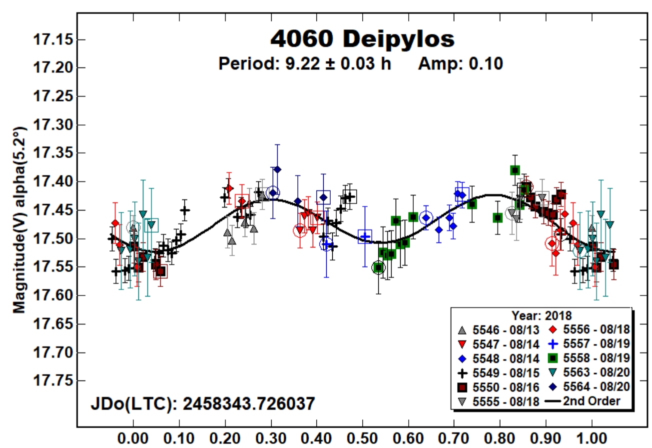

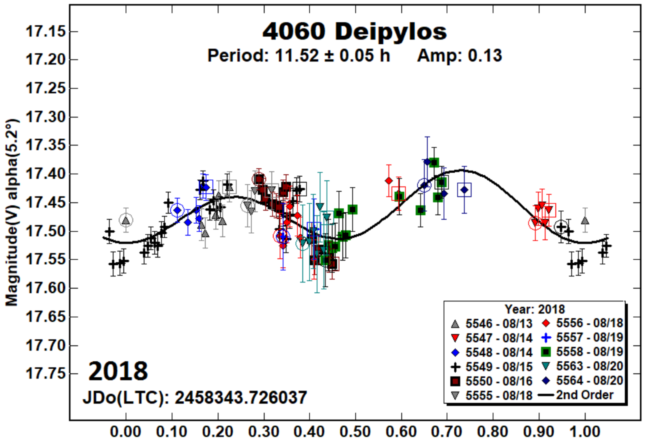

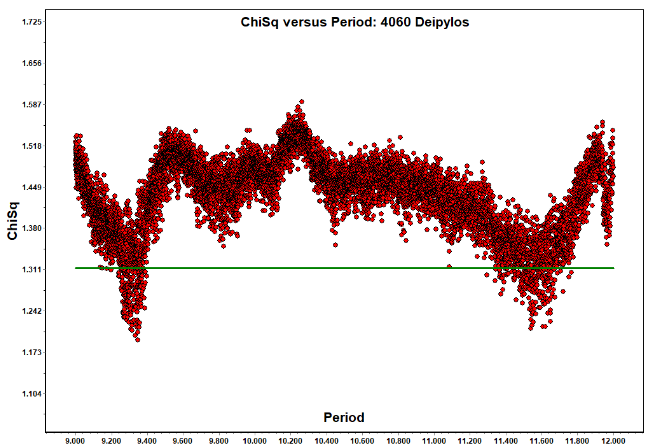

Acknowledgements

Observations at CS3 and continued support of the asteroid lightcurve database (LCDB; Warner et al., 2009) are supported by NASA grant 80NSSC18K0851. Work on the asteroid lightcurve database (LCDB) was also partially funded by National Science Foundation grant AST-1507535. This research was made possible in part based on data from CMC15 Data Access Service at CAB (INTA-CSIC) (*http://svo2.cab.inta-csic.es/vocats/cmc15/*) and through the use of the AAVSO Photometric All-Sky Survey (APASS), funded by the Robert Martin Ayers Sciences Fund. The purchase of a FLI-1001E CCD cameras was made possible by a 2013 Gene Shoemaker NEO Grants from the Planetary Society.

References

French, L.M., Stephens, R.D., Lederer, S.M., Coley, D.R., Rohl, D.A. (2011). "Preliminary Results from a Study of Trojan Asteroids." *Minor Planet Bul.* **38**, 116-120.

Harris, A.W., Young, J.W., Scaltriti, F., Zappala, V. (1984). "Lightcurves and phase relations of the asteroids 82 Alkmene and 444 Gyptis." *Icarus* **57**, 251-258.

Harris, A.W., Young, J.W., Bowell, E., Martin, L.J., Millis, R.L., Poutanen, M., Scaltriti, F., Zappala, V., Schober, H.J., Debehogne, H., Zeigler, K.W. (1989). "Photoelectric Observations of Asteroids 3, 24, 60, 261, and 863." *Icarus* **77**, 171-186.

Harris, A.W., Pravec, P., Galád, B., Skiff, B., Warner, B., Világi, J., Gajdoš, S., Carbognani, A., Hornoch, K., Kušnirák, P., Cooney, W., Gross, J., Terrell, D., Higgins, D., Bowell, E., Koehn, B. (2014). "On the maximum amplitude of harmonics of an asteroid lightcurve." *Icarus* **235**, 55-59.

Henden, A.A., Terrell, D., Levine, S.E., Templeton, M., Smith, T.C., Welch, D.I. (2009). *http//www.aavso.org/apass*

Kassalainen, M., Torppa J. (2001a). "Optimization Methods for Asteroid Lightcurve Inversion. I. Shape Determination." *Icarus* **153**, 24-36.

Kassalainen, M., Torppa J., Muinonen, K. (2001b). "Optimization Methods for Asteroid Lightcurve Inversion. II. The Complete Inverse Problem." *Icarus* **153**, 37-51.

Molnar, L.A., Jaegert, M.J., Hoogeboom, K.M. (2008). "Lightcurve Analysis of an Unbiased Sample of Trojan Asteroids." *Minor Planet Bull.* **35**, 82-84.

Mottola, S., Di Martino, M., Erikson, A., Gonano-Beurer, M., Carbognani, A., Carsenty, U., Hahn, G., Schober, H., Lahulla, F., Delbò, M., Lagerkvist, C. (2011). "Rotational Properties of Jupiter Trojans. I. Light Curves of 80 Objects." *Astron. J.* **141**, A170.

Stephens, R.D. (2010). "Trojan Asteroids Observed from GMARS and Santana Observatories: 2009 October - December." *Minor Planet Bull*. **37**, 47-48.

Stephens, R.D., Coley, D.R., French, L.M. (2016a). "Large L5 Jovian Trojan Asteroid Lightcurves from the Center for Solar System Studies." *Minor Planet Bull.* **43**, 15-22.

Stephens, R.D., Coley, D.R., Warner, B.D., French, L.M. (2016b). "Lightcurves of Jovian Trojan Asteroids from the Center for Solar System Studies: L4 Greek Camp and Spies." *Minor Planet Bull.* **43**, 323-331.

Stephens, R.D., Warner B.W. (2017). "Lightcurve Analysis of L4 Trojan Asteroids at the Center for Solar System Studies 2017 April-June." *Minor Planet Bull.* **44**, 312-316.

Stephens, R.D., Warner, B.D. (2018). "Lightcurve Analysis of L4 Trojan Asteroids at the Center for Solar System Studies 2017 July – September." *Minor Planet Bull*. **45**, 48-50.

Warner, B.D., Harris, A.W., Pravec, P. (2009). "The Asteroid Lightcurve Database." *Icarus* **202**, 134-146. Updated 2018 April. *http://www.minorplanet.info/lightcurvedatabase.html*

Waszczak, A., Chang, C., Ofek, E.O., Laher, R., Masci, F., Levitan, D., Surace, J., Cheng, Y., Ip, W., Kinoshita, D., Helou, G., Prince, T.A., Kulkarni, S. (2015). "Asteroid lightcurves from the Palomar Transient Factory survey: Rotation periods and phase functions from sparse photometry." *Astron. J.* **150**, A75.

LIGHTCURVE ANALYSIS AND ROTATION PERIOD FOR (11650) 1997 CN

M. Mollica
AstroCampania Associazione
via Servio Tullio 101, 80126 Naples (Italy)
m.mollica@astrocampania.it

A. Vecchione
AstroCampania Associazione Naples (Italy)

(Received: 2018 Oct 10)

Photometric data for asteroid (11650) 1997 CN were collected from 2018 September 16-30. Analysis led to a well-covered lightcurve with a period of 7.7175 ± 0.0007 hr and amplitude of 0.27 mag.

The main-belt asteroid (11650) 1997 CN was discovered by T. Kobayashi, at Oizumi in 1997. Its orbit has a semi-major axis of 2.458 AU, period of 3.85 years, eccentricity of 0.254, and inclination of 6.338 deg. This 5-km diameter asteroid has an absolute magnitude of H = 13.2 and geometric albedo of 0.466 (JPL, 2018). To the best of our knowledge, no rotation period or lightcurve have been reported for this object.

Observations were conducted by using a 0.25-m *f*/8 Ritchey-Chrétien telescope with a KAF-8300M CCD camera (3358x2536x5.4-microns), and were unfiltered. A total of 225 lightcurve data points were collected in six observing sessions from 2018 September 16-30. Exposure times were 240 s at 1x1 binning, except on September 17 and 21, when 2x2 binning was used. Master darks and flats were obtained using *CCD STACK*.

The MPOSC3 catalog distributed with *MPO Canopus* (Warner, 2016) was used for comparison star magnitudes. This catalogue provides BVRI magnitudes derived from 2MASS J-K color indexes (Warner, 2007). The MPOSC3 Rc magnitudes were used to find the asteroid magnitude, which was then corrected to unity Sun-asteroid and Earth-asteroid distances and normalized to a phase angle of 6.3° using G = 0.15.

Night-to-night zero-point calibration was accomplished by selecting up to five comparison stars with near-solar colors using the "Comp Star Selector" feature in *MPO Canopus*. The "StarBGone" routine in *MPO Canopus* was used to subtract stars on the images that merged with the asteroid. *MPO Canopus* was also used for rotation period analysis using the FALC method by Harris (Harris et al., 1989). We found a lightcurve period of 7.7175 ± 0.0007 hr and amplitude of 0.27 mag, which was the one most favored by the best (lowest RMS) solution in the period spectrum. Table I gives the observing circumstances and results.

Despite the object's magnitude being very close to the limit for useful photometric data with our optics, the data were of good quality, except those from the cloudy night of Sept 29.

References

Harris, A.W., Young, J.W., Scaltriti, F., Zappala, V. (1984). "Lightcurves and phase relations of the asteroids 82 Alkmene and444 Gyptis." *Icarus* **57**, 251-258.

Harris, A.W., Young, J.W., Bowell, E., Martin, L.J., Millis, R.L., Poutanen, M., Scaltriti, F., Zappala, V., Schober, H.J., Debehogne, H., Zeigler, K.W. (1989). "Photoelectric Observations of Asteroids 3, 24, 60, 261, and 863." *Icarus* **77**, 171-186.

JPL (2018). Small-Body Database Browser. *http://ssd.jpl.nasa.gov/sbdb.cgi#top*

Warner, B.D. (2007). "Initial Results of a Dedicated H-G Program." *Minor Planet Bull*. **34**, 113-119.

Warner, B.D., Harris, A.W., Pravec, P. (2009). "The Asteroid Lightcurve Database." *Icarus* **202**, 134-146. Updated 2018 June. *http://www.minorplanet.info/lightcurvedatabase.html*

Warner, B.D. (2016). MPO Software, *MPO Canopus* version 10.7.7.0 Bdw Publishing. *http://minorplanetobserver.com*

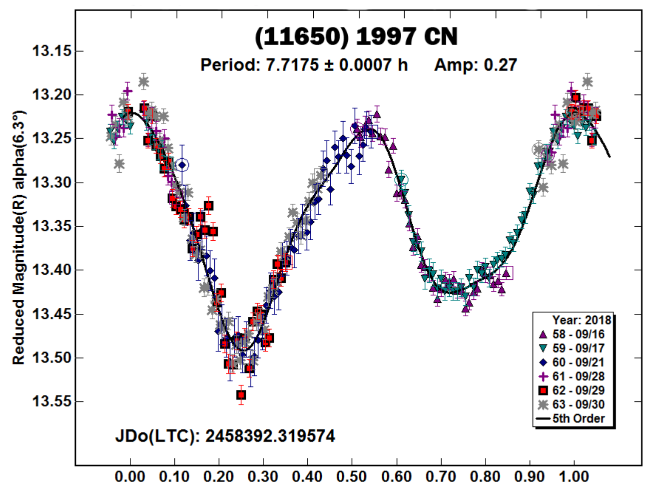

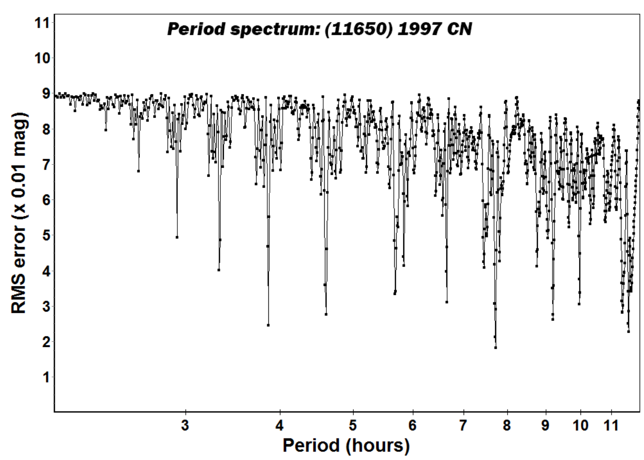

Number	Name	2018 mm/dd	Pts	Phase	L_{PAB}	B_{PAB}	Period(h)	P.E.	Amp	A.E.	U	Exp
11650	1997 CN	09/16-09/30	225	6.3,11.0	353.9	8.6	7.7175	0.0007	0.27	0.01	2	240

Table I. Observing circumstances and results. The phase angle is given for the first and last date. L_{PAB} and B_{PAB} are the approximate phase angle bisector longitude and latitude at mid-date range (see Harris *et al.*, 1984). The U rating is our estimate and not necessarily the one assigned in the asteroid lightcurve database (Warner *et al.*, 2009). Exp is average exposure, seconds.

ROTATION PERIOD DETERMINATION FOR 1229 TILIA

Alfonso Noschese
AstroCampania Associazione
via Servio Tullio 101, 80126 Naples (Italy)
and
Osservatorio Elianto (K68)
via V. Emanuele III, 95, 84098
Pontecagnano (SA) Italy
a.noschese@astrocampania.it

Antonio Vecchione
AstroCampania Associazione Naples (Italy)

(Received: 2018 Oct 8)

CCD photometric data of asteroid 1229 Tilia were collected from 2018 September 17-30. Lightcurve analysis led to a period of 7.0355 ± 0.0007 hr and amplitude of 0.35 mag.

The asteroid 1229 Tilia is a member of the Themis family; it was discovered on 1931 October 9 by Karl Reinmuth at the Heidelberg Observatory. It has a semi-major axis of 3.2243 AU, orbital period of 5.79 yr, eccentricity of 0.166, and inclination of 1.039 deg. The absolute magnitude is H = 11.3 and the albedo is 0.069 (JPL, 2018). At the time of the observations, there was no reported rotation period for Tilia. The spectral type and spin axis are unknown.

Observations were conducted at Elianto observatory (MPC K68) using a 0.30-m *f*/4.0 Newtonian telescope with a KAF-1603ME CCD camera with a 1536x1024 array of 9-micron pixels. The unfiltered exposures ranged from 240-300 s.

A total of 187 lightcurve data points were collected in six observing sessions from 2018 September 17-30. All images were astrometrically aligned dark and flat-field corrected using *Maxim DL* software. *MPO Canopus* (Warner, 2017) was used to measure the magnitudes with CMC-15 catalogue (Munos, 2017). The Rc derived magnitudes were reduced to unity Sun-asteroid and Earth-asteroid distances and normalized using G = 0.15.

Night-to-night zero-point calibration was accomplished by selecting up to five comparison stars with near-solar colors using the “Comp Star Selector” feature. The “StarBGone” routine within *MPO Canopus* was used to subtract stars that merged with the asteroid during the observations. *MPO Canopus*, which implements the FALC Fourier analysis method developed by Harris (Harris et al., 1989), was used to find the rotation period.

The individual sessions were divided in two parts, before and after passing the meridian. We found a period an unambiguous period of 7.0355 ± 0.0007 hours, as shown in the period spectrum. The lightcurve amplitude is 0.35 magnitudes. Table I gives the observing circumstances and results.

References

Harris, A.W., Young, J.W., Scaltriti, F., Zappala, V. (1984). “Lightcurves and phase relations of the asteroids 82 Alkmene and 444 Gyptis.” *Icarus* **57**, 251-258.

Harris, A.W., Young, J.W., Bowell, E., Martin, L.J., Millis, R.L., Poutanen, M., Scaltriti, F., Zappala, V., Schober, H.J., Debehogne, H., Zeigler, K.W. (1989). “Photoelectric Observations of Asteroids 3, 24, 60, 261, and 863.” *Icarus* **77**, 171-186.

JPL (2018). Small-Body Database Browser. *http://ssd.jpl.nasa.gov/sbdb.cgi#top*

Munos, J.L. (2017). Carlsberg Meridian Catalog web site. *http://svo2.cab.inta-csic.es/vocats/cmc15/*

Warner, B.D., Harris, A.W., Pravec, P. (2009). “The Asteroid Lightcurve Database.” *Icarus* **202**, 134-146. Updated 2018 June. *http://www.minorplanet.info/lightcurvedatabase.html*

Warner, B.D. (2017). MPO Software, *MPO Canopus* version 10.7.11.1 Bdw Publishing. *http://minorplanetobserver.com*

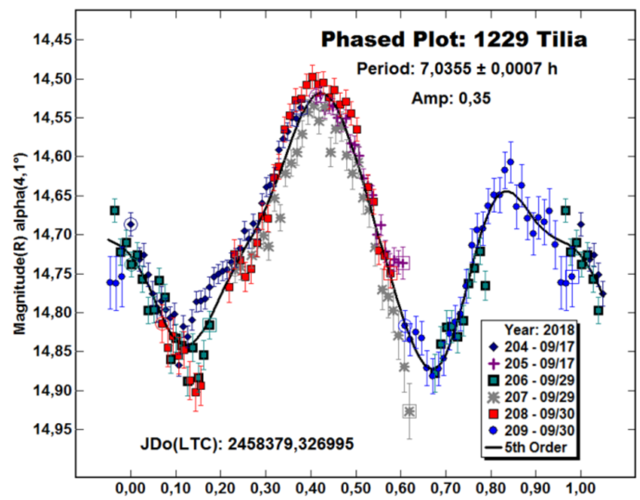

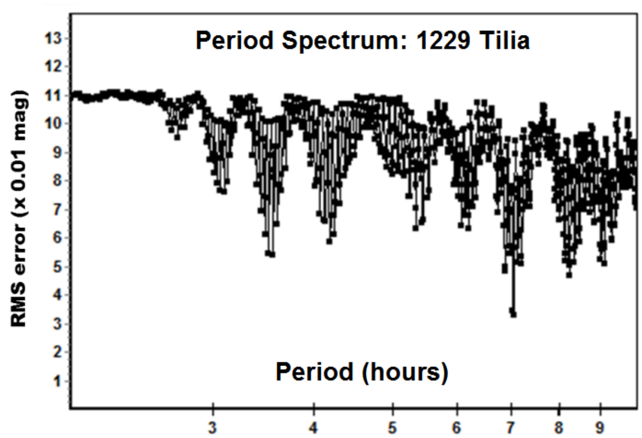

Number	Name	2018 mm/dd	Pts	Phase	L_{PAB}	B_{PAB}	Period(h)	P.E.	Amp	A.E.	Exp
1229	Tilia	09/17-09/30	187	4.1,9.4	346	1	7.0355	0.0007	0.35	0.01	240-300

Table I. Observing circumstances and results. The phase angle is given for the first and last date. L_{PAB} and B_{PAB} are the approximate phase angle bisector longitude and latitude at mid-date range (see Harris *et al.*, 1984). Exp is exposure range, seconds.

LIGHTCURVE ANALYSIS FOR SEVEN MAIN-BELT MINOR PLANETS

Tom Polakis
Command Module Observatory
121 W. Alameda Dr.
Tempe, AZ 85282 USA
tpolakis@cox.net

(Received: 2018 October 12)

Synodic rotation periods were determined for seven main-belt asteroids: 831 Stateira, 860.7 ± 7.1 h; 983 Gunila, 16.633 ± 0.023 h; 1006 Lagrangea, 19.497 ± 0.024 h; 1149 Volga, 27.262 ± 0.049 h; 1409 Isko, 11.639 ± 0.004 h; 1539 Borrelly, 15.922 ± 0.007 h; and 2406 Orelskaya, 6.109 ± 0.001 h. All the data have been submitted to the ALCDEF database.

CCD photometric observations of seven main-belt asteroids were performed at Command Module Observatory (MPC V02) in Tempe. Images at V02 were taken using a 0.32-m *f*/6.7 Modified Dall-Kirkham telescope, SBIG STXL-6303 CCD camera, and a 'clear' glass filter. Exposure time for all the images was 2 minutes. The image scale after 2x2 binning was 1.76 arcsec/pixel. Table I shows the observing circumstances and results. All of the images for these seven asteroids were obtained during 2018 September and October.

Images were calibrated using a dozen bias, dark, and flat frames. Flat-field images were made using an electroluminescent panel. Image calibration and alignment was performed using MaxIm DL software.

The data reduction and period analysis were done using *MPO Canopus* (Warner, 2017). The 45'x30' field of the CCD typically enables the use of the same field center for three consecutive nights. In these fields, the asteroid and three to five comparison stars were measured. Comparison stars were selected with colors within the range of 0.5 < B-V < 0.95 to correspond with color ranges of asteroids. In order to reduce the internal scatter in the data, the brightest stars of appropriate color that had peak ADU counts below the range where chip response becomes nonlinear were selected. The *MPO Canopus* internal star catalogue was useful in selecting comp stars of suitable color and brightness.

Comp star magnitudes were derived from a combination of CMC15 (Muiñoz et al. 2014), APASS DR9 (Munari et al. 2015), and GAIA2 G (Sloan r´ = G for stars of asteroidal color) catalogues to set the zero-points each night. In most regions the Sloan r´ data sources for brighter stars yielded very similar magnitudes (within about 0.05 mag total range), so mean values rounded to 0.01 mag precision were used.

This careful adjustment of the comp star magnitudes and color-indices allowed the separate nightly runs to be linked often with no zero-point offset required, or shifts of only a few hundredths of a magnitude in a series.

A 9-pixel (16 arcsec) diameter measuring aperture was used for asteroids and comp stars. It was typically necessary to employ star subtraction to remove contamination by field stars. For the asteroids described here, I note the RMS scatter on the phased lightcurves, which gives an indication of the overall data quality including errors from the calibration of the frames, measurement of the comp stars, the asteroid itself, and the period-fit. Period determination was done using the *MPO Canopus* Fourier-type FALC fitting method (cf. Harris et al., 1989). Phased lightcurves show the maximum at phase zero. Magnitudes in these plots are apparent, and scaled by *MPO Canopus* to the first night.

In most cases, asteroids were selected from the CALL website (Warner, 2011) using the criteria of magnitude greater than 15.0 and quality of results, U, less than 3-.

The Asteroid Lightcurve Database (LCDB; Warner et al., 2009) was consulted to locate previously published results. All the new data for these seven asteroids may be found in the ALCDEF database.

831 Stateira is a Flora-family asteroid discovered by Max Wolf at Heidelberg in 1916. The only rotation period in the LCDB is that of Behrend (2008), whose sparse data yielded >4 h.

During the course of 31 nights, 1209 data points were gathered. Nearly one rotation of 831 Stateira was covered during the 34-night observing interval. A fourth-order fit produced a period solution of 860.7 ± 7.1 h, disagreeing with Behrend's result, and placing it among the 30 longest known rotation periods. Despite its long period, the lightcurve exhibits no evidence of tumbling. The amplitude is 0.64 ± 0.03 mag, and the RMS scatter on the fit shown in the phased plot is 0.033 mag.

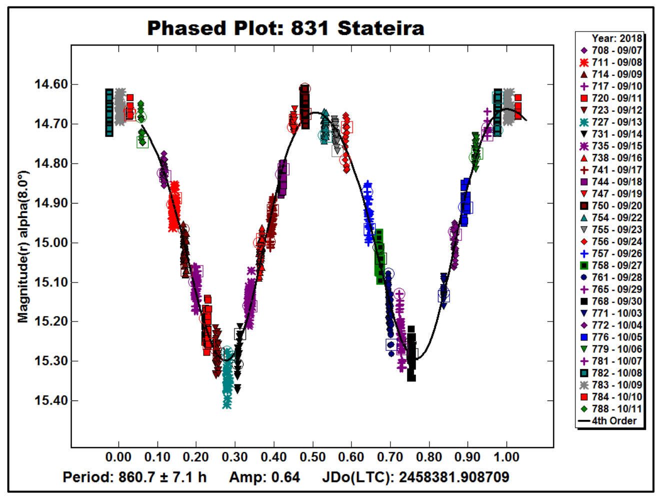

983 Gunila. This outer-belt asteroid was discovered at Heidelberg in 1922 by Karl Reinmuth. Hayes-Gehrke (2014) published a period of 8.37 ± 0.12 h.

During six nights, 329 images were gathered, yielding a period solution of 16.633 ± 0.023 h. This double-mode result is roughly twice that of Hayes-Gehrke. The amplitude is 0.12 ± 0.02 mag. The RMS scatter on the fit is 0.015 mag.

Number	Name	2018/mm/dd	Pts	Phase	L_{PAB}	B_{PAB}	Period (h)	P.E.	Amp	A.E.	Grp
831	Stateira	09/07-10/11	1209	8.0,0.0,12.8	357	0	860.7	7.1	0.64	0.03	FLOR
983	Gunila	09/15-09/20	329	6.5,6.9	349	18	16.633	0.023	0.12	0.02	MB-O
1006	Lagrangea	09/07-09/11	400	12.4,11.2	359	14	19.497	0.024	0.11	0.01	MB-O
1149	Volga	09/15-09/21	427	7.7,9.1	344	15	27.262	0.049	0.14	0.02	MB-O
1409	Isko	09/27-10/06	371	1.9,6.1	0	-1	11.639	0.004	0.14	0.03	MB-M
1539	Borrelly	09/07-09/11	314	6.3,4.6	358	-1	15.922	0.007	0.54	0.04	MB-O
2406	Orelskaya	09/27-10/05	363	10.0,14.7	351	-1	6.109	0.001	0.37	0.04	FLOR

Table I. Observing circumstances and results. The phase angle (α) is given at the start and end of each date range, unless it reached a minimum or maximum, which is then the second of three values. LPAB and BPAB are each the average phase angle bisector longitude and latitude (see Harris et al., 1984). Grp is the asteroid family/group (Warner et al., 2009).

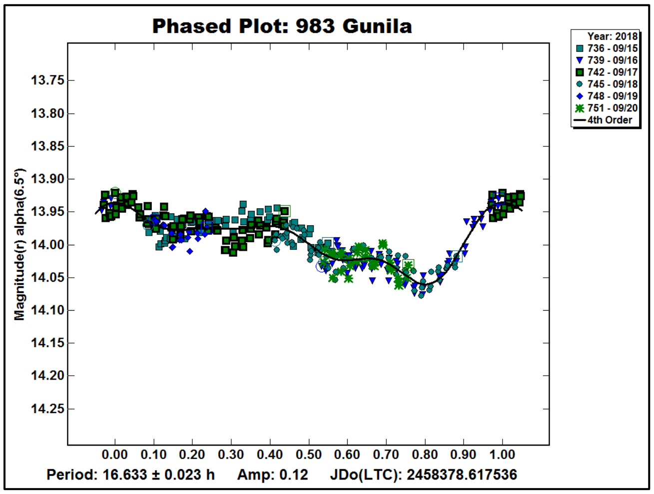

1006 Lagrangea. Sergey Belyavsky discovered this asteroid at Simeis in 1923. Its highly eccentric orbit results in opposition distances ranging from 1.1 to 4.5 a.u.; the 2018 opposition was favorably placed near the minor planet's perihelion.

The rotation period published by Behrend (2001) is 32.79 ± 0.06 h. A total of 400 data points were acquired on five nights. A rotation period of 19.497 ± 0.024 h was computed, disagreeing with Behrend's. The full amplitude is 0.11 ± 0.01 mag, and the RMS scatter of the fit is 0.014 mag.

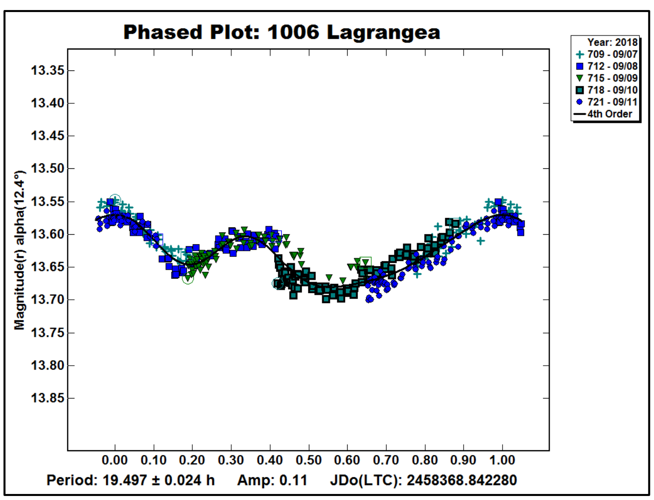

1149 Volga. This outer-belt asteroid was discovered in 1929 by Evgenii Skvortsov at Semeis. The LCDB shows one period solution: Binzel (1987), who published 27.5 h.

After seven nights, 427 images were gathered, producing a period solution of 27.262 ± 0.049 h, in accordance with Binzel's result. The lightcurve has an amplitude of 0.14 ± 0.02 mag, and the RMS error on the fit of 0.017 mag.

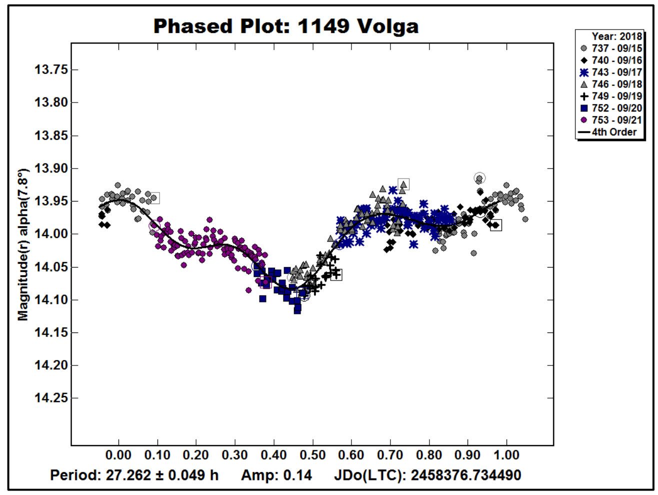

1409 Isko was discovered at Heidelberg by Karl Reinmuth in 1937. Behrend (2001) obtained a period of 11.6426 ± 0.0007 h.

A total of 371 images were acquired during seven nights. The period solution of 11.639 ± 0.004 h agrees with Behrend's value. The RMS scatter on the fit is 0.025 mag. The amplitude is 0.14 ± 0.03 mag.

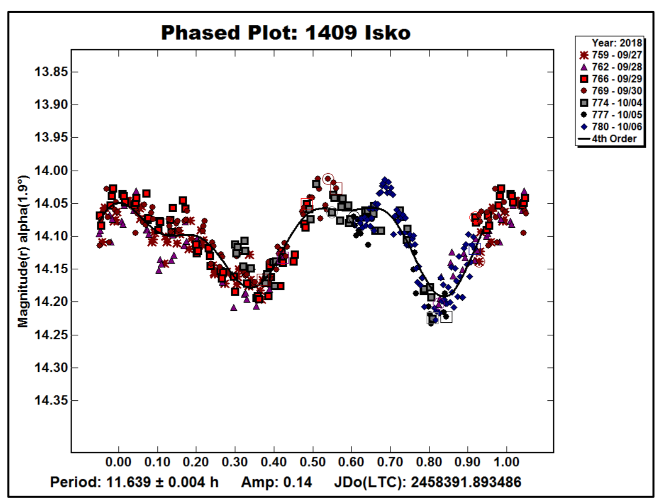

1539 Borrelly. In 1940, André Patry discovered this asteroid at Nice. No period solutions for it appear in the LCDB.

Due to its large amplitude, sufficient data were acquired to derive its rotation period in only five nights, using 314 images. A synodic period of 15.922 ± 0.007 h was computed. The amplitude of the lightcurve is 0.54 ± 0.04 mag, and the RMS error on the fit is 0.038 mag.

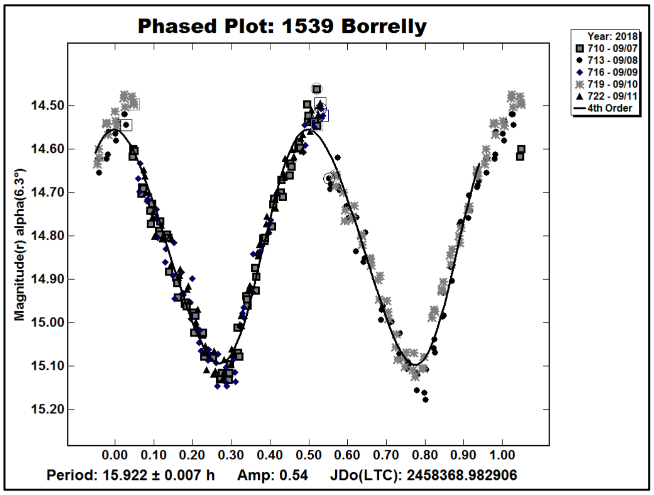

2406 Orelskaya was discovered at the Crimean Astrophysical Observatory in 1966. The only period published in the LCDB is that of Waszczak et al. (2015), who used sparse data from the Palomar Transient Factory to calculate 6.11 ± 0.009 h.

During six nights, 363 images were obtained. The period solution of 6.109 ± 0.001 h is in close agreement with Waszczak's result. Two very steep minima required an 11th order fit, whose RMS error is 0.040 mag. The amplitude is 0.37 ± 0.04 mag.

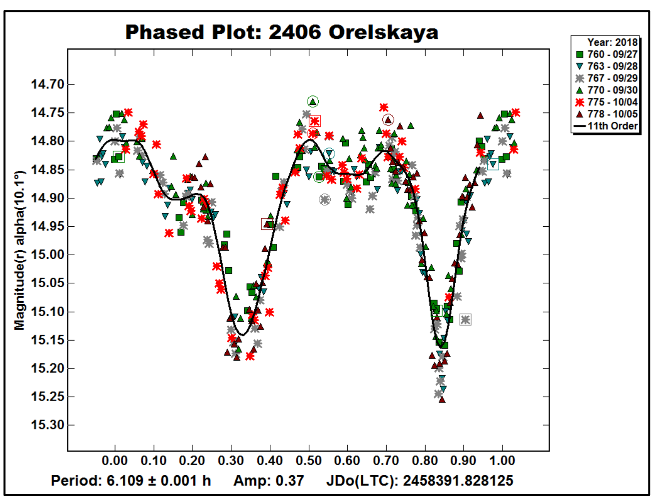

Acknowledgments

The author would like to express his gratitude to Brian Skiff for his indispensable mentoring in data acquisition and reduction. Thanks also go out to Brian Warner for support of his *MPO Canopus* software package.

References

Behrend, R. (2001, 2008). Observatoire de Geneve web site. *http://obswww.unige.ch/~behrend/page_cou.html*

Binzel, R.P. (1987). "A photoelectric survey of 130 asteroids." *Icarus* **72**, 135-208.

Harris, A.W., Young, J.W., Scaltriti, F., Zappala, V. (1984). "Lightcurves and phase relations of the asteroids 82 Alkmene and 444 Gyptis." *Icarus* **57**, 251-258.

Hayes-Gehrke, M.; Berenhaus, J.; Mascone, A.; Lopez-Lahocki, M; Levantis, G.; Haigh, E.; Yang, Z.; Guerci, J.; Wasli, Z.; Koester, K. (2014). "Rotation Period of 983 Gunila." *Minor Planet Bull*., **41**, 77.

VizieR (2017). *http://vizier.u-strasbg.fr/viz-bin/VizieR*

Warner, B.D. (2002). "Asteroid Photometry at the Palmer Divide Observatory: Results for 573 Recha, 1329 Eliane, and 8041 Masumoto." *Minor Planet Bull*. **29**, 14-15.

Warner, B.D., Harris, A.W., Pravec, P. (2009). "The Asteroid Lightcurve Database." *Icarus* **202**, 134-146. Updated 2016 Feb. *http://www.minorplanet.info/lightcurvedatabase.html*

Warner, B.D., (2011). Collaborative Asteroid Lightcurve Link website. *http://www.minorplanet.info/call.html*

Warner. B.D. (2017). *MPO Canopus* software. *http://bdwpublishing.com*

Waszczak, A., Chang, C.-K., Ofeck, E.O., Laher, F., et al. (2015). "Asteroid Light Curves from the Palomar Transient Factory Survey: Rotation Periods and Phase Functions from Sparse Photometry." *Astron. J*. **150**, A75.

ETSCORN ASTEROIDS: 2018 JULY - SEPTEMBER

Daniel A. Klinglesmith III, Erin Aaron Lovato
Etscorn Campus Observatory
New Mexico Tech
101 East Road
Socorro, NM 87801
dklinglesmith@mro.nmt.edu

(Received: 2018 October 4)

Analysis of CCD photometric data led to finding lightcurve parameters for three asteroids: 1229 Tilia, P = 7.035 ± 0.001 hr, A = 0.30 mag; 3677 Magnusson: P = 9.47 ± 0.01 hr, A = 0.68 mag; and 4262 DeVorkin: P = 7.067 ± 0.001 hr, A = 0.47mag.

Our observations of the three asteroids reported here were obtained with two Celestron 0.35-m telescopes equipped with SBIG STL1001E CCD camera systems at the Etscorn Campus Observatory. (Klinglesmith and Franco, 2016). The images were processed and calibrated using *MPO Canopus* 10.7.2.0 (Warner, 2017). Exposures were between 300 and 420 seconds through clear filters depending on the brightness of the asteroids. The multi-night data sets for each asteroid were combined with the FALC algorithm (Harris et al., 1989) within *MPO Canopus* to provide synodic periods for each asteroid. Discovery information was obtained from the JPL Small Bodies Node (JPL, 2017). Table I contains the observation circumstances and results.

1229 Tilia is a main-belt asteroid discovered by K. Reinmuth at Heidelberg on 1931 Oct 9. It is also known as 1931 TP1. We observed it on seven nights between 2018 Sep 9-18. We obtained a synodic period of 7.035 ± 0.001 hr. The amplitude is 0.30 ± 0.05 mag. The little bump at about phase 0.5 appears to be real. We find no previous record of a period for this object.

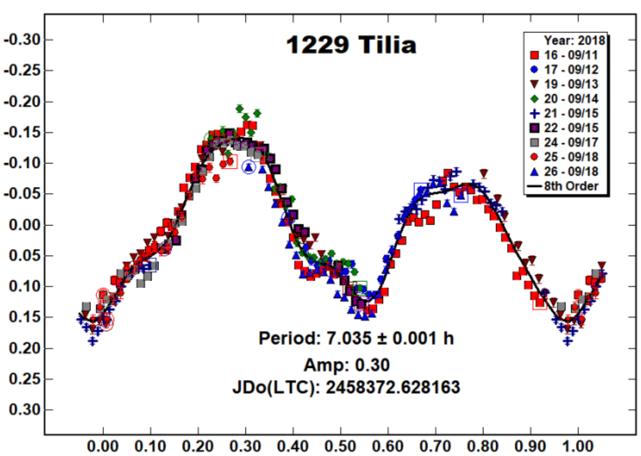

3677 Magnusson is a main-belt asteroid discovered by E. Bowell at Flagstaff, Anderson Mesa Station on 1984 Aug 31. It is also known as 1984 QJ1. We observed it on five nights between 2018 Aug 8 and Sep 11. We obtained a synodic period 9.47 ± 0.01 hr. The amplitude is 0.68 ± 0.10 mag. It could use more complete coverage. We find no previous record of a period for this object.

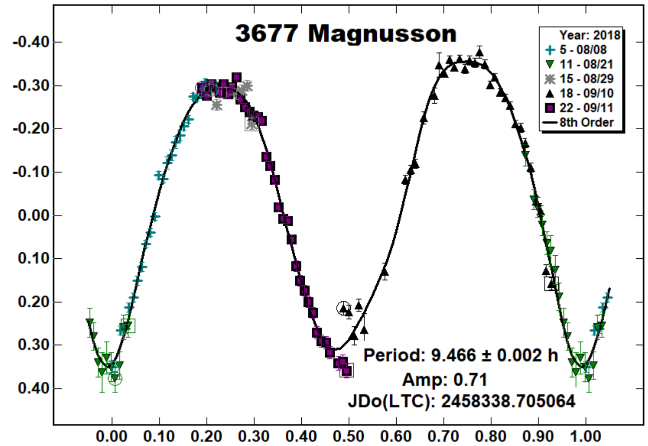

4262 DeVorkin is a main-belt asteroid discovered by M. Arai and H. Mori at Yorii on 1989 Feb 5. It is also known as 1989 CO. We observed in on eight nights between 2018 Aug 1-26. We obtained a synodic period of 7.067 ± 0.001 hr. The amplitude is 0.47 ± 0.1 mag. We find no previous record of a period for this object.

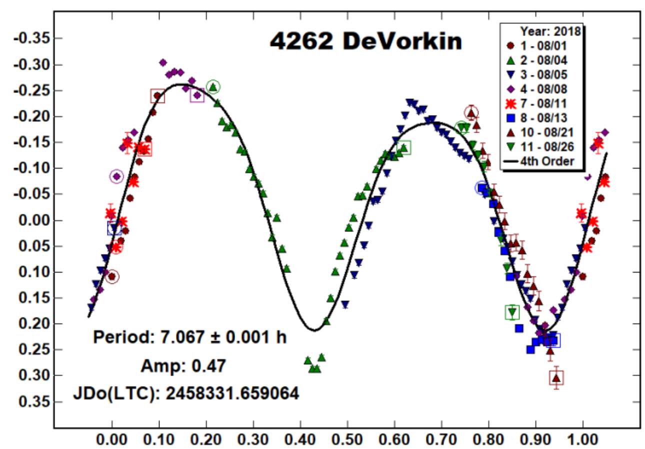

Acknowledgements

The Etscorn Campus Observatory operations are supported by the Research and Economic Development Office of New Mexico Institute of Mining and Engineering.

Number	Name	2018 mm/dd	Pts	Phase	L_{PAB}	B_{PAB}	Period(h)	P.E.	Amp	A.E.	Grp
1229	Tilia	09/11-09/18	322	1.2,4.2	345	0	7.035	0.001	0.30	0.05	THM
3677	Magnusson	08/08-09/11	116	5.0,18.9	320	6	9.47	0.01	0.68	0.10	FLOR
4262	DeVorkin	08/01-08/26	162	13.6,25.2	293	1	9.067	0.001	0.47	0.10	FLOR

Table I. Observing circumstances and results. Pts is the number of data points. The phase angle is given for the first and last date. L_{PAB} and B_{PAB} are the approximate phase angle bisector longitude and latitude at mid-date range (see Harris *et al.*, 1984). Grp is the asteroid family/group (Warner *et al.*, 2009). THM: Themis; FLOR: Flora.

References

Harris, A.W., Young, J.W., Scaltriti, F., Zappala, V. (1984). "Lightcurves and phase relations of the asteroids 82 Alkmene and 444 Gyptis." *Icarus* **57**, 251-258.

Harris, A.W., Young, J.W., Bowell, E., Martin, L.J., Millis, R.L., Poutanen, M., Scaltriti, F., Zappala, V., Schober, H.J., Debehogne, H., Zeigler, K.W. (1989). "Photoelectric Observations of Asteroids 3, 24, 60, 261, and 863." *Icarus* **77**, 171-186.

JPL (2017). Small-Body Database Browser. *http://ssd.jpl.nasa.gov/sbdb.cgi#top*

Klinglesmith III, D.A., Franco, L. (2016). "Lightcurves for 1531Hartmut and 4145 Maximova." *Minor Planet Bull.* **43**, 121.

Warner, B.D., Harris, A.W., Pravec, P. (2009). "The Asteroid Lightcurve Database." *Icarus* **202**, 134-146. Updated 2018 June. *http://www.minorplanet.info/lightcurvedatabase.html*

Warner. B.D. (2017). MPO Canopus software. *http://bdwpublishing.com*

PHOTOMETRIC STUDY OF ASTEROID 4730 XINGMINGZHOU FROM GAOYAZI AND XINGMING OBSERVATORIES

Hanjie Tan
Department of Physics
National Central University
No.300 Zhongda Rd., Taoyuan, TAIWAN
h.tan1996@hotmail.com

Xing Gao
Xinjiang Astronomical Observatory
150 Science 1-StreetUrumqi, Xinjiang, CHINA PR

Received (2018 October 15)

Lightcurve and filter photometry of main-belt asteroid 4730 Xingmingzhou were made at Gaoyazi and Xingming Observatories in 2018 October. We find the asteroid has a synodic rotation period of 3.396 ± 0.001 hr and amplitude of 0.15 ± 0.02 mag. We also found color indices of B-V = 0.783 ± 0.068, V-R = 0.367 ± 0.074, and R-I = 0.722 ± 0.054 mag. According to these color indices, 4730 Xingmingzhou can be classified as a C-type asteroid.

CCD photometric observations were made of main-belt asteroid 4730 Xingmingzhou in 2018 October. At Gaoyazi Observatory we used a 50-cm *f*/4 reflector and QHY11 CCD camera. The image scale was 0.9 arcsec/pixel; exposures were unfiltered and 90 seconds. Filtered photometric observations were made using the Ningbo Bureau of Education and Xinjiang Observatory Telescope (NEXT). The instrument was a 60-cm *f*/8.0 Ritchey-Chretien and LI PL230 CCD camera; this gave a pixel scale of 0.64 arcsec/pixel. Observations were made in Johnson-Cousins BVR_CI_C filters. Each image was taken with 90 seconds exposure. All images were calibrated using standard procedures, including flat-correction and dark and bias frames using *Maxim DL*.

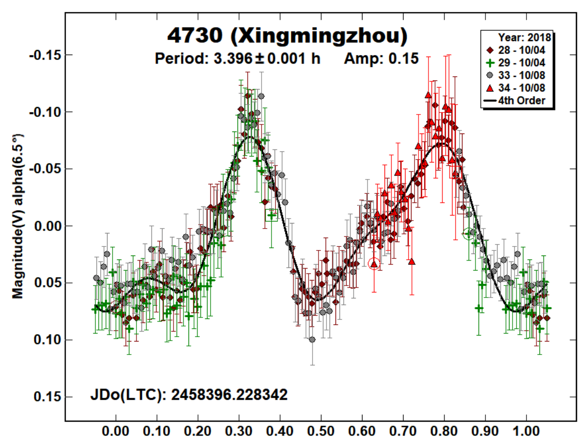

Fig.1. Lightcurve for asteroid 4730 Xingmingzhou fit to a period of 3.396 ± 0.001 hr; the peak-to-peak amplitude is 0.15 ± 0.02 mag.

Number	Name	2018/ mm/dd	Pts	Phase	L_{PAB}	B_{PAB}	Period(h)	P.E.	Amp	A.E.	Grp
4730	Xingmingzhou	10/04-10/08	288	6.4,5.5	23	-13	3.0396	0.001	0.16	0.02	MB-O

Table III. Observing circumstances and results. Pts is the number of data points. The phase angle is given for the first and last date. L_{PAB} and B_{PAB} are the approximate phase angle bisector longitude and latitude at mid-date range (see Harris *et al.*, 1984). Grp is the asteroid family/group (Warner et al., 2009): MB-O: Main-belt Outer

We observed the asteroid for nearly 9 hours under good conditions on 2018 Oct 4 and 8. The relative photometry and Fourier period analysis were obtained using *MPO Canopus*. Analysis of our observations with a total of 285 data points provides a good fit to a lightcurve with $P = 3.396 \pm 0.001$ h and $A = 0.15$ mag (Fig. 1). Prior to our work, the only previous rotational period result for 4730 Xingmingzhou was by Waszczak et al. (2015; 3.396 hr) with an uncertainty degree U = 2. Our results confirm those from Waszczak et al. (2015).

Four images each in B, V, R_C and I_C filters were obtained alternately in ten minutes on 2018 Oct 6 and 7. For example, on these two nights, we observed the asteroid in the following order: BVRI-BVRI.

We used the AAVSO Photometric All-Sky Survey (APASS) catalog (Henden, 2016) as the photometric reference stars catalog to reduce data to B and V band directly. The APASS catalog does not have R_C or I_C magnitudes. For these two filters, we used the equations derived by Lupton (2005) to transform Sloan r´ and i´ magnitudes to R_C and I_C. Aperture and differential photometry of five field stars and asteroid were used to find the asteroid's magnitude.

Date(UT)	B	ΔB	V	ΔV	R	ΔR	I	ΔI
Oct.2018								
6.715	16.803	0.04	16.022	0.04	15.658	0.01	15.315	0.01
7.702	16.831	0.03	16.045	0.02	15.670	0.05	15.310	0.02

Table I. A summary of the apparent brightness of 4730 Xingmingzhou on 2018 Oct 6 and 7.

These measurements allowed us to calculate the color indices from the mean of values (Table. II). The results from the two nights were consistent with one another.

Mean color Indices of 4730 Xingmingzhou	
B-V	0.783±0.068
V-R	0.367±0.074
V-I	0.722±0.054

Table II. A summary of the mean color indices of 4730 Xingmingzhou.

The distribution of the color indices of different taxonomic types is shown in Figures 2 and 3. Based on these plots, we suggest that 4730 Xingmingzhou is a type G class asteroid using classification method proposed by Dandy et al. (2003) that used Tholen taxonomy classes (Tholen, 1984).

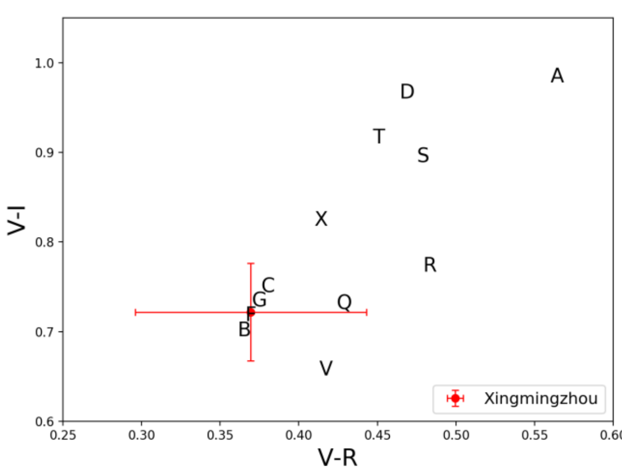

Fig.2. The V-R vs. V-I color-color diagram with 4730 Xingmingzhou and different taxonomic types based on Dandy et al. (2003).

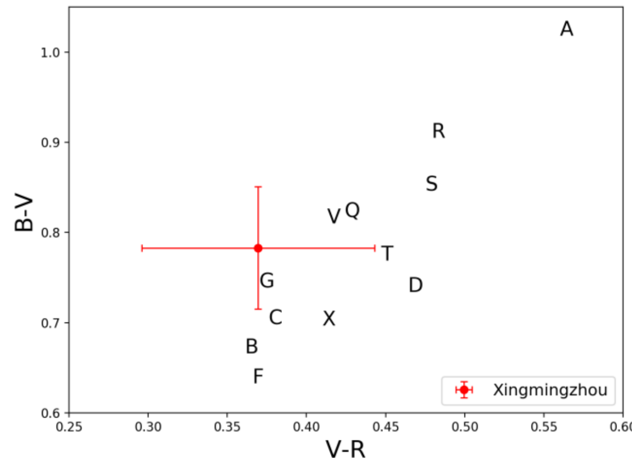

Fig.3. The V-R vs. B-V color-color diagram with 4730 Xingmingzhou and different taxonomic types based on Dandy et al. (2003).

We subtracted the solar color index in each band from the color index for asteroid (Howell, 1995) and then calculated relative reflectance values (Lin et al., 2014). The comparisons of the resulting relative reflectance spectra of against spectra of Bus-DeMeo (DeMeo et al., 2009; DeMeo et al., 2013) classes Cgh, Cg, Q, V, and C classes are shown in Fig. 4. These show a best fit for the asteroid to the Cgh class.

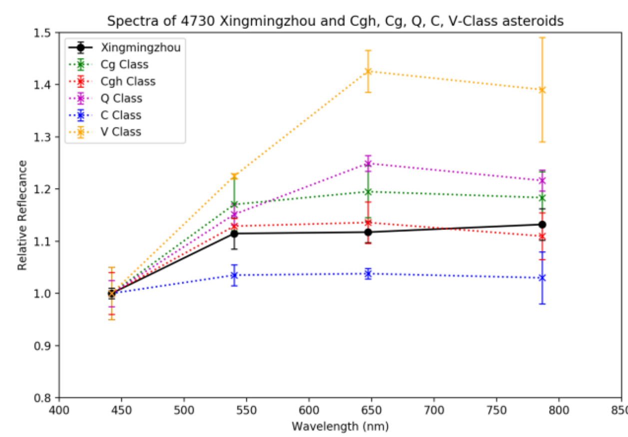

Fig.4. The relative reflectance spectrum of 4730 Xingmingzhou determined using BVRI observations in comparison with spectra of five Bus-DeMeo clases.

In some cases, Cgh-type and G-type were classified as C-type or C-subtypes (Binzel et al., 2004; Lin et al., 2018; Stuart et al., 2004; Ye, 2011) because their spectra are very similar. For this asteroid, our result showed the B-V color is slightly redder than a normal C-type asteroid but closer to G-type and the asteroid's spectrum shows little differences from a typical C-type.

The only classification before our work was from Pan-STARRS observations that suggested a C-class asteroid (Vereš, 2015) based on *H* and *G* parameters (absolute magnitude and phase slope parameter). It's hard to distinguish among Cgh, G, and C-type using only BVRI photometry and so, in this work, a conservative assignment of type C in the Tholen classification scheme is given (Dandy et al., 2003; Tholen, 1984). This puts our result in agreement with that from Vereš (2015).

Acknowledgements

We would like to give special thanks to Dr.Chan-Kao Chang and Prof. Wing-Huen Ip at the Graduate Institute of Astronomy, National Central University, for their invaluable assistance that greatly helped this study.

Asteroid 4730 Xingmingzhou was named after the Chinese amateur astronomer Xing-Ming Zhou (1965-2004). He was an exceptional comet hunter, logging around 1500 hours in night sky comet hunting in almost 20 years. He discovered 63 SOHO comets and one SWAN comet: C/2004 H6 (SWAN). He was ranked fourth in the world among SOHO hunters before he left us. In 2000, Xingming was the first and only Chinese SOHO discoverer; there are now 24. He inspired a generation of hundreds of amateurs in China that are now searching for comets, asteroids, and supernova using the data from the Xingming Observatory, which is named in his honor. We would like to offer our highest respect and admiration to him and his family in this paper.

References

Binzel, R.P., Rivkin, A.S., Stuart, J.S., Harris, A.W., Bus, S.J., Burbine, T.H. (2004). "Observed spectral properties of near-Earth objects: results for population distribution, source regions, and space weathering processes." *Icarus* **170**, 259-294.

Dandy, C.L., Fitzsimmons, A., Collander-Brown, S.J. (2003). "Optical colors of 56 near-Earth objects: trends with size and orbit." *Icarus* **163**, 363-373.

DeMeo, F.E., Binzel, R.P., Slivan, S.M., Bus, S.J. (2009). "An extension of the Bus asteroid taxonomy into the near-infrared." *Icarus* **202**, 160-180.

DeMeo, F.E., Carry, B. (2013). "The taxonomic distribution of asteroids from multi-filter all-sky photometric surveys." *Icarus* **226**, 723-741.

Harris, A.W., Young, J.W., Scaltriti, F., Zappala, V. (1984). "Lightcurves and phase relations of the asteroids 82 Alkmene and 444 Gyptis." *Icarus* **57**, 251-258.

Howell, E.S. (1995). "Probing Asteroid Composition Using Visible and Near-Infrared Spectroscopy." Ph. D. Thesis, The University of Arizona.

Lin, C.H., Ip, W.H., Lin, Z.Y., Yoshida, F., Cheng, Y.C. (2014). "Detection of large color variation in the potentially hazardous asteroid (297274) 1996 SK." *Research in Astron. Astrophys.* **14**, 311.

Lin, C.H., Ip, W.H., Lin, Z.Y., Cheng, Y.C., Lin, H.W., Chang, C.K. (2018). "Photometric survey and taxonomic identifications of 92 near-Earth asteroids." *Plan. Space Sci.* **152**, 116-135.

Lupton,R. (2005) *http://classic.sdss.org/dr4/algorithms/sdssUBVRITransform.html*

Stuart, J.S., Binzel, R.P. (2004). "Bias-corrected population, size distribution, and impact hazard for the near-Earth objects." *Icarus* **170**, 295-311.

Tholen, D.J. (1984). "Asteroid taxonomy from cluster analysis of Photometry." Doctoral Thesis. Univ. Arizona, Tucson.

Vereš, P., Jedicke, R., Fitzsimmons, A., Denneau, L., Granvik, M., Bolin, B., Chastel, S., Wainscoat, R.J., Burgett, W.S., Chambers, K.C., Flewelling, H., Kaiser, N., Magnier, E.A., Morgan, J.S., Price, P.A., Tonry, J.L., Waters, C. (2015). "Absolute magnitudes and slope parameters for 250,000 asteroids observed by Pan-STARRS PS1 - Preliminary results." *Icarus* **241**, 34-47.

Warner, B.D., Harris, A.W., Pravec, P. (2009). "The Asteroid Lightcurve Database." *Icarus* **202**, 134-146. Updated 2018 Nov. *http://www.minorplanet.info/lightcurvedatabase.html*

Waszczak, A., Chang, C.-K., Ofek, E.O., Laher, R., Masci, F., Levitan, D., Surace, J., Cheng, Y.-C., Ip, W.-H., Kinoshita, D., Helou, G., Prince, T.A., Kulkarni, S. (2015). "Asteroid Light Curves from the Palomar Transient Factory Survey: Rotation Periods and Phase Functions from Sparse Photometry." *Astron. J.* **150**, A75.

Ye, Q.Z. (2010). "BVRI photometry of 53 unusual asteroids." *AJ* **141**, 32.

LIGHTCURVES FOR 131 VALA, 374 BURGUNDIA, 734 BENDA AND 929 ALGUNDE

Lorenzo Franco
Balzaretto Observatory (A81), Rome, ITALY
lor_franco@libero.it

Alessandro Marchini
Astronomical Observatory, DSFTA - University of Siena (K54)
Via Roma 56, 53100 - Siena, ITALY

Giorgio Baj
M57 Observatory (K38), Saltrio, ITALY

Giulio Scarfi
Iota Scorpii Observatory (K78), La Spezia, ITALY

Paolo Bacci, Martina Maestripieri
San Marcello Pistoiese (104), Pistoia, ITALY

Roberto Bacci
G. Pascoli Observatory (K63), Castelvecchio Pascoli, ITALY

Riccardo Papini, Fabio Salvaggio, Massimo Banfi
Wild Boar Remote Observatory (K49)
Spedaletto, Florence, ITALY

(Received: 2018 October15)

Photometric observations of four main-belt asteroids were made in order to acquire lightcurves for shape/spin axis models. The synodic period and lightcurve amplitude were found for: 131 Vala: 5.1796 ± 0.0003 hr, 0.14 mag; 374 Burgundia: 6.9637 ± 0.0005 hr, 0.07 mag.; 734 Benda: 7.105 ± 0.001 hr, 0.25 mag; and 929 Algunde: 3.3104 ± 0.0003 hr, 0.11 mag.

Collaborative observations of asteroids were made inside the UAI (Italian Amateur Astronomers Union) group. The targets were listed in the Shape/Spin Modeling Opportunities section from the most recent issues of the *Minor Planet Bulletin*. The CCD observations were made in 2018 August-October using the instrumentation described in the Table I. Lightcurve analysis was done at the Balzaretto Observatory with *MPO Canopus* (Warner, 2016). All the images were calibrated with dark and flat frames and converted to R magnitudes using solar colored field stars from CMC15 catalogue distributed with *MPO Canopus*. Table II shows the observing circumstances and results.

131 Vala is an X-type inner main-belt asteroid discovered on 1873 May 24 by C.H.F. Peters at Clinton. Observations were made over four nights. We found a synodic period of P = 5.1796 ± 0.0003 hr and amplitude A = 0.14 ± 0.02 mag. The period is close to the previously published results in the asteroid lightcurve database (LCDB; Warner et al., 2009).

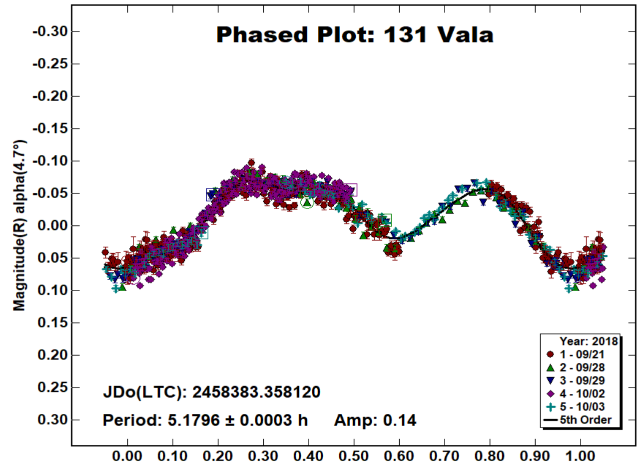

374 Burgundia is an S-type middle main-belt asteroid, discovered on 1893 September 18 by A. Charlois at Nice. Observations were made over seven nights. The period spectrum shows two stronger solutions near 6.9 and 13.8 hours with, respectively, a monomodal and bimodal lightcurve. The split-halves plot let us solve the ambiguity by showing that the two halves of the 13.8-hr solution were very symmetrical. This made the monomodal solution possible, but still not certain. Assuming a monomodal lightcurve, we found a synodic period of P = 6.9637 ± 0.0005 hr and amplitude A = 0.07 ± 0.01 mag. This period is close to that determined by Worman et al. (2004). The small amplitude and the monomodal solution could indicate a near polar aspect.

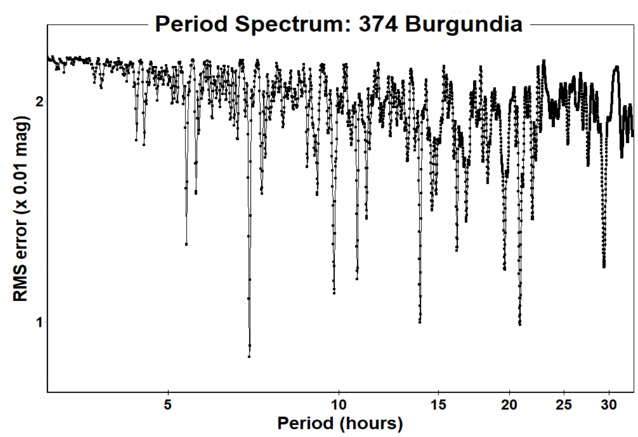

Observatory (MPC code)	Telescope	CCD	Filter	Observed Asteroids
Università Siena (K54)	0.30-m MCT f/5.6	SBIG STL-6303e (bin 2x2)	Rc	131, 374, 734, 929
M57 (K38)	0.30-m RCT f/5.5	SBIG STT-1603	C	131, 374
Iota Scorpii(K78)	0.40-m RCT f/8	SBIG STXL-6303e (bin 2x2)	Rc	374
GAMP(104)	0.60-m NRT f/4	Apogee Alta	C	131
G.Pascoli (K63)	0.40-m NRT f/3.2	QHY22 C 1318	C	131
WBRO (K49)	0.235-m SCT f/10	SBIG ST8-XME	C	734

Table I. Observing Instrumentations. MCT: Maksutov-Cassegrain, NRT: Newtonian Reflector, RCT: Ritchey-Chretien, SCT: Schmidt-Cassegrain.

Number	Name	2018 mm/dd	Pts	Phase	L_{PAB}	B_{PAB}	Period(h)	P.E	Amp	A.E.
131	Vala	09/21-10/03	722	4.7,3.3	6	-6	5.1796	0.0003	0.14	0.02
374	Burgundia	09/15-10/08	678	3.5,9.0	354	8	6.9637	0.0005	0.07	0.01
734	Benda	09/09-09/30	157	6.3,1.7	3	0	7.105	0.001	0.25	0.04
929	Algunde	08/15-08/30	223	3.5,8.8	323	6	3.3104	0.0003	0.11	0.04

Table II. Observing circumstances and results. Pts is the number of data points. The phase angle values are for the first and last date. L_{PAB} and B_{PAB} are the approximate phase angle bisector longitude and latitude at mid-date range (see Harris *et al.*, 1984).

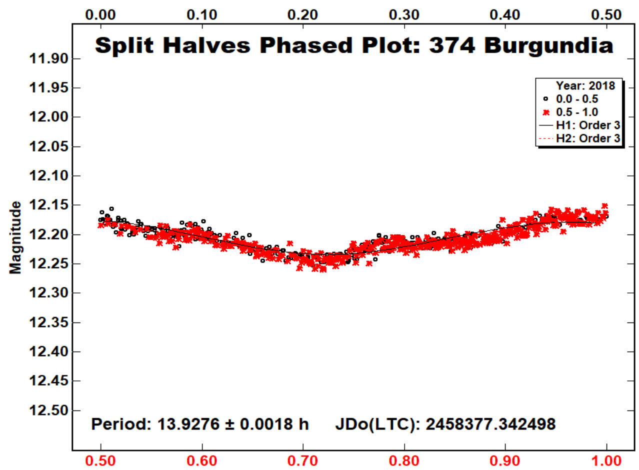

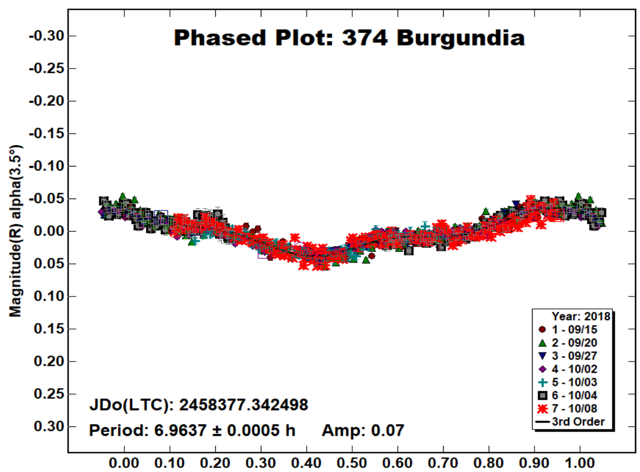

[734 Benda](#) is a C-type outer main-belt asteroid discovered on 1912 October 11 by J. Palisa Vienna. Observations were made over three nights.

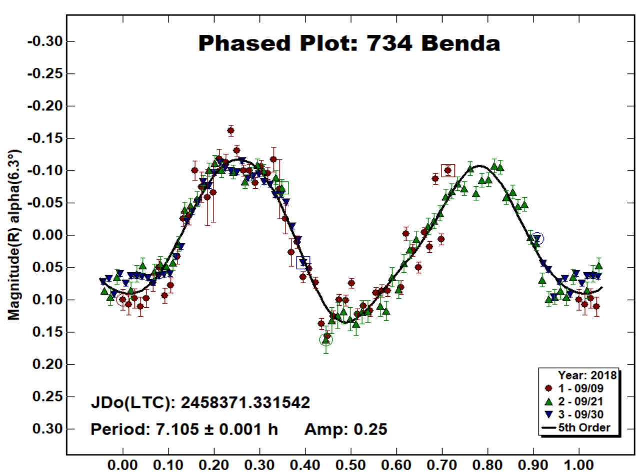

We found a synodic period of $P = 7.105 \pm 0.001$ hr and amplitude $A = 0.25 \pm 0.04$ mag. The period is consistent with previously published results in the LCDB (Warner et al., 2009).

929 Algunde is an S-type inner main-belt asteroid discovered on 1920 March 10 by K. Reinmuth at Heidelberg. Observations were made over five nights. We found a synodic period of $P = 3.3104 \pm 0.0003$ hr and amplitude $A = 0.11 \pm 0.04$ mag. The period is consistent with other results in the LCDB (Warner et al., 2009).

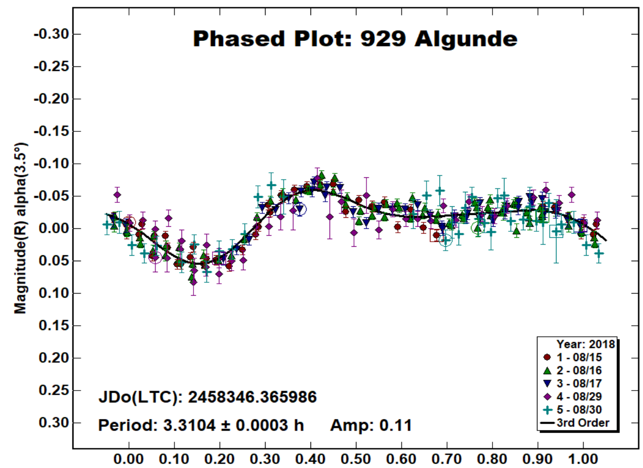

References

DSFTA (2018), Dipartimento di Scienze Fisiche, della Terra e dell'Ambiente – Astronomical Observatory. *https://www.dsfta.unisi.it/en/research/labs-eng/astronomical-observatory*

Harris, A.W., Young, J.W., Scaltriti, F., Zappala, V. (1984). "Lightcurves and phase relations of the asteroids 82 Alkmene and 444 Gyptis." *Icarus* **57**, 251-258.

Warner, B.D., Harris, A.W., Pravec, P. (2009). "The asteroid lightcurve database." *Icarus* **202**, 134-146. Updated 2018 August. *http://www.minorplanet.info/lightcurvedatabase.html*

Warner, B.D. (2016). MPO Software, *MPO Canopus* v10.7.7.0. Bdw Publishing. *http://minorplanetobserver.com*

Worman, W.E., Fieber, S., Hulet, K. (2004). "Photometry of 374 Burgundia." *Minor Planet Bull.* **31**, 66-67.

LIGHTCURVES AND ROTATION PERIODS FOR TEN ASTEROIDS

Vladimir Benishek
Belgrade Astronomical Observatory
Volgina 7, 11060 Belgrade 38, SERBIA
vlaben@yahoo.com

(Received: 2018 October 15)

CCD photometric observations of ten asteroids were conducted from 2018 April through September. A review of the results obtained for synodic rotation periods as well as the lightcurves established is presented here.

Photometric observations of ten asteroids were conducted at Sopot Astronomical Observatory (SAO) between 2018 April-September in order to determine the asteroids' synodic rotation periods. For this purpose, two 0.35-m *f*/6.3 Meade LX200GPS Schmidt-Cassegrain telescopes were employed. The telescopes are equipped with a SBIG ST-8 XME and a SBIG ST-10 XME CCD cameras. The exposures were unfiltered and unguided for all targets. Both cameras were operated in 2x2 binning mode, which produces image scales of 1.66 arcsec/pixel and 1.25 arcsec/pixel for ST-8 XME and ST-10 XME cameras, respectively. Prior to measurements, all images were corrected using dark and flat field frames.

Photometric reduction, lightcurve construction, and period analysis were conducted using *MPO Canopus* (Warner, 2018a). Differential photometry with up to five comparison stars of near solar color (0.5 ≤ B-V ≤ 0.9) was performed using the Comparison Star Selector (CSS) utility. This helped ensure a satisfactory quality level of night-to-night zero point calibrations and correlation of the measurements within the standard magnitude framework. Field comparison stars were calibrated using standard Cousins R magnitudes derived from the Carlsberg Meridian Catalog 15 (VizieR, 2018) Sloan r' magnitudes using the formula: R = r' - 0.22 in all cases presented in this paper. In some instances, small zero point adjustments were necessary in order to achieve the best match between individual data sets in terms of minimum RMS residual of a Fourier fit.

Some of the targets presented in this paper were observed within the Photometric Survey for Asynchronous Binary Asteroids (BinAstPhot Survey) under the leadership of Dr Petr Pravec from Ondřejov Observatory, Czech Republic.

Table I gives the observing circumstances and results.

Observations and results

<u>2119 Schwall</u>. No records on previous rotation period determinations have been found in the asteroid lightcurve database (LCDB; Warner et al., 2009). As a BinAstPhot Survey target it was observed at SAO in August 2018 over 4 nights. An unambiguous bimodal solution for period of P = 3.9394 ± 0.0004 h was found. An independent period analysis conducted upon SAO data by Pravec finds a value for period of 3.9393 ± 0.0004 h (Pravec, 2018).

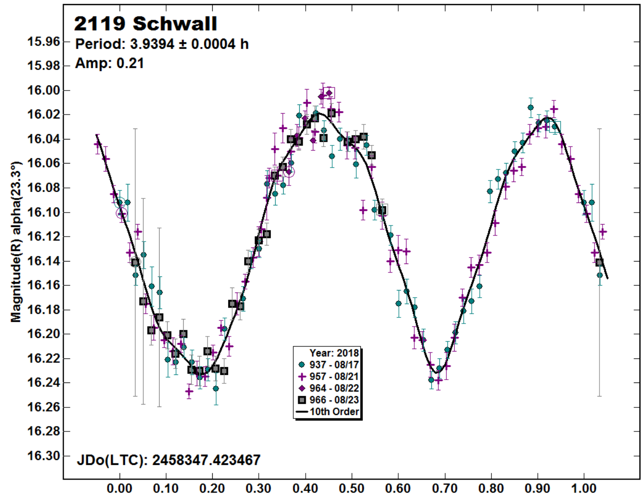

<u>3146 Dato</u>. This was a BinAstPhot Survey program target during its apparition in 2014. The only previous period determination is from the observations carried out in that campaign that found a value of 5.0540 ± 0.0002 h (Pravec, 2014). The SAO observations conducted during the 2018 apparition within the framework of the same Survey showed a good consistency with the previous result. Period analysis yielded an unambiguous bimodal solution of 5.0528 ± 0.0007 h.

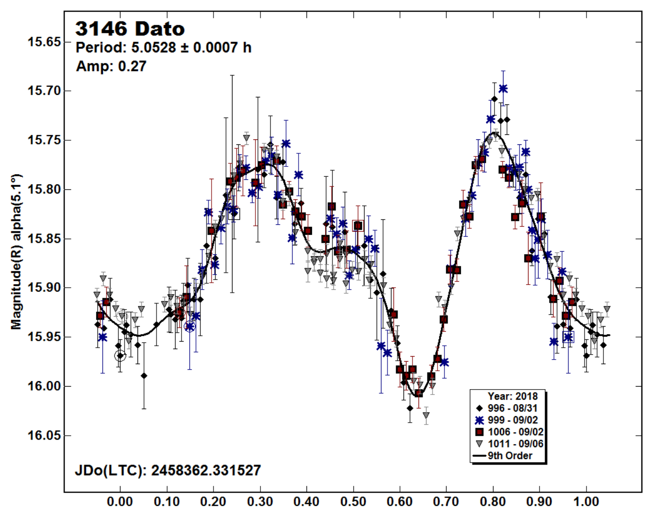

<u>3287 Olmstead</u>. Prior to this work only one period determination was known. Wisniewski et al. (1997) found a period of 4.80 ± 0.05 h, marked as fully reliable in the LCDB with an uncertainty flag of U=3. The SAO observations in late 2018 August led to a bimodal lightcurve with a moderately large amplitude of 0.34 mag. and phased to a period of 4.954 ± 0.003 h. This is fairly consistent with the result published on the Center for Solar System Studies website by Warner (2018; 4.963 h) obtained from his 2018 June observations of this asteroid.

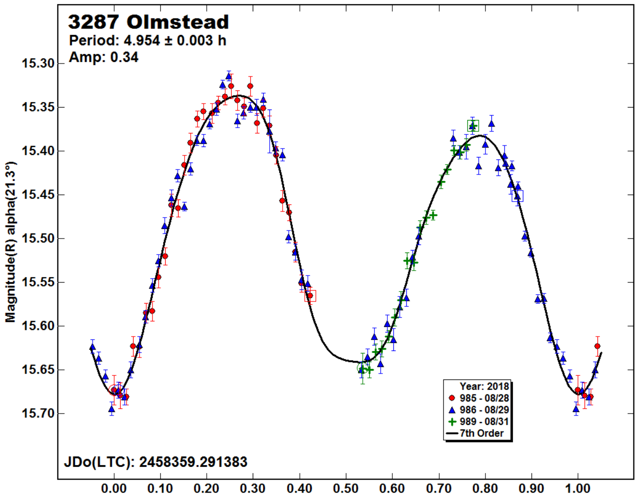

3552 Don Quixote. This is an exceptionally interesting near-Earth asteroid known for the large eccentricity of its orbit (e = 0.7089), a quite large size (~ 19 km; third largest known NEA) and certain cometary activity discovered in 2013. Binzel et al. (1987) suggest that its rotation period might be as short as 3 hours. Weidenschilling et al. (1990) state a value of 7.7 hours (U=2 in the LCDB) derived from their 1983 October photometric observations. In order to check plausibility of the latter result the photometric observations were conducted over 4 nights in 2018 August at SAO, which yielded in a high-amplitude (0.51 mag.) bimodal lightcurve and a period result quite different from that reported previously. The newly-established value for synodic rotaion period from the SAO observations is: P = 6.662 ± 0.001 h.

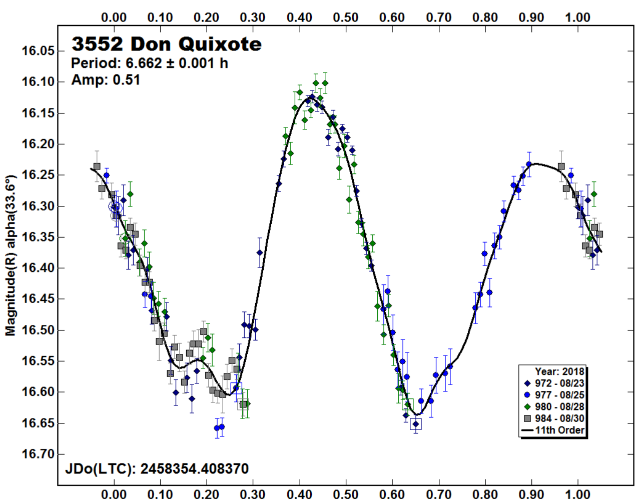

(14510) 1996 ES2. Another target followed up in the framework of the BinAstPhot Survey in 2018 September during 3 nights. A search for previously determined rotation periods has given no results. The SAO photometric observations resulted in a fairly large amplitude (0.37 mag.) bimodal lightcurve with a period of 6.2442 ± 0.0004 h. Period analysis by Pravec encompassing both SAO and Sugarloaf Observatory data sets founds very slightly different value for period: 6.2443 ± 0.0003 h (Pravec, 2018).

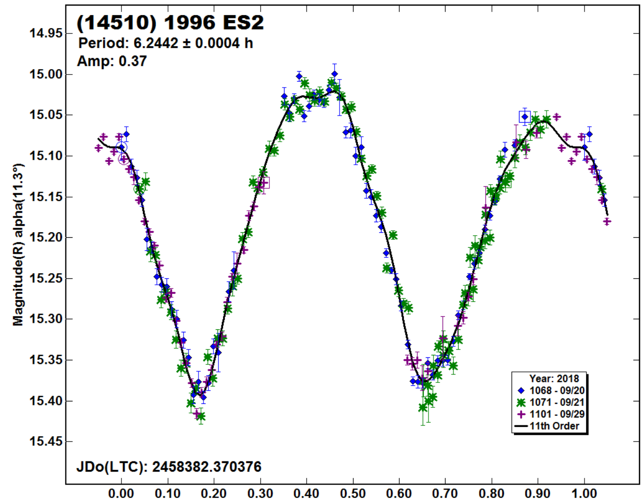

(15633) 2000 JZ1. Period analysis conducted on the photometric observations carried out over 2 nights in late April and early May of 2018 suggest a result of 3.941 ± 0.001 h as the plausible one for a synodic rotation period of this Phocaea family asteroid. Any records on previous period determinations for this asteroid have not been found.

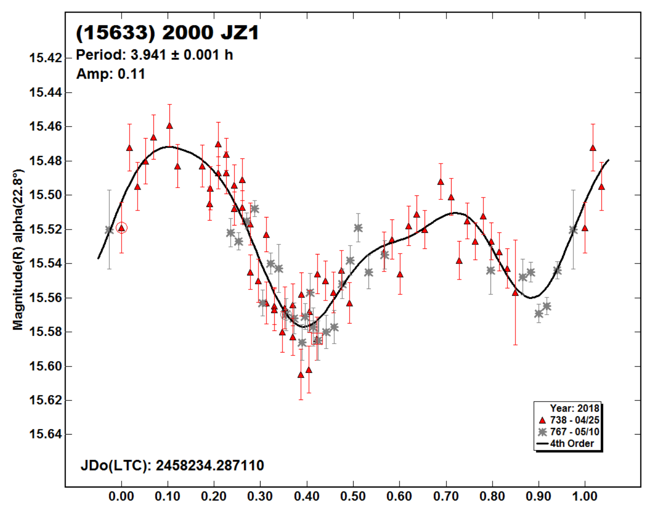

Number	Name	2018/mm/dd	Pts	Phase	L_{PAB}	B_{PAB}	Period (h)	P.E.	Amp	A.E.	Grp
2119	Schwall	08/16-08/23	149	23.3,21.2	6	5	3.9394	0.0004	0.21	0.02	FLOR
3146	Dato	08/31-09/07	220	5.1,2.4	346	4	5.0528	0.0007	0.27	0.02	MB-I
3287	Olmstead	08/28-08/31	112	21.3,22.1	317	19	4.954	0.003	0.34	0.01	MC
3552	Don Quixote	08/23-08/30	136	33.6,32.1	37	21	6.662	0.001	0.51	0.02	NEA
14510	1996 ES2	09/20-09/30	209	11.4,6.2	13	4	6.2442	0.0004	0.37	0.01	BAP
15633	2000 JZ1	04/25-05/10	83	22.8,23.5	212	32	3.941	0.001	0.11	0.03	PHO
27135	1998 XB12	08/23-08/30	165	23.4,23.0	343	34	4.482	0.002	0.14	0.03	PHO
51258	2000 JU59	09/16-09/18	96	8.1,7.6	6	7	3.391	0.003	0.15	0.02	MB-I
76978	2001 BY60	07/10-07/16	194	32.0,31.4	278	34	6.889	0.005	0.05	0.02	MC
82298	2001 KL40	08/05-08/16	75	13.8,12.7,12.8	320	17	4.3822	0.0003	0.39	0.01	MB-M

Table I. Observing circumstances and results. Pts is the number of data points. Phase is the solar phase angle given at the start and end of the date range, the middle value is the minimum solar phase angle. L_{PAB} and B_{PAB} are the average phase angle bisector longitude and latitude. Grp is the asteroid family/group (Warner *et al.*, 2009): BAP = Baptistina, FLOR = Flora, MB-I/M = main-belt inner/middle, MC = Mars - crosser, NEA = near-Earth asteroid, PHO = Phocaea.

(27135) 1998 XB12. Another Phocaea family asteroid with previously unknown rotation period. The 2018 August SAO data yielded 4.482 ± 0.002 h rotation period value.

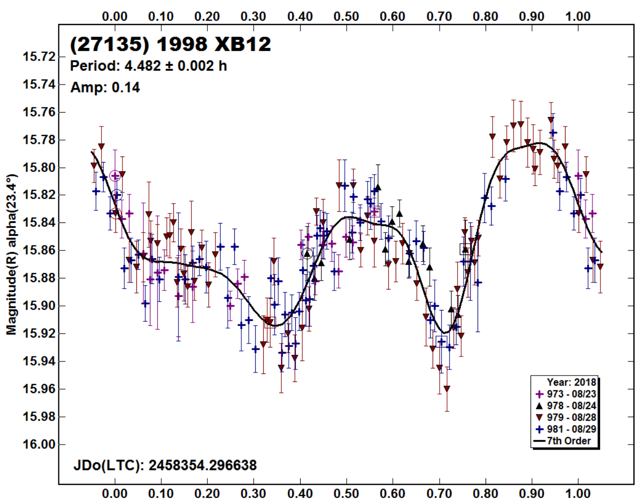

(51258) 2000 JU59. Period analysis on the data gathered in 2018 September over 2 nights indicates a period of 3.391 ± 0.003 h as the most favorable value for this inner main-belt asteroid with previously unknown period according to the LCDB.

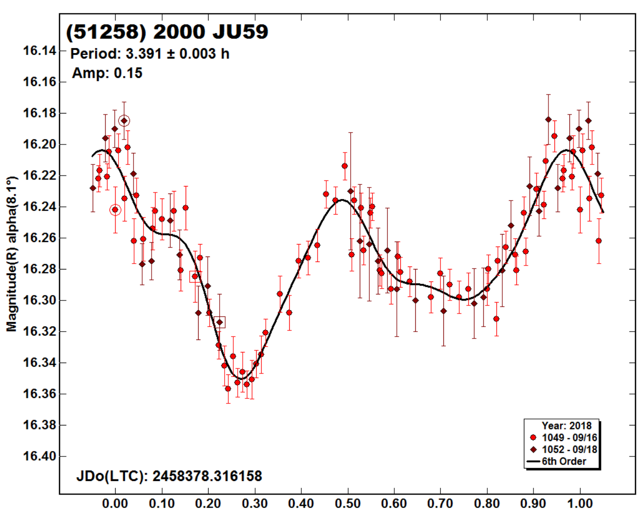

(76978) 2001 BY60. The lightcurve of this Mars-crosser as obtained from the SAO photometric data shows considerable "flatness" (0.05 mag. amplitude) with a very few discernible features in 2018 apparition. Considering a small lightcurve amplitude and somewhat higher range of phase angles at which the observations were made, a unique solution for period can hardly be singled out in the period spectrum. Noneheless, a value that stands out for its lowest RMS error is adopted as a likely period solution (P = 6.889 ± 0.005 h). It should be noted that this value differs very little from the period solution for this asteroid found by Warner, published on the Center for Solar System Studies website (2018; 6.897 ± 0.005 h) found from Warner's 2018 May observations.

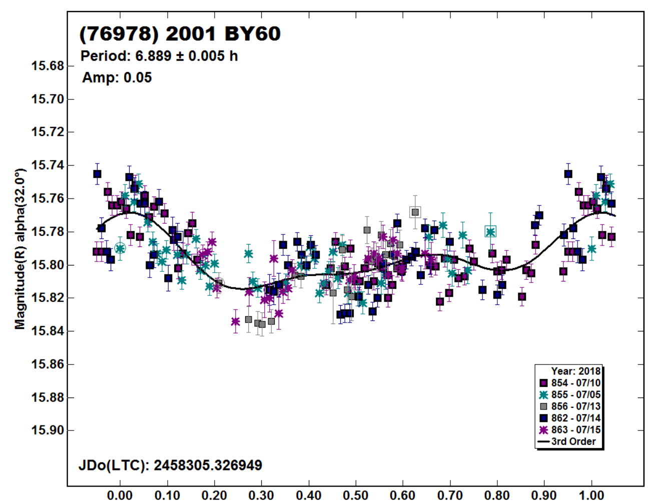

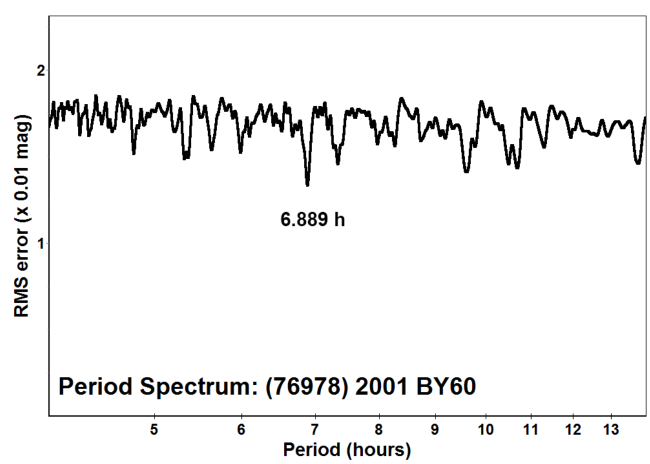

(82298) 2001 KL40. Prior to this work there were no rotation period determinations on this main-belt asteroid. The photometric observations were carried out at SAO in 2018 August on 4 nights. Period analysis resulted in a bimodal lightcurve with an amplitude of 0.39 mag. and a period of 4.3822 ± 0.0003 h.

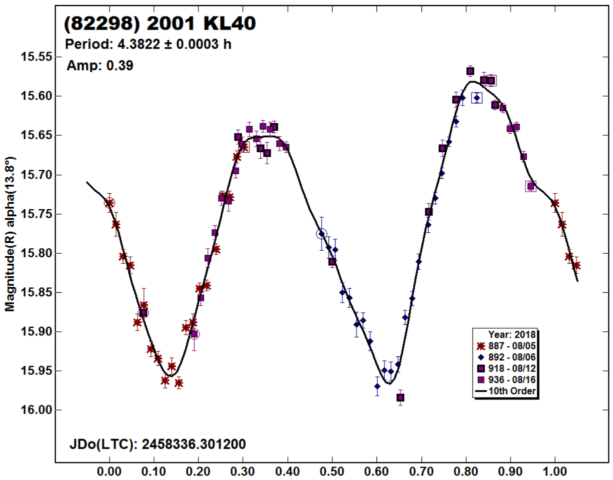

Acknowledgements

Observational work at Sopot Astronomical Observatory is supported by a 2018 Gene Shoemaker NEO Grant from The Planetary Society.

References

Binzel, R. P. (1987). "A photoelectric survey of 130 asteroids." *Icarus* **72**, 135-208.

Pravec, P. (2014, 2018). Photometric Survey for Asynchronous Binary Asteroids web site. *http://www.asu.cas.cz/~ppravec/newres.txt*

VizieR (2018). *http://vizier.u-strasbg.fr/viz-bin/VizieR*.

Warner, B.D., Harris, A.W., Pravec, P. (2009). "The Asteroid Lightcurve Database." *Icarus* **202**, 134-146. Updated 2018 June. *http://www.minorplanet.info/lightcurvedatabase.html*

Warner, B.D. (2018a). MPO Canopus software, version 10.7.11.3. *http://www.bdwpublishing.com*

Warner, B.D. (2018b). Center for Solar System Studies web site. CS3 Lightcurves Page. *http://www.planetarysciences.org/PHP/CS3_Lightcurves.php*

Weidenschilling, S.J., Chapman, C.R., Davis, D.R., Greenberg, R., Levy, D.H., Binzel, R.P., Vail, S.M., Magee, M., Spaute, D. (1990). "Photometric Geodesy of Main-Belt Asteroids." *Icarus* **86**, 402-447.

Wisniewski, W.Z., Michalowski, T.M., Harris, A.W., McMillan, R.S. (1997). "Photometric Observations of 125 Asteroids." *Icarus* **126**, 395-449.

ROTATION PERIOD DETERMINATION FOR 5351 DIDEROT AND 7230 LUTZ

Alessandro Marchini
Astronomical Observatory, DSFTA - University of Siena (K54)
Via Roma 56, 53100 - Siena, ITALY
alessandro.marchini@unisi.it

Riccardo Papini, Massimo Banfi, Fabio Salvaggio
Wild Boar Remote Observatory (K49)
San Casciano in Val di Pesa (FI), ITALY

(Received: 2018 October 15)

Photometric observations of two main-belt asteroids were conducted from the Astronomical Observatory of the University of Siena (Italy) in order to determine their synodic rotation periods. For 5351 Diderot we found a period of 9.984 ± 0.003 hr with an amplitude of 0.45 ± 0.01 mag; for 7230 Lutz we found a period of 5.682 ± 0.007 hr with an amplitude of 0.18 ± 0.02 mag.

CCD photometric observations of two main-belt asteroids were carried out in 2018 April and October at the Astronomical Observatory of the University of Siena (K54) at the Department of Physical Sciences, Earth and Environment (DSFTA, 2018). We used a 0.30-m *f*/5.6 Maksutov-Cassegrain telescope, a SBIG STL-6303E CCD camera, and clear or R filter. The pixel scale was 2.30 arcsec when binned at 2x2 pixels. All exposures were 300 sec. Data processing and analysis were done with *MPO Canopus* (Warner, 2017). All the images were calibrated with dark and flat-field frames and converted to R magnitudes using solar-colored field stars from a version of the CMC-15 catalogue distributed with *MPO Canopus*. Table I shows the observing circumstances and results.

A search through the asteroid lightcurve database (LCDB; Warner et al., 2009) indicates that our results may be the first lightcurve observations and results for these objects, which were chosen from the list of lightcurve photometry opportunities in the *Minor Planet Bulletin* (Warner et al., 2018a; 2018b).

5351 Diderot (1989 SG5) was discovered on 1989 Sep 26 at La Silla by E.W. Elst. It was named in memory of Denis Diderot (1713-1784), a French author of dramas, novels and philosophical essays. It is a main-belt asteroid with a semi-major axis of 2.426 AU, eccentricity 0.144, inclination 5.596 deg, and an orbital period of 3.78 years. Its absolute magnitude is H = 13.2 (JPL, 2018; MPC, 2018). The WISE satellite infrared radiometry survey (Masiero et al., 2011) found a diameter D = 3.66 ± 0.15 km using an absolute magnitude H = 13.0. From these, an optical albedo of p_V = 0.83 ± 0.14 was derived.

Our observations were conducted on four nights from 2018 April 20-24 and led to 217 data points. The period analysis shows a bimodal solution for the rotational period P = 9.984 ± 0.003 hr with an amplitude A = 0.45 ± 0.01 mag.

Number	Name	2018/mm/dd	Pts	Phase	L_{PAB}	B_{PAB}	Period(h)	P.E.	Amp	A.E.
5351	Diderot	04/20-04/25	217	4.8,4.5	214	7	9.984	0.003	0.45	0.01
7230	Lutz	10/03-10/05	157	4.8,3.9	17	-1	5.682	0.007	0.18	0.02

Table I. Observing circumstances and results. Pts is the number of data points. The phase angle is given for the first and last date. L_{PAB} and B_{PAB} are the approximate phase angle bisector longitude and latitude at mid-date range (see Harris *et al.*, 1984).

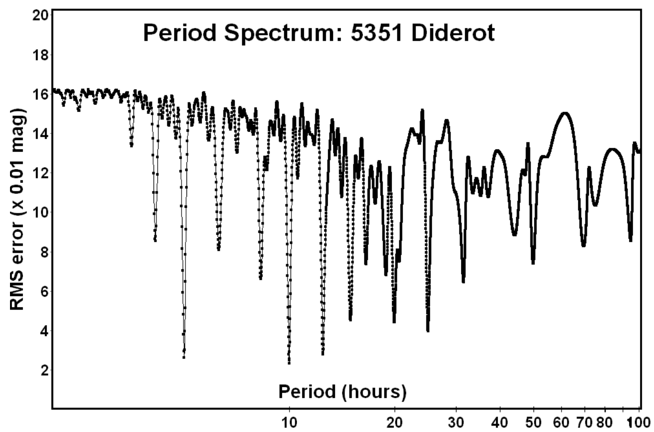

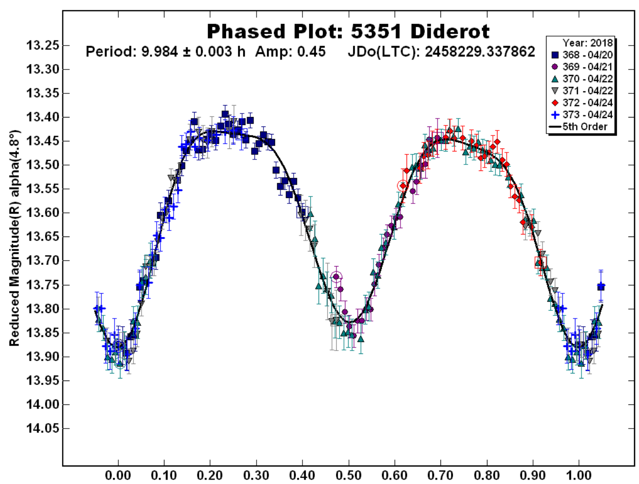

7230 Lutz (1985 RZ1) was discovered on 1985 Sep 12 by E. Bowell at the Anderson Mesa Station of the Lowell Observatory. It is named after Barry L. Lutz (b. 1944), professor of physics and astronomy and department chair at Northern Arizona University. It is a main-belt asteroid with the semi-major axis of 2.373 AU, eccentricity 0.241, inclination 3.14 deg, and an orbital period of 3.66 years. Its absolute magnitude is H = 13.8 (JPL, 2018; MPC, 2018).

Observations of this asteroid were conducted on two nights, 2018 Oct 3 and 4, and provided 157 data points. The period analysis shows a bimodal solution for the rotational period P = 5.682 ± 0.007 hr with an amplitude A = 0.18 ± 0.02 mag.

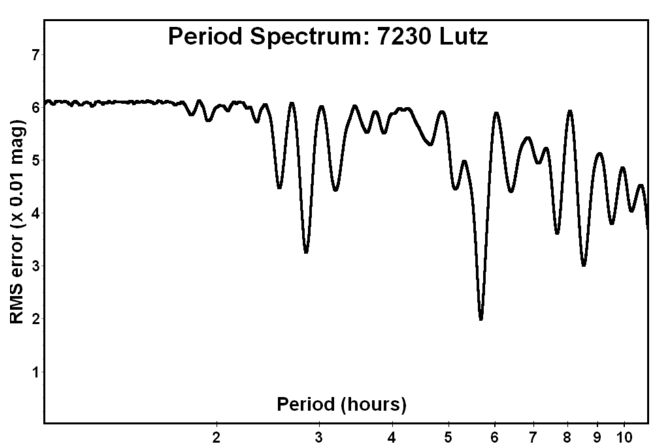

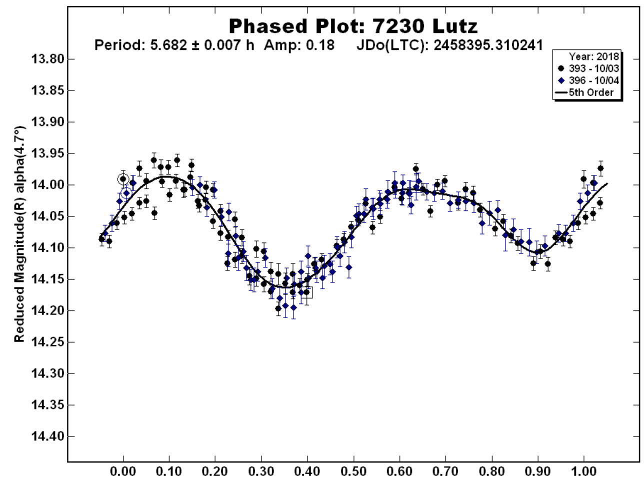

References

DSFTA (2018), Dipartimento di Scienze Fisiche, della Terra e dell'Ambiente – Astronomical Observatory. *https://www.dsfta.unisi.it/en/research/labs-eng/astronomical-observatory*

Harris, A.W., Young, J.W., Scaltriti, F., Zappala, V. (1984). "Lightcurves and phase relations of the asteroids 82 Alkmene and 444 Gyptis." *Icarus* **57**, 251-258.

JPL (2018). Small-Body Database Browser. *http://ssd.jpl.nasa.gov/sbdb.cgi#top*

Masiero, J.R., Mainzer, A.K., Grav, T., Bauer, J.M., Cutri, R.M., Dailey, J., Eisenhardt, P.R.M., McMillan, R.S., Spahr, T.B., Skrutskie, M.F., Tholen, D., Walker, R.G., Wright, E.L., DeBaun, E., Elsbury, D., Gautier, T., IV, Gomillion, S., Wilkins, A. (2011). "Main Belt Asteroids with WISE/NEOWISE. I. Preliminary Albedos and Diameters." *Astrophys. J.* **741**, A68.

MPC (2018). MPC Database. *http://www.minorplanetcenter.net/db_search/*

Warner, B.D., Harris, A.W., Pravec, P. (2009). "The Asteroid Lightcurve Database." *Icarus* **202**, 134-146. Updated 2018 June. *http://www.minorplanet.info/lightcurvedatabase.html*

Warner, B.D., Harris, A.W., Ďurech, J., Benner, L.A.M. (2018a). "Lightcurve photometry opportunities: 2018 April-June." *Minor Planet Bull.* **45**, 208-213.

Warner, B.D., Harris, A.W., Ďurech, J., Benner, L.A.M. (2018b). "Lightcurve photometry opportunities: 2018 October-December." *Minor Planet Bull.* **45**, 404-408.

Warner, B.D. (2017). MPO Software, MPO Canopus v10.7.7.0. Bdw Publishing. *http://minorplanetobserver.com*

LIGHTCURVE ANALYSIS OF 6 ASTEROIDS FROM RMS OBSERVATORY

Basil Rowe
RMS Observatory (W25)
Cincinnati, OH USA
basilrowe@gmail.com

(Received: 2018 October 15)

CCD images of 6 asteroids were taken from 2018 January 18 to 2018 June 18 for the purpose of determining their synodic rotation periods. The asteroids were: 1513 Matra, 2661 Bydzovsky, 4181 Kivi, 11830 Jessenius, 12237 Coughlin, and (42701) 1998 MD13.

CCD photometric observations of 6 asteroids were made from the RMS Observatory (W25) from 2018 January 18 to 2018 June 18. Observations were taken with a 0.35-m SCT operating at f/7.6 using an Atik One 6.0 CCD (unfiltered) binned at 3x3 with an image scale of 1.05 arcseconds per pixel. Exposure times varied from 30s to 300s.

The images were calibrated (bias, dark, and flat) with *AstroImageJ* (Collins and Kielkopf, 2013). Differential photometry measurements were made in *MPO Canopus* (Warner, 2017) using the FALC routine (Harris *et al.*, 1989) to derive the asteroid synodic periods. The StarBGone utility in *MPO Canopus* was applied to measure images when asteroids where located in the vicinity of stars. The *MPO Canopus* Comp Star Selector utility was employed to select comparison stars of near solar-color for differential photometry for all asteroids. R band magnitudes were taken from the CMC-15 catalog (Munos, 2017) and were chosen to best match the unfiltered CCD measurements.

Table I lists the observing circumstances and the analysis results.

1513 Matra Pervious work indicated an approximate period of 24 h and amplitude of 0.1 mag (Binzel, 1983), however the period is given U = 1 in the LCDB (Warner et al., 2009). Analysis indicates two possible bimodal periods: 34.48 h, or 51.92 h. The solution with the lowest RMS is 34.48 h (RMS = 0.049), however the 51.90 h period has only a sleightly larger RMS = 0.053.

A split halves plot of both options shows different halves, so the 34.48 h period is proposed based on the lower RMS.

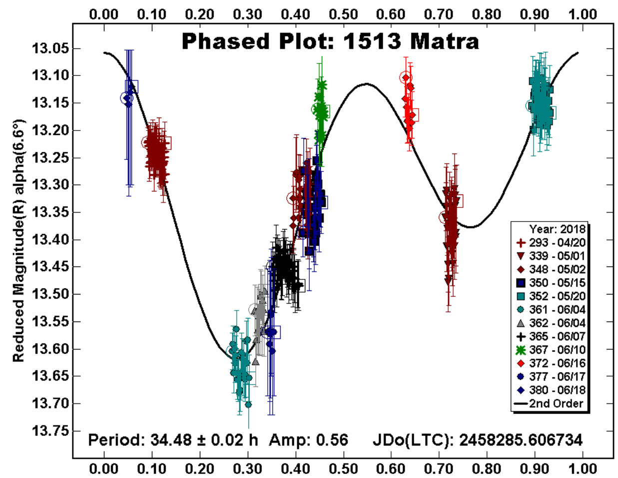

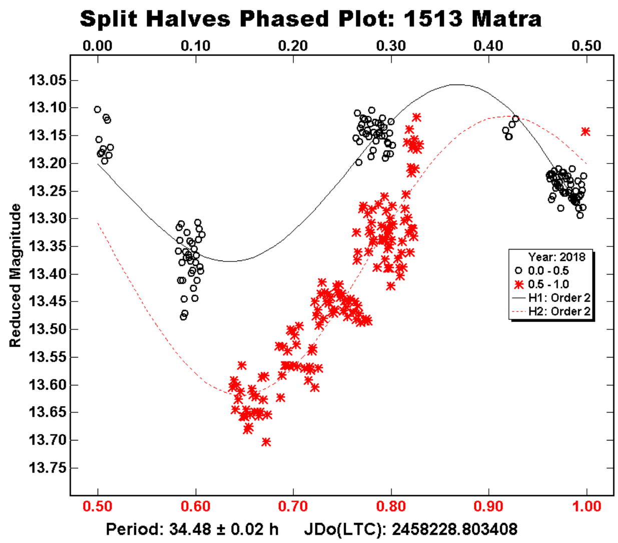

2661 Bydzovsky A search of the LCDB (Warner et al., 2009) did not find any previously reported period. Analysis indicated a bimodal 48.32 h period, however the period spectrum also showed a monomodal period of about 24 h. The 48.32 h period was the only bimodal period that fit the data and has a lower RMS than the 24 period (0.028 vs 0.031). It should be noted both periods are very close to multiples of the Earth's rotation period which could be influencing the Fourier analysis.

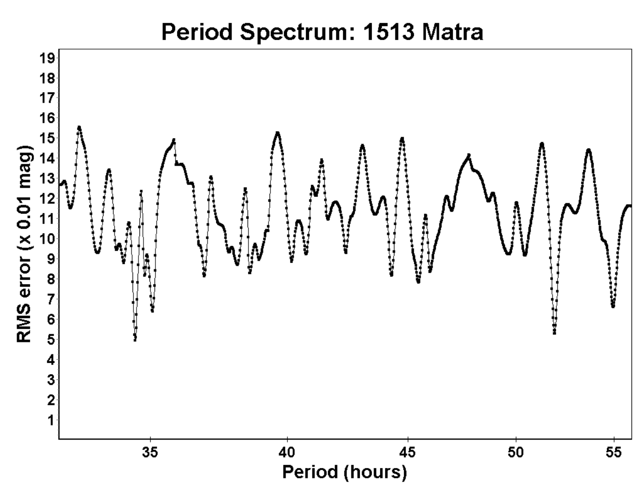

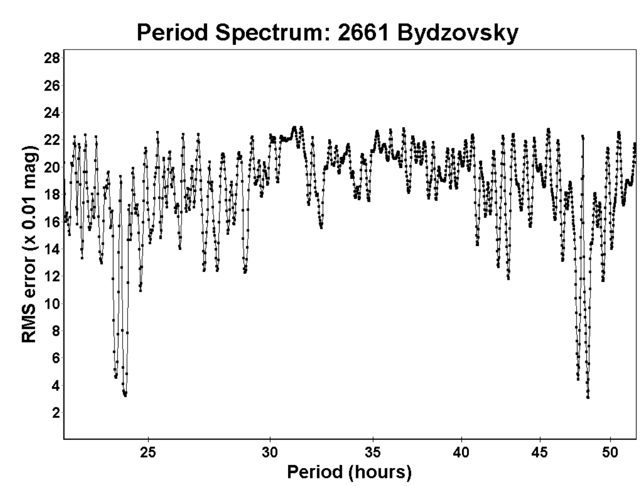

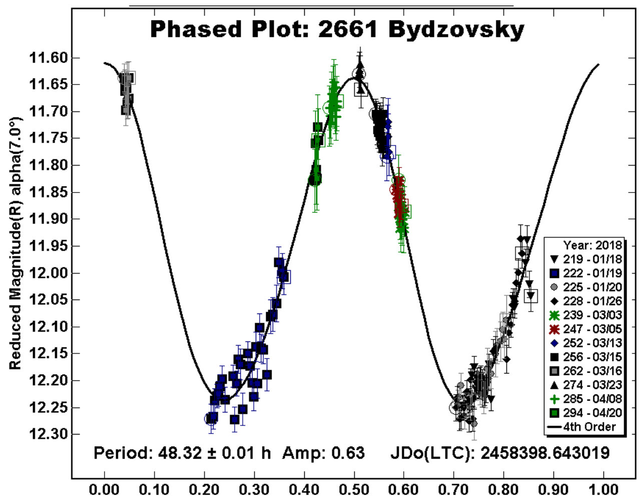

4181 Kivi A search of the LCDB (Warner et al., 2009) did not find any previously reported period. A second order analysis favors a bimodal period of 178.0 h, however higher order solutions (3, 4) sleightly favor a period around 89 h with a monomodal curve. A split halves plot of the 178.0 h plot shows nearly identical halves, therefore the 89 h period is proposed.

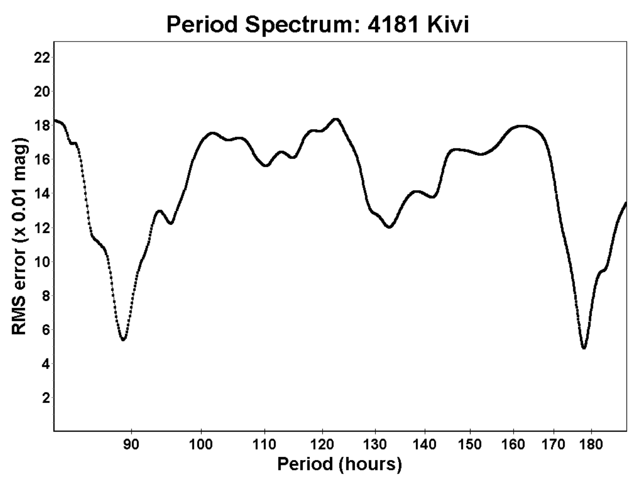

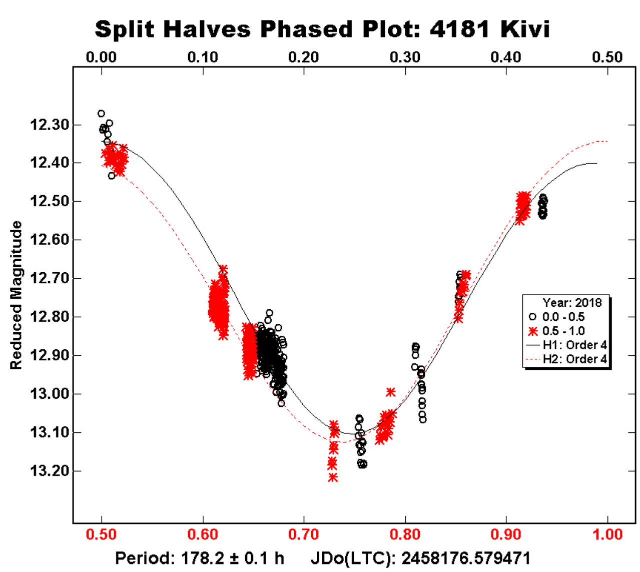

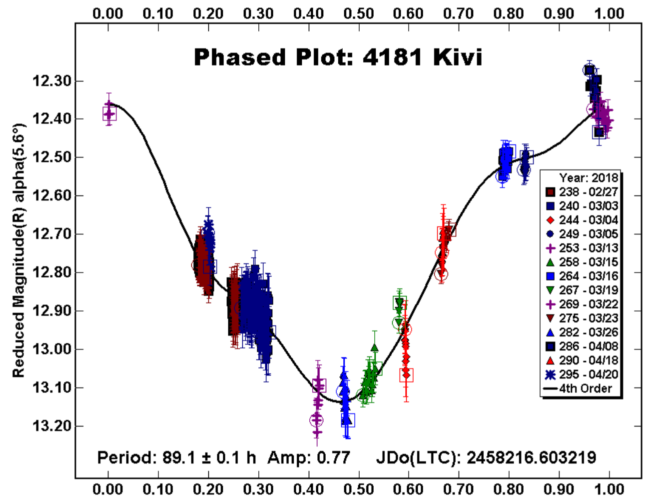

11830 Jessenius A search of the LCDB (Warner et al., 2009) did not find any previously reported period. Observations over approximately one month did not show any obvious rotation period. The best bimodal fit to the data is a period of 46.8 h.

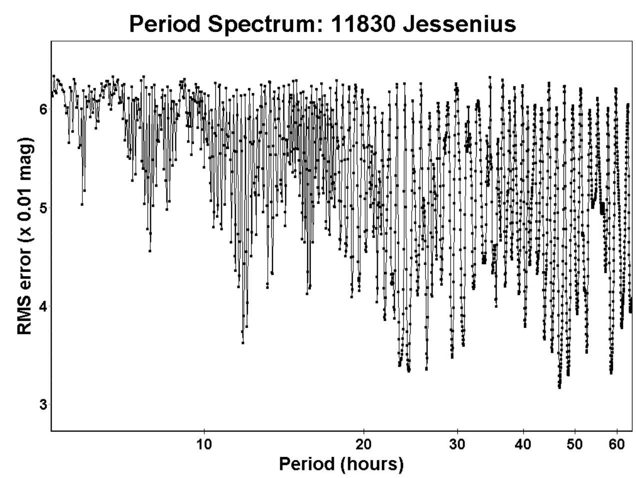

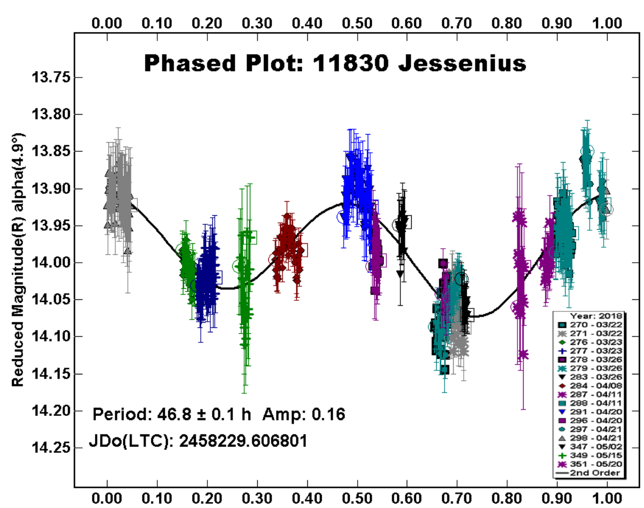

Number	Name	2018 mm/dd	Pts	Phase	L_{PAB}	B_{PAB}	Period(h)	P.E.	Amp	A.E.	Grp
1513	Matra	4/20-6/18	278	6.5,27.2	206	6	34.48	0.02	0.56	0.05	FLOR
2661	Bydzovsky	1/18-4/20	183	7.0,20.2	103,116	7,3	48.32	0.01	0.63	0.03	EOS
4181	Kivi	2/27-4/20	526	5.5,23.6	151	2	89.1	0.1	0.77	0.04	EUN
11830	Jessenius	3/22-4/21	505	5.1,13.5	188	3	46.8	0.1	0.16	0.03	MB
12237	Coughlin	3/4-4/21	302	11.8,30.5	154	-3	80.4	0.1	1.62	0.04	PHO
(42701)	1998 MD13	5/20-6/7	633	8.4,12.8	239	12	2.603	0.001	0.09	0.02	MB

Table I. Observing circumstances and results. Pts is the number of data points. The phase angle is given for the first and last date. L_{PAB} and B_{PAB} are the approximate phase angle bisector longitude and latitude at mid-date range (see Harris *et al.* 1984). Grp is the asteroid family/group. The definitions and values are those used in the LCDB (Warner *et al.* 2009).

12237 Coughlin A search of the LCDB (Warner et al., 2009) did not find any previously reported period. Initial second order analysis indicated a well defined monomodal period of about 40 h. However, a fourth order fit indicated a 80.4 h period of large amplitude. This incomplete lightcurve is the proposed period which fit the data fairly well.

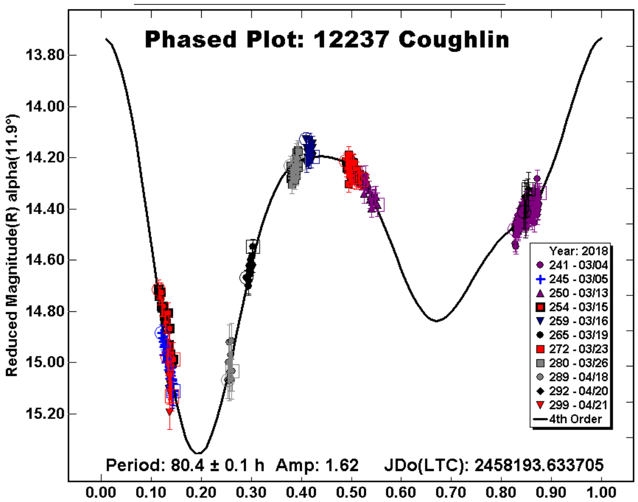

(42701) 1998 MD13 A search of the LCDB (Warner et al., 2009) did not find any previously reported period. Analysis showed a well defined bimodal period of 2.603 h with a low amplitude of 0.09 magnitudes.

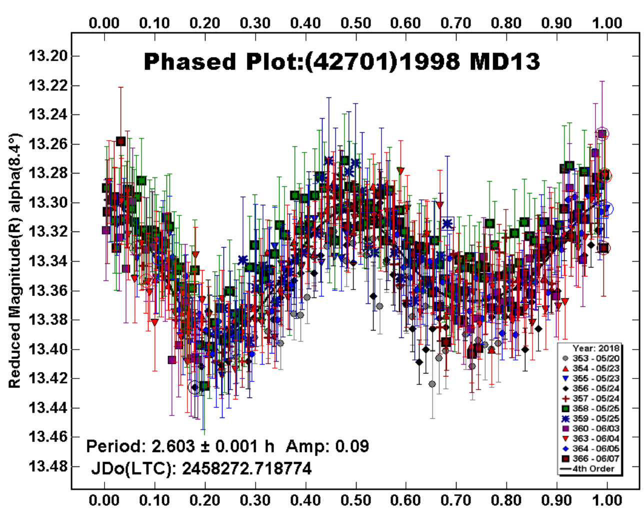

References

Binzel, R.P., Mulholland, J.D. (1983). "A photoelectric lightcurve survey of small main belt asteroids." *Icarus* **56**, 519-533.

Collins, K., Kielkopf, J. (2013). *AstroImageJ: ImageJ for astronomy.* Astrophysics Source Code Library. *http://www.astro.louisville.edu/software/astroimagej/*

Harris, A.W., Young, J.W., Scaltriti, F., Zappala, V. (1984). "Lightcurves and phase relations of the asteroids 82 Alkmene and 444 Gyptis." *Icarus* **57**, 251-258.

Harris, A.W., Young, J.W., Bowell, E., Martin, L.J., Millis, R.L., Poutanen, M., Scaltriti, F., Zappala, V., Schober, H.J., Debehogne, H., Zeigler, K.W. (1989). "Photoelectric Observations of Asteroids 3, 24, 60, 261, and 863." *Icarus* **77**, 171-186.

Munos, J.L. (2017). Carlsberg Meridian Catalog web site. *http://svo2.cab.inta-csic.es/vocats/cmc15/*

Warner, B.D., Harris, A.W., Pravec, P. (2009). "The Asteroid Lightcurve Database." *Icarus* **202**, 134-146. Updated 2017 Nov 9. *http://www.minorplanet.info/lightcurvedatabase.html*

Warner, B.D. (2017). *MPO Canopus*, v.10.7.11.1. BDW Publishing, *http://www.bdwpublishing.com/*

LIGHTCURVE AND REVISED ROTATION PERIOD FOR 1277 DOLORES

Rui M. D. Gonçalves
Linhaceira Observatory (938)
Instituto Politécnico de Tomar
2300-313 Tomar, Portugal
rui.goncalves@ipt.pt

(Received: 2018 October 15)

Photometric observations of 1277 Dolores were performed over six nights from 2018 September 15-30. The rotation period was found to be 12.676 ± 0.001 hr with amplitude of 0.43 ± 0.03 mag. The period differs from the period reported by (Stephens, 2001; 17.19 hr).

1277 Dolores is a main-belt asteroid discovered by G.N. Neujmin on 1933 April 18. Photometric observations were performed at Linhaceira Observatory from 2018 September-15 using a Meade 0.25-m LX-200 Classic reduced to *f*/6.73 and cooled Starlight Xpress MX916 CCD camera. The rectangular pixels of 11.2x11.6 µm were binned 2x2, giving 1.8x1.7 arcsec/pixel image scale. The images were unfiltered. Exposure times were 150 s except for the last session, when the exposures were 180 s. Flat field frames were taken at twilight before beginning observations.

All data processing of the calibrated images and subsequent period analysis was performed using *MPO Canopus*. Differential photometry measurements were performed using the StarBGone procedure to overcome stars close stars to minor planet. Many sessions were affected by poor sky conditions.

About 28.5 hours of observations produced 554 data points for analysis. The rotation period was found to be 12.676 ± 0.001 hr with amplitude of 0.43 ± 0.03 mag.

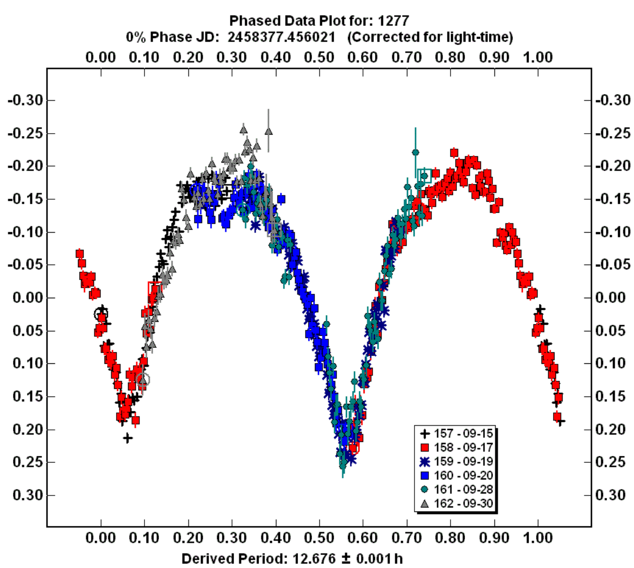

A search of the asteroid lightcurve database (LCDB, Warner et al., 2009) indicated one previously reported lightcurve, which was by Stephens (2001; P = 17.19 hr, A = 0.50 mag). His observations produced 330 data points spread over seven nights from 2000 July 2-11. The new data from 2018 could not be fit to the longer period found by Stephens (2001). Unfortunately, the original raw data points were lost (Stephens, personal communication) and so it was not possible to see if his data fit the shorter period found here.

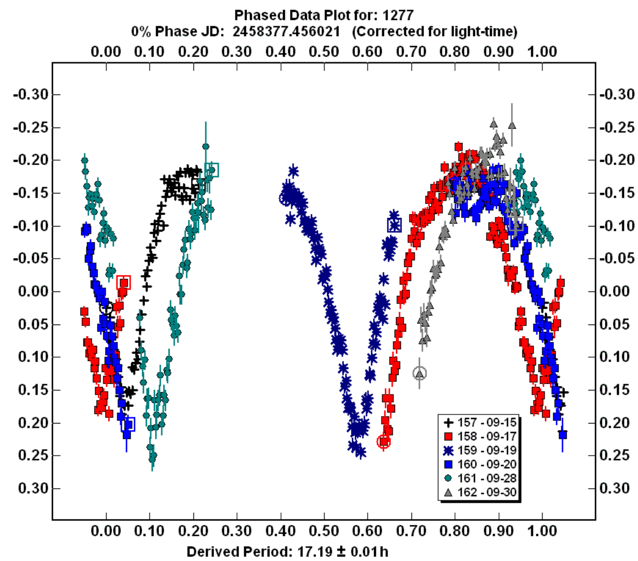

References

Harris, A.W., Young, J.W., Scaltriti, F., Zappala, V. (1984). "Lightcurves and phase relations of the asteroids 82 Alkmene and 444 Gyptis." *Icarus* **57**, 251-258.

Stephens, R.D. (2001). "Rotational Periods and Lightcurves of 1277 Dolores, 666 Desdemona and (7505) 1997 AM2." *Minor Planet Bulletin* **28**, 28-29.

Warner, B.D., Harris, A.W., Pravec, P. (2009). "The Asteroid Lightcurve Database." *Icarus* **202**, 134-146. Updated 2018 Oct. *http://www.minorplanet.info/lightcurvedatabase.html*

Number	Name	2018 mm/dd	Pts	Phase	L_{PAB}	B_{PAB}	Period(h)	P.E.	Amp	A.E.	Grp
1277	Dolores	09/15-09/30	554	5.5,7.3	356	9.0	12.676	0.001	0.43	0.03	MB-M

Table I. Observing circumstances and results. Pts is the number of data points. The phase angle is given for the first and last date. L_{PAB} and B_{PAB} are the approximate phase angle bisector longitude and latitude at mid-date range (see Harris *et al.*, 1984). Grp is the asteroid family/group (Warner *et al.*, 2009). H: Hungaria.

PHOTOMETRY OF NEA (144332) 2004 DV24 AT THE TERSKOL OBSERVATORY

Volodymyr Reshetnyk, Vira Godunova, Inna Izvekova, Andrii Simon, Oleksandr Sergeev
ICAMER Observatory of NASU (MPC B18)
27 Acad Zabolotnoho Str.
Kyiv, 03680 UKRAINE
V_Godunova@bigmir.net

Vitalii Polyakov
Research and Training Center for Applied Informatics of NASU,
Kyiv, UKRAINE

(Received: 2018 Oct 16)

We present analysis of photometric observations obtained in 2018 August at the Terskol Observatory of the potentially hazardous asteroid (144332) 2004 DV24. We found the rotation period to be P = 7.985 ± 0.009 h with a lightcurve amplitude of 1.17 ± 0.05 mag. We also determined two color indices: V-R = 0.20 ± 0.06 and B-V = 0.72 ± 0.21.

Asteroid 2004 DV24 was discovered at Haleakala by NEAT on 2004 February 21. This is an Amor-type asteroid with an absolute magnitude (H) of 16.5, which suggests – depending of albedo – a diameter of 1.1-2.7 km. It has been classified as a "Potentially Hazardous Asteroid" by the Minor Planet Center and passed close to Earth (within 0.0556 AU) on 2018 September 16.

Follow-up photometry of 2004 DV24 was carried out at the Terskol Observatory over six nights on 2018 August 19-24. Observations were obtained using the 60-cm Cassegrain telescope (Zeiss-600) and a SBIG STL-1001 CCD with 1024x1024x24-micron pixels that provides a field of view of 10.9x10.9 arcmin. During the observations, the phase angle ranged from 71.6 to 74.2 degrees and the R magnitude varied from 17.8 to 16.6. BVRI filters were used for the 120 s exposures.

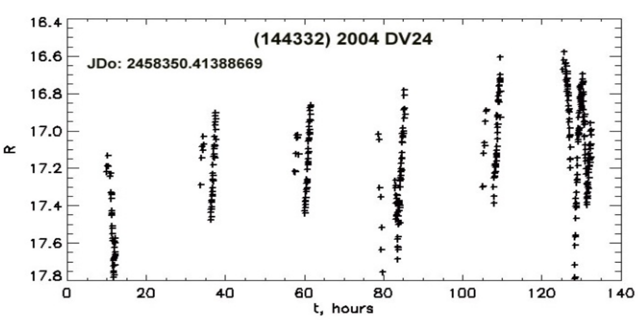

Data processing was performed using *MaxIm DL* and our own software. A total of 424 data points were employed in the analysis. Images were calibrated with bias, flat, and dark frames. Photometric standard stars from the AAVSO catalog were used to reduce data to R band. Observations with Johnson-Cousins B, V, and R allowed us to find mean color indices of V- R = 0.20 ± 0.06 and B-V = 0.72 ± 0.21.

To find the periodicity in the lightcurve, the PDM technique was applied (Stellingwerf, 1978). Furthermore, we checked the result by the aid of the Lomb normalized periodogram method (Lomb, 1976) and the Θ-statistic. All these techniques produced a similar result, namely, a rotational period of 7.985 ± 0.009 h with a lightcurve amplitude of 1.17 ± 0.05 mag.

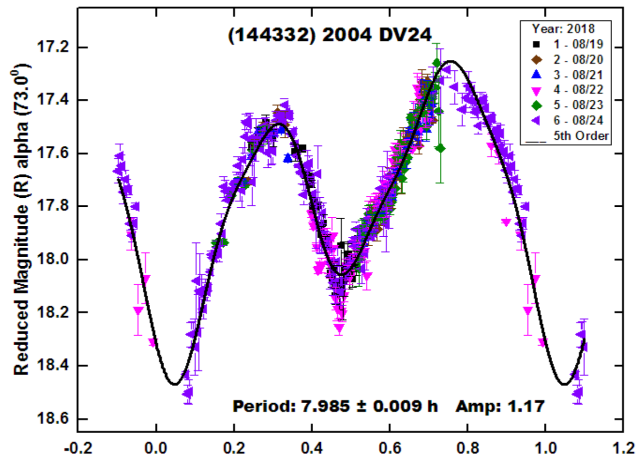

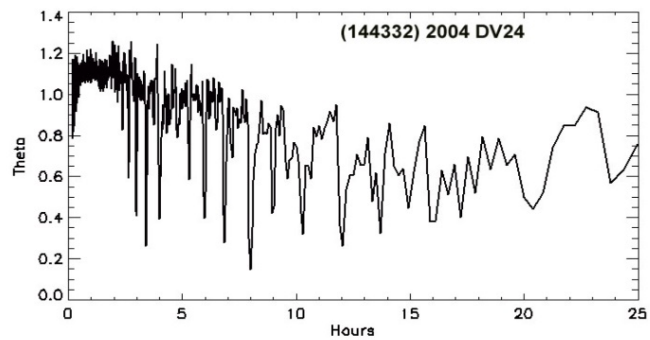

Acknowledgements

This work was supported by the NASU-NSA project No. 0118U003858.

References

Harris, A.W., Young, J.W., Scaltriti, F., Zappala, V. (1984). "Lightcurves and phase relations of the asteroids 82 Alkmene and 444 Gyptis." *Icarus* **57**, 251-258.

Lomb, N.R. (1976). "Least-squares frequency analysis of unequally spaced data." *Ap&SS* **39**, 447-462.

Stellingwerf, R.F. (1978). "Period determination using phase dispersion minimization." *ApJ* **224**, 953-960.

Warner, B.D., Harris, A.W., Pravec, P. (2009). "The asteroid lightcurve database." *Icarus* **202**, 134-146. Updated 2016 Sept 6. *http://www.minorplanet.info/lightcurvedatabase.html*

Number	Name	2018 mm/dd	Pts	Phase	L_{PAB}	B_{PAB}	Period(h)	P.E.	Amp	A.E.	Grp
(144332)	2004 DV24	08/19-08/24	424	71.6,74.2	349	+57	7.985	0.009	1.17	0.05	NEA

Table I. Observing circumstances and results. Pts is the number of data points. The phase angle is given for the first and last date. L_{PAB} and B_{PAB} are the approximate phase angle bisector longitude and latitude at mid-date range (see Harris *et al.*, 1984). Grp is the asteroid family/group (Warner *et al.*, 2009).

LIGHTCURVE BASED ROTATIONAL PERIOD DETERMINATION FOR ASTEROIDS AT UNISON OBSERVATORY: FIRST HALF OF 2018

Pablo Loera-González, Lorenzo Olguín & Julio C. Saucedo
Departamento de Investigación en Física
Universidad de Sonora
Hermosillo, Sonora, MEXICO
pabloloerag@gmail.com

Ramona Núñez-López
Departamento de Física, Matemáticas e Ingeniería
Universidad de Sonora, Unidad Regional Norte
Caborca, Sonora, MEXICO

Nadia Amina Yahia-Keith
Departamento de Física
Universidad de Sonora
Hermosillo, Sonora, MEXICO

(Received: 2018 Oct 19)

Lightcurve period determinations for four asteroids were carried out at the Universidad de Sonora Observatory. Results of the analysis are: 1903 Adzhimushkaj: P = 4.622 ± 0.001 hr, A = 0.04 mag; 2746 Hissao: P = 3.1848 ± 0.0015 hr, A = 0.41 mag; 3617 Eicher: P = 10.3050 ± 0.0193 hr, A = 0.07 mag; (47606) 2000 AA238: P = 7.2125 ± 0.0152 hr, A = 0.22 mag;

After a successful participation in the Mexican Asteroid Photometry Campaign (MAPC) since 2015 (Sada et al. 2016; 2017; 2018; Haro et al. 2018), the asteroid research team at the Universidad de Sonora (UNISON) decided to undertake a local program to study a sample of asteroids in addition to those that were selected for the MAPC runs. The objects included in our sample for the first semester of 2018 were taken from CALL website (Warner et al. 2009).

In total, 27 observing nights were recorded at the Carl Sagan Observatory belonging to the Universidad de Sonora (UNISON) in Hermosillo, Mexico. This observatory operates a Meade LX-200GPS 0.41-m *f*/10 telescope equipped with a 3056×3056×12 µm Apogee Alta F9000 CCD for imaging. The image frame was trimmed to a subframe of 2000×2000 pixels and then binned 2×2, yielding an effective 1000×1000 pixel array and ~20×20 arcmin FOV with an image scale of about 1.2 arcsec/pix. Images were unguided and unfiltered. Exposure times ranged from 180-240 s.

Images from the observatory were reduced in the standard manner using nightly flat-field files as well as dark-current and bias images using *CCDSoft* v5.00.071. Photometric measurements and lightcurve analysis were performed using *MPO Canopus* (version 10.7.3.0; Warner 2017). Although all observations were unfiltered, differential magnitudes were calculated based on R band stellar magnitudes.

1903 Adzhimushkaj is a main-belt object belonging to the Eos family; it was discovered on 1972 May 9 at Nauchnyj by T.M. Smyrnova (Schmadel 2003). We observed on six nights (2018 March 13, 16, 18-20, and April 8) to obtain photometric data. Due to bad weather conditions, data obtained on March 13 and 19 were split into two sessions each. The total observing time for this object was 18 hours and included 360 data points. The resulting period was P = 4.622 ± 0.001 hr and A = 0.04 mag using a 3rd order fit. Notice that the vertical axis in the lightcurve plot was set to ±0.10 mag to emphasize the structure of the derived light curve. Ditteon et al. (2017) reported an amplitude of A = 0.05 ± 0.05 mag, which is similar to ours, but did not report a period. It must be noticed that due to our large data scattering, comparable to the amplitude value, we should be cautious to draw any conclusion based on this lightcurve.

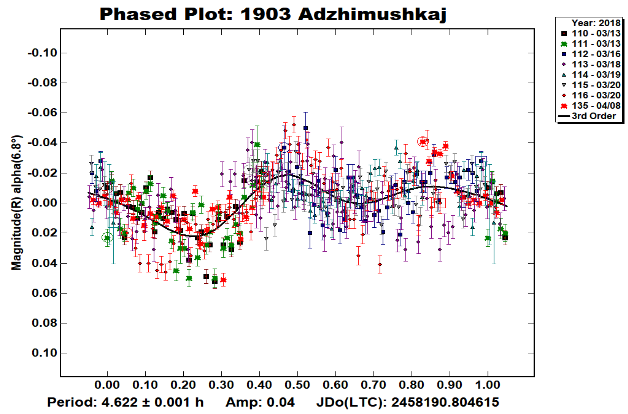

2746 Hissao. Discovered on 1979 Sept. 22 at Nauchnyj by N.S. Chernykh, 2746 Hissao is a main-belt asteroid. It was observed during 6 nights (2018 March 27, 28 and April 2, 3, 9, and 10), compiling a total of 23.7 h of data. During the first two nights (2018 April 2 and 3), only two hours of data were taken. The complete data set consisted of 318 points from which we derived a period of P = 3.1848 ± 0.0015 hr and amplitude of A = 0.41 mag when using a 5th order fit. Based on our period, the asteroid rotated 7.4 times during the total observing time.

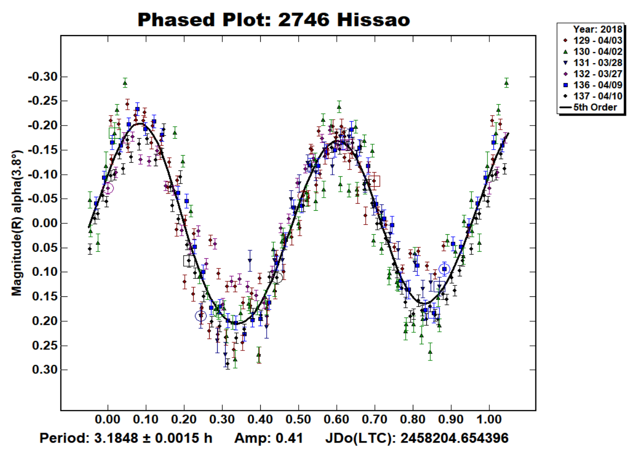

(47606) 2000 AA238. This asteroid was discovered by LONEOS at Anderson Mesa Observatory on 2000 January 6. 2000 AA238 is the brightest of three additional asteroids (2000 AA238, 2000 WB123, and 2006 UX272) found in our images of 1903 Adzhimushkaj. This object was detected during five out of six nights. A total of 18 hours of observing time were used to build its final lightcurve. It should be noticed that since the images had an exposure time chosen for 1903 Adzhimushkaj, the resulting signal to noise ratio for 2000 AA238 was low. The derived period obtained with *MPO Canopus*, using a 5th order fit, was P = 7.2125 ± 0.0152 hr and amplitude A = 0.22 mag.

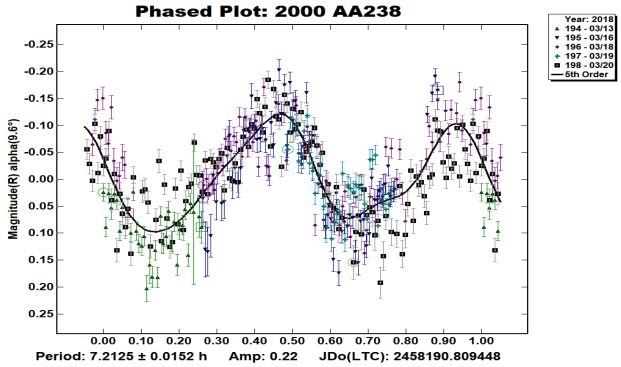

3617 Eicher. This asteroid was discovered at Anderson Mesa by B.A. Skiff on 1984 June 2. It is a main-belt object, named in honor of David J. Eicher, editor-in-chief of Astronomy magazine (Schmadel 2003). Data for this object were collected during 10 nights (2018 May 8, 10, 13-15, 17, 18, and 20-22). We obtained a total of 597 data points over 39.8 h of observing time. A period of P = 10.3050 ± 0.0193 hr and amplitude of A = 0.07 mag were found using a 4th order Fourier fit. The low amplitude indicates that it is a rather spherical object, or that it was observed nearly pole-on. Warner et al. (2018) found P = 5.81 hr, A = 0.21 mag. The discrepancy in the determination of both parameters may be due to the low signal to noise of our data. Images with longer exposure times or larger aperture telescopes may be necessary to better constrain the rotation period.

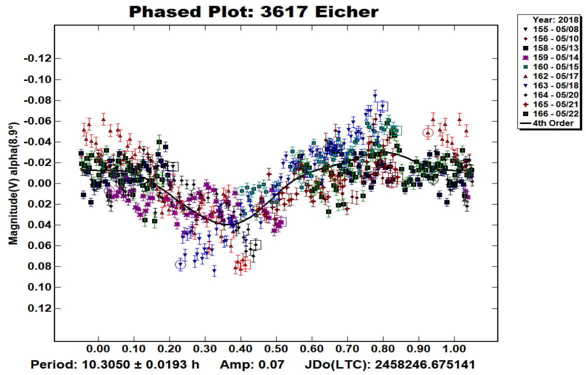

References

Ditteon, R., Adam, A., Doyel, M., Gibson, J., Lee, S., Linville, D., Michalik, D., Turner, R., Washburn, K. (2017). "Lightcurve Analysis of Minor Planets Observed at the Oakley Southern Sky Observatory." *Minor Planet Bull.* **45**, 13-16.

Haro-Corzo, S.A.R., Villegas, L.A., Olguín, L., Saucedo, J.C., Contreras, M.E., Sada, P.V., Ayala, S.A., Garza, J.R., Segura-Sosa, J., Benítez-Benítez, C.P. (2018). "Lightcurves for Asteroids 2022 West and 18301 Konyukhov." *Minor Planet Bull.* **45**, 233-234.

Harris, A.W., Young, J.W., Scaltriti, F., Zappala, V. (1984). "Lightcurves and phase relations of the asteroids 82 Alkmene and 444 Gyptis." *Icarus* **57**, 251-258.

Sada, P.V., Navarro-Meza, S., Reyes-Ruiz, M., Olguín, L., Saucedo, J.C., Loera-González, P. (2016). "Results of the 2015 Mexican Asteroid Photometry Campaign." *Minor Planet Bull.* **43**, 154-156.

Sada, P.V., Olguín L., Saucedo, J.C., Loera-González, P., Cantú-Sánchez, L., Garza, J.R., Ayala-Gómez, S.A., Avilés, A., Pérez-Tijerina, E., Navarro-Meza, S., Silva, J.S., Reyes-Ruiz, M., Segura-Sosa, J., López-Valdivia, R., Álvarez-Santana, F. (2017). "Results of the 2016 Mexican Asteroid Photometry Campaign." *Minor Planet Bull.* **44**, 239-242.

Sada, P.V., Loera-González, P., Olguín, L., Saucedo-Morales, J. C., Ayala-Gómez, S.A., Garza, J.R. (2018). "Results of the 2017 Mexican Asteroid Photometry Campaign - Part 1." *Minor Planet Bull.* **45**, 122-124.

Schmadel, L.D. (2003). *Dictionary of Minor Planet Names*, pp. 163. Springer, New York.

Warner, B.D., Harris, A.W., Pravec, P. (2009). "The Asteroid Lightcurve Database." *Icarus* **202**, 134-146. Updated 2018 Nov. *http://www.minorplanet.info/lightcurvedatabase.html*

Warner. B.D. (2017). *MPO Canopus software*. *http://bdwpublishing.com*

Warner B.D., Harris A.W., Durech J., Benner L.A.M. (2018). "Lightcurve photometry opportunities: 2018 April-June." *Minor Planet Bull.* **45-2**, 208-213.

Number	Name	2018 mm/dd	Pts	Phase	L_{PAB}	B_{PAB}	Period(h)	P.E.	Amp	A.E.	Grp
1903	Adzhimushkaj	03/13-04/08	360	6.7,14.9	156.9	6.2	4.622	0.001	0.04	0.03	Eos
2746	Hissao	04/03-04/10	318	9.4,13	177.6	0.5	3.1848	0.0015	0.41	0.15	MBO
3617	Eicher	05/08-05/22	597	8.8,14.0	219.3	12.6	10.3050	0.0193	0.07	0.03	EMB
47606	2000 AA238	03/13-03/20	360	11.4,9.2	202.9	-6.6	7.2125	0.0152	0.22	0.1	MBO

Table I. Observing circumstances and results. Pts is the number of data points. The phase angle is given for the first and last date. L_{PAB} and B_{PAB} are the approximate phase angle bisector longitude and latitude at mid-date range (see Harris *et al.*, 1984). Grp is the asteroid family/group (Warner *et al.*, 2009).

ROTATION PERIOD DETERMINATION OF ASTEROIDS 7736 NIZHNIJ NOVGOROD AND (42701) 1998 MD13

Riccardo Papini, Massimo Banfi, Fabio Salvaggio
Wild Boar Remote Observatory (K49)
via Potente 52, 50026 San Casciano in val di Pesa (FI), ITALY
riccardo.papini@yahoo.it

Alessandro Marchini
Astronomical Observatory, DSFTA - University of Siena (K54)
Via Roma 56, 53100 – Siena, ITALY

(Received: 2018 Oct 15)

Photometric observations were made in 2018 of the main-belt asteroids 7736 Nizhnij Novgorod and (42701) 1998 MD13. Analysis of the data suggests a likely period of 2.858 ± 0.001 hr for 7736 Nizhnij Novgorod and a period of 2.603 ± 0.001 hr for (42701) 1998 MD13.

Photometric observations of the main-belt asteroids 7736 Nizhnij Novgorod and (42701) 1998 MD13 were nade at the Astronomical Observatory of the University of Siena (K54), Italy, and at the Wild Boar Remote Observatory (K49), Italy. Exposure time was 300 seconds at both the observatories. Table I shows the main features of the instruments used while Table II gives the observation circumstances and results.

Obs	Telescope	Filter	CCD
K54	0.30 m f/5.6 MCT	Clear	SBIG STL-6303 2x2 2.3”/pixel
K49	0.24 m f/10 SCT	Clear	SBIG ST8-XME 2x2 1.6”/pixel

Table I. Main features of the instruments used at the observatories involved in the research. MCT: Maksutov-Cassegrain; SCT: Schmidt-Cassegrain.

The authors performed differential photometry measurements using the Comp Star Selector (CSS) procedure in *MPO Canopus* (Warner, 2018) that allows selecting of up to five comparison stars of near-solar color. The magnitudes from the CMC-15 catalog (Munos, 2017) were used for the comparison stars. Period analysis was performed using *MPO Canopus* and its FALC (Fourier Analysis for Light Curves) algorithm (Harris *et al.*, 1989). In the end we carried out additional adjustments of the magnitude zero-points for each data set out in order to reach the minimum RMS value from the Fourier analysis and so achieve the best alignment among light curves.

A search of the Asteroid Light Curve Database (LCDB; Warner *et al.*, 2009) and literature found no previous entries.

<u>7736 Nizhnij Novgorod</u> is a main-belt asteroid that was discovered at Nauchnyj on 1981 September 8 by L.V. Zhuravleva. Nizhnij Novgorod is an old Russian city located at the confluence of the Volga and Oka rivers. Founded in 1221, the city is now a large industrial, scientific and cultural center. It is known for many architectural monuments and the famous Nizhnij Novgorod Fair.

The asteroid orbits with a semi-major axis of about 2.586 AU, eccentricity 0.197, and a period of 4.16 years (JPL, 2018). Observations were made on four nights from 2018 June 10-23, collecting 175 useful data points. The period analysis yielded a few possible solutions with nearly comparable RMS values. We concluded that the most likely value of the synodic period is associated with a bimodal lightcurve phased to 2.858 ± 0.001 hr with an amplitude of 0.16 ± 0.03 mag.

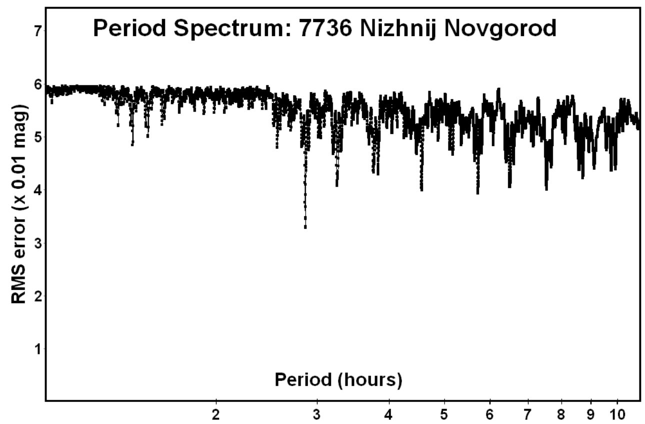

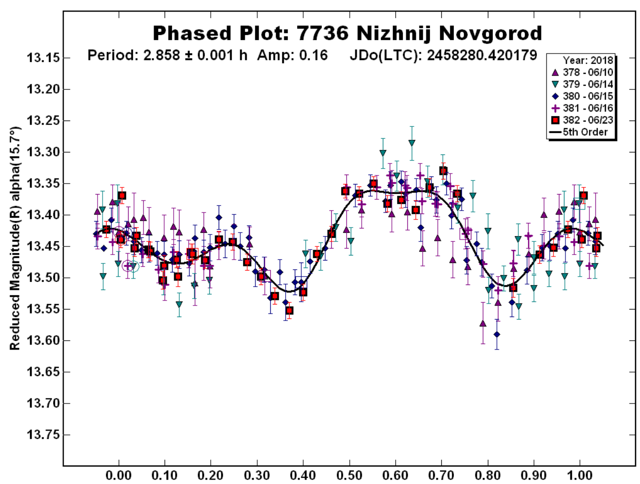

<u>(42701) 1998 MD13</u> is a main-belt asteroid discovered on 1998 June 19 by LINEAR at Socorro. It orbits with a semi-major axis of about 2.534 AU, eccentricity 0.214, and a period of 4.03 years (JPL, 2018). Observations were made on three nights from 2018 May 19 through June 9 with 135 data points collected.

The period analysis yielded several possible solutions with comparable RMS errors. We concluded that the most likely value of the synodic period is associated with a bimodal lightcurve phased to 2.603 ± 0.001 hr with an amplitude of 0.10 ± 0.03 mag.

Number	Name	2018 mm/dd	Pts	Phase	L_{PAB}	B_{PAB}	Period(h)	P.E.	Amp	A.E.	Grp
7736	Nizhnij Novgorod	06/10-06/23	175	15.7,12.5	281	19	2.858	0.001	0.16	0.03	MB
42701	1998 MD13	05/19-06-09	135	8.4,13.9	240	13	2.603	0.001	0.10	0.03	MB

Table II. Observing circumstances and results. Pts is the number of data points. The phase angle is given for the first and last date. L_{PAB} and B_{PAB} are the approximate phase angle bisector longitude and latitude at mid-date range (see Harris *et al.*, 1984). Grp is the asteroid family/group (Warner *et al.*, 2009).

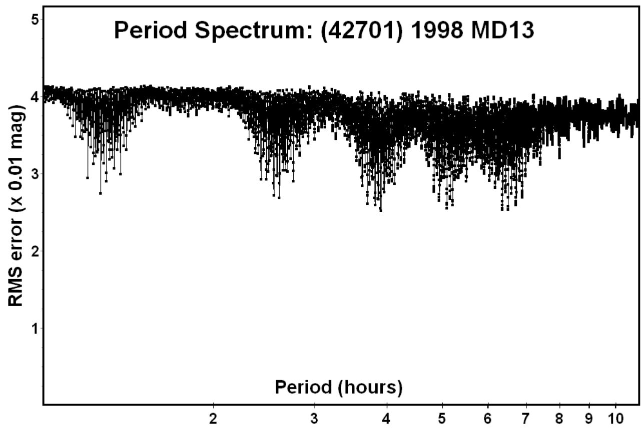

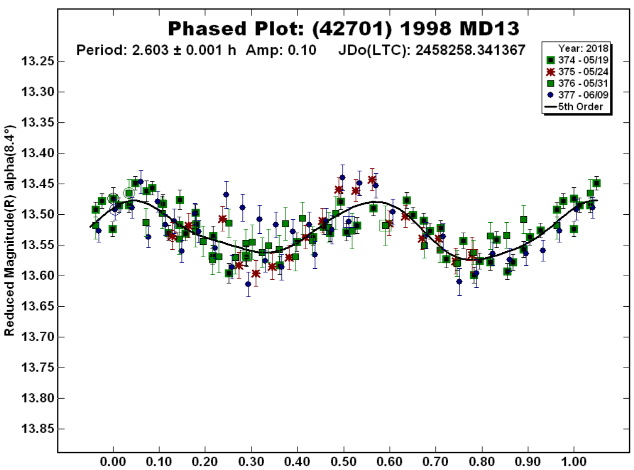

Acknowledgements

The authors want to thank here Chiara Firenzani, Enrico Monti, Giulio Senesi who are high school students from Liceo Scientifico "Federigo Enriques" (Castelfiorentino) involved in an interesting vocational guidance project about astronomy at the Astronomical Observatory of the University of Siena. They attended some observing sessions and participated in data analysis.

References

Harris, A.W., Young, J.W., Scaltriti, F., Zappala, V. (1984). "Lightcurves and phase relations of the asteroids 82 Alkmene and 444 Gyptis." *Icarus* **57**, 251-258.

Harris, A.W., Young, J.W., Bowell, E., Martin, L.J., Millis, R.L., Poutanen, M., Scaltriti, F., Zappala, V., Schober, H.J., Debehogne, H., Zeigler, K. (1989). "Photoelectric observations of asteroids 3, 24, 60, 261, and 863." *Icarus* **77**, 171-186.

JPL (2018). Small-Body Database Browser. *http://ssd.jpl.nasa.gov/sbdb.cgi#top*

Munos, J.L. (2017). Carlsberg Meridian Catalog web site. *http://svo2.cab.inta-csic.es/vocats/cmc15/*

Warner, B.D., Harris, A.W., Pravec, P. (2009). "The asteroid lightcurve database." *Icarus* **202**, 134-146. Updated 2016 Sept. *http://www.minorplanet.info/lightcurvedatabase.html*

Warner, B. D. (2018). MPO Software, Canopus version 10.7.12.1. Bdw Publishing. *http://minorplanetobserver.com*

LIGHTCURVE PHOTOMETRY OPPORTUNITIES: 2019 JANUARY-MARCH

Brian D. Warner
Center for Solar System Studies / MoreData!
446 Sycamore Ave.
Eaton, CO 80615 USA
brian@MinorPlanetObserver.com

Alan W. Harris
MoreData!
La Cañada, CA 91011-3364 USA

Josef Ďurech
Astronomical Institute
Charles University
18000 Prague, CZECH REPUBLIC
durech@sirrah.troja.mff.cuni.cz

Lance A.M. Benner
Jet Propulsion Laboratory
Pasadena, CA 91109-8099 USA
lance.benner@jpl.nasa.gov

We present lists of asteroid photometry opportunities for objects reaching a favorable apparition and have no or poorly-defined lightcurve parameters. Additional data on these objects will help with shape and spin axis modeling via lightcurve inversion. We also include lists of objects that will or might be radar targets. Lightcurves for these objects can help constrain pole solutions and/or remove rotation period ambiguities that might not come from using radar data alone.

We present several lists of asteroids that are prime targets for photometry during the period 2019 January-March.

In the first three sets of tables, "Dec" is the declination and "U" is the quality code of the lightcurve. See the asteroid lightcurve data base (LCDB; Warner et al., 2009) documentation for an explanation of the U code:

http://www.minorplanet.info/lightcurvedatabase.html

The ephemeris generator on the CALL web site allows you to create custom lists for objects reaching V ≤ 18.0 during any month in the current year, e.g., limiting the results by magnitude and declination.

http://www.minorplanet.info/PHP/call_OppLCDBQuery.php

We refer you to past articles, e.g., *Minor Planet Bulletin* **36**, 188, for more detailed discussions about the individual lists and points of advice regarding observations for objects in each list.

Once you've obtained and analyzed your data, it's important to publish your results. Papers appearing in the *Minor Planet Bulletin* are indexed in the Astrophysical Data System (ADS) and so can be referenced by others in subsequent papers. It's also important to make the data available at least on a personal website or upon request. We urge you to consider submitting your raw data to the ALCDEF database. This can be accessed for uploading and downloading data at

http://www.alcdef.org

Containing almost 3.2 million observations for more than 13380 objects, we believe this to be the largest publicly available database of raw asteroid time-series lightcurve data.

Now that many backyard astronomers and small colleges have access to larger telescopes, we have expanded the photometry opportunities and spin axis lists to include asteroids reaching V = 15.5 and brighter (sometimes 15.0 when the list has more than 100 objects.

Lightcurve/Photometry Opportunities

Objects with U = 3– or 3 are excluded from this list since they will likely appear in the list for shape and spin axis modeling. Those asteroids rated U = 1 should be given higher priority over those rated U = 2 or 2+, but not necessarily over those with no period. On the other hand, d*o not overlook asteroids with* U = 2/2+ *on the assumption that the period is sufficiently established.* Regardless, do not let the existing period influence your analysis since even high quality ratings have been proven wrong at times. Note that the lightcurve amplitude in the tables could be more or less than what's given. Use the listing only as a guide.

An entry in italics is a near-Earth asteroid (NEA).

		Brightest			LCDB Data		
Number	Name	Date	Mag	Dec	Period	Amp	U
6941	Dalgarno	01 02.4	15.5	+5			
7520	1990 BV	01 03.9	15.0	+24			
7865	Francoisgros	01 05.3	15.5	+24			
7261	Yokootakeo	01 07.0	15.5	+0			
2745	San Martin	01 07.9	15.3	-3		0.04	
11151	Oodaigahara	01 08.2	15.1	+16			
2670	Chuvashia	01 08.4	14.8	+22		0.14	
22106	Tomokoarai	01 10.0	15.3	-16			
2595	Gudiachvili	01 10.4	15.5	+12	4.72	0.5	1
5131	*1990 BG*	*01 16.1*	*15.0*	*+29*	*37.2*	*0.34*	*2-*
18348	1990 BM1	01 17.1	14.6	+17			
1212	Francette	01 17.6	14.1	+15	22.433	0.13	2
69971	Tanzi	01 19.0	15.0	+21			
4970	Druyan	01 19.3	15.5	+19		0.30	
449	Hamburga	01 20.2	11.6	+23	18.263	0.08-0.17	2+
3658	Feldman	01 20.7	15.3	+23			
4056	Timwarner	01 22.8	15.3	+12			
4156	Okadanoboru	01 23.4	15.0	+22	12.015	0.47	2
1435	Garlena	01 25.7	15.0	+12			
394130	*2006 HY51*	*01 25.7*	*13.8*	*-20*			
100006	1987 DA7	01 27.0	15.1	+19			
4163	Saaremaa	01 27.9	15.1	+18			
10111	Fresnel	01 28.8	15.5	+14			
27027	1998 QA98	01 29.1	15.4	+19			
5924	Teruo	01 31.3	15.5	+20			
1269	Rollandia	02 01.9	13.6	+17	19.98	0.02-0.13	2
6258	Rodin	02 02.0	15.3	+17	6.1	0.03	1
3549	Hapke	02 07.6	15.1	+8	7.071	0.24-0.31	2
4148	McCartney	02 08.5	14.6	+16			
16058	1999 JP75	02 10.6	15.4	+6			
1802	Zhang Heng	02 10.9	15.1	+14	3.162	0.27-0.37	2+
69270	1989 BB	02 13.1	15.1	+13		0.71	
4215	Kamo	02 19.4	15.2	+2	12.6	0.11-0.21	2
5297	Schinkel	02 24.0	15.2	+11			
488	Kreusa	02 27.1	11.6	+25	32.666	0.08-0.2	2+
2602	Moore	02 27.3	14.9	+8		0.30	
2727	Paton	02 28.5	15.0	+4			
1614	Goldschmidt	03 02.4	14.3	+7	8.873	0.14-0.14	2-
6918	Manaslu	03 05.4	15.4	+5	8.97	0.21	2
16578	Essjayess	03 07.0	15.5	+5			
2761	Eddington	03 07.2	15.4	+9			
6843	Heremon	03 10.1	15.2	+14		0.5	
37652	1994 JS1	03 11.9	14.9	+5			
12265	1990 FG	03 14.8	15.4	+6	56.6	0.65	2
2640	Hallstrom	03 17.5	15.1	+3	22.9	0.15	1
4533	Orth	03 20.1	14.5	+1	>24.	0.1-0.68	2
4171	Carrasco	03 24.9	15.4	-2	33.53	0.17-0.22	2

Low Phase Angle Opportunities

The Low Phase Angle list includes asteroids that reach very low phase angles. The "α" column is the minimum solar phase angle for the asteroid. Getting accurate, calibrated measurements (usually V band) at or very near the day of opposition can provide important information for those studying the "opposition effect." Use the on-line query form for the LCDB to get more details about a specific asteroid.

http://www.minorplanet.info/PHP/call_OppLCDBQuery.php

You will have the best chance of success working objects with low amplitude and periods that allow covering at least half a cycle every night. Objects with large amplitudes and/or long periods are much more difficult for phase angle studies since, for proper analysis, the data must be reduced to the average magnitude of the asteroid for each night. This reduction requires that you determine the period and the amplitude of the lightcurve; for long period objects that can be difficult. Refer to Harris *et al.* (1989; *Icarus* **81**, 365-374) for the details of the analysis procedure.

As an aside, some use the maximum light to find the phase slope parameter (G). However, this can produce a significantly different value for both H and G versus when using average light, which is the method used for values listed by the Minor Planet Center.

The International Astronomical Union (IAU) has adopted a new system, H-G_{12}, introduced by Muinonen *et al.* (2010; *Icarus* **209**, 542-555). It will be some years before H-G_{12} becomes the standard. Furthermore, it still needs refinement. That can be done mostly by having data for more asteroids, but only if at very low and moderate phase angles. We strongly encourage obtaining data every degree between 0° to 7°, the non-linear part of the curve that is due to the opposition effect. At angles $\alpha > 7°$, well-calibrated data every 2° or so out to about 25-30°, if possible, should be sufficient. Coverage beyond about 50° is not generally helpful since the H-G system is best defined with data from 0-30°.

Num	Name	Date	α	V	Dec	Period	Amp	U
277	Elvira	01 05.2	0.48	13.6	+21	29.69	0.34-0.59	3
638	Moira	01 05.3	0.16	13.9	+23	9.875	0.10-0.31	3
1107	Lictoria	01 06.6	0.37	13.1	+22	8.562	0.16-0.30	3
607	Jenny	01 06.9	0.09	13.8	+22	8.521	0.16-0.26	3
370	Modestia	01 07.8	0.40	13.3	+23	22.530	0.24-1.39	3
24	Themis	01 14.0	0.40	10.7	+23	8.374	0.09-0.14	3
738	Alagasta	01 25.6	0.25	14.0	+18	18.86	0.11-0.20	2
89	Julia	01 31.0	0.16	10.2	+18	11.387	0.10-0.25	3
159	Aemilia	01 31.3	0.22	11.7	+17	24.476	0.16-0.24	3
1269	Rollandia	02 01.8	0.09	13.6	+17	19.98	0.02-0.13	2
65	Cybele	02 04.8	0.47	11.6	+15	6.081	0.02-0.12	3
558	Carmen	02 08.3	0.39	12.7	+14	11.387	0.2 -0.31	3
335	Roberta	02 15.0	0.14	12.5	+13	12.054	0.05-0.78	3
334	Chicago	02 15.1	0.42	13.1	+14	7.361	0.20-0.67	3
208	Lacrimosa	02 19.4	0.52	12.7	+13	14.085	0.15-0.33	3
435	Ella	02 20.4	0.79	13.9	+13	4.623	0.30-0.38	3
108	Hecuba	02 25.5	0.48	12.3	+11	14.256	0.09-0.12	3
64	Angelina	03 02.8	0.50	10.4	+06	8.752	0.04-0.42	3
167	Urda	03 09.1	0.08	13.0	+05	13.07	0.24-0.39	3
50	Virginia	03 16.6	0.14	13.8	+02	14.315	0.07-0.20	3
175	Andromache	03 17.1	0.47	13.7	+03	8.324	0.28-0.30	3
337	Devosa	03 17.1	0.09	11.1	+01	4.653	0.08-0.75	3
59	Elpis	03 18.6	0.56	11.9	+03	13.671	0.07-0.42	3
126	Velleda	03 22.5	0.65	12.7	+01	5.367	0.07-0.22	3
302	Clarissa	03 24.1	0.20	13.9	-01	14.381	0.6	3
291	Alice	03 25.4	0.67	13.3	+00	4.313	0.15-0.55	3
1453	Fennia	03 28.0	0.23	13.7	-02	4.412	0.10-0.20	3
670	Ottegebe	03 29.5	0.76	14.0	-01	10.045	0.34-0.35	3
737	Arequipa	03 30.6	0.55	12.6	-02	7.026	0.10-0.27	3
161	Athor	03 31.3	0.90	12.2	-02	7.280	0.08-0.27	3

Shape/Spin Modeling Opportunities

Those doing work for modeling should contact Josef Ďurech at the email address above. If looking to add lightcurves for objects with existing models, visit the Database of Asteroid Models from Inversion Techniques (DAMIT) web site

http://astro.troja.mff.cuni.cz/projects/asteroids3D

An additional dense lightcurve, along with sparse data, could lead to the asteroid being added to or improving one in DAMIT, thus increasing the total number of asteroids with spin axis and shape models.

Included in the list below are objects that:

1. Are rated U = 3– or 3 in the LCDB
2. Do not have reported pole in the LCDB Summary table
3. Have at least three entries in the Details table of the LCDB where the lightcurve is rated U ≥ 2.

The caveat for condition #3 is that no check was made to see if the lightcurves are from the same apparition or if the phase angle bisector longitudes differ significantly from the upcoming apparition. The last check is often not possible because the LCDB does not list the approximate date of observations for all details records. Including that information is an on-going project.

Favorable apparitions are in bold text. NEAs are in italics.

		Brightest			LCDB Data		
Num	Name	Date	Mag	Dec	Period	Amp	U
651	Antikleia	01 01.8	14.2	+37	20.299	0.13-0.41	3
1562	Gondolatsch	01 05.0	14.4	+19	8.78	0.30- 0.4	3-
1123	Shapleya	01 06.1	13.6	+28	52.92	0.25-0.38	3-
1107	**Lictoria**	**01 06.6**	**13.1**	**+22**	**8.562**	**0.16-0.30**	**3**
663	Gerlinde	01 07.5	13.5	+1	10.251	0.19-0.35	3
850	Altona	01 11.6	14.2	+18	11.191	0.09-0.17	3
3873	Roddy	01 12.8	14.5	-16	2.478	0.05-0.11	3
9068	**1993 OD**	**01 12.8**	**14.4**	**+31**	**3.407**	**0.19-0.20**	**3**
418	Alemannia	01 13.6	13.2	+14	4.671	0.14-0.33	3
1309	Hyperborea	01 15.6	14.2	+5	13.88	0.34-0.54	3
1717	**Arlon***	**01 17.9**	**13.9**	**+29**	**5.148**	**0.07-0.12**	**3**
420	Bertholda	01 20.1	13.0	+12	11.04	0.24-0.29	3
5806	**Archieroy**	**01 20.8**	**14.4**	**+21**	**12.163**	**0.34-0.47**	**3**
300	Geraldina	01 23.2	14.2	+21	6.842	0.04-0.32	3
2167	Erin	01 23.8	14.5	+11	5.719	0.3-0.53	3
658	Asteria	01 24.9	14.2	+21	21.034	0.22-0.28	3
224	Oceana	01 25.1	12.3	+26	9.401	0.09-0.14	3
895	Helio	01 26.4	12.7	-10	9.347	0.10-0.23	3
219	Thusnelda	01 27.2	13.2	+3	59.74	0.19-0.24	3
1028	Lydina	01 31.2	13.9	+30	11.68	0.22- 0.7	3
2460	**Mitlincoln**	**02 04.0**	**14.4**	**+12**	**3.01**	**0.03-0.20**	**3**
909	Ulla	02 07.8	14.1	+12	8.73	0.08-0.24	3
558	**Carmen**	**02 08.3**	**12.7**	**+14**	**11.387**	**0.2-0.31**	**3**
972	Cohnia	02 12.1	14.3	+6	18.472	0.19-0.21	3
781	Kartvelia	02 16.1	14.4	+17	19.04	0.16-0.28	3-
790	Pretoria	02 21.4	13.7	-14	10.37	0.05-0.18	3
388	Charybdis	02 24.0	13.0	+13	9.516	0.14-0.25	3
454	Mathesis	02 25.0	12.3	+18	8.378	0.20-0.37	3
712	Boliviana	02 25.0	12.1	-10	11.743	0.10-0.12	3
359	Georgia	02 26.3	13.2	+13	5.537	0.16-0.54	3
653	Berenike	02 28.5	13.3	+15	12.489	0.03-0.11	3
779	Nina	03 05.8	12.7	-11	11.186	0.06-0.32	3
1304	Arosa	03 05.9	13.7	+32	7.748	0.13-0.38	3
1590	Tsiolkovskaja	03 09.1	14.3	-1	6.731	0.10- 0.4	3
1084	Tamariwa	03 11.2	14.5	+2	6.196	0.25-0.42	3
100	Hekate	03 17.2	12.5	+8	27.066	0.11-0.23	3
175	Andromache	03 17.2	13.7	+3	8.324	0.28-0.30	3
59	Elpis	03 18.5	11.9	+3	13.671	0.07-0.42	3
696	Leonora	03 20.7	14.7	-15	26.896	0.04-0.31	3
151	Abundantia	03 21.3	12.3	+6	9.864	0.15-0.20	3
111	Ate	03 21.5	11.1	-7	22.072	0.08-0.18	3
851	Zeissia	03 21.8	13.5	+2	9.34	0.38-0.53	3
1146	Biarmia	03 22.3	14.1	-13	5.47	0.20-0.32	3
126	Velleda	03 22.5	12.7	+1	5.367	0.07-0.22	3
1113	Katja	03 22.8	13.8	-12	18.465	0.08-0.17	3
868	Lova	03 23.3	14.4	+6	41.118	0.10-0.40	3
1817	Katanga	03 26.9	14.0	+43	8.481	0.22-0.42	3
1453	**Fennia**	**03 28.0**	**13.7**	**-2**	**4.412**	**0.10-0.20**	**3**
197	Arete	03 28.8	13.6	+9	6.608	0.10-0.16	3
535	Montague	03 30.3	12.6	+6	10.248	0.18-0.25	3
737	Arequipa	03 30.7	12.6	-2	7.026	0.10-0.27	3
191	Kolga	03 30.8	13.5	+4	17.604	0.21- 0.5	3

Radar-Optical Opportunities

Future radar targets:
http://echo.jpl.nasa.gov/~lance/future.radar.nea.periods.html

Past radar targets:
http://echo.jpl.nasa.gov/~lance/radar.nea.periods.html

Arecibo targets:
http://www.naic.edu/~pradar/sched.shtml
http://www.naic.edu/~pradar

Goldstone targets:
http://echo.jpl.nasa.gov/asteroids/goldstone_asteroid_schedule.html

These are based on *known* targets at the time the list was prepared. It is very common for newly discovered objects to move up the list and become radar targets on short notice. We recommend that you keep up with the latest discoveries the Minor Planet Center observing tools

In particular, monitor NEAs and be flexible with your observing program. In some cases, you may have only 1-3 days when the asteroid is within reach of your equipment. Be sure to keep in touch with the radar team (through Dr. Benner's email or their Facebook or Twitter accounts) if you get data. The team may not always be observing the target but your initial results may change their plans. In all cases, your efforts are greatly appreciated.

Use the ephemerides below as a guide to your best chances for observing, but remember that photometry may be possible before and/or after the ephemerides given below. Note that *geocentric* positions are given. Use these web sites to generate updated and *topocentric* positions:

MPC: *http://www.minorplanetcenter.net/iau/MPEph/MPEph.html*
JPL: *http://ssd.jpl.nasa.gov/?horizons*

In the ephemerides below, ED and SD are, respectively, the Earth and Sun distances (AU), V is the estimated Johnson V magnitude, and α is the phase angle. SE and ME are the great circles distances (in degrees) of the Sun and Moon from the asteroid. MP is the lunar phase and GB is the galactic latitude. "PHA" indicates that the object is a "potentially hazardous asteroid", meaning that at some (long distant) time, its orbit might take it very close to Earth.

About YORP Acceleration

Many, if not all, of the targets in this section are near-Earth asteroids. These objects are particularly sensitive to YORP acceleration. YORP (Yarkovsky–O'Keefe–Radzievskii–Paddack) is the asymmetric thermal re-radiation of sunlight that can cause an asteroid's rotation period to increase or decrease. High precision lightcurves at multiple apparitions can be used to model the asteroid's *sidereal* rotation period and see if it's changing.

It usually takes four apparitions to have sufficient data to determine if the asteroid rotation rate is changing under the influence of YORP. This is why observing asteroids that already have well-known periods is still a valuable use of telescope time. It is even more so when considering the BYORP (binary-YORP) effect among binary asteroids that has stabilized the spin so that acceleration of the primary body is not the same as if it would be if there were no satellite.

To help focus efforts in YORP detection, Table I gives a quick summary of this quarter's radar-optical targets. The family or group for the asteroid is given under the number name. Also under the name will be additional flags such as "PHA" for Potentially Hazardous Asteroid, NPAR for a tumbler, and/or "Bin" to indicate the asteroid is a binary (or multiple) system. If "Bin" is followed by "?" it means that the asteroid is a suspected but not confirmed binary. The period is in hours and, in the case of binary, for the primary. The Amp column gives the known range of lightcurve amplitudes. The App columns gives the number of different apparitions at which a lightcurve period was reported while the Last column gives the year for the last reported period. The R SNR column indicates the estimated radar SNR using the tool at

http://www.naic.edu/~eriverav/scripts/index.php

The "A" is for Arecibo and "G" is for Goldstone. Note that this calculator assumes full power at Arecibo.

Asteroid	Period	Amp	App	Last	R SNR
(141053) 2001 XT1 NEA	**-**	**-**	**-**	**-**	**A 14 G -**
(418884) 2008 WM64 NEA	**-**	**-**	**-**	**-**	**A 1590 G 90**
2004 XP14 NEA	**>100**	**-**	**1**	**2007**	**A 1850 G 210**
433 Eros NEA	**5.27**	**0.08 1.40**	**13+**	**2016**	**A 900 G 100**
2016 AZ8 NEA	**-**	**-**	**-**	**-**	**A 1850 G 210**
(90403) 2003 YE45 NEA	-	-	-	-	A *52 June
(454177) 2013 GJ35 NEA	-	-	-	-	A 43
(18736) 1998 NU NEA	-	-	-	-	A 11
(180186) 2003 QZ30 NEA	-	-	-	-	A 14
(419880) 2011 AH37 NEA	-	-	-	-	A 40
(137805) 1999 YK5 NEA	3.930	0.09 0.38	2	2016	A 55
2013 CW32 NEA	**-**	**-**	**-**	**-**	**A 510 G 55**
(455176) 1999 VF22 NEA	-	-	-	-	A 370 G 41
(381677) 2009 BJ81 NEA	-	-	-	-	A 10
(162361) 2000 AF6 NEA	-	-	-	-	A 20
(86667) 2000 FO10 NEA	26	0.7 1.0	1	2004	A 32
(163081) 2002 AG29 NEA	19.70	0.25	1	2011	A 299 G 26
(88254) 2001 FM129 NEA	-	-	-	-	A 300 G 33
(5189) 1990 UQ NEA	6.676	1.02	1	2017	A *11 July

Table I. Summary of radar-optical opportunities in 2018 July-October. Data from the asteroid lightcurve database (Warner *et al.*, 2009; *Icarus* **202**, 134-146). *The SNRs for 2003 SD220 will be enormous: A: 1.76E+6, G: 96800.

The estimated SNR uses the current MPCORB absolute magnitude (*H*), a period of 4 hours (2 hours if $D \leq 170$ m) if it's not known, and the approximate minimum Earth distance during the current quarter.

If the SNR value is in bold text, the object was found on the radar planning pages listed above. Otherwise, the planning tool at

http://www.minorplanet.info/PHP/call_OppLCDBQuery.php

was used to find known NEAs that were V < 18.0 during the quarter. An object is usually placed on the list only if the estimated Arecibo SNR > 10. This would produce a marginal signal, not enough for imaging, but might allow improving orbital parameters.

(141053) 2001 XT1 (Jan, *H* = 18.7)
There's no reported period in the LCDB for this 500-meter NEA. This ephemeris covers the first few days of 2019. If you can, observe it during the last week of 2018 December as well.

DATE	RA	Dec	ED	SD	V	α	SE	ME	MP	GB
01/01	07 08.9	+28 36	0.34	1.32	17.5	5.9	172	116	-0.23	+16
01/02	07 05.1	+28 30	0.35	1.33	17.5	5.0	173	130	-0.15	+15
01/03	07 01.5	+28 24	0.36	1.34	17.5	4.3	174	143	-0.09	+15
01/04	06 58.1	+28 18	0.37	1.35	17.6	4.0	174	156	-0.04	+14
01/05	06 54.8	+28 12	0.38	1.36	17.6	4.1	174	168	-0.01	+13
01/06	06 51.7	+28 05	0.39	1.37	17.7	4.5	174	173	+0.00	+12
01/07	06 48.8	+27 59	0.40	1.38	17.8	5.2	173	163	+0.01	+12
01/08	06 46.0	+27 52	0.41	1.39	17.9	6.0	172	151	+0.03	+11
01/09	06 43.4	+27 46	0.42	1.39	18.0	6.8	170	139	+0.08	+11
01/10	06 40.9	+27 39	0.43	1.40	18.1	7.7	169	127	+0.14	+10

(418849) 2008 WM64 (Dec-Jan, *H* = 20.6)
Both Rowe (2018) and Warner (2018) found a period of 2.4 h based on observations in mid- to late-December of 2017. This makes it a potential binary candidate, so careful observations are in order. Note the ephemeris starts in late December 2018. Make it a New Year's Resolution.

DATE	RA	Dec	ED	SD	V	α	SE	ME	MP	GB
12/25	03 25.3	+15 24	0.05	1.02	15.5	38.4	140	72	-0.93	-33
12/26	03 07.1	+25 42	0.05	1.02	15.7	41.1	137	87	-0.85	-28
12/27	02 49.9	+33 57	0.06	1.02	16.1	44.8	133	102	-0.76	-23
12/28	02 33.9	+40 21	0.06	1.02	16.4	48.4	129	114	-0.65	-18
12/29	02 19.2	+45 17	0.07	1.03	16.8	51.5	125	124	-0.54	-15
12/30	02 05.8	+49 05	0.08	1.03	17.1	54.2	122	131	-0.43	-12
12/31	01 53.5	+52 04	0.09	1.03	17.4	56.4	119	134	-0.33	-10
01/01	01 42.4	+54 27	0.10	1.03	17.7	58.2	117	134	-0.23	-8
01/02	01 32.3	+56 21	0.11	1.03	17.9	59.6	115	132	-0.15	-6
01/03	01 23.2	+57 55	0.12	1.03	18.2	60.8	113	128	-0.09	-5

2004 XP14 (Jan, *H* = 19.3, PHA)
The radar observers are hoping for hi-res imaging of this 300 meter NEA. Some astrometry and photometry before, during, and after their runs on Jan 2-5 will be a great help. The bad news is that the period is possibly more than 100 hours. Given that and the short observing window for photometry, a collaboration of several observers at widely separated longitudes is in order.

DATE	RA	Dec	ED	SD	V	α	SE	ME	MP	GB
01/01	04 10.3	+48 00	0.08	1.05	15.4	36.5	141	139	-0.23	-3
01/02	04 01.7	+41 19	0.08	1.04	15.3	36.5	141	153	-0.15	-9
01/03	03 54.4	+34 04	0.07	1.04	15.3	37.7	140	162	-0.09	-15
01/04	03 48.1	+26 29	0.07	1.04	15.3	40.0	137	158	-0.04	-22
01/05	03 42.6	+18 50	0.07	1.04	15.4	43.4	134	145	-0.01	-28
01/06	03 37.9	+11 25	0.08	1.03	15.5	47.4	129	130	+0.00	-34
01/07	03 33.8	+04 27	0.08	1.03	15.7	51.6	125	115	+0.01	-40
01/08	03 30.2	-01 53	0.08	1.03	16.0	55.7	120	100	+0.03	-44
01/09	03 27.0	-07 34	0.09	1.02	16.2	59.6	116	86	+0.08	-48
01/10	03 24.2	-12 34	0.09	1.02	16.4	63.1	112	74	+0.14	-51

433 Eros (Jan-Mar, *H* = 11.2)
Yes, there's still reason to observe this NEA even after it was studied in depth by the NEAR-Shoemaker space craft. The main purpose is to extend the time span of observations and so get a good handle on how much the YORP (Yarkovsky–O'Keefe–

Radzievskii–Paddack) thermal effect is decreasing or increasing Eros' period.

DATE	RA	Dec	ED	SD	V	α	SE	ME	MP	GB
01/01	04 13.0	+50 59	0.22	1.16	9.1	33.3	140	136	-0.23	+0
01/11	04 25.0	+43 06	0.21	1.15	9.1	36.0	137	89	+0.21	-4
01/21	04 44.3	+34 15	0.21	1.14	9.2	39.6	133	45	+1.00	-8
01/31	05 08.2	+25 29	0.22	1.13	9.3	43.4	128	174	-0.20	-9
02/10	05 34.7	+17 37	0.24	1.14	9.6	46.7	123	67	+0.22	-8
02/20	06 02.6	+11 07	0.27	1.14	9.9	49.1	119	67	-1.00	-6
03/02	06 31.0	+05 59	0.30	1.15	10.2	50.6	116	159	-0.18	-2
03/12	06 59.7	+02 01	0.34	1.17	10.5	51.2	113	55	+0.26	+3
03/22	07 28.5	-01 02	0.38	1.19	10.8	51.2	111	83	-0.99	+8
04/01	07 57.2	-03 25	0.43	1.21	11.1	50.9	110	147	-0.17	+13

2016 AZ8 (Jan, *H* = 21.0, PHA)

This is another target for hi-res imaging. It's also an NHATS target, i.e., a potential target for human missions. The rotation period is not known for the 190 meter NEA.

DATE	RA	Dec	ED	SD	V	α	SE	ME	MP	GB
01/08	17 42.6	+48 09	0.03	0.98	17.2	104.8	74	79	+0.03	+31
01/09	17 03.9	+55 48	0.03	0.98	16.8	95.0	83	92	+0.08	+37
01/10	16 14.1	+61 49	0.03	0.99	16.6	86.1	92	103	+0.14	+42
01/11	15 14.2	+65 47	0.04	0.99	16.5	78.1	100	110	+0.21	+45
01/12	14 10.4	+67 41	0.04	1.00	16.4	71.3	107	114	+0.29	+48
01/13	13 11.8	+67 56	0.04	1.00	16.4	65.5	112	113	+0.38	+49
01/14	12 23.6	+67 08	0.05	1.01	16.5	60.5	117	109	+0.47	+50
01/15	11 46.3	+65 49	0.05	1.01	16.6	56.2	121	102	+0.58	+50
01/16	11 18.0	+64 17	0.05	1.02	16.7	52.6	125	93	+0.68	+50
01/17	10 56.3	+62 44	0.06	1.02	16.7	49.4	128	83	+0.77	+50

(90403) 2003 YE45 (Jan-Mar, *H* = 17.6)

This is one of two targets this quarter where the date of brightest magnitude is several months removed from the date of closest approach. For 2003 YE45, closest approach is June 29 (0.135 AU). The rotation period for the 900-meter NEA is not known.

DATE	RA	Dec	ED	SD	V	α	SE	ME	MP	GB
01/01	07 56.6	+22 24	0.41	1.38	17.1	12.0	163	105	-0.23	+24
01/11	07 25.3	+16 47	0.36	1.34	16.4	3.8	175	126	+0.21	+15
01/21	06 49.8	+09 53	0.33	1.30	16.7	16.4	158	20	+1.00	+4
01/31	06 17.4	+02 52	0.34	1.26	17.1	30.6	139	156	-0.20	-6
02/10	05 53.3	-03 07	0.35	1.22	17.4	42.9	123	71	+0.22	-14
02/20	05 38.6	-07 47	0.38	1.17	17.8	52.7	110	76	-1.00	-20
03/02	05 31.8	-11 26	0.40	1.13	18.1	60.4	99	136	-0.18	-23
03/12	05 30.7	-14 28	0.42	1.08	18.3	66.7	90	43	+0.26	-24
03/22	05 33.4	-17 13	0.44	1.04	18.4	72.3	83	110	-0.99	-25
04/01	05 38.0	-19 54	0.44	1.00	18.5	77.6	77	110	-0.17	-25

(454177) 2013 GJ35 (Jan-Mar, *H* = 15.8)

This is one of the larger asteroids in the list: 2.1 km. The rotation period is not known. The first 2-3 weeks of January favor northern observers. Southern observers get the rest of the observing window.

DATE	RA	Dec	ED	SD	V	α	SE	ME	MP	GB
01/01	09 30.5	+32 18	0.27	1.21	14.7	29.9	142	87	-0.23	+46
01/11	08 43.5	+04 40	0.20	1.17	13.7	21.1	155	144	+0.21	+27
01/21	07 40.5	-30 17	0.21	1.13	14.4	42.4	129	51	+1.00	-4
01/31	06 37.6	-49 31	0.30	1.11	15.5	58.4	107	108	-0.20	-22
02/10	05 49.1	-57 19	0.40	1.10	16.3	63.9	95	81	+0.22	-31
02/20	05 17.2	-60 45	0.50	1.09	16.8	64.6	88	96	-1.00	-35
03/02	04 58.3	-62 32	0.60	1.11	17.1	63.2	84	91	-0.18	-37
03/12	04 49.3	-63 43	0.68	1.13	17.4	60.9	83	79	+0.26	-38
03/22	04 48.2	-64 45	0.74	1.16	17.6	58.3	82	102	-0.99	-37
04/01	04 54.5	-65 51	0.79	1.20	17.7	55.7	84	82	-0.17	-36

(18736) 1998 NU (Jan-Mar, *H* = 15.8)

This NEA also has a diameter of about 2.1 km. There is no rotation period given in the LCDB. Its size virtually assures that the period will be > ≈2.2 hours. The large range of phase angles make this a good subject for finding the H-G parameters.

DATE	RA	Dec	ED	SD	V	α	SE	ME	MP	GB
01/01	07 47.2	+23 15	0.44	1.41	15.4	10.2	165	108	-0.23	+22
01/11	07 45.5	+22 21	0.38	1.36	14.7	3.0	176	130	+0.21	+21
01/21	07 42.3	+21 08	0.33	1.31	14.4	5.0	173	4	+1.00	+20
01/31	07 40.0	+19 34	0.30	1.28	14.5	13.2	163	144	-0.20	+19
02/10	07 41.4	+17 39	0.28	1.25	14.6	20.9	153	97	+0.22	+19
02/20	07 48.9	+15 28	0.27	1.22	14.6	27.5	145	40	-1.00	+20
03/02	08 03.5	+13 05	0.27	1.21	14.8	32.6	139	168	-0.18	+22
03/12	08 24.9	+10 34	0.28	1.21	14.9	36.0	134	74	+0.26	+26
03/22	08 51.8	+07 57	0.29	1.21	15.1	37.9	132	62	-0.99	+30
04/01	09 22.2	+05 19	0.32	1.23	15.3	38.7	130	168	-0.17	+36

(180186) 2003 QZ30 (Jan-Mar, *H* = 17.4)

The rotation period for the 1-km 2003 QZ30 is not known. The lightcurve shape could be affected by shadowing effects at the large phase angles during the apparition. Expect the unexpected.

DATE	RA	Dec	ED	SD	V	α	SE	ME	MP	GB
01/01	00 12.4	-36 39	0.25	0.93	17.6	95.1	71	120	-0.23	-77
01/08	01 23.1	-36 40	0.21	0.96	17.1	88.9	79	63	+0.03	-78
01/15	02 47.3	-33 15	0.20	1.01	16.6	78.1	91	42	+0.58	-64
01/22	04 10.1	-25 45	0.20	1.05	16.3	64.4	105	84	-0.99	-46
01/29	05 17.2	-16 22	0.22	1.11	16.2	51.5	119	139	-0.38	-28
02/05	06 06.6	-07 53	0.26	1.16	16.4	41.9	128	126	+0.00	-14
02/12	06 42.9	-01 18	0.31	1.22	16.8	35.9	134	61	+0.41	-2
02/19	07 10.5	+03 30	0.37	1.28	17.2	32.7	135	38	+0.99	+6
02/26	07 32.5	+06 56	0.45	1.34	17.6	31.4	135	128	-0.55	+12
03/05	07 51.0	+09 24	0.53	1.41	18.1	31.0	133	149	-0.02	+17

(419880) 2011 AH37 (Jan-Feb, *H* = 19.5)

There's no rotation period given in the LCDB for 2011 AH37, which has an estimated diameter of 370 meters. This makes it unlikely to have a super-fast period. However, rules are made to be broken.

DATE	RA	Dec	ED	SD	V	α	SE	ME	MP	GB
01/20	00 35.8	+23 11	0.11	0.97	18.0	95.0	79	86	+0.98	-40
01/23	01 24.8	+36 09	0.10	0.99	17.4	82.8	91	110	-0.95	-26
01/26	02 32.1	+47 25	0.11	1.02	17.1	70.2	104	128	-0.70	-12
01/29	03 53.3	+54 17	0.12	1.04	17.1	59.3	115	139	-0.38	+0
02/01	05 11.9	+56 35	0.14	1.07	17.2	50.9	123	143	-0.13	+10
02/04	06 13.9	+56 03	0.16	1.09	17.4	44.9	129	135	-0.01	+17
02/07	06 58.1	+54 21	0.19	1.12	17.7	40.5	132	117	+0.04	+23
02/10	07 29.3	+52 19	0.21	1.15	17.9	37.4	135	92	+0.22	+27
02/13	07 51.8	+50 20	0.24	1.18	18.2	35.1	137	63	+0.51	+30

(137805) 1999 YK5 (Jan-Feb, *H* = 16.6)

This is one of the few asteroids with a reported rotation period (Warner, 2016; 3.390 h) and Aznar (2018, 3.468 h). These differ by more than several times the formal errors. Maybe new observations will lead to a more secure result.

DATE	RA	Dec	ED	SD	V	α	SE	ME	MP	GB
01/01	11 44.2	+46 34	0.47	1.27	17.2	44.0	117	70	-0.23	+66
01/08	11 47.1	+50 44	0.42	1.25	16.8	42.6	121	132	+0.03	+63
01/15	11 44.3	+56 06	0.36	1.23	16.5	41.6	124	110	+0.58	+59
01/22	11 30.0	+62 52	0.32	1.20	16.1	41.8	126	51	-0.99	+52
01/29	10 46.1	+70 51	0.28	1.16	15.8	44.4	124	97	-0.38	+43
02/05	08 26.8	+77 31	0.25	1.12	15.7	50.5	118	120	+0.00	+32
02/12	04 48.1	+74 04	0.23	1.08	15.7	60.4	108	66	+0.41	+18
02/19	03 15.5	+62 17	0.22	1.03	15.9	73.4	94	77	+0.99	+4
02/26	02 39.7	+48 52	0.22	0.97	16.4	88.0	79	143	-0.55	-10
03/05	02 19.8	+36 02	0.24	0.91	17.1	103.4	63	81	-0.02	-23

2013 CW32 (Jan-Feb, *H* = 16.6)

Despite its diminutive size of 120 meters, this NEA will pass close enough to Earth to provide large SNR values at Arecibo and Goldstone. The rotation period is not known but there's a good chance that it is shorter than 2 hours. With that in mind, keep exposures as short as possible for the initial observations and until there is a better idea of the period. The rapid sky motion will make short exposures necessary regardless.

DATE	RA	Dec	ED	SD	V	α	SE	ME	MP	GB
01/25	10 46.9	-68 42	0.06	0.98	18.8	88.0	89	75	-0.80	-9
01/27	09 43.5	-55 16	0.04	1.00	17.7	72.8	105	69	-0.59	-2
01/29	09 00.9	-31 45	0.04	1.01	16.5	48.4	130	88	-0.38	+10
01/31	08 32.0	-02 43	0.04	1.02	15.8	20.1	159	125	-0.20	+21
02/02	08 11.9	+19 26	0.05	1.03	16.0	11.2	168	161	-0.07	+26
02/04	07 57.5	+32 39	0.06	1.04	17.0	21.4	157	165	-0.01	+27
02/06	07 47.0	+40 30	0.08	1.05	17.7	29.1	149	140	+0.01	+27
02/08	07 39.1	+45 27	0.10	1.06	18.4	34.3	143	116	+0.09	+27

(455176) 1999 VF22 (Feb, *H* = 20.6)
The estimated size is 225 meters, large enough that super-fast rotation is not likely but, again, not impossible.

DATE	RA	Dec	ED	SD	V	α	SE	ME	MP	GB
02/12	12 41.0	+15 24	0.14	1.09	18.1	38.5	136	140	+0.41	+78
02/13	12 50.9	+16 01	0.13	1.08	17.9	40.3	135	130	+0.51	+79
02/14	13 03.3	+16 46	0.11	1.07	17.7	42.7	133	119	+0.62	+79
02/15	13 19.1	+17 40	0.10	1.05	17.4	45.9	130	109	+0.72	+79
02/16	13 39.9	+18 43	0.09	1.04	17.2	50.2	126	99	+0.82	+76
02/17	14 08.1	+19 53	0.07	1.03	17.1	56.2	120	92	+0.90	+71
02/18	14 46.7	+21 01	0.06	1.01	16.9	64.6	112	86	+0.96	+63
02/19	15 39.5	+21 41	0.06	1.00	17.0	76.2	101	85	+0.99	+52
02/20	16 46.9	+21 01	0.05	0.99	17.3	91.2	86	88	-1.00	+36
02/21	18 01.0	+18 21	0.05	0.97	18.1	108.1	69	94	-0.97	+19

(381677) 2009 BJ81 (Jan-Mar, *H* = 20.6)
The rotation period is unknown. Mainzer et al. (2016) give a diameter of 470 meters and an albedo of 0.346.

DATE	RA	Dec	ED	SD	V	α	SE	ME	MP	GB
01/15	09 45.0	+18 31	0.38	1.33	17.8	20.6	152	110	+0.58	+46
01/25	09 58.6	+21 31	0.30	1.27	17.1	16.6	158	33	-0.80	+50
02/04	10 15.5	+26 15	0.23	1.21	16.4	14.9	162	155	-0.01	+55
02/14	10 40.8	+33 16	0.18	1.15	15.9	19.8	157	83	+0.62	+61
02/24	11 27.1	+42 45	0.14	1.11	15.6	31.3	144	64	-0.75	+67
03/06	13 02.0	+52 29	0.11	1.07	15.5	47.5	128	131	+0.00	+65
03/16	15 35.8	+53 51	0.10	1.03	15.8	65.0	110	92	+0.67	+50
03/26	17 37.2	+43 37	0.11	1.01	16.3	77.8	96	64	-0.71	+31

(162361) 2000 AF6 (Feb-Mar, *H* = 20.1)
The estimated diameter is 280 meters, making this an unlikely super-fast rotation candidate.

DATE	RA	Dec	ED	SD	V	α	SE	ME	MP	GB
02/20	11 58.8	+12 16	0.20	1.17	18.0	22.0	154	20	-1.00	+71
02/23	11 50.6	+14 39	0.18	1.16	17.7	18.5	158	29	-0.84	+71
02/26	11 39.9	+17 28	0.16	1.15	17.3	15.5	162	73	-0.55	+71
03/01	11 26.2	+20 46	0.15	1.14	17.1	14.1	164	113	-0.26	+70
03/04	11 08.7	+24 31	0.14	1.12	16.9	15.8	162	151	-0.06	+67
03/07	10 46.5	+28 40	0.13	1.11	16.9	21.0	156	157	+0.00	+62
03/10	10 18.8	+33 00	0.12	1.10	16.9	28.6	148	118	+0.10	+57
03/13	09 45.1	+37 13	0.11	1.08	17.1	37.6	138	74	+0.35	+50
03/16	09 05.4	+40 53	0.11	1.07	17.2	47.6	128	32	+0.67	+42
03/19	08 21.2	+43 35	0.11	1.05	17.5	57.9	117	37	+0.94	+34

(86667) 2000 FO10 (Mar-Apr, *H* = 17.6)
Polishook and Brosch (2008) reported a period of 26 hours, but it was very uncertain (U = 1 in the LCDB). They also gave an amplitude of > 0.5 mag. The diameter is about 900 meters.

DATE	RA	Dec	ED	SD	V	α	SE	ME	MP	GB
03/02	04 33.3	-56 28	0.19	0.98	17.1	87.2	82	94	-0.18	-41
03/07	05 58.9	-46 58	0.20	1.03	16.7	74.5	95	89	+0.00	-28
03/12	06 52.0	-35 57	0.21	1.07	16.7	63.9	105	70	+0.26	-15
03/17	07 26.1	-26 05	0.24	1.11	16.8	56.5	112	48	+0.78	-5
03/22	07 50.0	-18 07	0.28	1.14	17.0	51.9	115	78	-0.99	+4
03/27	08 08.2	-11 55	0.32	1.18	17.3	49.3	117	129	-0.61	+11
04/01	08 23.0	-07 10	0.37	1.21	17.6	48.0	116	149	-0.17	+17
04/06	08 35.7	-03 29	0.42	1.23	17.9	47.4	115	106	+0.01	+21

(163081) 2002 AG29 (Feb-Mar, *H* = 18.4)
The estimated diameter is 620 meters. Skiff (2011) found a secure period of 19.70 h and 0.25 mag lightcurve amplitude. This one's exclusively for southern observers.

DATE	RA	Dec	ED	SD	V	α	SE	ME	MP	GB
02/01	10 41.2	-42 44	0.30	1.15	18.0	50.9	115	89	-0.13	+14
02/08	10 43.8	-47 45	0.27	1.13	17.8	52.8	115	124	+0.09	+10
02/15	10 45.3	-53 05	0.24	1.10	17.5	55.5	113	100	+0.72	+5
02/22	10 46.0	-58 57	0.21	1.08	17.3	59.1	110	64	-0.92	+0
03/01	10 45.8	-65 43	0.18	1.06	17.1	64.1	106	81	-0.26	-6
03/08	10 45.1	-74 00	0.15	1.03	16.9	70.8	101	101	+0.02	-13
03/15	10 44.2	-84 50	0.13	1.01	16.8	80.0	93	110	+0.56	-23
03/22	22 44.0	-80 11	0.11	0.99	16.9	92.5	81	97	-0.99	-35
03/29	22 45.1	-60 06	0.10	0.96	17.4	108.2	66	53	-0.42	-51
04/05	22 47.6	-37 30	0.10	0.94	18.4	122.7	52	46	+0.00	-62

(88254) 2001 FM129 (Mar-Apr, *H* = 17.6)
Mainzer et al. (2014) reported a diameter of 800 meters and albedo of 0.252. Thomas et al. (2014) found 2001 FM129 to be a type Q asteroid, which is relatively uncommon among the inner main-belt asteroids.

DATE	RA	Dec	ED	SD	V	α	SE	ME	MP	GB
03/10	02 42.9	+01 05	0.10	0.93	17.6	124.1	51	15	+0.10	-51
03/13	04 16.4	+04 28	0.09	0.97	16.0	103.1	72	13	+0.35	-31
03/16	05 54.6	+07 13	0.09	1.00	15.3	81.0	94	22	+0.67	-9
03/19	07 10.2	+08 28	0.11	1.04	15.2	64.6	109	44	+0.94	+8
03/22	08 00.5	+08 47	0.14	1.07	15.5	54.4	119	75	-0.99	+19
03/25	08 33.8	+08 44	0.17	1.10	15.8	48.3	124	108	-0.80	+27
03/28	08 56.9	+08 35	0.21	1.14	16.2	44.6	127	141	-0.52	+32
03/31	09 13.9	+08 24	0.24	1.17	16.5	42.3	128	169	-0.24	+35
04/03	09 27.1	+08 12	0.28	1.20	16.8	40.9	129	153	-0.05	+38
04/06	09 37.7	+08 00	0.32	1.22	17.2	39.9	128	120	+0.01	+40

(5189) 1990 UQ (Mar-Apr, *H* = 17.8)
This is second object in the list where dates of brightest and closest are separated by several months. Closest approach for 1990 UQ is July 19 (0.207 AU). It will be only a few degrees from the Sun at that time.

Warner (2018) found a period of 6.676 h and 1.02 mag lightcurve amplitude. Here's another good opportunity to get an H-G phase curve. Being so faint, it may require very large scopes or careful transformation from clear/no filter to the V standard band.

DATE	RA	Dec	ED	SD	V	α	SE	ME	MP	GB
03/15	12 02.1	+06 37	0.58	1.57	18.0	4.7	173	87	+0.56	+66
03/18	11 57.0	+07 32	0.56	1.55	17.9	4.3	173	42	+0.87	+67
03/21	11 51.4	+08 30	0.54	1.53	17.8	5.6	171	5	-1.00	+67
03/24	11 45.4	+09 30	0.52	1.51	17.8	8.1	168	50	-0.88	+66
03/27	11 39.1	+10 31	0.50	1.49	17.9	11.0	163	91	-0.61	+66
03/30	11 32.5	+11 32	0.49	1.47	17.9	14.2	159	130	-0.33	+66
04/02	11 25.7	+12 33	0.48	1.45	17.9	17.5	154	167	-0.10	+65
04/05	11 18.9	+13 32	0.47	1.42	18.0	20.9	150	154	+0.00	+64
04/08	11 12.1	+14 28	0.46	1.40	18.0	24.3	145	115	+0.07	+64
04/11	11 05.5	+15 21	0.45	1.38	18.0	27.7	140	74	+0.31	+63

(This page deliberately left blank.)

IN THIS ISSUE

This list gives those asteroids in this issue for which physical observations (excluding astrometric only) were made. This includes lightcurves, color index, and H-G determinations, etc. In some cases, no specific results are reported due to a lack of or poor quality data. The page number is for the first page of the paper mentioning the asteroid. EP is the "go to page" value in the electronic version.

THE MINOR PLANET BULLETIN (ISSN 1052-8091) is the quarterly journal of the Minor Planets Section of the Association of Lunar and Planetary Observers (ALPO). Current and most recent issues of the *MPB* are available on line, free of charge from:

http://www.minorplanet.info/MPB/mpb.php

Nonmembers are invited to join ALPO by communicating with: Matthew L. Will, A.L.P.O. Membership Secretary, P.O. Box 13456, Springfield, IL 62791-3456 (will008@attglobal.net). The Minor Planets Section is directed by its Coordinator, Prof. Frederick Pilcher, 4438 Organ Mesa Loop, Las Cruces, NM 88011 USA (fpilcher35@gmail.com, assisted by Lawrence Garrett, 206 River Rd., Fairfax, VT 05454 USA (LSGasteroid@msn.com). Dr. Alan W. Harris (Space Science Institute; awharris@spacescience.org), and Dr. Petr Pravec (Ondrejov Observatory; ppravec@asu.cas.cz) serve as Scientific Advisors. The Asteroid Photometry Coordinator is Brian D. Warner, Palmer Divide Observatory, 446 Sycamore Ave., Eaton, CO 80615 USA (brian@MinorPlanetObserver.com).

The Minor Planet Bulletin is edited by Professor Richard P. Binzel, MIT 54-410, 77 Massachusetts Ave, Cambridge, MA 02139 USA (rpb@mit.edu). Brian D. Warner (address above) is Associate Editor, and Dr. David Polishook, Department of Earth and Planetary Sciences, Weizmann Institute of Science (david.polishook@weizmann.ac.il) is Assistant Editor. The *MPB* is produced by Dr. Robert A. Werner, 3937 Blanche St., Pasadena, CA 91107 USA (rawerner@polygrav.org) and distributed by Derald D. Nye. Direct all subscriptions, contributions, address changes, etc. to:

Mr. Derald D. Nye - Minor Planet Bulletin
10385 East Observatory Drive
Corona de Tucson, AZ 85641-2309 USA
(nye@kw-obsv.org) (Telephone: 520-762-5504)

Effective with Volume 38, the *Minor Planet Bulletin* is a limited print journal, where print subscriptions are available only to libraries and major institutions for long-term archival purposes. In addition to the free electronic download of the *MPB* noted above, electronic retrieval of all *Minor Planet Bulletin* articles (back to Volume 1, Issue Number 1) is available through the Astrophysical Data System

http://www.adsabs.harvard.edu/.

Authors should submit their manuscripts by electronic mail (rpb@mit.edu). Author instructions and a Microsoft Word template document are available at the web page given above. All materials must arrive by the deadline for each issue. Visual photometry observations, positional observations, any type of observation not covered above, and general information requests should be sent to the Coordinator.

* * * * *

The deadline for the next issue (46-2) is January 15, 2019. The deadline for issue 46-3 is April 15, 2019.